Proceedings of RIKEN BNL Research Center Workshop Volume 31

BNL-52617
Formal Report

RHIC SPIN PHYSICS III & IV

POLARIZED PARTONS AT HIGH Q^2 REGION

August 3, 2000 at BNL
October 14, 2000 at Kyoto University

Organizing Committee:
8/3 — Gerry Bunce, Steve Vigdor
10/14 — K. Imai, H. En'yo, N. Saito, T. Kunihiro, T. Uematsu, S. Kumano, Y. Koike, M. Okamura

Scientific Advisory Committee:
T. Roser, D. Underwood, X. Ji, J. Soffer, L.C. Bland, K. Yazaki, A. Masaike

RIKEN BNL Research Center
Building 510A, Brookhaven National Laboratory, Upton, NY 11973-5000, USA

Other RIKEN BNL Research Center Proceedings Volumes:

Volume 30 - RBRC Scientific Review Committee Meeting – BNL-52603

Volume 29 - Future Transversity Measurements - BNL-52612

Volume 28 - Equilibrium & Non-Equilibrium Aspects of Hot, Dense QCD – BNL-52613

Volume 27 – Predictions and Uncertainties for RHIC Spin Physics & Event Generator for RHIC Spin Physics III – Towards Precision Spin Physics at RHIC – BNL-52596

Volume 26 - Circum-Pan-Pacific RIKEN Symposium on High Energy Spin Physics - BNL-52588

Volume 25 - RHIC Spin - BNL-52581

Volume 24 - Physics Society of Japan Biannual Meeting Symposium on QCD Physics at RIKEN BNL Research Center - BNL-52578

Volume 23 - Coulomb and Pion-Asymmetry Polarimetry and Hadronic Spin Dependence at RHIC Energies – BNL-52589

Volume 22 - OSCAR II: Predictions for RHIC - BNL-52591

Volume 21 - RBRC Scientific Review Committee Meeting - BNL-52568

Volume 20 - Gauge-Invariant Variables in Gauge Theories – BNL-52590

Volume 19 - Numerical Algorithms at Non-Zero Chemical Potential - BNL-52573

Volume 18 - Event Generator for RHIC Spin Physics - BNL-52571

Volume 17 - Hard Parton Physics in High-Energy Nuclear Collisions - BNL-52574

Volume 16 - RIKEN Winter School - Structure of Hadrons - Introduction to QCD Hard Processes – BNL-52569

Volume 15 - QCD Phase Transitions - BNL-52561

Volume 14 - Quantum Fields In and Out of Equilibrium - BNL-52560

Volume 13 - Physics of the 1 Teraflop RIKEN-BNL-Columbia QCD Project First Anniversary Celebration – BNL-66299

Volume 12 - Quarkonium Production in Relativistic Nuclear Collisions – BNL-52559

Volume 11 - Event Generator for RHIC Spin Physics - BNL-66116

Volume 10 - Physics of Polarimetry at RHIC - BNL-65926

Volume 9 - High Density Matter in AGS, SPS and RHIC Collisions - BNL-65762

Volume 8 - Fermion Frontiers in Vector Lattice Gauge Theories - BNL-65634

Volume 7 - RHIC Spin Physics - BNL-65615

Volume 6 - Quarks and Gluons in the Nucleon - BNL-65234

Volume 5 - Color Superconductivity, Instantons and Parity (Non?)-Conservation at High Baryon Density – BNL-65105

Volume 4 - Inauguration Ceremony, September 22 and Non -Equilibrium Many Body Dynamics – BNL- 64912

Volume 3 - Hadron Spin-Flip at RHIC Energies - BNL-64724

Volume 2 - Perturbative QCD as a Probe of Hadron Structure - BNL-64723

Volume 1 - Open Standards for Cascade Models for RHIC - BNL-64722

Inside

Preface to the Series

The RIKEN BNL Research Center (RBRC) was established in April 1997 at Brookhaven National Laboratory. It is funded by the "Rikagaku Kenkysho" (RIKEN, The Institute of Physical and Chemical Research) of Japan. The Center is dedicated to the study of strong interactions, including spin physics, lattice QCD and RHIC physics through the nurturing of a new generation of young physicists.

During the first year, the Center had only a Theory Group. In the second year, an Experimental Group was also established at the Center. At present, there are seven Fellows and nine post docs in these two groups. During the third year, we started a new Tenure Track Strong Interaction Theory RHIC Physics Fellow Program, with six positions in the academic year 1999-2000; this program will increase to include eleven theorists in the next academic year, and, in the year after, also be extended to experimental physics. In addition, the Center has an active workshop program on strong interaction physics, about ten workshops a year, with each workshop focussed on a specific physics problem. Each workshop speaker is encouraged to select a few of the most important transparencies from his or her presentation, accompanied by a page of explanation. This material is collected at the end of the workshop by the organizer to form proceedings, which can therefore be available within a short time.

The construction of a 0.6 teraflop parallel processor, which was begun at the Center on February 19, 1998, was completed on August 28, 1998.

T. D. Lee
September 29, 2000

*Work performed under the auspices of U.S.D.O.E. Contract No. DE-AC02-98CH10886.

CONTENTS

Preface to the Series i

Summary – RSC2000 International Workshop on Polarized Partons at High Q^2 Region, October 13-14, 2000, Yukawa Institute, Kyoto University, Japan 1

Workshop Program 2

List of Participants 4

Summary – RIKEN BNL Workshop on Year 2 Spin Physics at RHIC
S. Vigdor & G. Bunce 7

A New Optically-Pumped Polarized H Ion Source (OPPIS) for the RHIC Spin Physics
A. Zelenski 13

Polarized Proton Commissioning Run 2000
Haixin Huang 29

Polarimetry at RHIC
D. Svirida 43

Suppressing Intrinsic Spin Harmonics at the AGS
A. Lehrach 53

Partial Helical Snake for AGS
M. Okamura 59

Spin Tracking with "Real" Siberian Snakes in RHIC
M. Xiao 67

Spin Flipping in RHIC
M. Bai 85

Overview of RHIC Spin Commissioning and Plans
T. Roser 93

Polarized Parton Distribution Functions with Estimate of Uncertainties
H. Kobayashi 101

How Well Do We Know The Polarized Parton Densities in the Nucleon At Present?
E. Leader 113

Soft-Gluon Effects in Polarized Prompt Photon Production
W. Vogelsang 129

Future Transversity Measurement with PHENIX
M. Grosse Perdekamp 145

Short Comment
A. Ogawa 159

Sudakov Suppression of Azimuthal Spin Asymmetries
D. Boer 163
New Prospects for Polarized Fragmentation Functions
J. Soffer 175
Polarized A_c^+ Production at RHIC
K. Ohkuma 191
Large Momentum Transfer Electroproduction of Mesons
Hanwen Huang 199
PHENIX Detector Commissioning and Prospects for Polarized Proton Running
K. Barish 211
The STAR Level-3 Trigger System – Year 0 Experiences
J. Soeren Lange 233
Short Comment
A. Ogawa 249
Short Comment
H. Spinka 253
Polarized Jet Target for Absolute Measurement of RHIC Proton Beam Polarization
T. Wise 255
Beyond Standard Model Physics at RHIC
J. Murata 263
Summary of Previous Meeting (August 3rd)
S. Vigdor 275
Discussion for FY2001 Running & Beyond
G. Bunce 281

RSC2000

International Workshop on Polarized Partons at High Q^2 region

October 13(Fri.)-14(Sat), 2000,
Yukawa Institute, Kyoto University, Japan

International workshop on " Polarized Partons at High Q^2 region " was held at the Yukawa Institute for Theoretical Physics, Kyoto University, Kyoto, Japan, on October 13-14, 2000, as a satellite of the international conference "SPIN 2000" (Osaka, Japan, October 16-21,2000). This workshop was supported by RIKEN (The Institute of Physical and Chemical Research) and by Yukawa Institute. The scientific program was focused on the upcoming polarized collider RHIC. The workshop was also an annual meeting of RHIC Spin Collaboration (RSC).

The number of participants was 55, including 28 foreign visitors and 8 foreign-resident Japanese participants, reflecting the international nature of the RHIC spin program.

At the workshop there were 25 oral presentations in four sessions, 1) RHIC Spin Commissioning, 2) Polarized Partons, Present and Future, 3) New Ideas on Polarization Phenomena, 4) Strategy for the Coming Spin Running. In 1) the successful polarized proton commissioning and the readiness of the accelerator for the physics program impressed us. In 2) and 3) active discussions were made on the new structure function *h1* to be firstly measured at RHIC, and several new theoretical ideas were presented. In session 4) we have established a plan for the beam time requirement toward the first collision of polarized protons.

These proceedings include the transparencies presented at the workshop. The discussion on "Strategy for the Coming Spin Running" was summarized by the chairmans of the session, S. Vigdor and G. Bunce.

At the dinner party, all the participants sit on the floor in the traditional Japanese-style restaurant, and enjoyed *nabe*, Japanese Fondue.

Local organizers: K. Imai (Kyoto University), H. En'yo (Kyoto University,), N. Saito (RIKEN & RBRC), T. Kunihiro (Yukawa Institute, Kyoto University), T. Uematsu (Kyoto University), S. Kumano (Saga University), Y. Koike (Niigata University), M. Okamura (RIKEN)

Scientific Advisers: G. Bunce (BNL & RBRC), T. Roser (BNL), D. Underwood (ANL), X. Ji (University of Maryland), J. Soffer (Marseill), L. C. Bland (ICUF Indiana), K. Yazaki (TWU), A. Masaike (Fukui Institute of Technology)

Workshop program

2000/OCT/13

9:00 Welcome (Imai Ken'ichi),

1st Session: RHIC Spin Commissioning (Chair Y. Makdisi)

9:30 The new Optically Pumped Polarized Ion Source (A. Zelenski)
9:50 Polarized proton commissioning run 2000 (H. Huang)
10:30 Polarimetry at RHIC (D. Svirida)
10:50 Break
11:00 Suppressing intrinsic spin harmonics at the AGS (A. Lehrach)
11:15 Partial helical snake for AGS (M. Okamura)
11:30 Spin tracking with real Siberian snakes in RICH (M. Xiao)
11:45 Spin flipping in RHIC (M. Bai)
12:00 Overview of RHIC spin commissioning and plans (T. Roser, discussion leader)
12:30 Lunch

2nd Session: Polarized Partons, present and future (Chair V. Rykov)

14:00 Polarized Parton Distribution Functions with Estimate of Uncertainties (H. Kobayashi)
14:30 How well do we know the polarized parton densities in the nucleon at present (D. Stamenov)
15:00 Soft-gluon effects in Prompt Photon Production (W. Vogelsang)
15:30 Transversity measurements at RHIC (M. Perdekamp, A.Ogawa)
16:10 Break

3rd Session: New Idea on Polarization Phenomena (Chair W. Vogelsang)

16:40 Sudakov Suppression of Azimuthal Spin Asymmetries (D. Boer)
17:10 New Prospects for Polarized Fragmentation Functions (J.Soffer)
17:40 Polarized Λc^+ Production at RHIC (K. Ohkuma)
18:10 Large momentum transfer electro-production of mesons (Hanwen Huang)
18:40 Move to Dinner at Tozan-sou

2000/OCT/14

4th Session: Strategy for Coming Spin Running (Chair G. Bunce)

9:00 Summary of Pervious meeting (Aug 3rd) (S. Vigdor)
9:15 Phenix detector commissioning and prospects for the spin runs (K.Barish)
9:45 STAR detector commissioning and prospects for the spin runs (L.Bland)
10:10 First Experiences with STAR level-3 trigger (J.S. Lange)
10:30 Discussion and planning for FY2001 running
11:00 Break

5th Session: Strategy for the Long Range Plan (Chair S. Vigdor)

11:15 Polarized Jet Target for Absolute Measurement of RHIC Proton Beam Polarization (T. Wise)
11:45 Beyond Standard Model at RHIC (J. Murata)
12:15 Discussion for long range plan (G. Bunce discussion leader)
13:00 Adjourn
14:00 RSC business meeting

List of Participants

	name		Email	Organization
	Last	First		
1	Bai	Mei	mbai@bnl.gov	Brookhaven National Laboratory
2	Barish	Kenneth N.	barish@phyun0.ucr.edu	University of California Riverside
3	Bland	Leslie C.	bland@iucf.indiana.edu	IUCF, Indiana University
4	Boer	Daniel	dboer@bnl.gov	RIKEN-BNL Research Center
5	Bunce	Gerry	bunce@bnl.gov	BNL/RIKEN-BNL Research Center
6	En'yo	Hideto	enyo@ne.scphys.kyoto-u.ac.jp	Kyoto University
7	Goto	Yuji	goto@bnl.gov	RIKEN-BNL Research Center
8	Guryn	Wlodek	guryn@bnl.gov	Brookhaven National Laboratory
9	Haeberli	Willy	whaeberli@uwnuc0.physics.wisc.edu	University of Wisconsin, Madison
10	Hayashi	Naoki	hayashi@rarfaxp.riken.go.jp	RIKEN
11	Hirai	Masanori	98td25@edu.cc.saga-u.ac.jp	Saga University
12	Huang	Haixin	huanghai@bnl.gov	Brookhaven National Laboratory
13	Huang	Hanwen	huanghw@radix.h.kobe-u.ac.jp	Kobe University
14	Hughes	Vernon	vernon.hughes@yale.edu	Yale University
15	Ichihara	Takashi	ichihara@riken.go.jp	RIKEN
16	Imai	Ken'ichi	imai@ne.scphys.kyoto-u.ac.jp	Kyoto University
17	Kamihara	Nobuyuki	kamihara@nucl.phys.titech.ac.jp	Tokyo Institute of Technology
18	Katayama	Takeshi	katayama@postman.riken.go.jp	RIKEN
19	Kobayashi	Hideyuki	hyuki@rarfaxp.riken.go.jp	RIKEN
20	Kohama	Akihisa	kohama@rarfaxp.riken.go.jp	RIBF Project Office, RIKEN
21	Kurita	Kazuyoshi	kurita@bnl.gov	RIKEN BNL Research Center
22	Lange	Jens Soeren	soeren@bnl.gov	Brookhaven National Laboratory
23	Lehrach	Andreas	lehrach@sun2.bnl.gov	Brookhaven National Laboratory
24	Makdisi	Yousef	makdisi@bnl.gov	Brookhaven National Laboratory
25	Masaike	Akira	masaike@mvb.biglobe.ne.jp	Fukui University of Technology
26	Miyama	Masanori	miyama@comp.metro-u.ac.jp	Tokyo Metropolitan University
27	Morii	Toshiyuki	morii@kobe-u.ac.jp	Kobe University
28	Murata	Jiro	murata@bnl.gov	RIKEN
29	Nakamura	Masanobu	nakamura@nh.scphys.kyoto-u.ac.jp	Kyoto University

30	Ogawa	Akio	akio@bnl.gov	Pennsylvania State University
31	Ohkuma	Kazumasa	ohkuma@radix.h.kobe-u.ac.jp	Kobe University
32	Okamura	Masahiro	mokamura@postman.riken.go.jp	RIKEN
33	Perdekamp	Matthias G.	matthias@bnl.gov	RIKEN-BNL Research Center
34	Roser	Thomas	roser@bnl.gov	Brookhaven National Laboratory
35	Rykov	Vladimir	rykov@physics.wayne.edu	Wayne State University
36	Saito	Naohito	saito@bnl.gov	RIKEN/RBRC
37	Sato	Hiroki, D.	satohiro@bnl.gov	Kyoto University
38	Shibata	Tshi-Aki	shibata@nucl.phys.titech.ac.jp	Tokyo Institute of Technology
39	Soffer	Jacques F.	Jacques.Soffer@cpt.univ-mrs.fr	Centre de Physique Theorique
40	Spinka	Harold M.	hms@hep.anl.gov	Argonne National Laboratory
41	Stamenov	Dimiter, B	stamenov@inrne.bas.bg	Institute for Nuclear Research and Nuclear Energy
42	Stephenson	Edward, J	stephens@iucf.indiana.edu	Indiana University Cyclotron Facility
43	Svirida	Dmitry M.	svirida@vitep5.itep.ru	Institute of Theoretical and Experimental Physics
44	Tannenbaum	Michael J.	mjt@bnl.gov	Brookhaven National Laboratory
45	Tojo	Junji	tojo@bnl.gov	Kyoto University
46	Torii	Hiyayuki	htorii@bnl.gov	Kyoto University
47	Uematsu	Tsuneo	uematsu@phys.h.kyoto-u.ac.jp	FIHS, Kyoto University
48	Vigdor	Steven E.	vigdor@iucf.indiana.edu	Indiana University
49	Vogelsang	Werner	vogelsan@quark.phy.bnl.gov	RIKEN-BNL Research Center
50	Watanabe	Yasushi	watanaby@riken.go.jp	RIKEN
51	Wise	Thomas S.	wise@uwnuc0.physics.wisc.edu	University of Wisconsin
52	Wissink	Scott W.	wissink@iucf.indiana.edu	Indiana University
53	Xiao	Meiqin	meiqin@bpmail.fnal.gov	Fermi National Accelerator Laboratory
54	Yasui	Yoshiaki	yasui@taro02.riken.go.jp	RIKEN Radiation Lab.
55	Zelenski	Anatoli	zelenski@bnl.gov	Institute for Nuclear Research

Summary of RIKEN-BNL Workshop on Year 2 Spin Physics at RHIC

August 3 at BNL and October 14 at Kyoto
Steve Vigdor and Gerry Bunce

The RHIC Spin Collaboration met twice to develop a spin run plan and request for 2001, the first year of spin collisions at RHIC. The first meeting was held August 3 at BNL, with presentations by Yousef Makdisi on polarimetry, Thomas Roser on the plans for the September commissioning and plans for the installation of Siberian Snakes for the 2001 run, Naohito Saito presented PHENIX goals for the 2001 run, Steve Vigdor gave STAR plans and goals, and Wlodek Guryn gave the pp2pp plans. This meeting took place prior to RHIC running reliably for heavy ion collisions (which started about August 5), and prior to the September spin commissioning.

There were a number of interesting and potentially important points made in the presentations and discussion. However, it was clear that we would have many of the concerns voiced August 3 answered by the September commissioning, and that we should meet with that information in hand, to develop the 2001 spin request. This second meeting took place in Kyoto October 14. We summarize both meetings here.

A list of August 3 Concerns and Comments

1. Proton-carbon Coulomb-Nuclear Interference scattering is the planned relative polarimeter for RHIC. How to absolutely calibrate pC CNI? Tie to the AGS internal polarimeter until 2003. Then use a polarized hydrogen jet target in RHIC for absolute calibration to $\pm 5\%$. A pp "elastic" recoil spectrometer ($-t=0.15$) was also installed in RHIC looking at the pC CNI polarimeter target for the September commissioning run, in order to measure quasi-elastic pp from the carbon target.
2. Transferring the calibration of the polarimeter from injection to higher energy is to be done by decelerating from the higher energy to injection energy to re-measure the polarization to learn whether polarization has been lost in acceleration (and deceleration). (If not, then one can apply the polarization to the measured asymmetry at the higher energy to obtain the analyzing power. If polarization was lost, we will need to compare asymmetry measurements before and after acceleration and finding the higher energy analyzing power will be less straight forward.)
3. The September spin commissioning used a single Snake. In this mode, the Snake must be turned on after injection, with the stable spin direction then moving from vertical at injection to the horizontal plane with the Snake on. Calculations show that acceleration to 100 GeV should work with one snake, with the orbit errors controlled to the planned level for the spin program. Radial and longitudinal orientation of the polarization at the experiments can be arranged for one snake by controlling the snake rotation axis and the beam energy.

4. For longitudinally polarized beam at the experiments (using either one snake, or two snakes with spin rotators), different collision angles at the IPs due to orbit errors can create a radial component of polarization. This effect was estimated at the meeting to be small, but should be checked.
5. The 2001 plan is to have all 4 snakes and no spin rotators. With 2 snakes the stable spin direction is vertical. It may be possible to accelerate with 2 snakes, and then to turn off one snake to obtain longitudinal polarization at the experiments. (This mode became important when we found that we apparently lose some polarization when we inject into RHIC without snakes on, which is required when using only 1 snake. For 2 snakes injection is done with the snakes on, so that polarization should not be affected by spin resonances.)
6. A spin flipper will be installed in 2001 permitting reversal of the polarization direction of each beam independently.
7. All 8 spin rotators, for STAR and PHENIX, will be installed for 2002.
8. The PHENIX spin goal for 2001 is to measure the longitudinal asymmetry A_{LL} for $\pi^{\pm,0}$ production, which is sensitive to the gluon polarization. On August 3 sensitivities were shown for 70% polarization and 32 pb^{-1}. For the expected 5 weeks $\times$ 1.5 pb^{-1} and 50% polarization, a factor $\times 5$ larger errors than those shown are expected, which still represents a significant measurement when compared with "models" of the gluon polarization. (It was pointed out on August 3 that the proposed errors were much smaller than expected systematic errors, for example from imperfect knowledge of the beam polarization.)
9. STAR views the 2001 polarized beam operation as the engineering run for the spin physics program, with goals of demonstrating acceleration and storage of well-polarized beams, reliability of beam polarization measurements, reliability of measurements of small asymmetries at the detectors, and production of first publishable results. The STAR collaboration feels these goals are most likely to be met with a concentration on vertically polarized beam and measurement with a left-right symmetric detector of transverse single spin asymmetries (A_N) for hadron production at high p_T. The advantages of such measurements are that they provide an essential test of the importance of higher-twist contributions to perturbative QCD amplitudes, which are ignored in all the calculations relevant to the extraction of Δg, while minimizing sensitivity to the experimental systematic errors that will most probably dominate polarization measurement uncertainties in year 2. These systematic errors are associated with large absolute beam polarization uncertainties, reliance on very precise understanding of RHIC energies and orbit dynamics to predict horizontal spin orientations, unknown spin-dependence of reactions to be used for luminosity monitoring, and possible small instrumental asymmetries in the detectors and polarimeters. Statistically meaningful measurements of A_N for inclusive charged and neutral pion production can be made out to p_T = 20 GeV/c with 5 pb^{-1} of integrated luminosity. In addition to vertically polarized

beam, STAR would also want some time to begin studying luminosity monitoring for collisions of longitudinally polarized beams.

10. pp2pp will have 1 Roman Pot installed in each ring for 2001 and will start measuring pp elastic scattering with the standard RHIC tune.
11. For a $\pm 25\%$ absolute uncertainty of the beam polarization in 2001 (a suggested likely error), a 2-spin asymmetry such as proposed by PHENIX would have a normalization uncertainty of $\pm$ 50%; for the 1-spin transverse asymmetry proposed by STAR, the polarization scale uncertainty would be $\pm 25\%$.
12. The ideal geometry for the A_N measurement proposed by STAR would be at larger x_F than either STAR or PHENIX can reach, and can possibly be done with reasonable sensitivity with the BRAHMS detector.
13. The need and projected accuracy for luminosity monitoring were debated. It is not essential for single-spin transverse asymmetries measured with a symmetric detector. However, for A_{LL} measurements it is essential to determine the relative normalization of the collisions with the same *vs.* opposite beam helicities to a precision better than the error goal on the measured asymmetries. For example, if one wants to measure A_{LL} to a net uncertainty of ± 0.004 with beam polarizations of 0.50, then the relative normalization has to be determined to considerably better than 0.1%. One must worry not only about reproducibility of luminosity monitor measurements at this level, but also about possible real spin-dependences (*i.e.,* $A_{LL} \neq 0$ for the monitoring reactions) that are *a priori* unknown. An alternative concept for relative normalization, that would not rely on luminosity monitoring, was suggested and discussed. In this approach, one would simply assume that over a long run fluctuations in luminosity from beam crossing to beam crossing, and hence from spin combination to spin combination, would average to zero, unless there were some unexpected *correlation* between spin orientation in the bunches and bunch intensity or emittance. Correlations of the latter type would lead with longitudinally polarized beams to sizable apparent parity-violating single-spin asymmetries, and so could presumably be monitored. Correlations of bunch properties with the *combination* of spin orientations in the two colliding bunches were considered less likely. This idea was new enough to most of the attendees that people felt the need for more time to assess it.
14. Both STAR and PHENIX will try to develop local polarimeters to measure residual transverse polarization at their IPs. These local polarimeters will be calibrated (after first determining that they, indeed, have a non-zero analyzing power) with transverse polarization in RHIC, either vertical or radial or both. This is very attractive to do--these measurements would verify whether the polarization is indeed longitudinal at the IPs (for either the one-snake scenario or later with spin rotators to obtain longitudinal polarization), and the measurements with transverse polarization in RHIC would confirm handling of the data (+ and – polarization labeled properly). A meeting was organized for December 13 to develop local polarimetry.

CONCLUSIONS from August 3:

The PHENIX and STAR spin groups are in basic agreement concerning the most important ultimate goals of the RHIC spin program. The detailed differences revealed and discussed at this meeting arise from two sources: a different degree of optimism in the two collaborations concerning the timescale for commissioning polarized beam operation and measurements in this unexplored energy regime, and different installation schedules within the two detectors for equipment important to the spin program. Despite these differences, the meeting concluded by enumerating many areas of agreement between the two groups, which should lead to a joint polarized beam use request for year 2:

- The chances of a healthy and productive RHIC spin program are greatly enhanced by cooperation among all the interested groups.
- Sufficient polarized beam operation will be needed in RHIC year 2 to permit commissioning of polarized proton collisions, systematic studies of CNI polarimeter operation and reproducibility, studies relevant to calibrating other systematic errors discussed above, and production running with both longitudinally and transversely polarized beams. It was estimated that 10 weeks of running would probably be needed to accomplish all these goals, but a detailed time request must await further work outlined below.
- The deployment of all four Siberian snakes for the year 2 run was strongly endorsed, as it provides the flexibility to meet needs of all the interested experiments.
- Some of the engineering run goals outlined by Vigdor should be accomplished during the anticipated September 2000 polarized beam commissioning study within the blue ring. Therefore, a more informed decision regarding the optimal breakdown of requested time among the goals listed above can be made after the Sept. 19 end of the current running period. The spin groups will reconvene shortly thereafter to try to converge on a beam use request.
- In the time before the next meeting, more detailed thought needs to be given to quantitative year 2 systematic error concerns and goals for both STAR and PHENIX, and to realistic measurement plans aimed at assessing whether these goals have been achieved. Progress on relevant calculations will be a prominent topic of discussion at the next meeting.
- The STAR spin group should consider in more detail the possibility of measuring transverse asymmetries with radially polarized beam. BRAHMS collaborators should be approached to gauge their interest and capabilities for transverse asymmetry measurements in inclusive hadron production at high x_F and p_T values.
- The PHENIX spin group should reassess the beam time needed for year 2 A_{LL} measurements, in light of more realistic estimates of integrated luminosity likely to be available, and in light of more realistic assessments of systematic errors. It makes no sense to push statistical

uncertainties to levels far smaller than the systematic ones.

- Installation of a full complement of spin rotators at both STAR and PHENIX at the earliest possible date is crucial to the future of the RHIC spin program. Different installation schedules for relevant equipment within the two detectors will inevitably lead to continuing differences in beam time demands for the various beam spin orientations. The rotators provide the flexibility to accommodate the needs of both collaborations. Continued cooperation will still be needed in dividing time between different beam energies.

Kyoto Summary for 2001 Spin Run

First, we learned much from the very successful September commissioning and further analysis of the AGS CNI polarimeter experiment E950 (after Kyoto):

1. The pC CNI polarimeter worked. Systematics were $\Delta P<2\%$.
2. $\Delta A_N/A_N$(CNI)=$\pm$10% $\pm$12% =$\pm$16% at RHIC injection, including energy calibration. The first error is statistical and connecting the data from the external pp elastic measurement (E925 at AGS) and the internal CNI measurement (E950 at AGS). The second error is on A_N for pp elastic scattering at $-t=0.15$, based on analyzing the world data (Hal Spinka).
3. The RHIC polarimeter commissioning took only about 12 hours! For 2001 we will have 10x the rate per crossing and a new readout (wave form digitizers) to commission. The prototype WFD worked in its September debut.
4. The polarization in RHIC was about 20%. We need commissioning time before the 2001 run to reach at least 50%.
5. We also need to inject into RHIC with the snakes on, using therefore 2 snakes in each ring. The polarization in RHIC achieved during September was tune-dependent due to injection with the snake off.
6. 1-snake running is stable.
7. There was a large bunch intensity variation (factor 2). Is it from AGS extraction jitter? Can we fix it? Do other beam characteristics vary?
8. The expected luminosity for 2001 will be 1.5 pb^{-1} per week.

We agreed to request

1. time to commission the AGS to improve the polarization. This work is parasitic to RHIC running.
2. 2 weeks to commission RHIC for pp collisions. This is independent of spin. About 1 week of the 2 week September spin commissioning was used to store and accelerate protons in the blue ring, independent of spin.
3. 1 week of spin commissioning

4. 5 weeks of pp collisions with spin, 5-6 pb^{-1}, 50% polarization.

The total time we request for pp is 8 weeks. The 5 weeks of pp collisions in the request are a reasonable match for the needs of the heavy ion program for pp comparison running, as well as the first data with a
spin collider. We noted that this plan does not fit the 25-week FY2001 run plan for RHIC, and that the plan requires an extra month to fit.

STAR and PHENIX spinners agreed to request that this plan be part of their experiment beam requests for the November PAC.

Epilogue

At the PAC, a run plan was decided upon including 2 weeks AGS spin commissioning, 3 weeks pp commissioning in RHIC including spin, and a 5-week pp spin/heavy ion comparison run.

A new Optically-Pumped Polarized H Ion Source (OPPIS) for the RHIC spin physics

A. Zelenski, J. Alessi, B. Briscoe, V. LoDestro, A. Lechrach, J. Macdisi, D. Raparia, T. Roser (BNL), Y. Mori (KEK), M. Okamura (RIKEN), V. Klenov, S. Kokhanovski, V. Zoubets,(INR Moscow), G. Dutto, P. Levy, P. Schmor and G. Wight (TRIUMF)

Abstract

In 1996 Y. Mori proposed to provide the KEK OPPIS for the RHIC polarization program. In October of 1997 the OPPIS was moved to TRIUMF for upgrade to higher intensity and longer (300 us) pulse duration. An ECR primary proton source was upgraded from 18 GHz to 29 GHz. A new sodium-jet ionizer was developed to reduce the sodium losses, increase current and polarization. The cell is floated and biased to -32 kV, which allowed to accelerate polarized beam to 35 keV for injection to RFQ. A long pulse laser based on solid-state LiSAF crystal was developed to produce up to 450 us pulse duration. A 1.6 mA H ion current of a 85% polarization was obtained at the test bench at TRIUMF. The upgrade has been completed and source was delivered to BNL in September of 1999. The OPPIS installation, laser room construction and a 35 keV LEBT construction was completed in May and first beam was accelerated to 200 MeV polarimeter in June. The polarization of a 72-74 % was measured at 200 MeV. The polarized H ion beam current of a 350 uA was obtained at 200 MeV, which corresponds to about 40% transmission from the source to the end of the linac. In July -August the beam was injected into AGS and used for depolarization studies in booster and AGS. In September 5-19 polarized run the beam was injected and stored in RHIC. The new source operation was quite reliable. The ionizer biasing worked well, a 2-3 % sparking rate can be reduced by vacuum improvement in the ionizer cell and electrode geometry optimization. The pulsed laser operation was reliable. The crystal dissolution rate is about 0.3 mm in diameter /month of operation.

The 200 MeV polarimeter has to be upgraded for the high-current operation.. The Lamb-shift polarimeter will be completed soon. It should help to investigate the possible polarization losses in the 35 keV LEBT. Apparently, a significant part of the OPPIS current has to be sacrificed to reduce the depolarization in the booster , AGS and RHIC. Therefore, the high intensity development should be continued.

A new Optically-Pumped Polarized H^- Ion Source (OPPIS) for the RHIC spin-physics

A.Zelenski, J.Alessi, B.Briscoe, V. LoDestro, A.Lechrach, J.Macdisi,
D.Raparia, T. Roser, BNL
Y Mori KEK, M.Okamura, T.Takeuchi RIKEN
V.Klenov, S.Kokhanovski, V.Zoubets, INR Moscow
G.Dutto, P.Levy, PSchmor, G. Wight TRIUMF

Kyoto RHIC-SPIN workshop
October 2000

BNL OPPIS

MILESTONES

Oct. 96 - Y. Mori proposed to use KEK OPPIS for RHIC.

Oct. 97 - KEK OPPIS arrived to TRIUMF for upgrade

Oct. 99 - OPPIS moved to BNL

Oct. 2000 - FIRST presentation of OPPIS operation for RHIC.

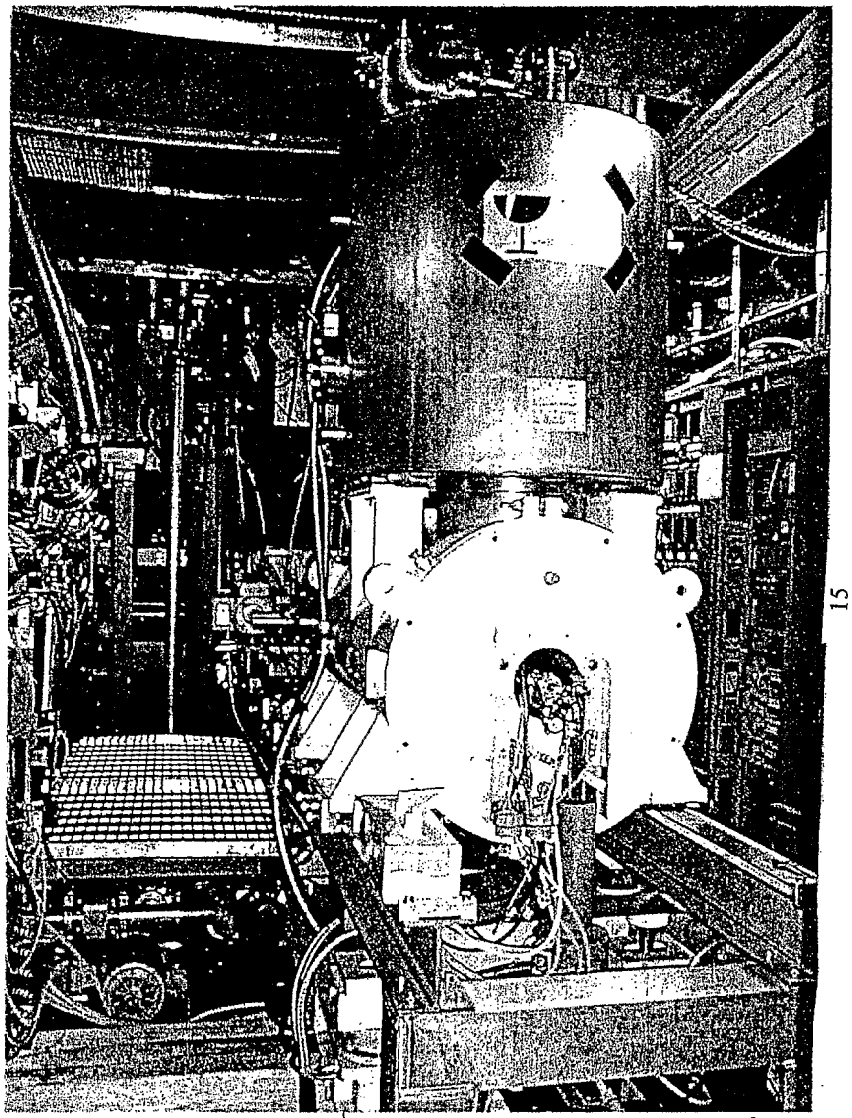

KEK OPPIS moved to TRIUMF in Oct. 97

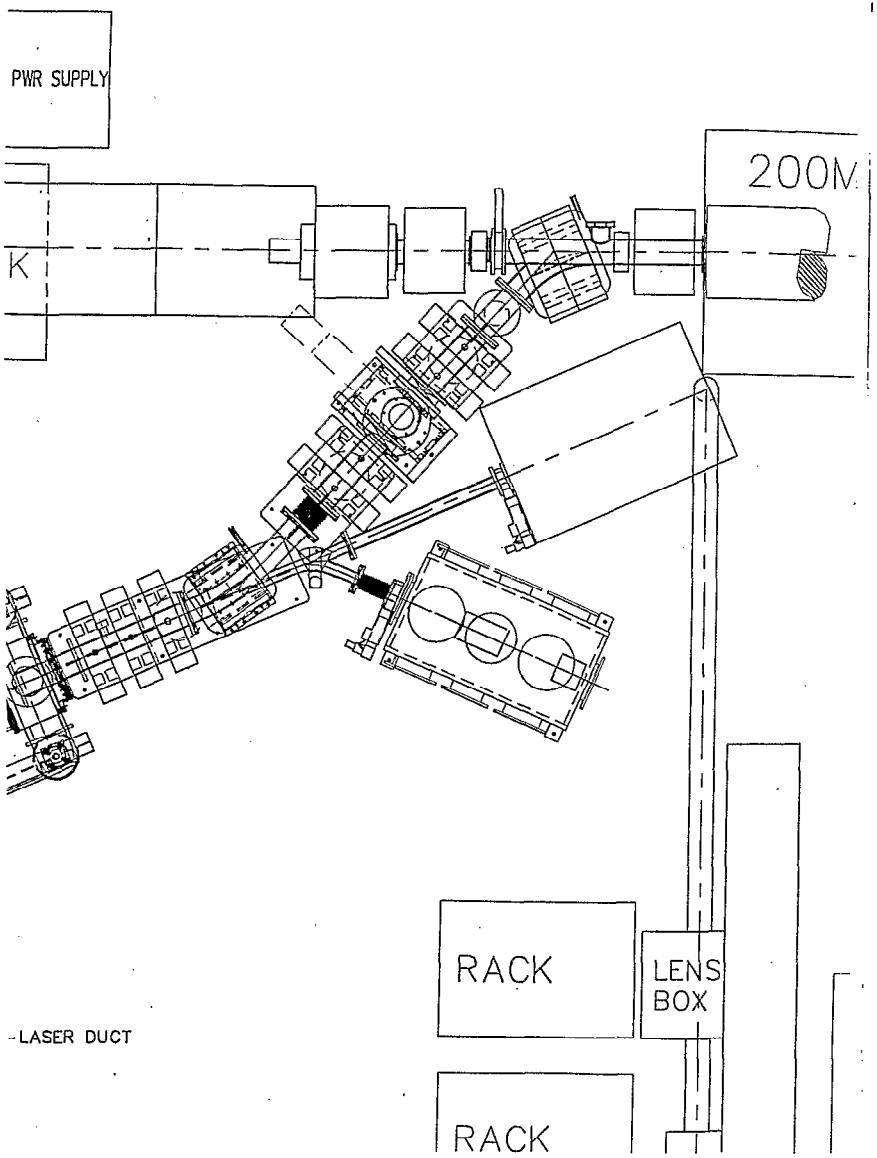

Polarized Proton Collisions at BNL

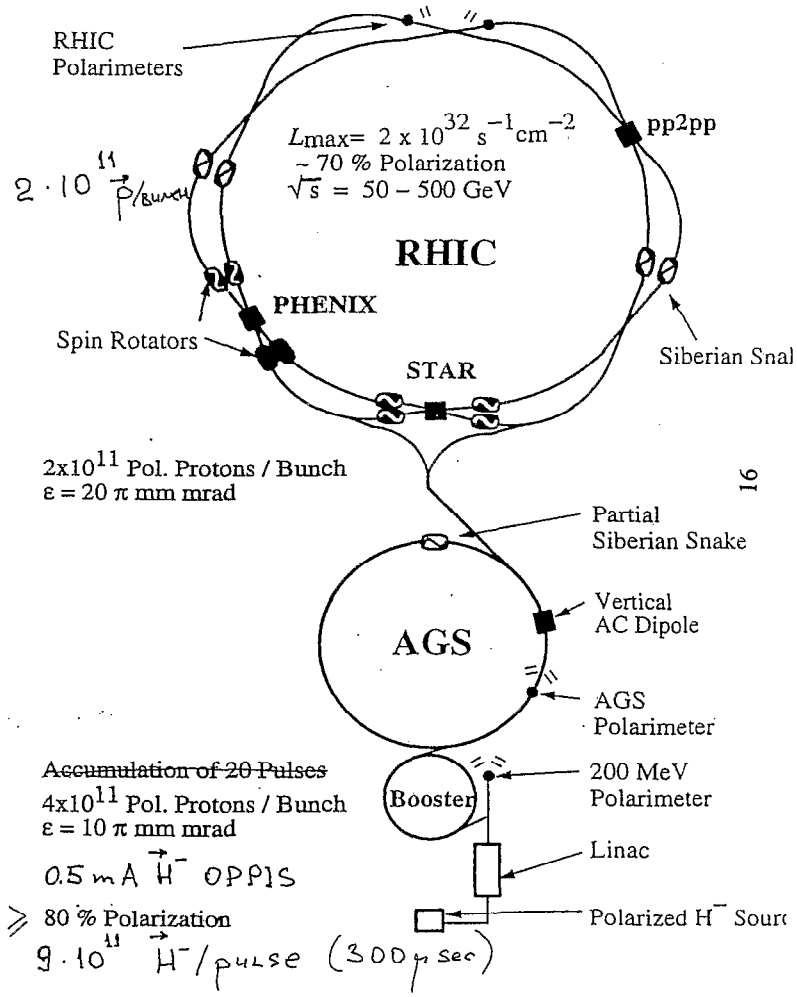

The TRIUMF Optically Pumped Polarized $\vec{H}^-$ Ion Source (OPPIS)

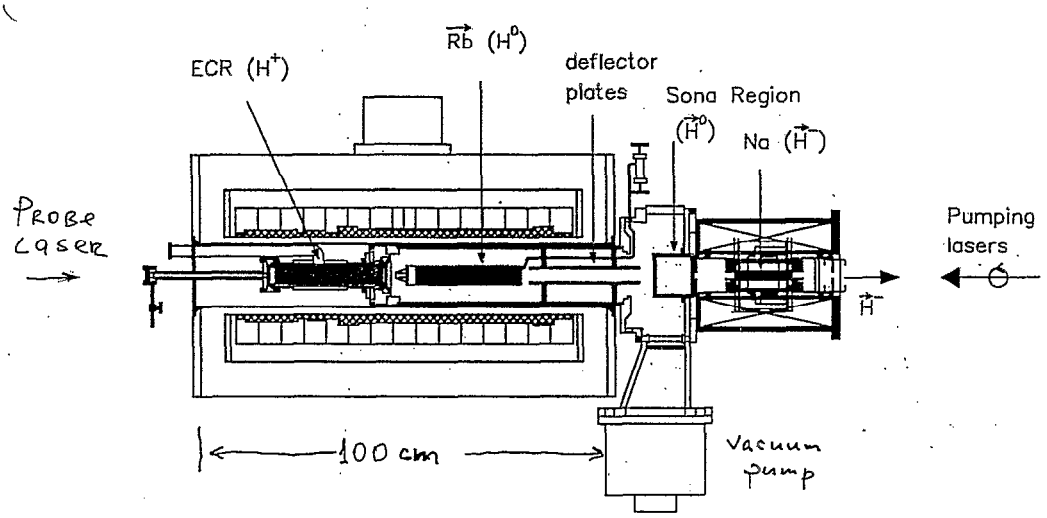

OPPIS delivers 30-40% of the beamtime for "Parity" experiment at TRIUMF.

18 GHz → 28 GHz ECR H^+ ECRFIGUR.PS .DWG .DSK

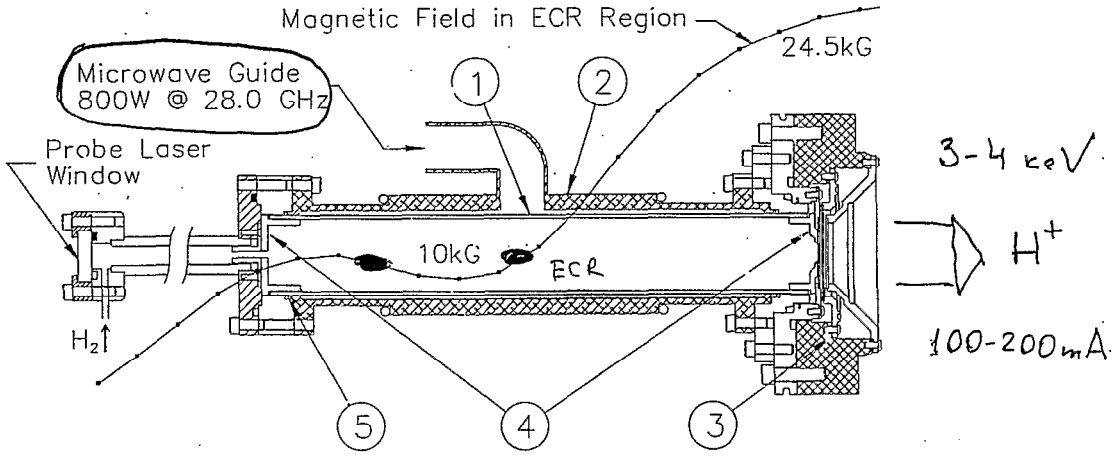

The TRIUMF OPPIS ECR primary proton source

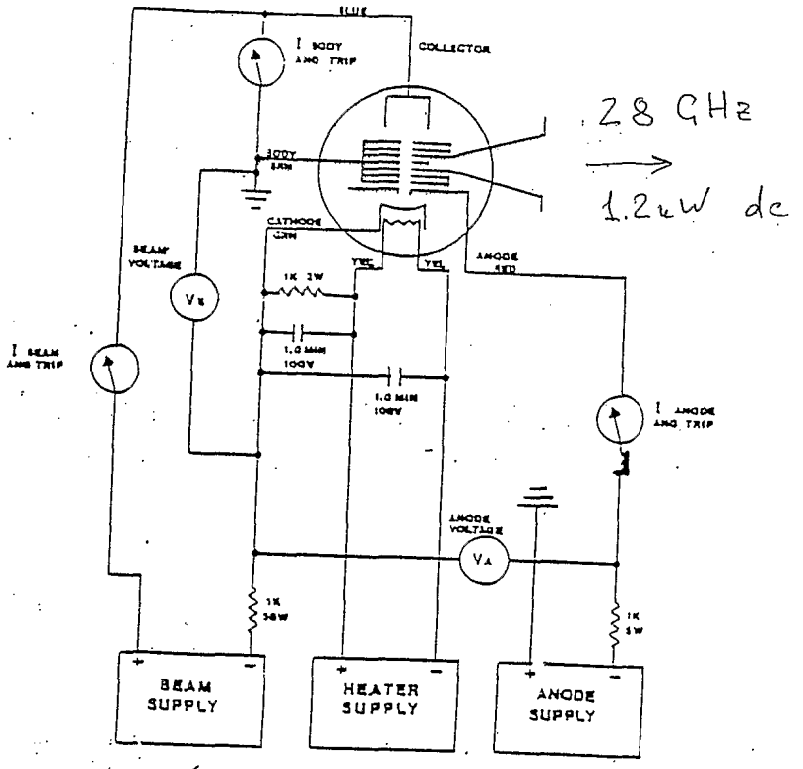

−12 kV (0.5mA) 7.0V (1.0A) 6.0kV (5mA)

NOTE

1. THIS CIRCUIT IS RECOMMENDED FOR TUBES WHICH MAY BE OPERATED WITH ANODE AT BODY POTENTIAL AND ONLY SUCH TUBES.
2. TRIPS MUST SHUT DOWN BEAM AND ANODE SUPPLY AND IN THAT SEQUENCE.
3. NORMAL ANODE CURRENT WILL FLOW IN REVERSE DIRECTION THROUGH THE ANODE SUPPLY.
4. RESISTANCE IN OHMS. CAPACITY IN MICROFARADS.

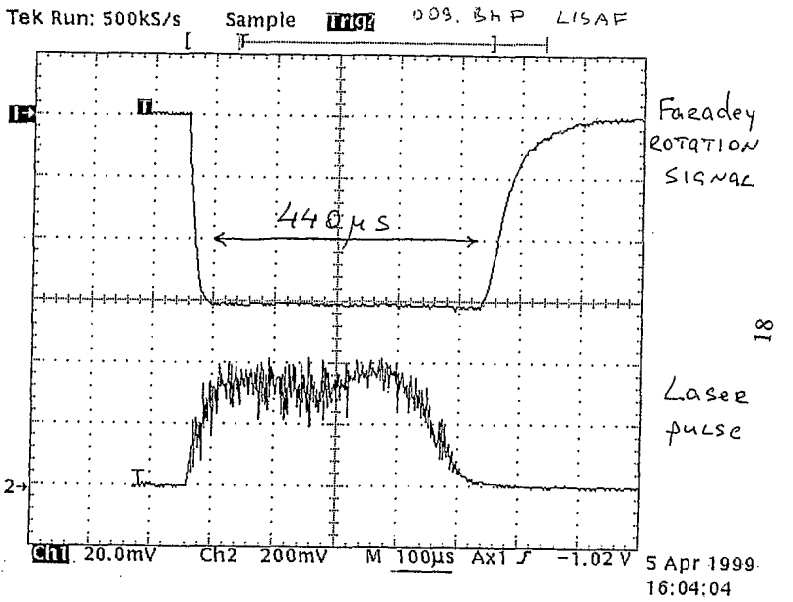

Optical pumping by LiSAF laser.

$LiSAF \longleftrightarrow LiSrAlF_6 : Cr^{3+}$

Laser power : $P_{laser} \sim 1.0\,kW$

Linewidth : $\sim 10\,GHz$

Sodium-jet IONIZER CELL.

NOZZLE - COLLECTOR ASSEMBLY.

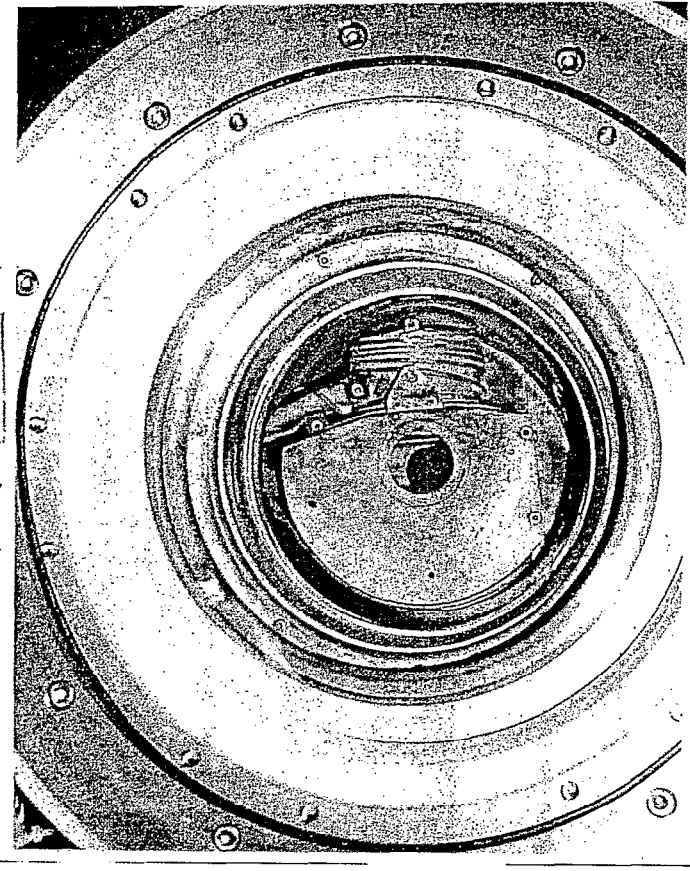

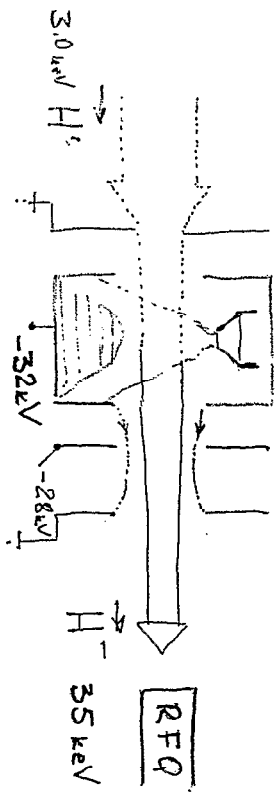

$\vec{H}^-$ beam acceleration after the Na-Jet IONIZER

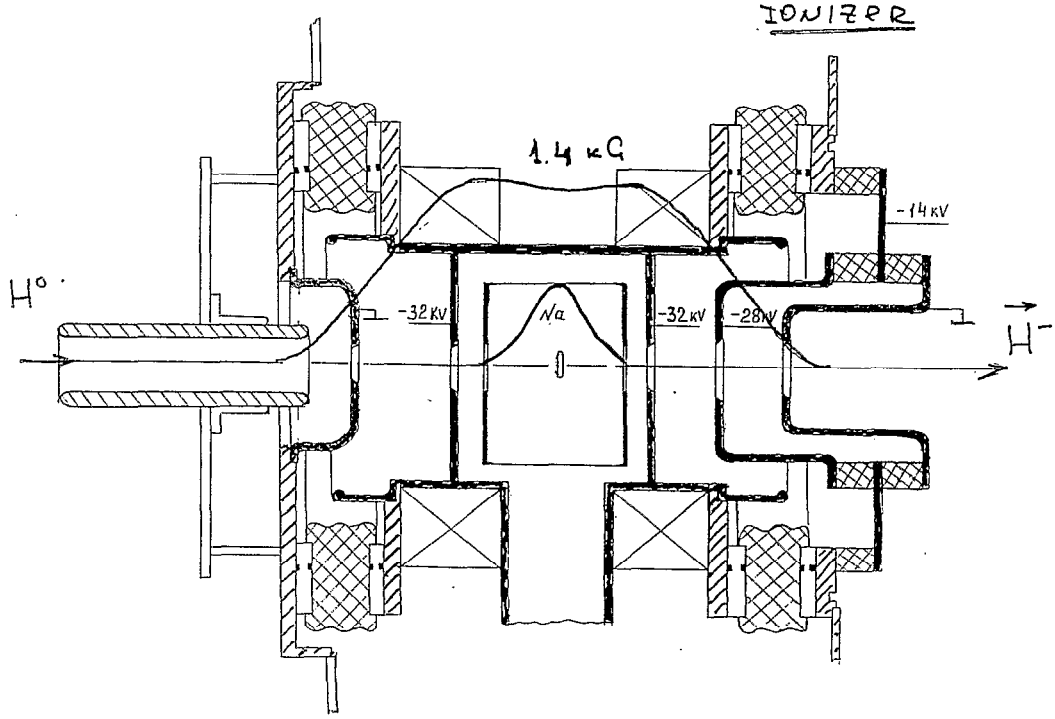

SODIUM JET IONIZER CELL

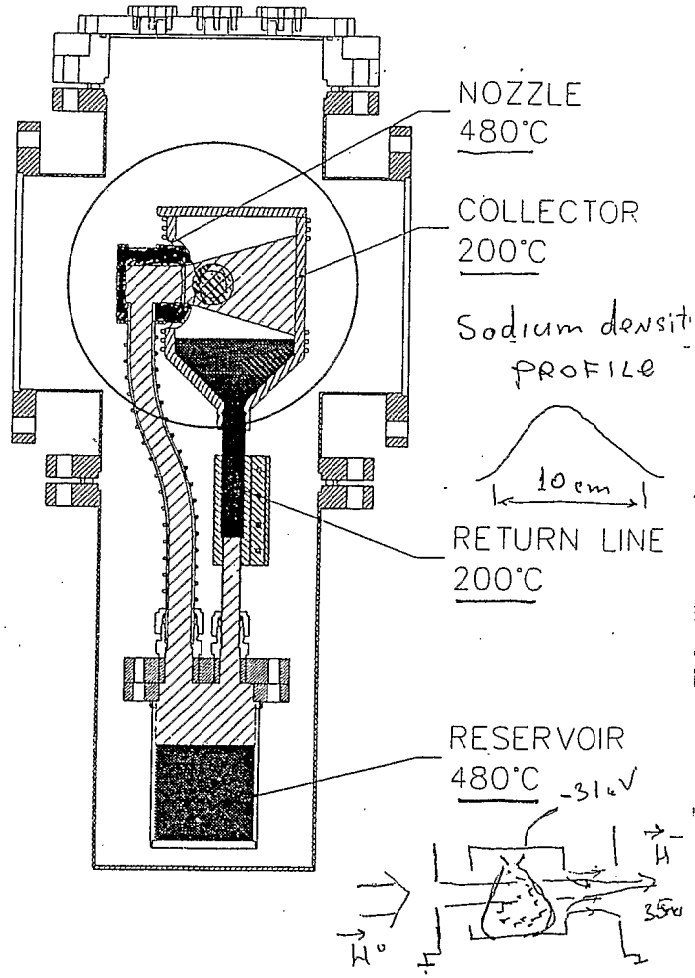

The OPPIS Laser System

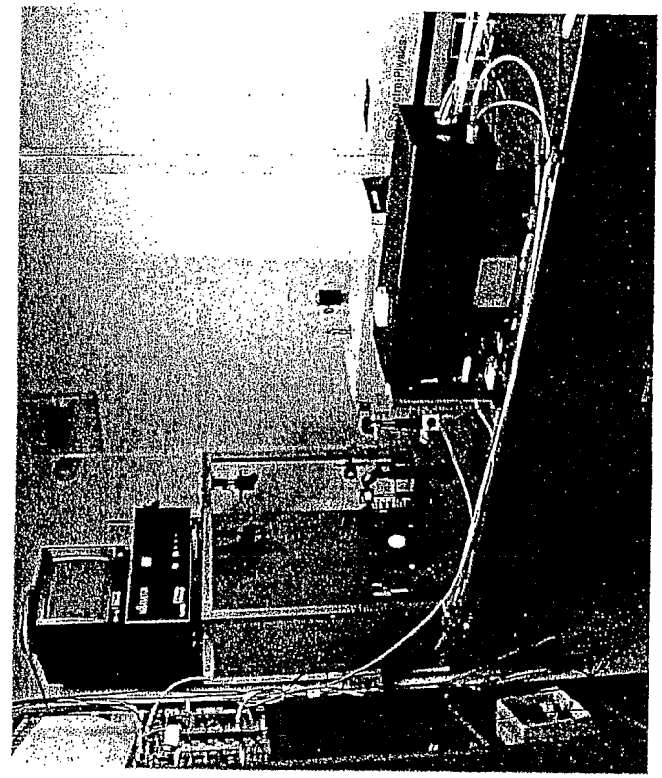

Pulsed LiSAF laser is used for optical pumping. Pulse duration ~400 μs, P ≈ 1.0 kW

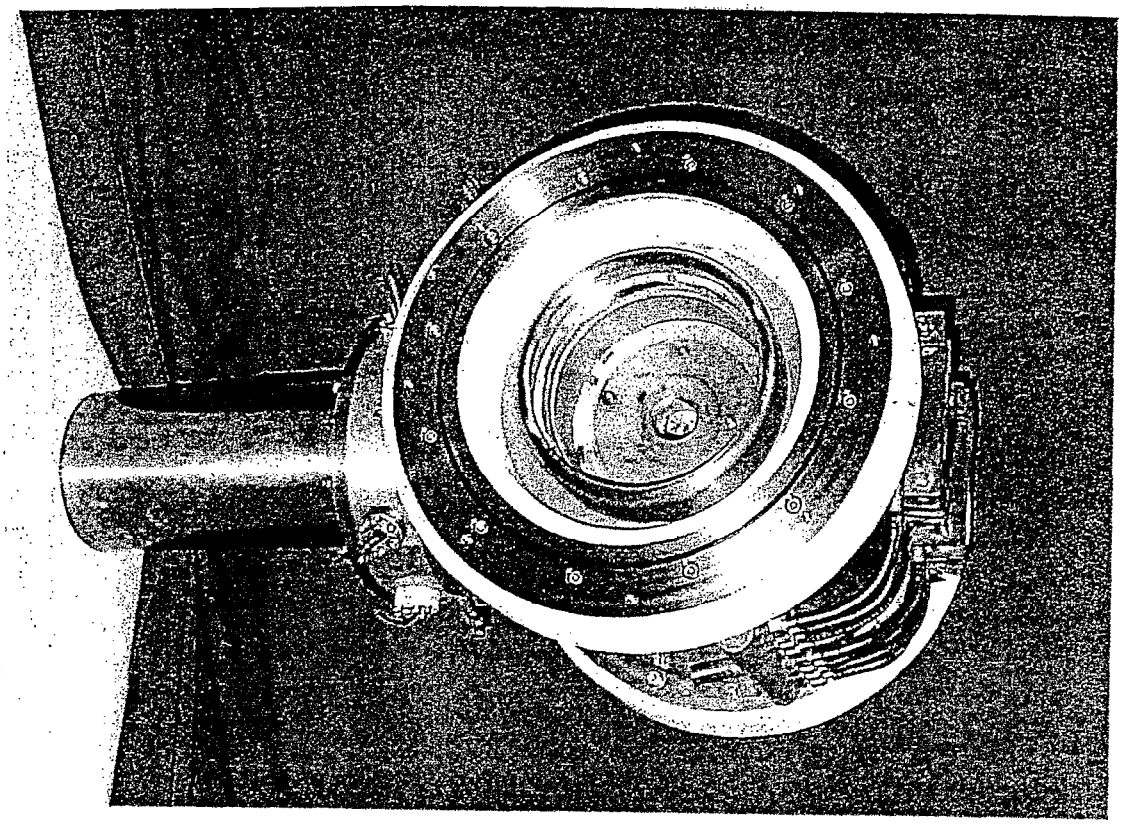

UPPIS FOR RHIC

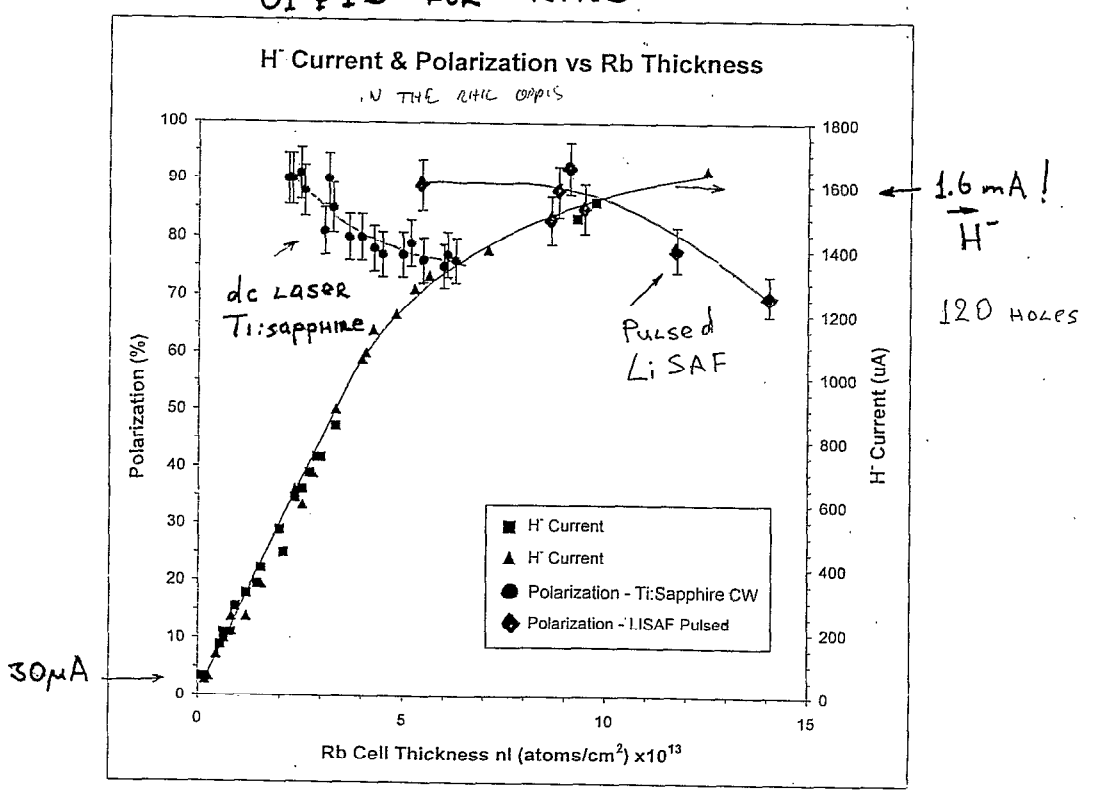

Polarized H^- ion current produced in the dc TRIUMF OPPIS

PAC 95.

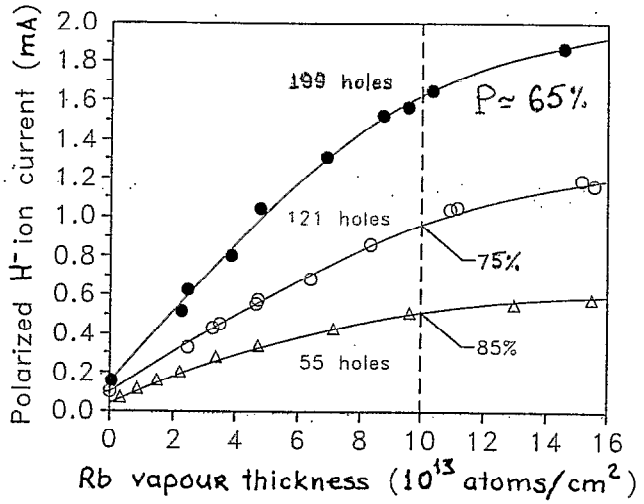

H^- ion polarized current dependence on Rb cell thickness. Na ionizer diameter – 20mm. Diameter of 199 hole pattern is 17.5mm, 121 holes – 14.5mm and 55 holes – 9mm.

Zelensky

OPPIS FOR RHIC Sept. 1999

		KEK	RHIC specified	RHIC achieved
H ion current	(mA)	0.1	0.5	1.6 mA !
Polarization	(%)	75	80	85-90 % !
Emittance	(pi mm mrad)	2.0	2.0	1.8
Pulse duration	(us)	100	300	400
Current * duration	(mA*us)	10	150	700
Repetition rate	(Hz)	25	7.5	7.5
Beam energy	(keV)		35	35

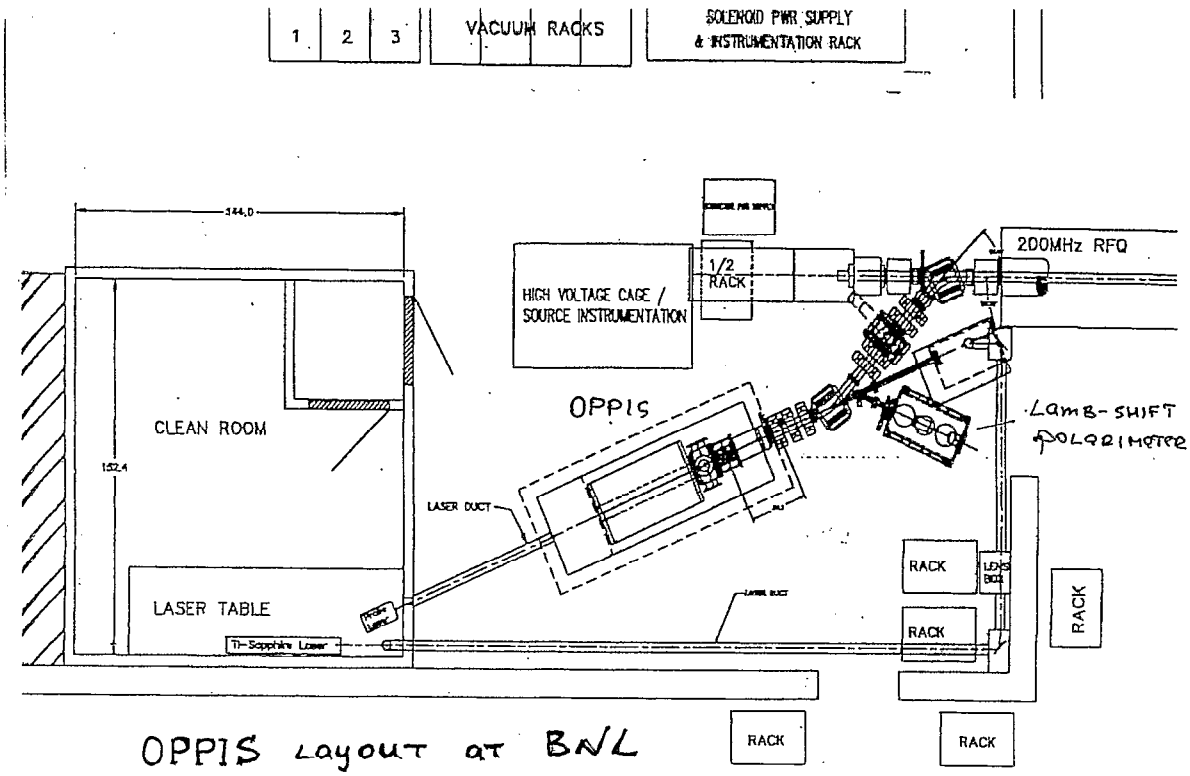

OPPIS Layout at BNL

BNL OPPIS Sept. 2000

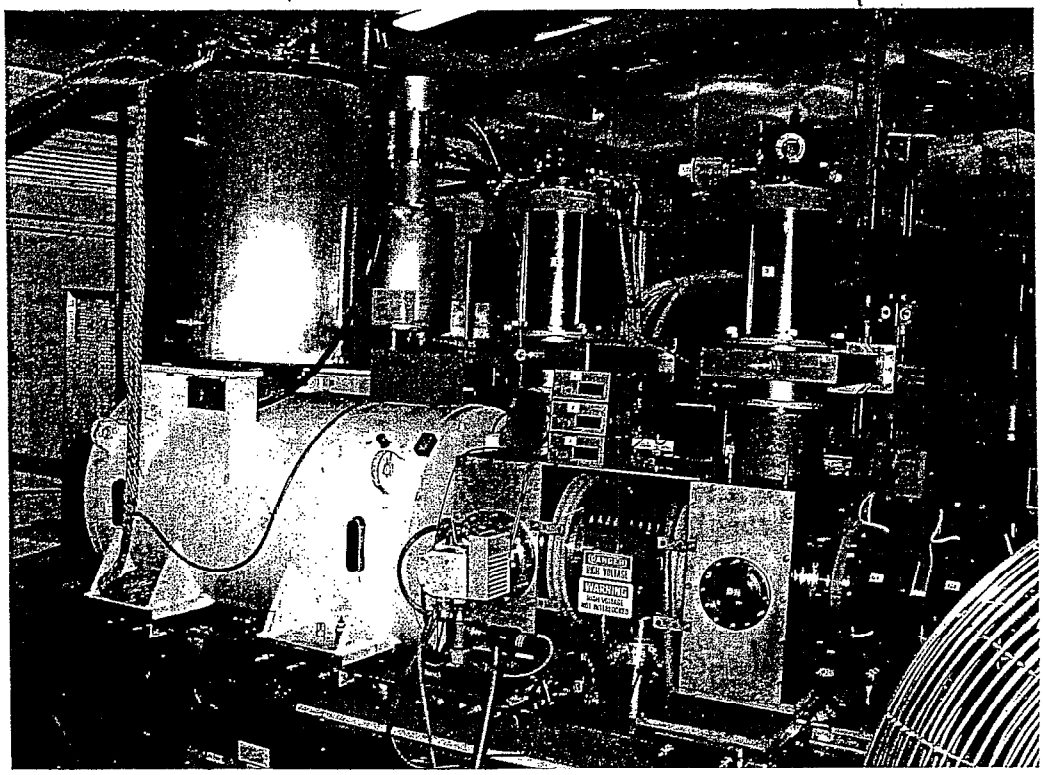

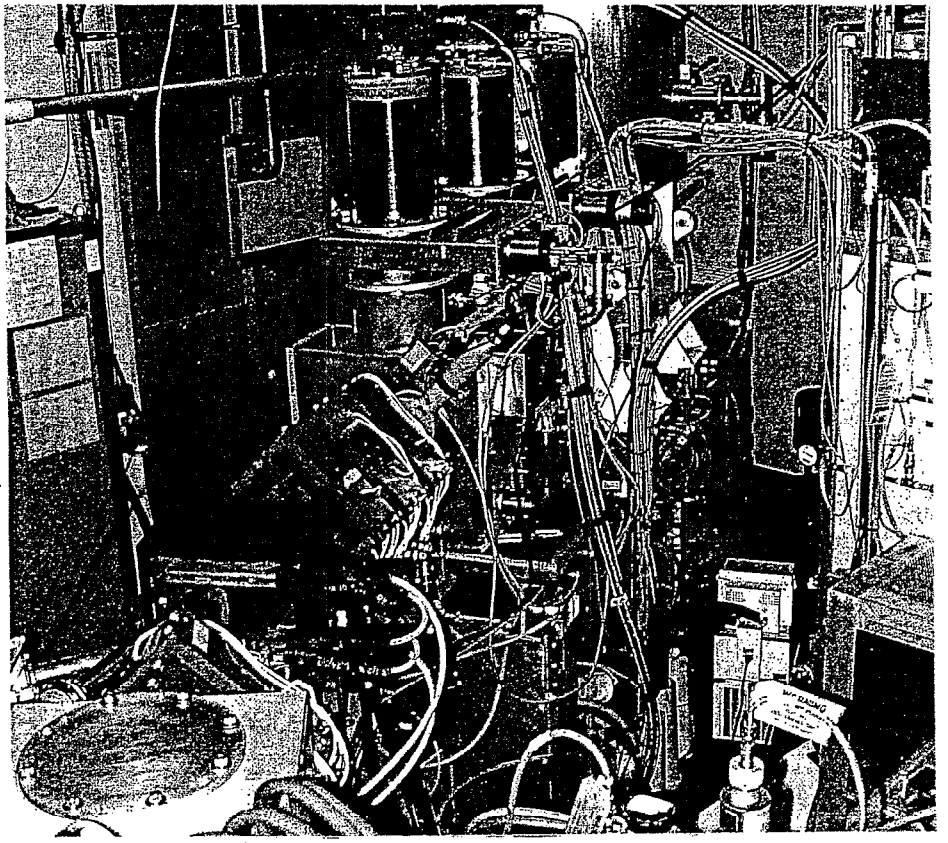

35 keV LEBT Sept. 2000

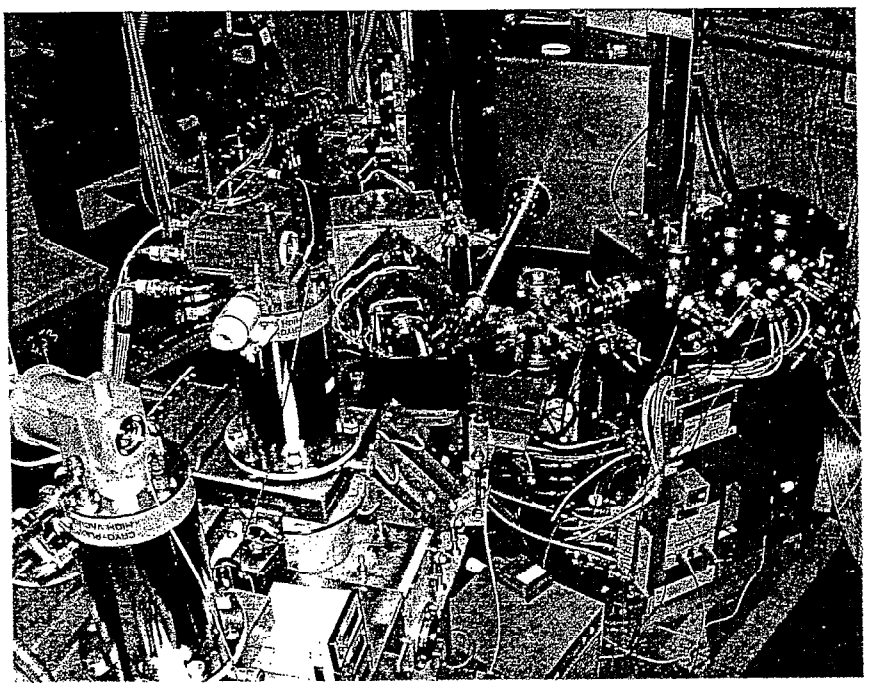

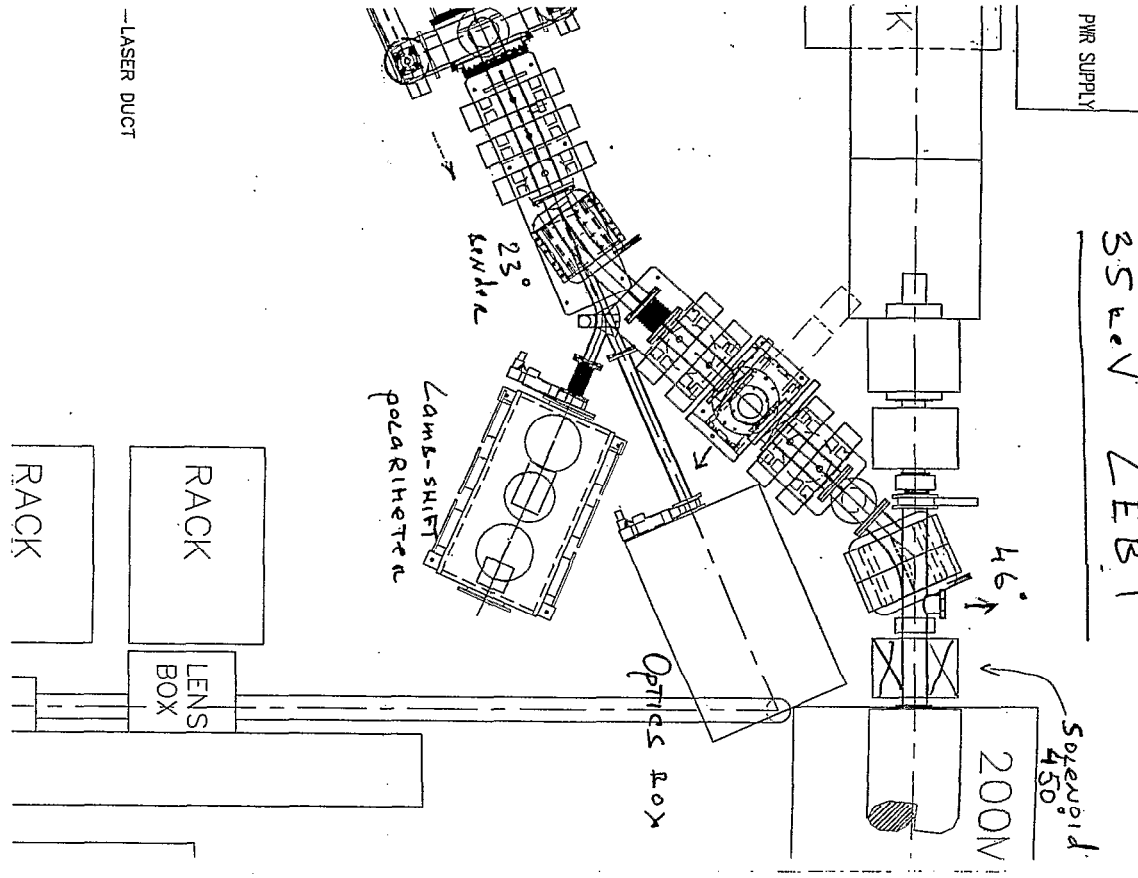
LASER DUCT
RACK
RACK
LENS BOX
LAMB-SHIFT POLARIMETER
23° BENDER
OPTICS BOX
46°
SOLENOID 450°
200N
35 keV LEBT
PWR SUPPLY

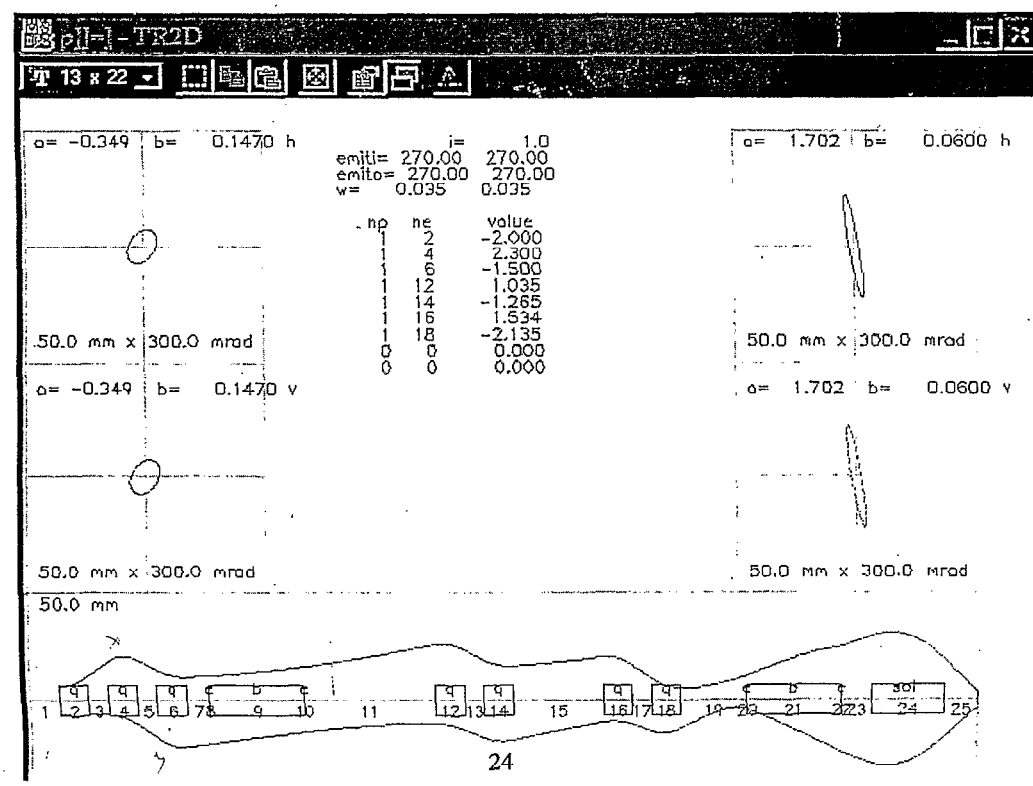
pII-1-TR2D
13 x 22
a= -0.349 b= 0.1470 h
50.0 mm x 300.0 mrad
a= -0.349 b= 0.1470 v
50.0 mm x 300.0 mrad
i= 1.0
emiti= 270.00 270.00
emito= 270.00 270.00
w= 0.035 0.035
np ne value
1 2 -2.000
1 4 2.300
1 6 -1.500
1 12 1.035
1 14 -1.265
1 16 1.534
1 18 -2.135
0 0 0.000
0 0 0.000
a= 1.702 b= 0.0600 h
50.0 mm x 300.0 mrad
a= 1.702 b= 0.0600 v
50.0 mm x 300.0 mrad
50.0 mm

Y 2000 polarized beam run

June – First acceration in RFQ and LINAC to 200 MeV

July – First polarization measure.
August at 200 MeV, Beam injected to AGS

Sept. – polarized beam injected to RHIC.
3 weeks continues OPPIS operation

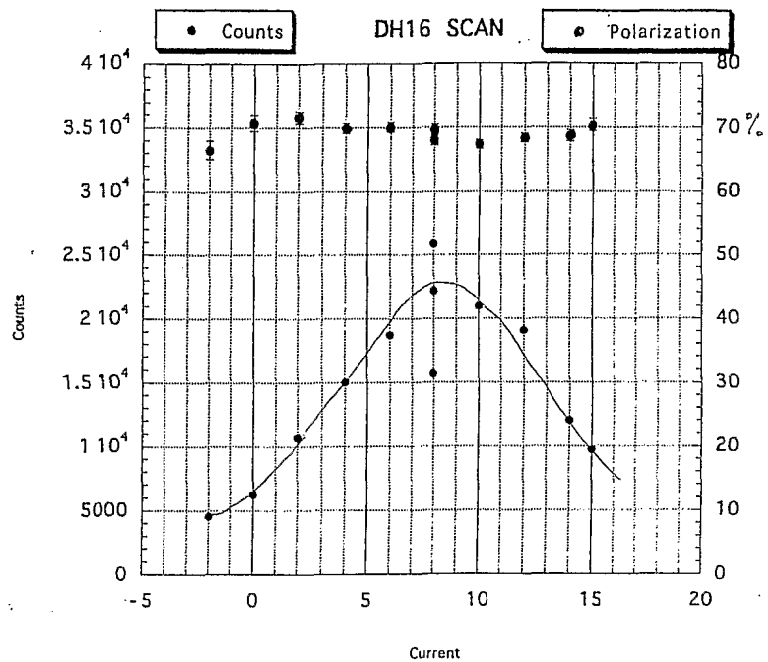

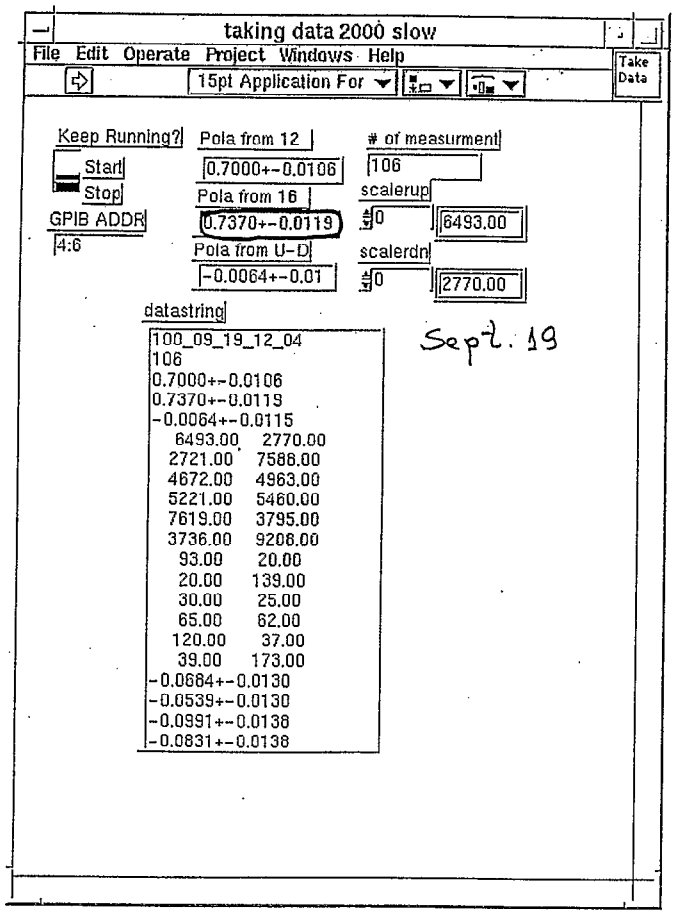
taking data 2000 slow
File Edit Operate Project Windows Help
15pt Application For
Take Data
Keep Running?
Start
Stop
GPIB ADDR
4:6
Pola from 12
0.7000+-0.0106
Pola from 16
0.7370+-0.0119
Pola from U-D
-0.0064+-0.01
# of measurment
106
scalerup
0
6493.00
scalerdn
0
2770.00
datastring
100_09_19_12_04
106
0.7000+-0.0106
0.7370+-0.0119
-0.0064+-0.0115
6493.00 2770.00
2721.00 7586.00
4672.00 4963.00
5221.00 5460.00
7619.00 3795.00
3736.00 9208.00
93.00 20.00
20.00 139.00
30.00 25.00
65.00 62.00
120.00 37.00
39.00 173.00
-0.0684+-0.0130
-0.0539+-0.0130
-0.0991+-0.0138
-0.0831+-0.0138
Sept. 19

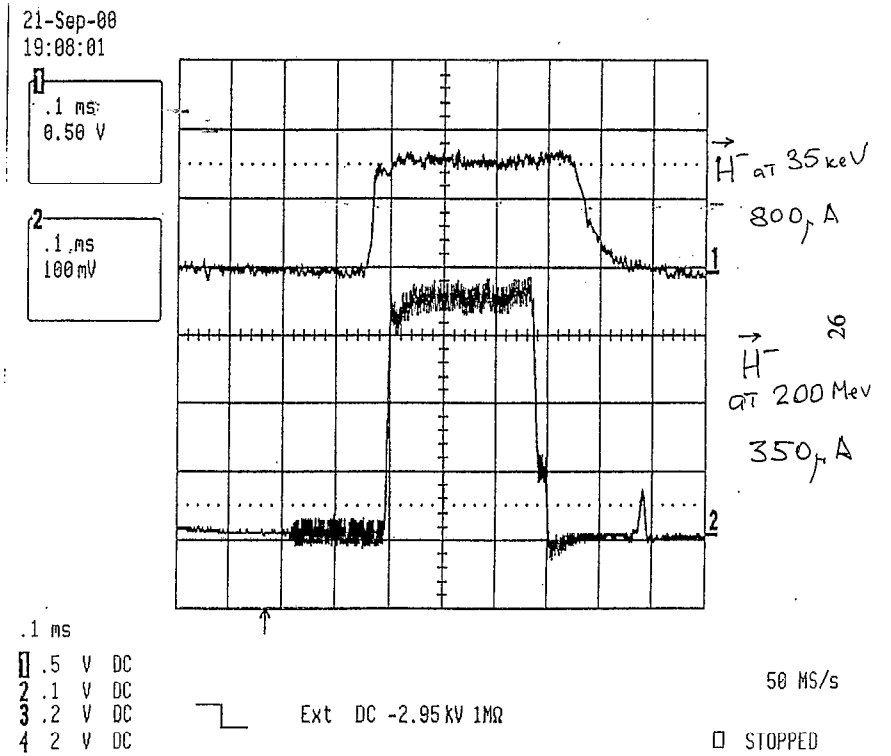
21-Sep-00
19:08:01
.1 ms
0.50 V
.1 ms
100 mV
H⁻ at 35 keV
800 μA
H⁻
at 200 MeV
350 μA
26
.1 ms
1 .5 V DC
2 .1 V DC
3 .2 V DC
4 2 V DC
Ext DC -2.95 kV 1MΩ
50 MS/s
STOPPED

CONCLUSIONS

- The new polarized source operation is quite reliable . The whole source biacing is not nessesary.
- The pulsed LiSAF laser works reliably. The crystal dissolution rate is about 0.3 mm in diameter/month of operation.
- About 40% of the source beam was accelerated to 200 MeV. A 350 uA was obtained at 200 MeV, which corresponds to 6 10^{11} H /pulse. However, the beam optics in LEBT is not well understood, better diagnostcs and more studies are nessesary.
- A 72+/-1 % polarization was measured in 200 MeV polarimeter. There are some indications of about 10% polarization losses in the 35 keV LEBT.
- The Lamb-shift polarimeter is near completion and will be used for the 3-4 keV beam polarization measurements and optimization.
- The beam diagnostics has to be upgraded for the beamlines and linac fine tuning and beam current monitoring.
- The 200 MeV polarimeter has to be upgraded to handle high intensity polarized beam.
- Apparently, a significant part of the source polarized current will be nessesary to sacrifice to reduce the depolarization in the booster, AGS and RHIC. Therefore, the high intensity development should be continued.

Zelensky

Polarized D^- source:

OPPIS with dual optical pumping.

Current: ~ 0.5 mA dc
~ 5-10 mA pulsed

Polarization: P_z ~ 80%

Polarized $^3He^{++}$ source:

Optically pumped ^3He gas + IBIS type ionizer.

Current: ~ 10^{10}–10^{11} $^3He^{++}$/pulse

Polarization: 70 – 80 %

Polarized Proton Commissioning Run 2000

Haixin Huang (Brookhaven National Laboratry)

Abstract

The recent year-2000 polarized proton commissioning run is summarized in this presentation. The AGS vertical RF dipole performed well in overcoming the intrinsic resonances. The ratio of final polarization vs the input polarization is estimated as 70%, improved from 55% years ago. The horizontal RF dipole was tried the first time to overcome both intrinsic and coupling resonance at 36+nu. It is demonstrated that in a full-coupled machine, the vertical coherence can be excited by using a horizontal RF dipole. No obvious improvement of beam polarization by using the horizontal RF dipole vs. vertical RF dipole is observed. But it looks promising and we plan to test it again in the future. RHIC p-Carbon CNI polarimeter worked beautifully. The RHIC snake magnets rotate spin to the expected direction as demonstrated by the polarimeter. The polarized proton beam has been accelerated in RHIC and the polarization is maintained up to 31 GeV.

Polarized Proton Commissioning Run 2000

1. AGS spin commissioning
   - Vertical RF dipole
   - Horizontal RF dipole
2. RHIC spin commissioning
3. Summary

Haixin Huang
RSC Meeting
Oct. 13-14, 2000

BROOKHAVEN
NATIONAL LABORATORY

Polarized proton collisions in RHIC

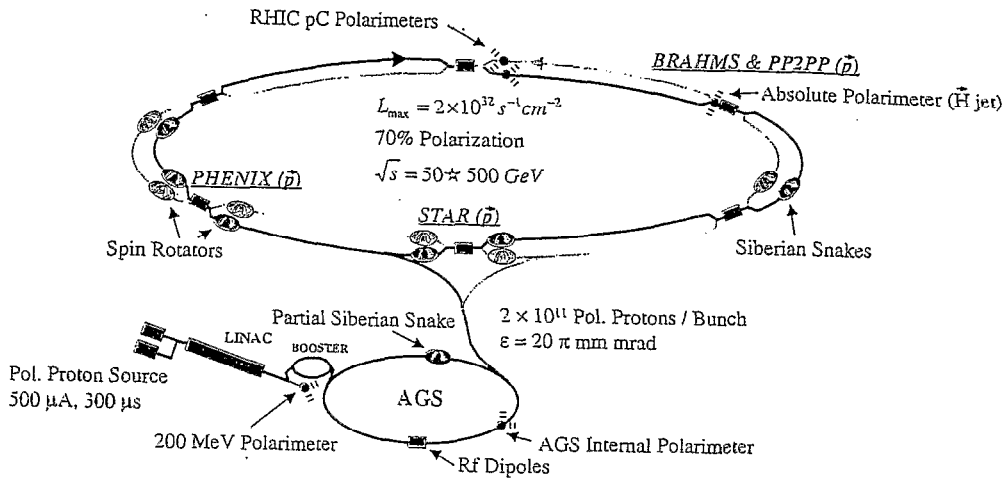

BROOKHAVEN NATIONAL LABORATORY

Depolarizing Resonances in the AGS

Imperfection Resonances	arising from vertical closed orbit distortion
$G\gamma=5,6,\ldots 47$	$G\gamma=n$ (integer)
Intrinsic Resonances strong ones	caused by vertical betatron motion
$G\gamma=0+\nu_y, 12+\nu_y, 36\pm\nu_y$ weak ones	$G\gamma=kP\pm\nu_y$
$G\gamma=24\pm\nu_y, 48-\nu_y$	
Coupling Resonances	horizontal betatron motion coupled to the vertical betatron motion by some coupling elements: solenoid
$G\gamma=0+\nu_x, 12+\nu_x, 36\pm\nu_x$	$G\gamma=kP\pm\nu_x$
Semi-intrinsic Resonance	caused by strong 1st order intrinsic resonance combined with large horizontal closed orbit distortion
$G\gamma=60-\nu_y-9$	$G\gamma=kP\pm\nu_y\pm[\nu_p]$

Crossing intrinsic resonance using RF dipole magnet...

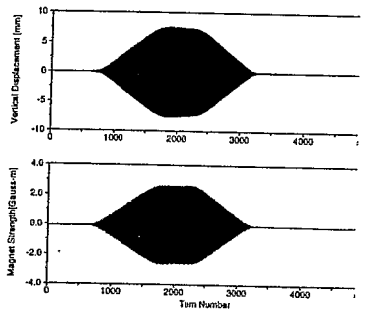

Vertical Displacement

RF Field Strength

Total Spin Flip is generated...

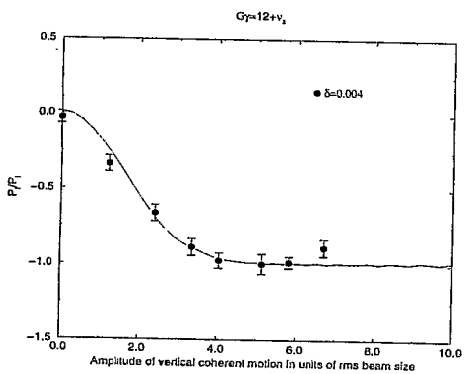

The RF dipole modulation tune was separated from the betatron tune by 0.004

Exciting coherent betatron oscillation when crossing the intrinsic spin resonance

The idea of exciting a vertical coherent betatron oscillation is to let all the particles have strong resonance strength so that a full spin can be obtained under the nominal acceleration rate

Intrinsic Resonance Crossing

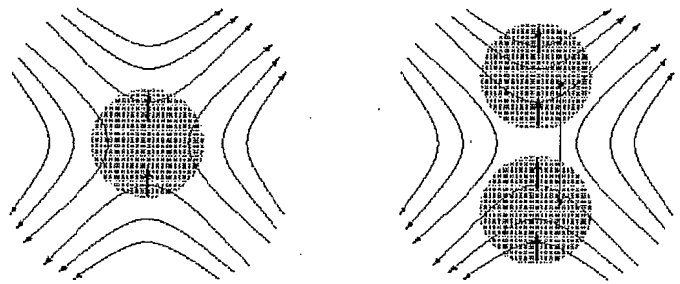

Vertical focusing fields cause depolarization

Driven beam oscillation
- whole beam sees the the same field
- spin flip

Key parameters to maintain beam polarization

- Both vertical and horizontal emittance should be small.
- Vertical betatron tune and modulation tune separation well controlled.
- Chromaticity small to get good coherence.
- Timing of firing RF dipoles.

BROOKHAVEN NATIONAL LABORATORY

Running Condition (1)

Resonance	Tune separation(FY 97)	Tune Separation(FY00)
$0+\nu$	0.009	0.009
$12+\nu$	0.0055	0.005
$36-\nu$	0.006	0.005
$36+\nu$	0.0065	0.0045

BROOKHAVEN NATIONAL LABORATORY

Running Condition (2)

- Horizontal emittance improved from 40π to $<20\pi$.
- Partial Snake is slightly weaker at top energy, ~3.5% instead of 5%.

BROOKHAVEN NATIONAL LABORATORY

Performance of AGS

- Polarization preservation efficiency improved in AGS(especially at 36+ν): from 55% up to 70%.
- Scale the polarization measured at $G\gamma=46.5$ back to injection, the estimated input polarization is (preliminary!)

  (55+- 9.8)%

BROOKHAVEN NATIONAL LABORATORY

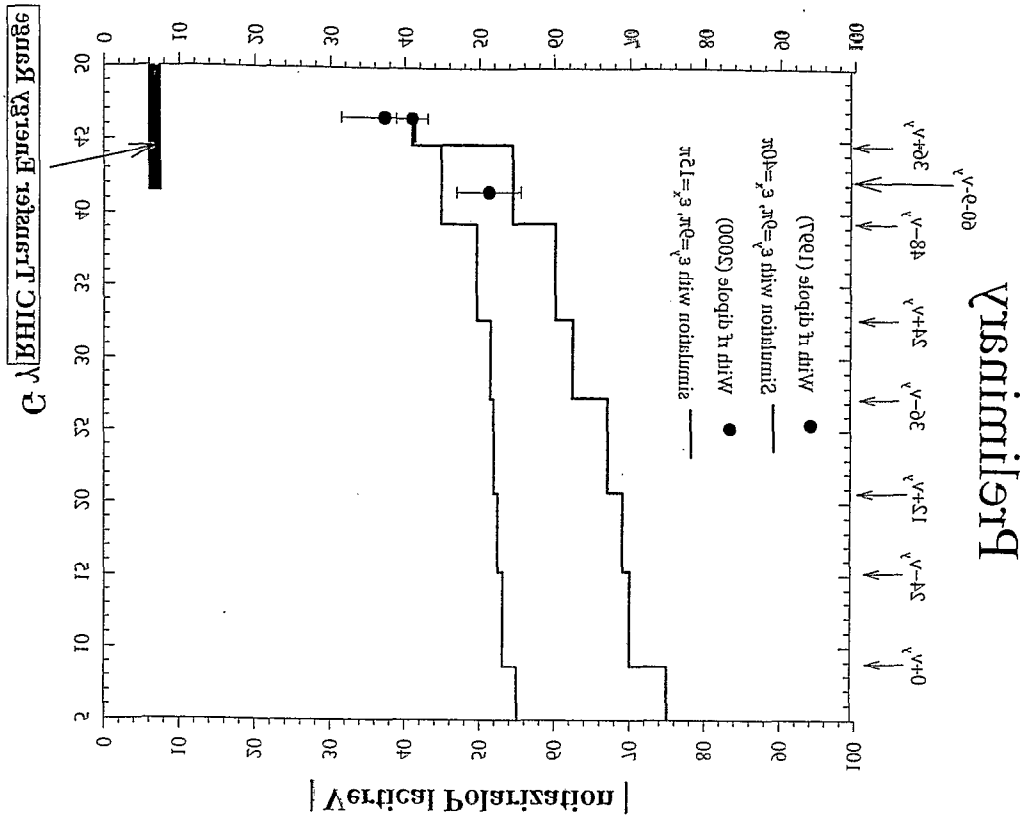

- Obtain a vertical coherence in a fully coupled machine

$$x'' + \omega^2 x - q^2 z = k \cos \omega_m \theta$$
$$z'' + \omega^2 z - q^2 x = 0$$

when the driving frequency = unperturbed betatron frequency, the driving force in the horizontal plane then results a coherence in the vertical plane.

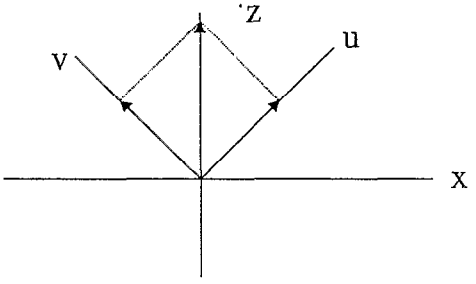

BROOKHAVEN NATIONAL LABORATORY

- beam turn by turn data in the AGS pp2000 run.

$\nu_m = 0.288$, $\nu_1 = 0.286$, $\nu_2 = 0.2932$

horizontal coherence sta
to show up as soon as th
driving frequency is awa
from the mid of the two
eigen betatron frequencie

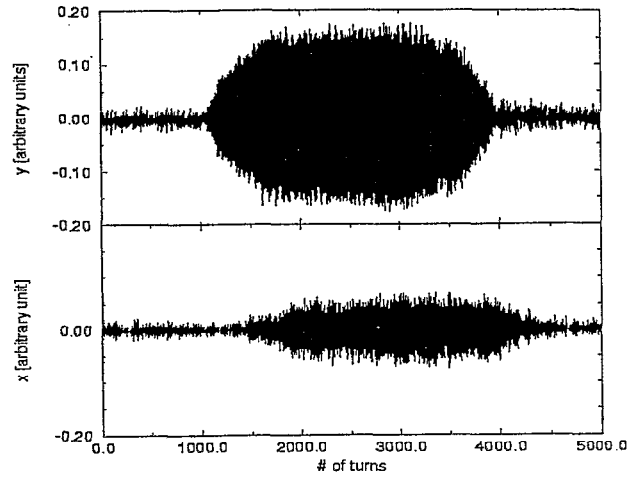

BROOKHAVEN NATIONAL LABORATORY

– comparison of the measured asymmetries with horizontal Rf dipole and vertical Rf dipole

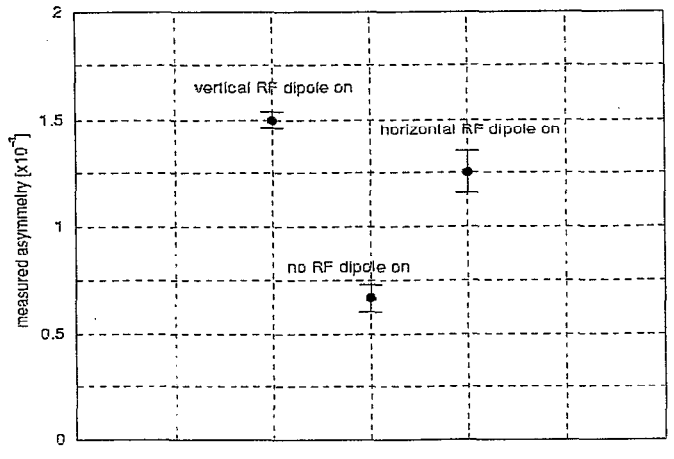

BROOKHAVEN NATIONAL LABORATORY

– Conclusion

- we demonstrated that in a full coupled machine, one can excite a vertical coherence using an horizontal RF dipole

- no obvious improvement of the beam polarization by using the horizontal RF dipole. We think this is because the vertical coherence excited by the horizontal dipole is not optimized and emittance growth was observed.

BROOKHAVEN NATIONAL LABORATORY

FY2000 commissioning plan

- June-July 2000: (independent of RHIC operation)
  - New pol. source (OPPIS) commissioned and beam transp. through linac: 65% polarization measured at 200 MeV polarimeter, 200 mA and 300 ms beam pulse (4×10^{11} polarized protons)
- August 2000: (during RHIC Au stores)
  - Accelerate single bunch (10^{11} pol. pr. / bunch) in Booster and AGS to $Gg = 46.5$ ($g = 25.94$) ✓
  - Commission coupled spin resonance crossing using horizontal rf dipole ✓
- September 2000: (dedicated RHIC operation)
  - Inject 6 bunches (+ – + – + –) into RHIC blue ring with snake off. ✓
  - Commission pC polarimeter and measure vertical polarization ✓
  - Turn on snake and measure radial polarization ✓
  - Accelerate and measure polarization ✓

BROOKHAVEN NATIONAL LABORATORY

Year-ONE polarimeter

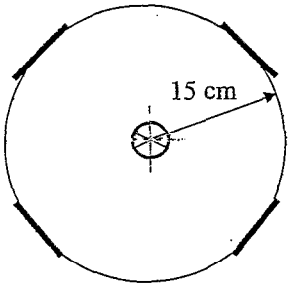

- Thin carbon target ~ 5 μg/cm^2 × 10μm;
- Horizontal and vertical targets;
- 4 Detectors 12strips × 2 mm;
- Strips in vertical direction;
- Trigger as 'or' of all strips;
- DAQ with LeCroy FERA 4300 ADC/TDC;
- 6-bunch mode;
- Up to $3 \cdot 10^{10}$ p/bunch

Carbon identification by time of flight/energy dependence:

E, keV	T, ns
100	118
200	84
500	53
1000	37

Polarized proton injection into RHIC

Injection at $G\gamma = 46.5$ without snake: vertical polarization!

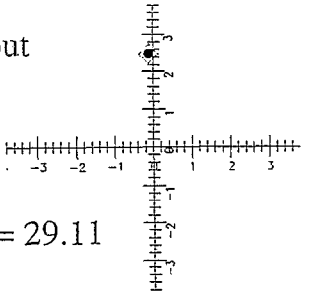

$\nu_y = 29.11$

Sensitive to betatron tune setting

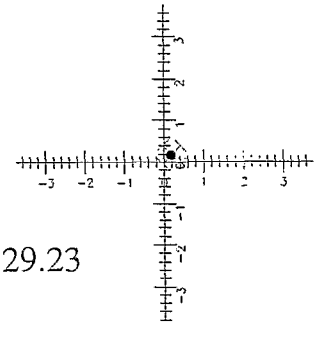

$\nu_y = 29.23$

BROOKHAVEN NATIONAL LABORATORY

Snake operating points

- Single snake RUN2000
  B1 = B2
- Two snakes for RUN2001

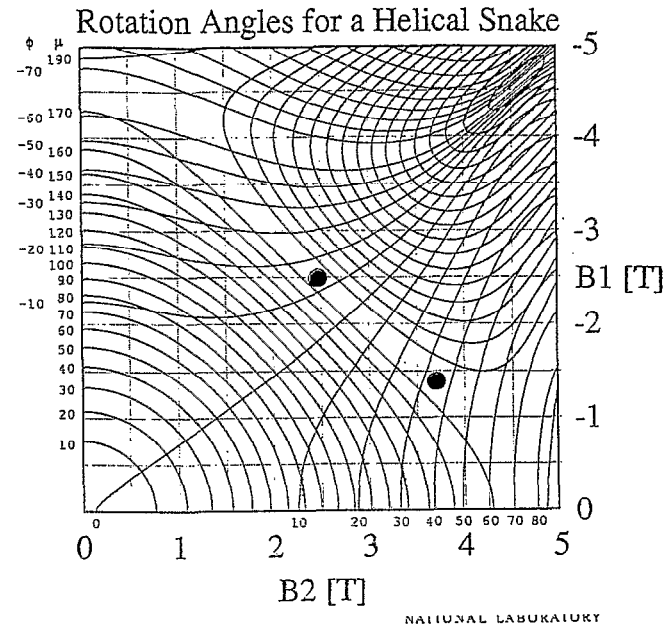

NATIONAL LABORATORY

Spin commissioning with a single Snake

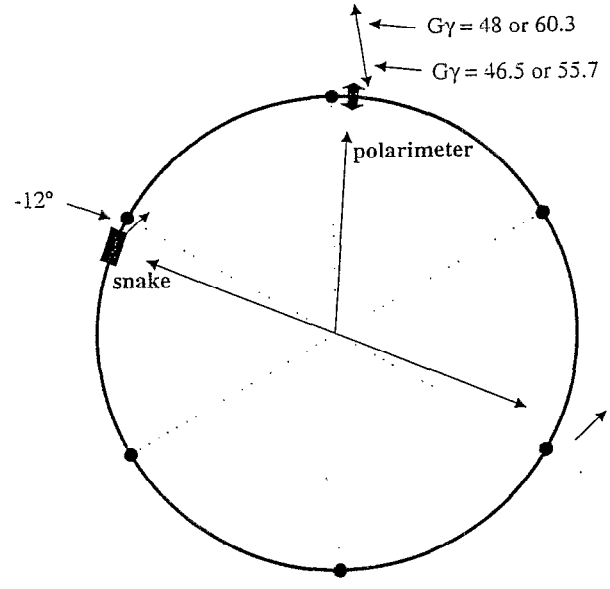

BROOKHAVEN
NATIONAL LABORATORY

Acceleration with single snake

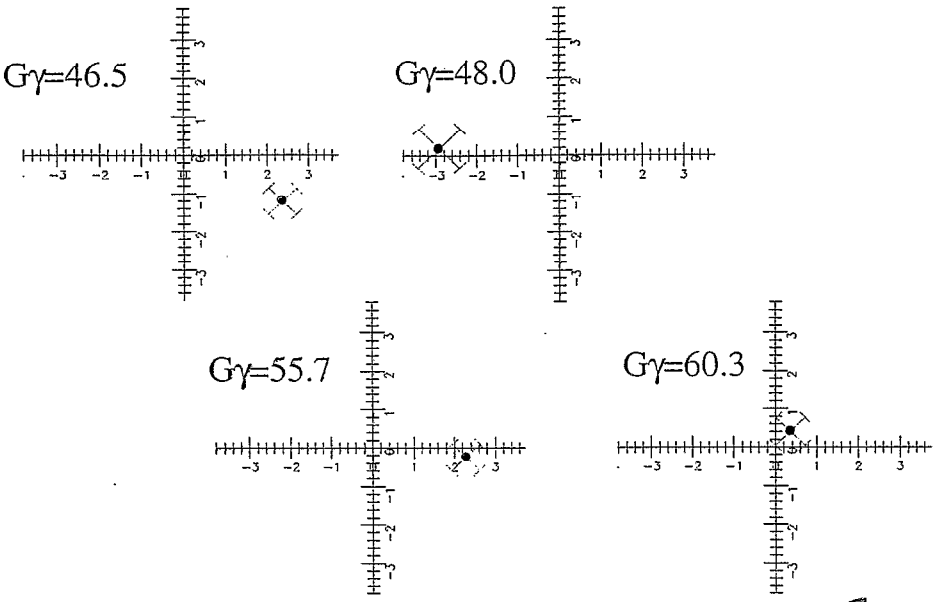

BROOKHAVEN NATIONAL LABORATORY

Spin resonances in RHIC (w/o Snakes)

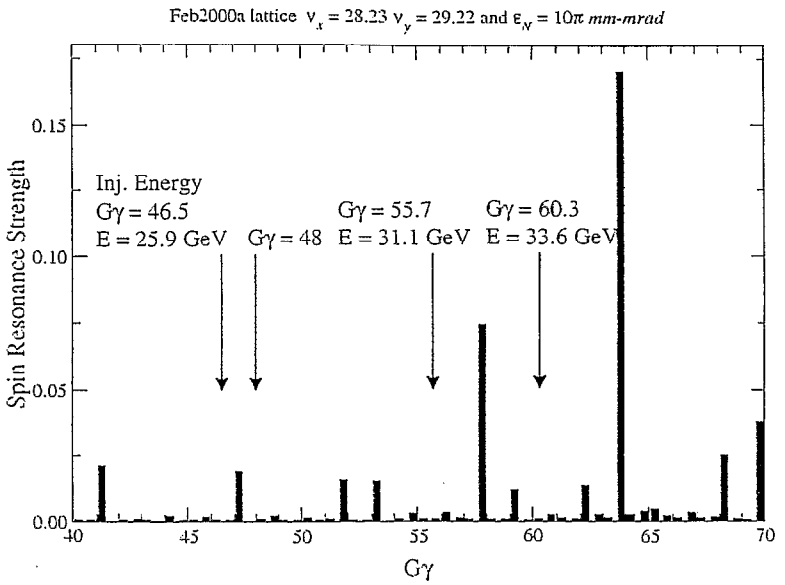

BROOKHAVEN NATIONAL LABORATORY

Asymmetries measured in RHIC

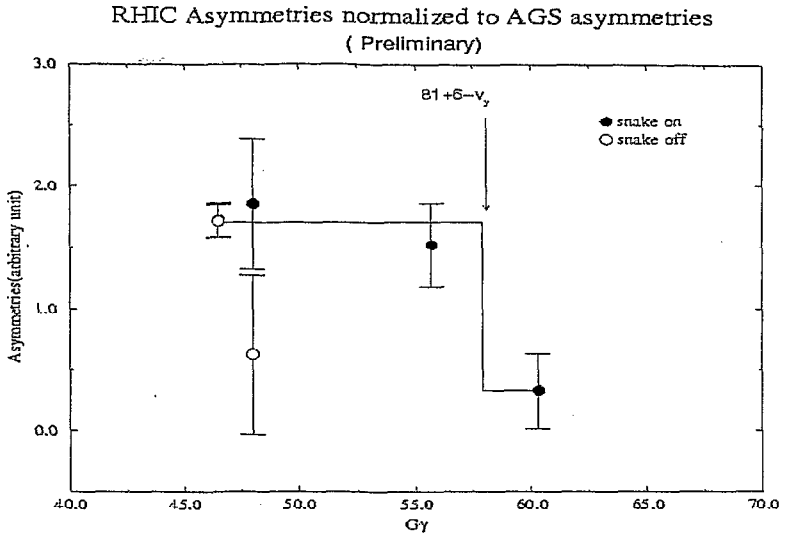

BROOKHAVEN NATIONAL LABORATORY

Summary

- AGS performed well with vertical rf dipole.
- First attempt to use horizontal rf dipole looks promising.
- RHIC pC CNI Polarimeter works very well.
- Snake Magnets work as expected.
- Polarized proton beam was accelerated in RHIC.

BROOKHAVEN NATIONAL LABORATORY

Polarimetry at RHIC

D. Svirida

POLARIMETRY AT RHIC (CNI)

- Results from E950
- RHIC year-one CNI polarimeter
- Latest results (September 2000)
- Future with wave front digitizers (WFD)
- Some physics

Why CNI ?

✓ Large crossection
✓ Simple equipment
✓ Weak asymmetry vs energy dependence

✗ Small effect (1-4)%
✗ No precise theoretical calculations

AGS E950 Experiment

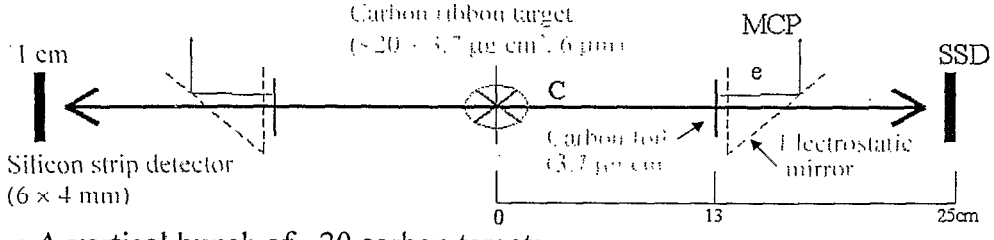

- A vertical bunch of ~20 carbon targets
- 2 detectors – 12 strips – only central 6 used for asymmetry calculations
- Trigger as 'OR' of all strips, carbon+prompts
- DAQ with LeCroy FERA 4300 ADC/TDC; dead time ~ 15 μs
- 1 bunch mode, ~ $5 \cdot 10^9$ p/bunch, ~ 40% polarization, 23 GeV
- About 10^7 carbon events in 2 day run
- Carbon selection by amplitude-TOF correlation
- Two independent methods of data treatment: 'banana' or linear cut, energy calibration by α-source or based on timing with MCP correction – – stable result

E950 Results and Fits

Asymmetry calculation :

$$A = \frac{\sqrt{LU}\sqrt{RD} - \sqrt{LD}\sqrt{RU}}{\sqrt{LU}\sqrt{RD} + \sqrt{LD}\sqrt{RU}}$$

Kopeliovich-Lapidus (old) :

$$A = \frac{\sqrt{-t}}{m} \cdot \frac{[(\mu-1)-2\mathrm{Im}r]\frac{t_c}{t} + 2(\rho\,\mathrm{Im}r - \mathrm{Re}r)}{1+(t_c/t+\rho+\delta)^2}$$

N. Buttimore improvement :

$$A = \frac{\sqrt{-t}}{m} \cdot \frac{[(\mu-1)-2\mathrm{Im}r]\frac{t_c}{t} - [(\mu-1)\rho - 2\mathrm{Re}r]\frac{t_c}{t}\delta + 2(\rho\,\mathrm{Im}r - \mathrm{Re}r)}{1+\left(\frac{t_c}{t}\right)^2 - 2(\rho+\delta)\frac{t_c}{t} + \rho^2 + (-t/m^2)[(\mathrm{Re}r)^2 + (\mathrm{Im}r)^2]}$$

$$\rho = \frac{\mathrm{Re}\, f_{++}(0)}{\mathrm{Im}\, f_{++}(0)} \qquad r = \frac{m}{\sqrt{-t}} \cdot \frac{f_{+-}}{\mathrm{Im}\, f_{++}}$$

δ – Bethe's phase

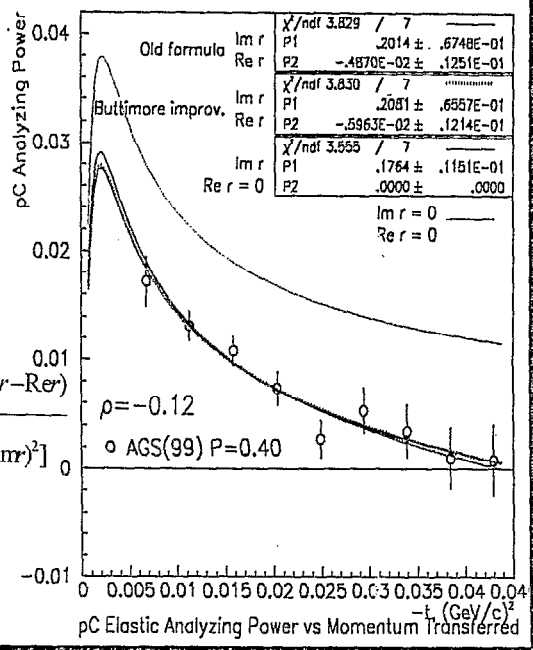

D. Svirida (ITEP)

RHIC Year-1 CNI Polarimeter

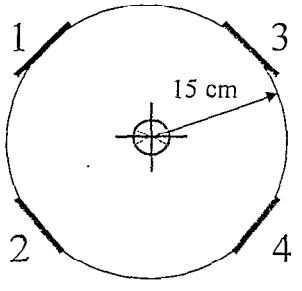

- Thin carbon target ~ 5 μg/sm² × 10μm
- Horizontal and vertical targets
- 4 Detectors 12 strips × 2 mm
- Strips in vertical direction
- Trigger as 'OR' of all strips
- No prompt particles in trigger
- DAQ with LeCroy FERA 4300 ADC/TDC
- Zero supression mode
- Dead time ~ 10 μs per event + 1.5 s per 40000 events
- 6-bunch mode
- Up to $5 \cdot 10^{10}$ p/bunch
- About 10^5 carbon events/min
- Carbon selection by amplitude-TOF correlation

D. Svirida (ITEP)

Energy Calibration

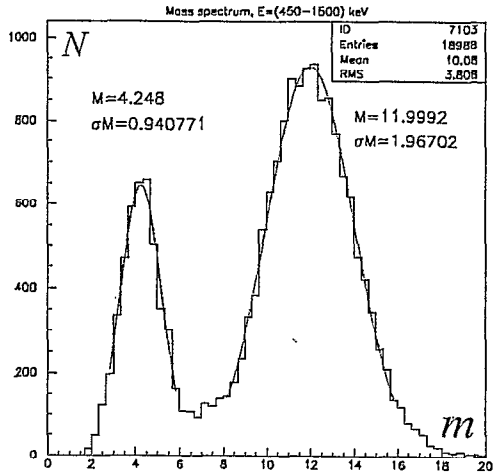

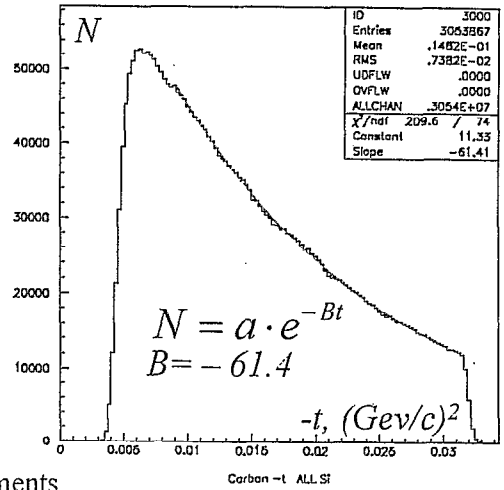

- Energy calibration by timing measurements
- Consistent with TANDEM test within 10%
- α-peak is at 4 with the account to Si dead layer

- ($-t$) spectrum corresponds to the elastic carbon (exponential)
- Spectrum slope is close to –60

D. Svinda (JINR)

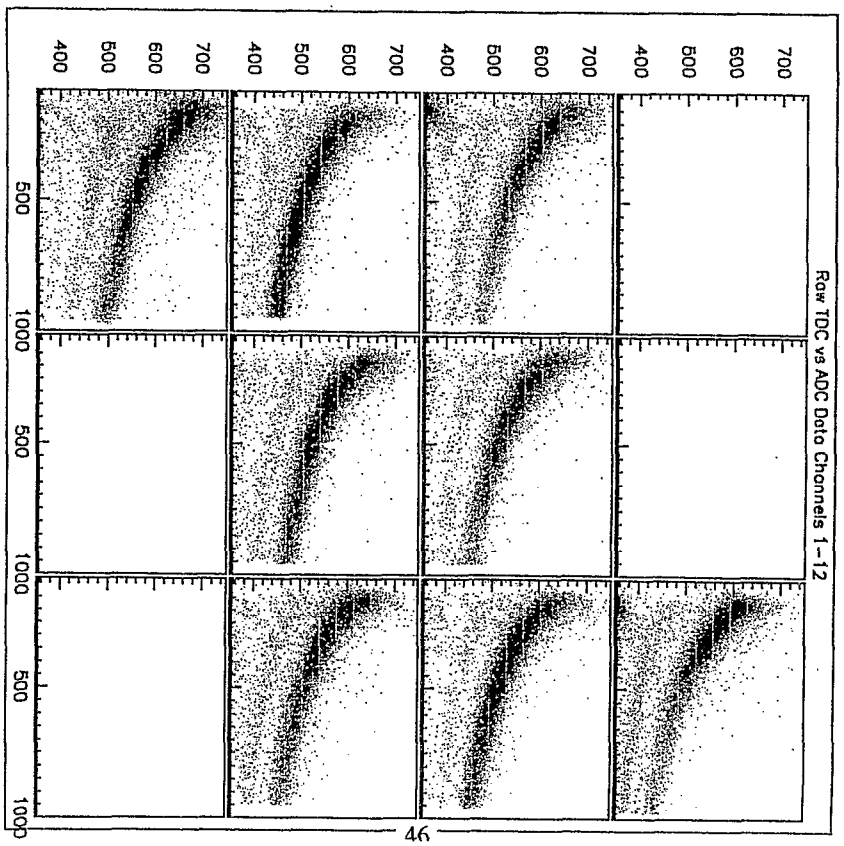

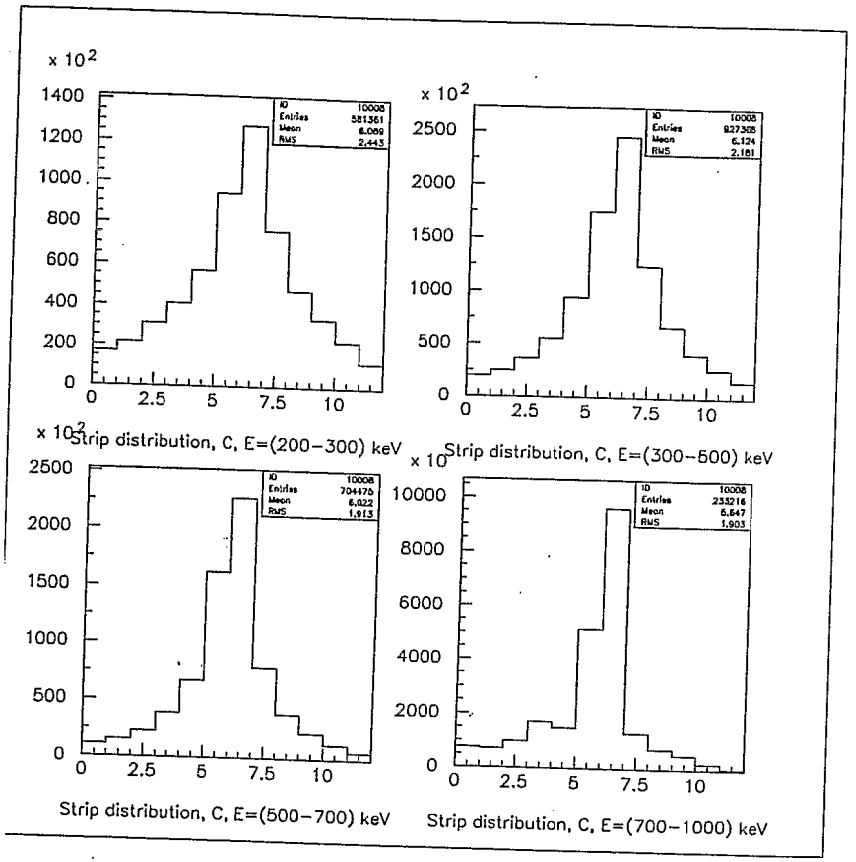
x 10^2
ID 10008
Entries 581361
Mean 6.069
RMS 2.443
Strip distribution, C, E=(200−300) keV
x 10^2
ID 10008
Entries 927305
Mean 6.124
RMS 2.181
Strip distribution, C, E=(300−500) keV
x 10^2
ID 10008
Entries 704476
Mean 6.022
RMS 1.915
Strip distribution, C, E=(500−700) keV
x 10
ID 10008
Entries 233216
Mean 6.647
RMS 1.903
Strip distribution, C, E=(700−1000) keV

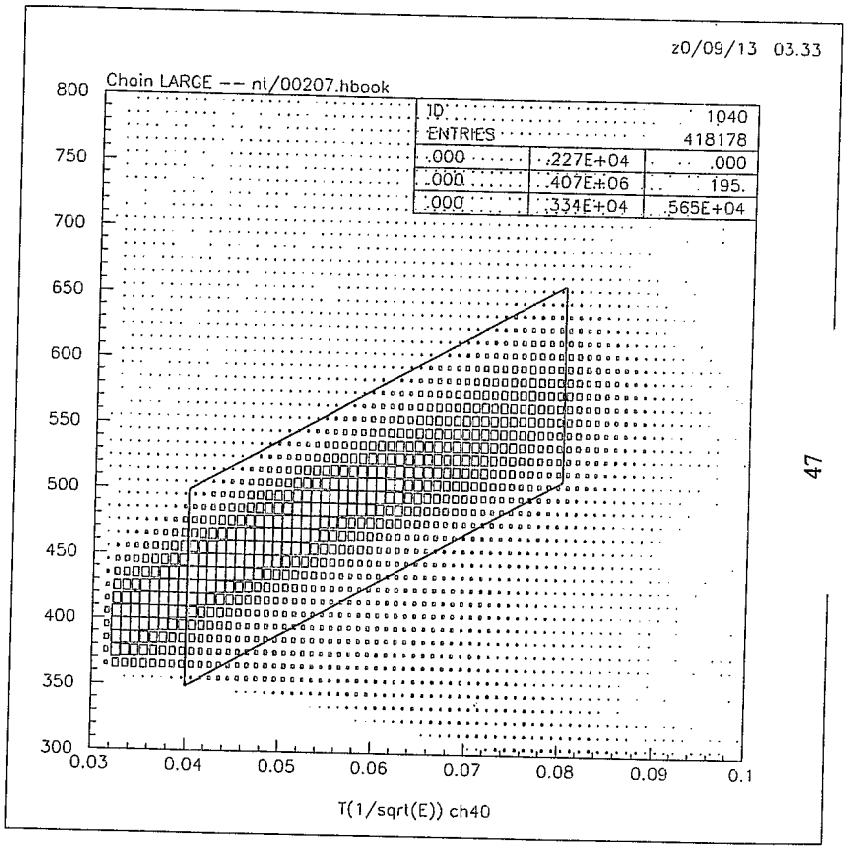
20/09/13 03.33
Chain LARGE -- ni/00207.hbook
ID 1040
ENTRIES 418178
.000 .227E+04 .000
.000 .407E+06 195.
.000 .334E+04 .565E+04
T(1/sqrt(E)) ch40

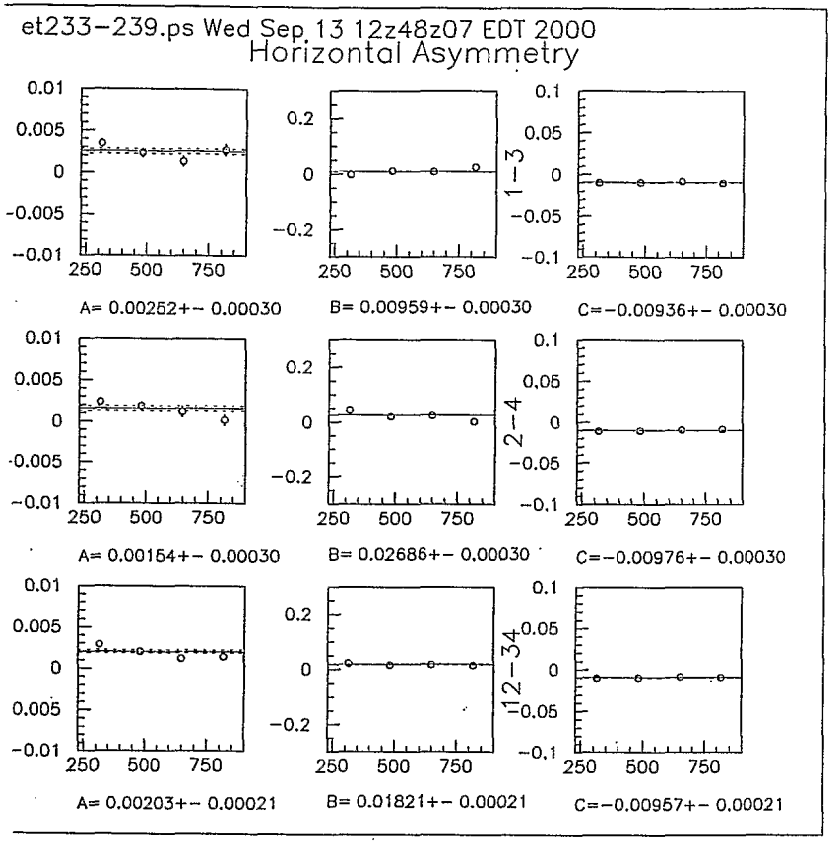
et233-239.ps Wed Sep 13 12z48z07 EDT 2000
Horizontal Asymmetry
1-3
A= 0.00262+- 0.00030
B= 0.00959+- 0.00030
C=-0.00936+- 0.00030
2-4
A= 0.00154+- 0.00030
B= 0.02686+- 0.00030
C=-0.00976+- 0.00030
12-34
A= 0.00203+- 0.00021
B= 0.01821+- 0.00021
C=-0.00957+- 0.00021

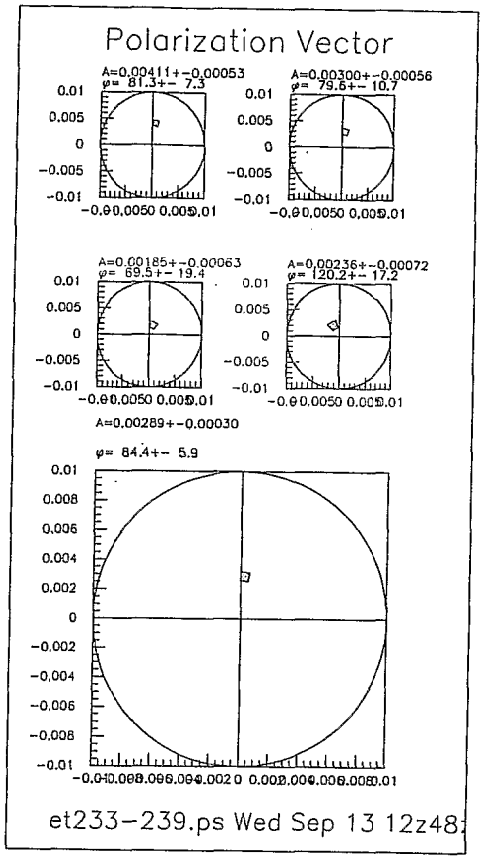
Polarization Vector
A=0.00411+-0.00053
φ= 81.3+- 7.3
A=0.00300+-0.00056
φ= 79.6+- 10.7
A=0.00185+-0.00063
φ= 69.5+- 19.4
A=0.00236+-0.00072
φ= 120.2+- 17.2
A=0.00289+-0.00030
φ= 84.4+- 5.9
et233-239.ps Wed Sep 13 12z48

Run History

RSC2000

Flip Test

Zero Test

- Statistically significant asymmetry values
- Correct correlation with polarization sign and/or direction
- Negligible systematic error with zero measurement

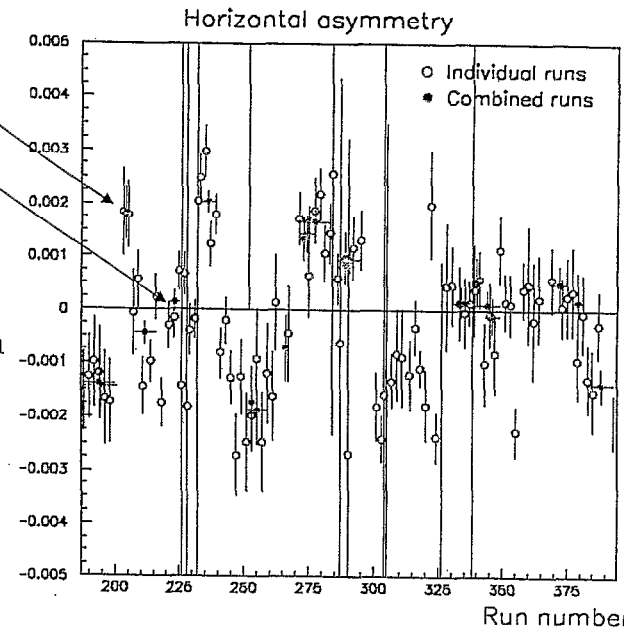

E950 Results and Fits + RHIC

RSC2000

Asymmetry calculation :

$$A = \frac{\sqrt{LU}\sqrt{RD} - \sqrt{LD}\sqrt{RU}}{\sqrt{LU}\sqrt{RD} + \sqrt{LD}\sqrt{RU}}$$

Kopeliovich-Lapidus (old) :

$$A = \frac{\sqrt{-t}}{m} \cdot \frac{[(\mu-1) - 2\,\mathrm{Im}\,r]\frac{t_c}{t} + 2(\rho\,\mathrm{Im}\,r - \mathrm{Re}\,r)}{1 + (t_c/t + \rho + \delta)^2}$$

N. Buttimore improvement :

$$A = \frac{\sqrt{-t}}{m} \cdot \frac{[(\mu-1) - 2\,\mathrm{Im}\,r]\frac{t_c}{t} - [(\mu-1)\rho - 2\,\mathrm{Re}\,r]\frac{t_c}{t}\delta + 2(\rho\,\mathrm{Im}\,r - \mathrm{Re}\,r)}{1 + \left(\frac{t_c}{t}\right)^2 - 2(\rho+\delta)\frac{t_c}{t} + \rho^2 + (-t/m^2)[(\mathrm{Re}\,r)^2 + (\mathrm{Im}\,r)^2]}$$

$$\rho = \frac{\mathrm{Re}\,f_{++}(0)}{\mathrm{Im}\,f_{++}(0)} \qquad r = \frac{m}{\sqrt{-t}} \cdot \frac{f_{+-}}{\mathrm{Im}\,f_{++}}$$

δ – Bethe's phase

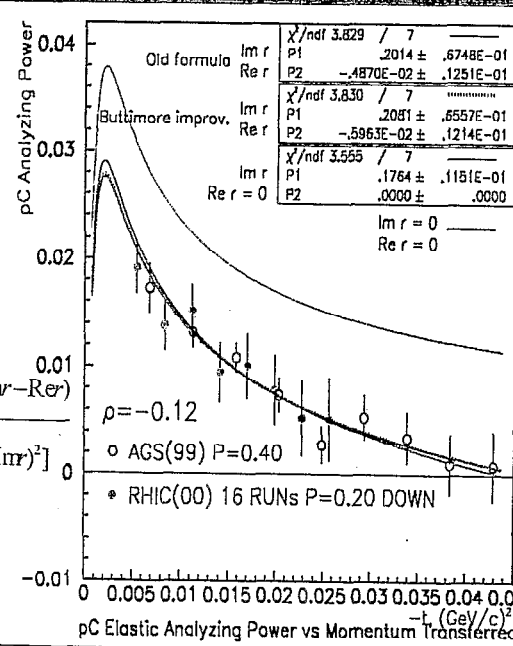

Future with WFD

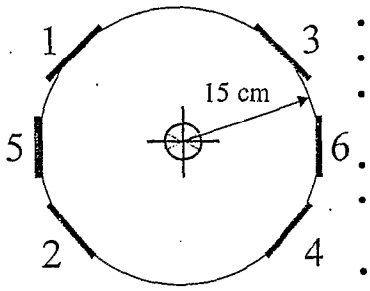

- 6 Detectors 12strips × 2 mm
- Strips in horizontal direction – all equivalent
- 72 independent self trigged channels with wave front digitizers (WFD)
- Large load ~ 1 event/bunch crossing (zero dead time)
- WFD allows to measure both time and amplitude of the signal
- Signal form analysis and zero level subtraction
- Flexible Xilinx configuration: on-board data storage
- Individual bunch polarization measurement

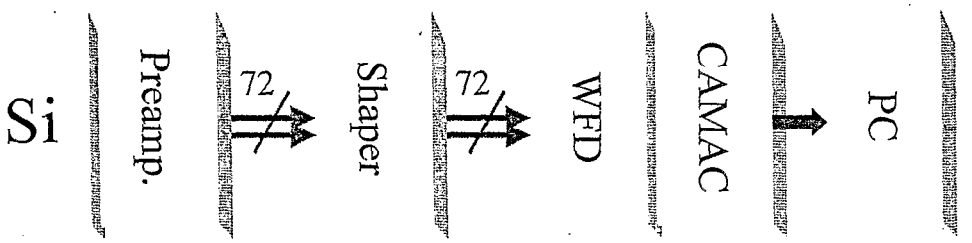

D. Svinda (ITEP)

WFD Test

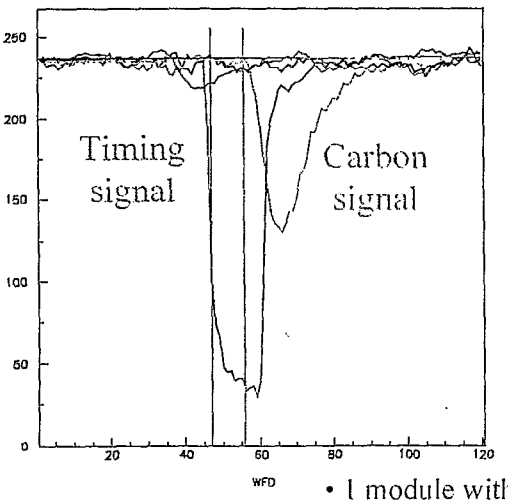

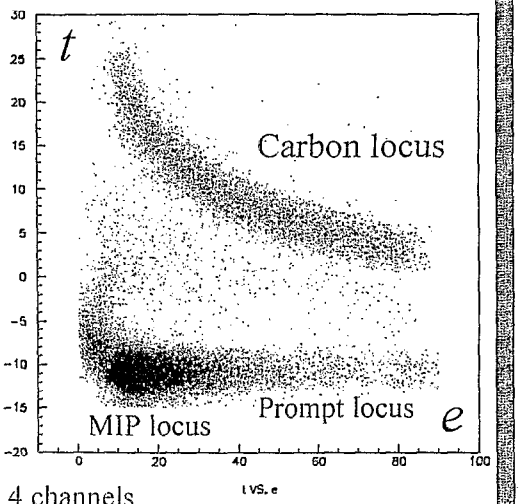

- 1 module with 4 channels
- External common trigger
- Waveform readout
- Software event reconstruction

D. Svinda (ITEP)

r : Beam Polarization Dependence

- Strong dependence on beam polarization P assumption
- Never consistent with zero
- Im r is well defined if Re r assumed 0
- χ^2 is smallest for P=(0.35-0.38)
- Reasonable values for reasonable P
- r phase is close to ρ

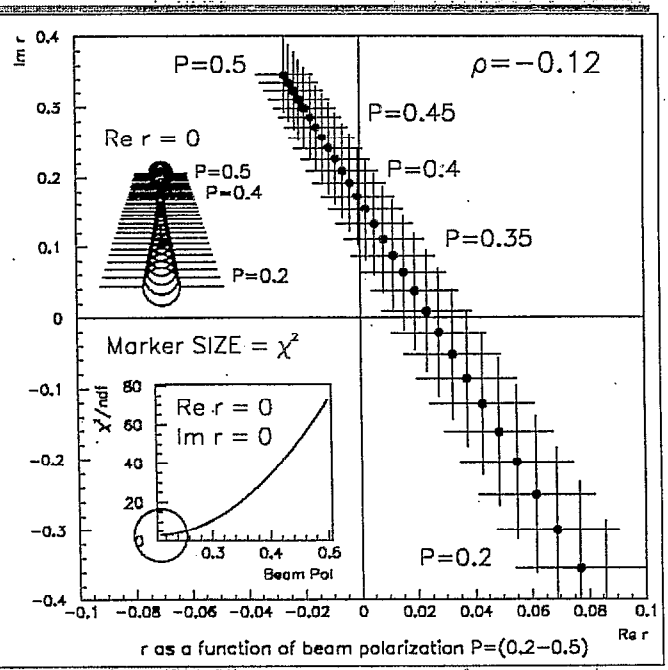

r as a function of beam polarization P=(0.2−0.5)

D. Svirida (ITEP)

r : ρ-dependence

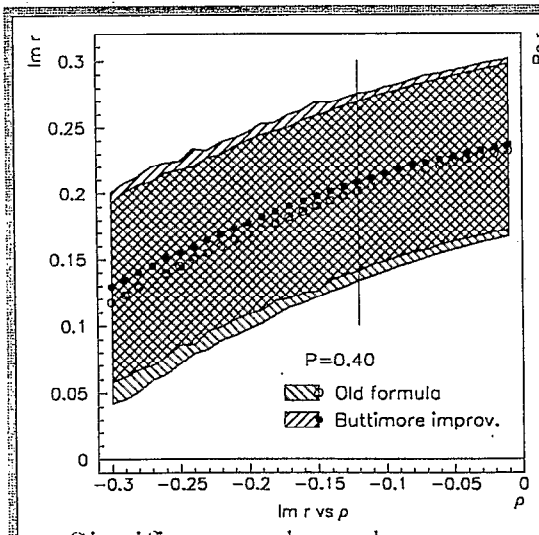

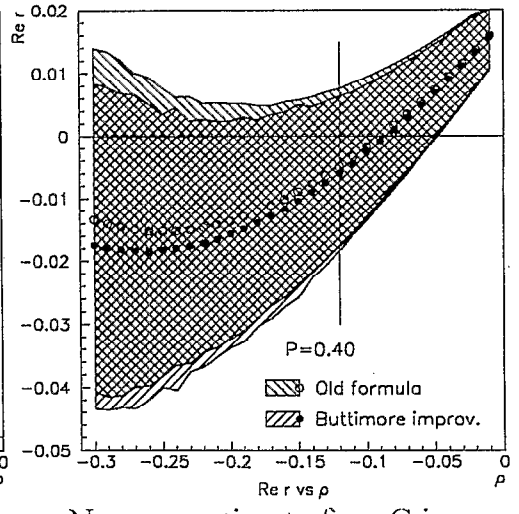

- Significant ρ-dependence
- Re r is nearly zero
- Im r is never consistent with 0

- New ρ estimate for pC in CNI region by B. Kopeliovich: $\rho = -0.12$

D. Svirida (ITEP)

Conclusions

RSC2000

- CNI Polarimeter proved to be a simple and reliable instrument for relative beam polarization measurements at RHIC
- WFD development will allow to achieve 5% accuracy at full RHIC luminosity and individual bunch polarization measurement
- Accurate estimate of spin-flip pC amplitude can be done, provided the absolute polarization value

Suppressing Intrinsic Spin Harmonics at the AGS

A.Lehrach [a], M. Bai [a], J.W. Glenn [a], W.W. MacKay [a], T. Roser [a], V. Ranjbar [a,b]
(a) Brookhaven National Laboratory, Upton,
(b) Indiana University, Bloomington, IN 47405, USA

Abstract

Over the last decade several improvements have been made to increase the polarization of the proton beam at the Brookhaven Alternating Gradient Synchrotron (AGS) [1]. A partial snake was installed to overcome all imperfection resonances in the energy range of the AGS [2]. The rf dipole concept to preserve polarization at strong intrinsic resonances has been demonstrated at the AGS for the first time [3]. Polarization losses have been observed at weak intrinsic resonances. One method to pre - serve polarization at weak intrinsic resonances is to change the betatron tune rapidly before crossing the resonance. Due to the non - adiabatic nature of this tune jump, the beam emittance will increase [4]. More efficient is a method called suppressing intrinsic spin harmonics, first successfully applied at the Cooler Synchrotron COSY [5]. In this presentation we describe how to use this method at the AGS.

References

[1] T. Roser, DESY-Proc-1999-03, 52 (1999).
[2] H. Huang et al., Phys. Rev. Lett. 73, 2982 (1994).
[3] M. Bai et al., Phys. Rev. E 56, 6002 (1997).
[4] L.A. Ahrens et al., AIP Conference Proceedings No. 187, 1068 (1988).
[5] A. Lehrach et al., Nucl. Inst. Meth. A 429, 26 (2000).

October 13th - 14th, 2000

Int. Workshop on Polarized Partons at High Q^2 region

Suppressing Intrinsic Spin Harmonics at the AGS

- introduction
- methode

- conclusion

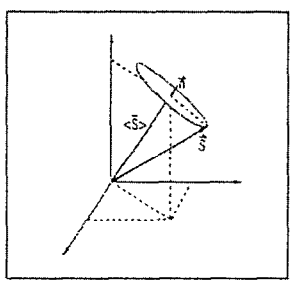

Andreas Lehrach, BNL

Depolarizing Resonances at AGS

1. imperfection

$\gamma G = 5, 6, \ldots$

→ 5% solenoidal partial snake

2. intrinsic

$\gamma G = kP \pm \nu_y$

P (GeV/c)	γG	$\varepsilon_R * 10^3$	P_{fi}
4.5	$0 + \nu_y$	6.1	- 0.42
8.0	$24 - \nu_y$	0.2	0.99
10.8	$12 + \nu_y$	2.4	0.45
14.3	$36 - \nu_y$	5.1	- 0.26
17.1	$24 + \nu_y$	0.4	0.95
20.5	$48 - \nu_y$	0.6	0.90
23.4	$36 + \nu_y$	11.0	- 0.77
24.8	$60 - \nu_y$	64.0	-1.99

→ 18 Gm rf dipole

3. couple

$\gamma G = 0 + \nu_x, 12 + \nu_x, 36 \pm \nu_x$

4. higher order

$\gamma G = 60 - \nu_y - 9$

resonance strength of intrinsic resonances

$$\epsilon_K = \frac{1+\gamma G}{2\pi}\sqrt{\frac{\epsilon_N}{\pi\gamma}}\oint \frac{\partial B_y/\partial x}{B\rho}\sqrt{\beta_y(s)}\,\cos(\nu_y\phi(s)+\eta)\,e^{iK\Theta(s)}\,ds,$$

ε_N : normalized vertical emittance

$\partial B_y/\partial x$: vertically focusing gradient field

$B\rho$: magnetic rigidity

β_y : vertical betatron amplitude

ν_y : vertical betatron tune

K : resonance tune

Θ : orbital bending angle

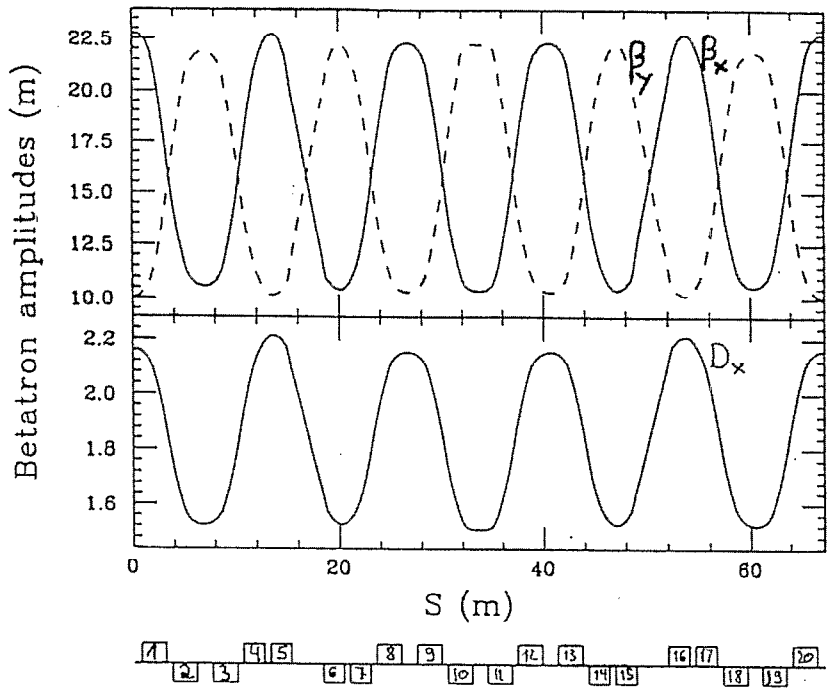

AGS unit cell

1	2	3	4	5	6	7	8	9	0	1	2	3	4	5	6	7	8	9	0
h	h	v	v	h	h	v	v	h	h	v	v	h	h	v	v	h	h	v	v
s	s	l	l	l	l	l	l	s	s	s	s	l	l	l	l	l	l	s	s

→ tuning quads at 3 and 17

→ symmetry points at 5 and 15

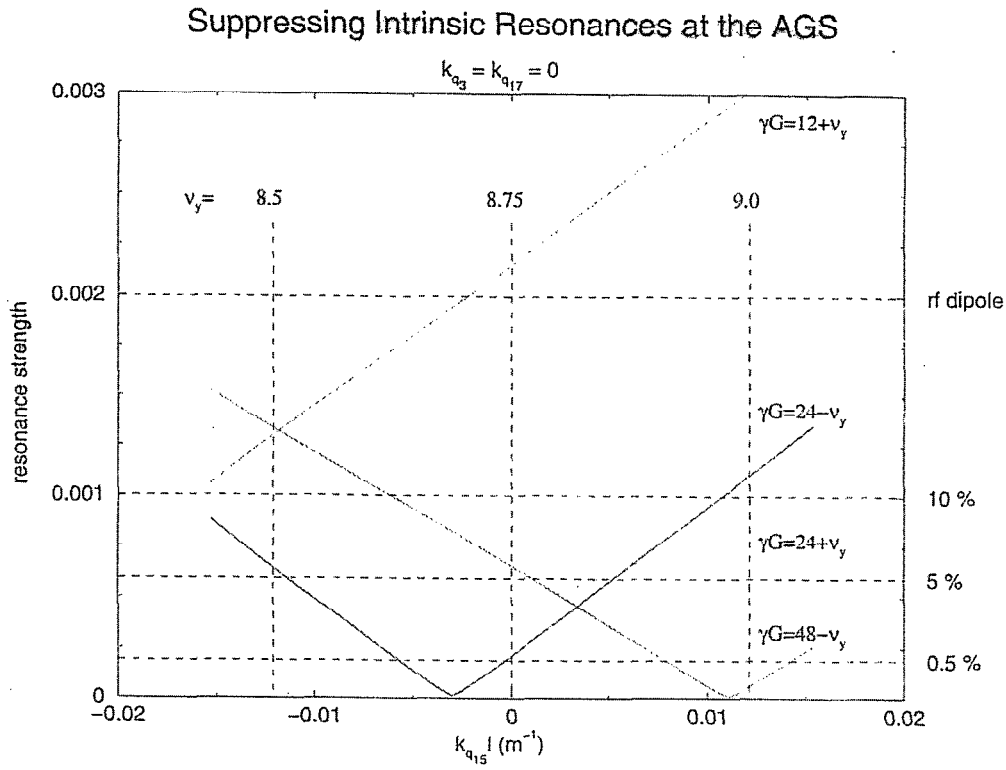

Hardware

- power supplies : I = 700A, V = ± 170V
- magnets : R = 0.161 Ω, L = 0.02567H
- rampe rate : 330A / 50msec

γG	t_{up} (msec)	t_{down} (msec)	I_{max} (A)
$24 - \nu_y$	60	40	-180
$24 + \nu_y$	50	30	-360
$48 - \nu_y$	30	50	+360

→ required ramp time : 110msec

factor two slower acceleration

Froissart-Stora

$$P_f = P_i(2e^{-\pi\ \varepsilon^2/2\alpha} - 1)$$

P_i : initial polarization
P_f : final polarization
α : resonance crossing rate
ε : resonance strength

- partial snake : $\theta \sim \sqrt{\alpha}$

Conclusion

- **quads at position 15**
- **slower acceleration**
  → weaker partial snake

$> 70\%$ polarization from AGS

Partial helical snake for AGS

M. Okamura, T. Tominaka, T. Katayama, RIKEN
N. Tsoupas, BNL

Abstract

In order to achieve high polarization of proton beams at RHIC, a helical partial snake magnet will be useful device. This new snake will be installed at AGS instead of existing solenoid partial snake magnet. With an RF dipole, the existing solenoid partial snake magnet could increase polarization up to 50 % at 21 GeV in AGS, however this result still does not fulfill the requirement of the project. It has been observed that much of the remaining depolarization occurring in the AGS is associated with transverse coupling resonance, which is due to the strong longitudinal field of the existing snake magnet itself. By replacing with the helical partial snake, the coupling will be reduced dramatically. The new partial snake system will be composed single normal conducting helical dipole and with steering magnet on both sides. Planned field strength, bore radius and length are 1.5 T, 75 mm and 1.5 m respectively. Detailed design of this magnet will be presented.

Partial Helical Snake for AGS

RHIC Spin Collaboration
October 13(Fri) 2000
Yukawa Institute, Kyoto University, Japan

M. Okamura / RIKEN

Contents:

1. Solenoid and Helical Magnets
2. Basic Design of the Helical Dipole Magnet.
3. XY coupling (Longitudinal Magnetic Field)
4. Conclusion

1. Solenoid and Helical Snake

Polarization are lost at spin resonances in a synchrotron.

At AGS,

Imperfection Resonances
→ Solenoidal partial Snake

Intrinsic Resonance
→ RF dipole

However,
strong longitudinal magnetic field
exists in the solenoidal snake.
↓
Transverse coupling.
↓
Additional Intrinsic Resonances.
Not only from vertical tune
but also from horizontal tune.

T-BMT equation

$$\frac{d\vec{S}}{dt} = \frac{qe}{\gamma m}\vec{S}\times\left[(1+G\gamma)\vec{B}_{\perp} + (1+G)\vec{B}_{=} + \left(G\gamma + \frac{\gamma}{\gamma+1}\right)\frac{\vec{E}\times\vec{\beta}}{c}\right]$$

Dipole field — Solenoidal field

Constant field strength — Should be ramped

Helical Dipole for the AGS

Net deflection = Zero
Orbit displacement → Steering Magnets

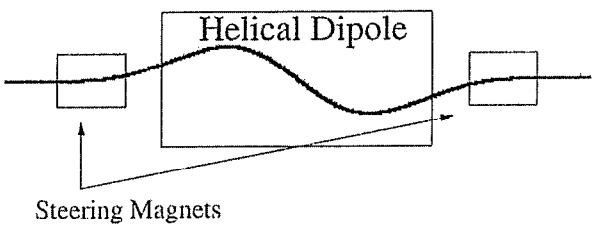

Still there are some longitudinal fields.
Operated high (constant) field at low beam energy.

2. Basic Design of the Helical Dipole Magnet

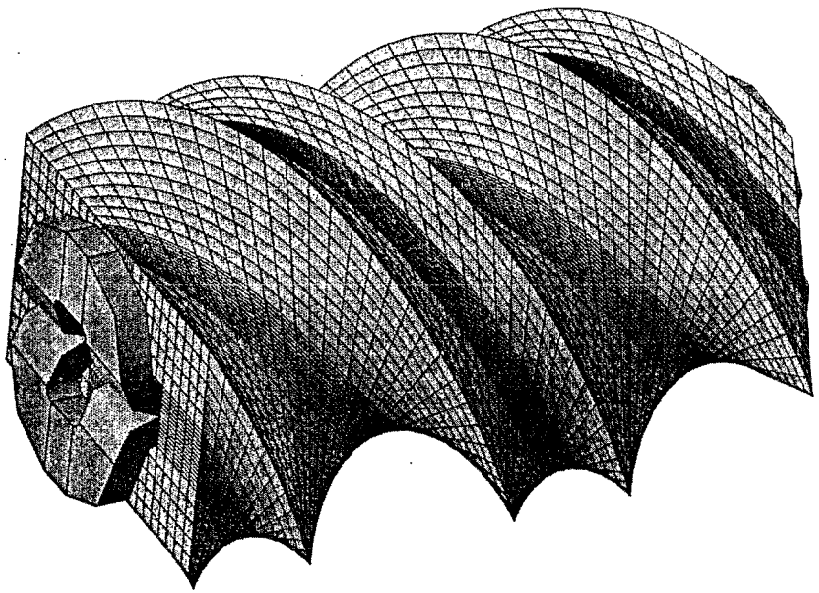

3D plot by OPERA/TOSCA

Effective magnetic length : 1500 mm
Bore: 150 x 150 mm
Field strength: 1.61 T (for 9 degree spin rotation)
Yoke length: 1393.2 mm (334.67 degree rotation)

Feild strength in the yoke

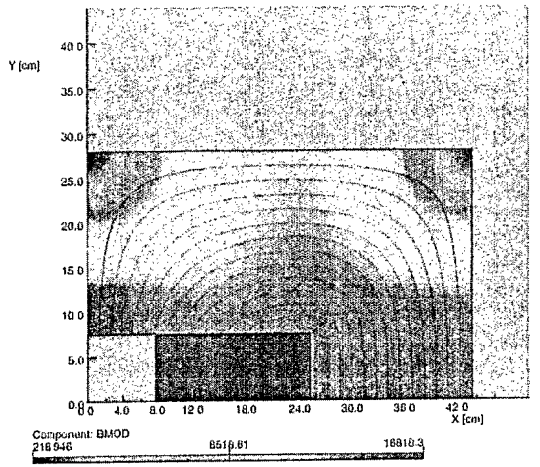

2D calculation

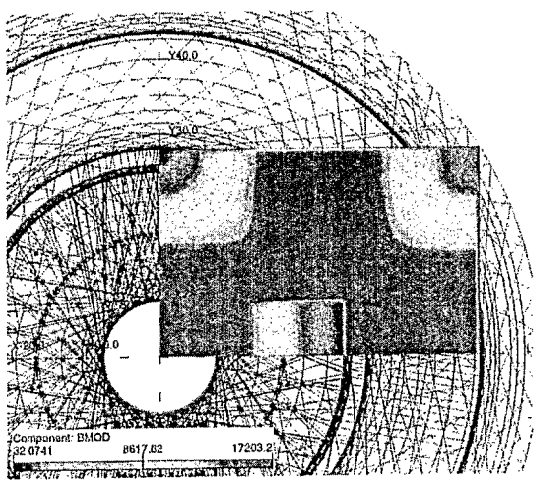

3D calculation

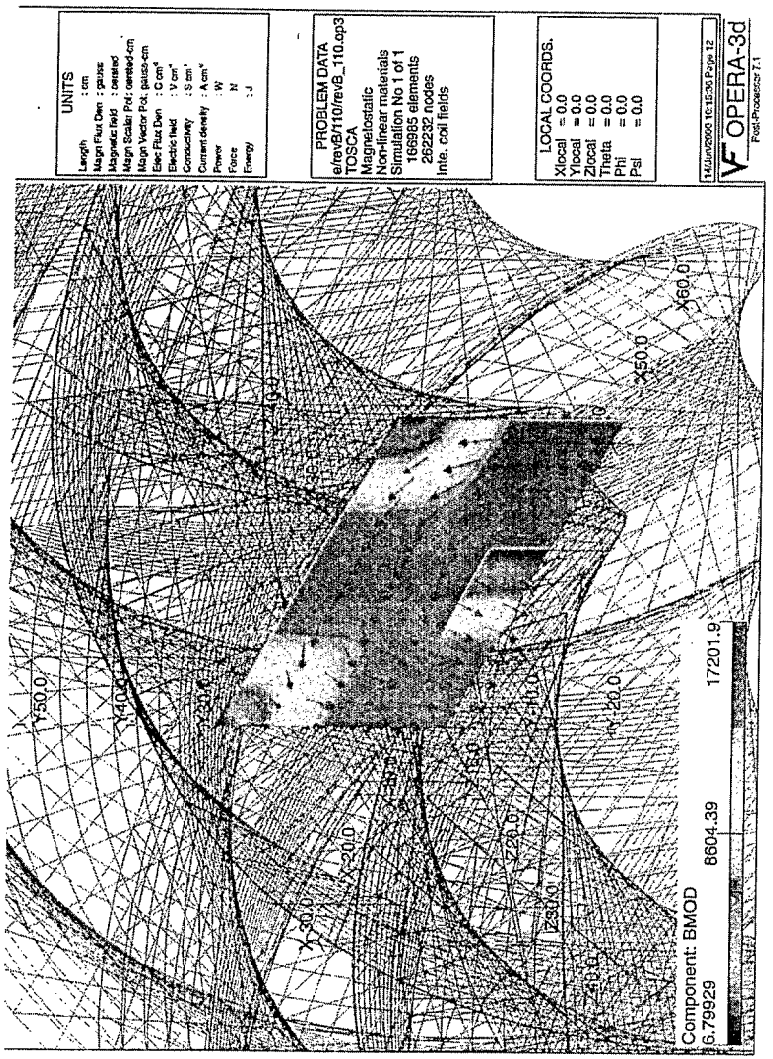

Table 1: Design Parameters

	Parameter	Value
Coils		
	Current density (A/cm^2)	754
	Total current (A turn)	198000
	Power dissipation (kW)	19
	Conductor size (mm)	11.5 x 11.5
	Diameter of hollow (mm)	7.5
	Inductance (mH)	95
	Number of turns	168 (14 x 12)
Yoke		
	Height (mm)	560
	Width (mm)	870
	Rotation angle (degree)	334.67
	Length (mm)	1393
	Packing factor (%)	99

Table 2: Multipole components

	2D	3D(azi.)	3D(ver.)
Dipole (T)	1.655	1.613	1.622
Sextupole / Dipole	4.2×10^{-4}	-4.0×10^{-3}	-9.3×10^{-3}
Decapole / Dipole	9.1×10^{-5}	6.1×10^{-4}	5.9×10^{-4}

Reference radius is set to 50 mm. All the values are based on normal components.

Optimization with 3D calculation

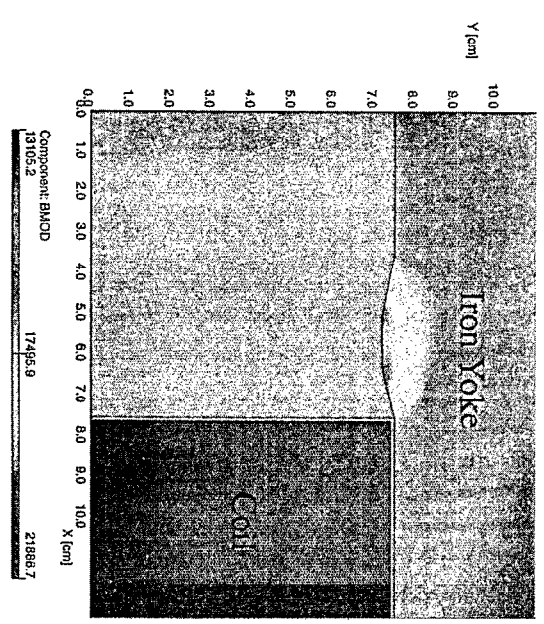

Pole shape with shim

The sextupole component with revised shape is 8.9 x 10-3 which is based on 2D code.

The 3D calculation gave the ratio of sextupole is 5.8 x 10-4.

3. Transverse Coupling (Longitudinal Magnetic Field)

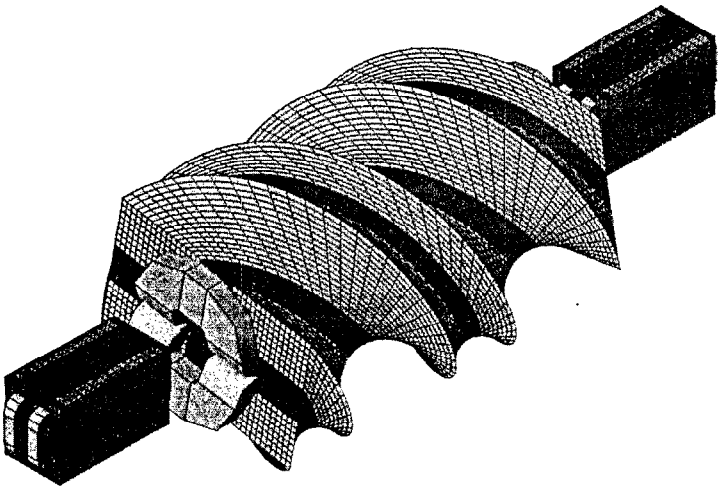

Partial Helical Snake

Tracking using 3D field map

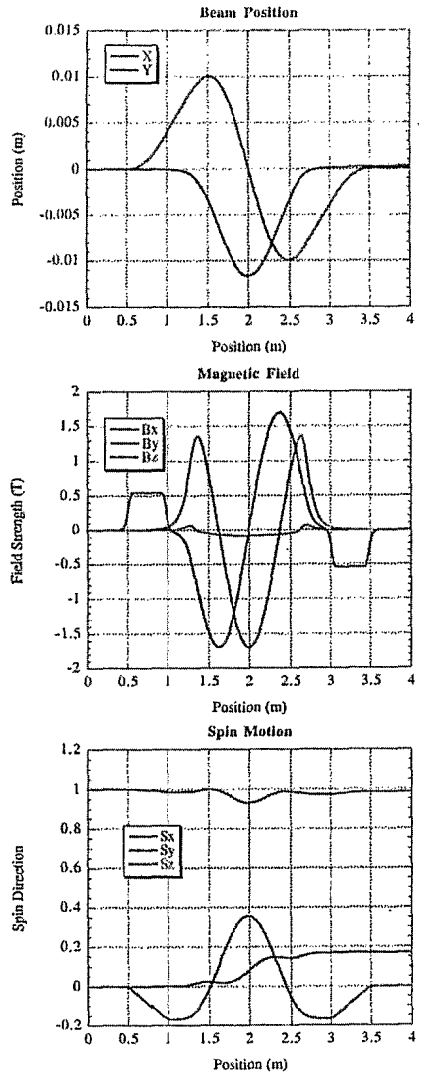

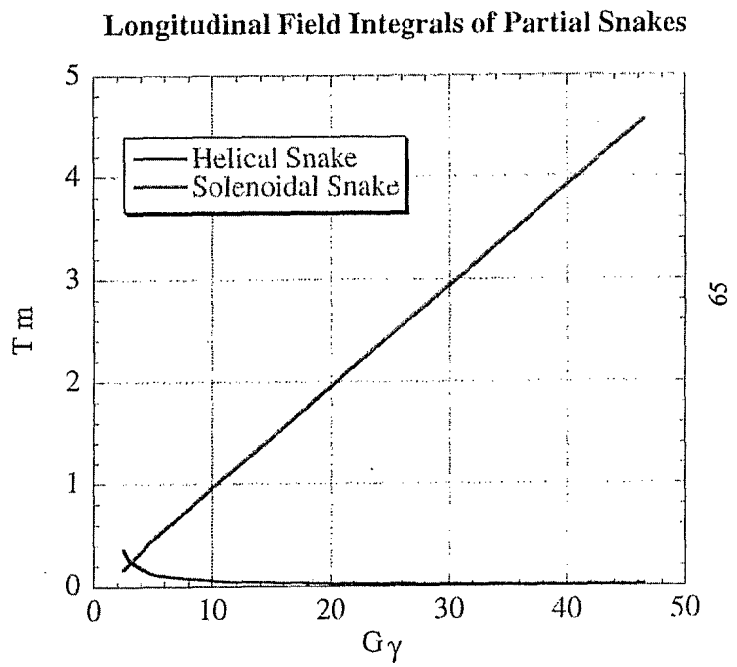

Conclusion

The new helical partial snake was designed using the 3D magnetic calculation. The longitudinal magnetic fields, which cause the transverse coupling, were estimated. We believe that the new snake system is effective to reduce depolarization in the AGS.

Spin Tracking with "Real" Siberian Snakes in RHIC

Meiqin Xiao* and Takeshi Katayama**
*Fermi National Accelerator Laboratory,
**Center for Nuclear Study (CNS), the University of Tokyo/RIKEN

Abstract

The numerical study of the spin depolarization in Relativistic Heavy Ion Collider (RHIC) at BNL due to the intrinsic and imperfection resonances has been carried out by tracking the orbital and spin motion of polarized protons with "real" Siberian Snakes in the ring, based on the magnetic field-map produced by TOSCA calculation, from the injection energy of 25GeV to the top energy of 250GeV. Firstly, the energy-dependent numerical orbital maps and the spin matrices of a Siberian Snake have been obtained by a method to combine spline interpolation functions for magnetic field fitting and TPSA (Truncated Power Series Algebra or Automatic Differentiation) approach for extracting an exact orbital map around any ray. Secondly, the symplectic problem of orbital map was solved for the spin tracking for 10^7 turns. And then, the code SPINK was upgraded to carry out spin tracking. Finally, the numerical spin tracking in RHIC with "real" Siberian snake was carried out. The single- and multi- particle tracking results show that "real" Siberian Snakes can keep the polarization of the protons through the acceleration to more than 95% in a RHIC machine with no misalignment and no field error, if the polarized protons are extracted from the emittance of 10pmm.mrad. In the machine with misalignments, it is found that the bigger the misalignments, the stronger the depolarization resonances. If r.m.s. misalignment is as large as 2.5mm, the corrected closed orbit distortion should be less than 0.2mm in the ring. The average polarization in this condition is about 73% at the top energy. On the other hand, it was found that "real" Siberian Snakes introduce the coupling of horizontal and vertical betatron motions in the low energy region. The operation points cross 10th order and 5th order sum resonance lines and difference resonance line during the acceleration. However, these motions in the low energy region do not affect so seriously the spin polarization.

Spin Tracking with "Real" Siberian Snakes in Relativistic Heavy Ion Collider (RHIC)

Meiqin Xiao* and Takeshi Katayama

CNS, the Univ. of Tokyo/RIKEN

*Present institution: Fermi National Accelerator Laboratory

1. Introduction

- RHIC-Spin Project (Figure 1) at Brookhaven National Laboratory, under the RIKEN-BNL agreements, has planed to install two Siberian Snakes in each RHIC main rings to accelerate polarized protons without losing their polarization from the injection energy 25 GeV to the top energy 250 GeV.
- Typically, there are two kinds of depolarizing resonances exist during the acceleration, intrinsic resonances, caused by the focusing fields, and imperfection resonances, derived by magnet errors and misalignments.
- Siberian Snake is a local spin rotator, Figure 2 indicates how one or two snakes to cure the imperfection depolarizing resonances. With the installation of two snakes in one ring, the spin tune of polarized proton becomes ½ and is independent of the energy. Figure 3 shows the stable spin directions in the ring with double snakes installed.

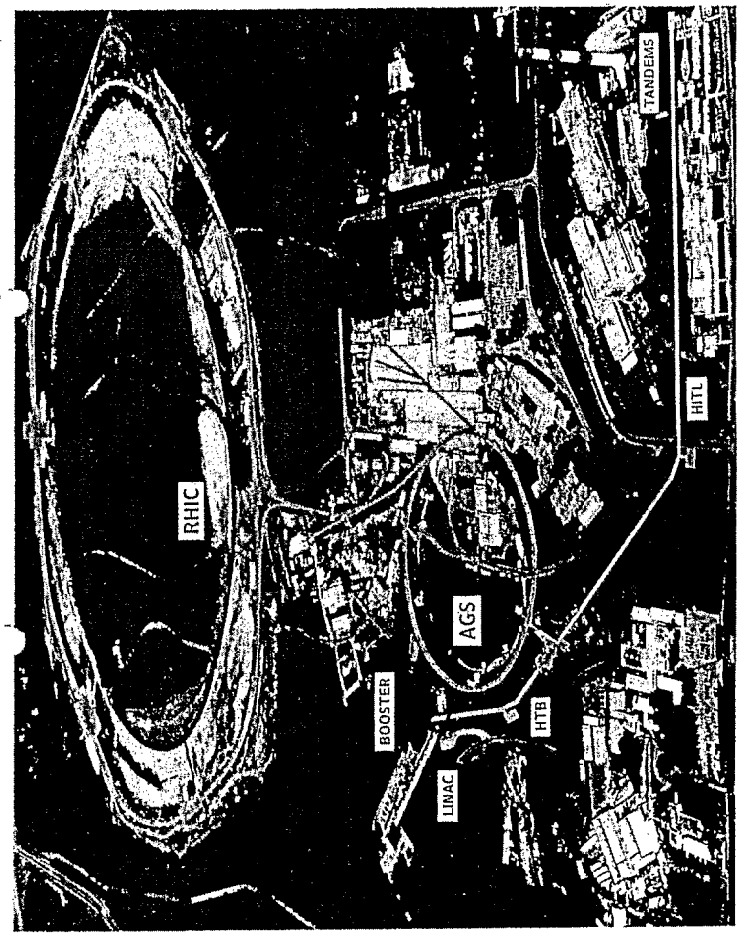

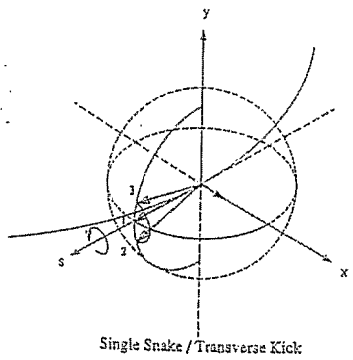

Single Snake / Transverse Kick

a. Stability of longitudinal spin with one snake.

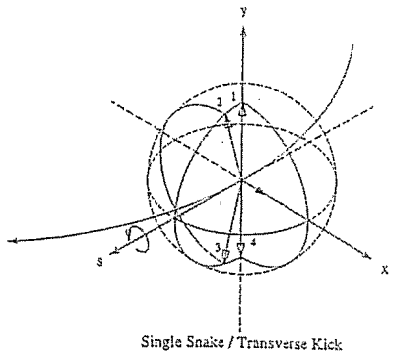

Single Snake / Transverse Kick

b. Stability of vertical spin with one snake and radial perturbation.

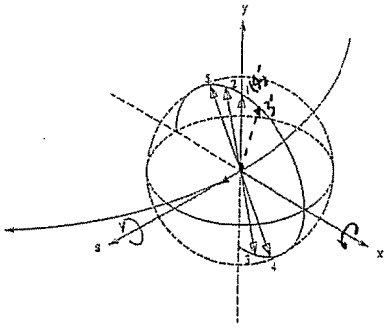

One Snake / Longitudinal Kick

Spin Tune = 1/2

c. Stability of vertical spin with one snake and longitudinal perturbation.

Fig 1.7 Single Snake with perturbation, can not cure the imperfection depolarizing resonances of vertical polarization due to stable direction: s-direction

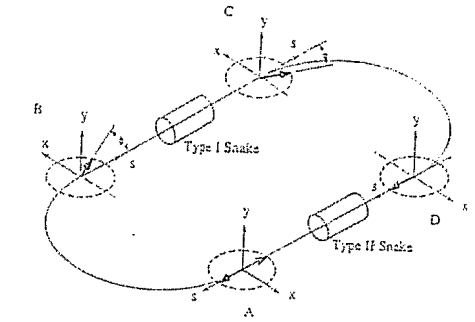

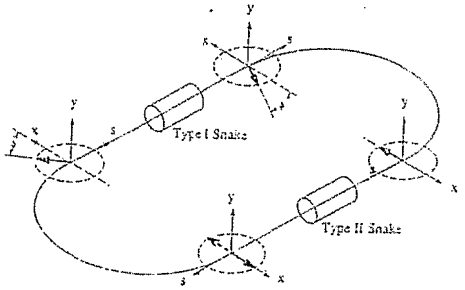

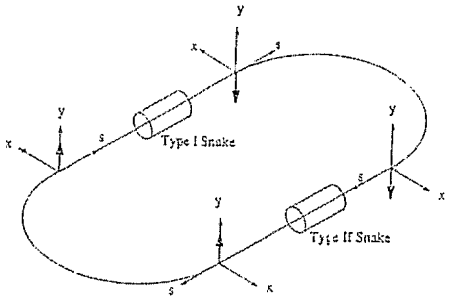

Fig 1.8 Double Snakes: stable spin directions: vertical (y-direction)

- Siberian Snake in RHIC consists of four superconducting helical dipole magnets (See Figure 4). The dipole field of a 2.4m long helical dipole magnet should rotate through a complete 360° from one end of the magnet to the other. A real helical dipole has no more idealistic magnetic fields, but large longitudinal magnetic field, as well as fringing field, which results in the incomplete cancellation of the perturbation.
- The simulation on spin dynamics with real Siberian Snakes is required to estimate the realistic depolarization phenomena. The present work was done based on three-dimensional numerical magnetic field map provided by TOSCA .

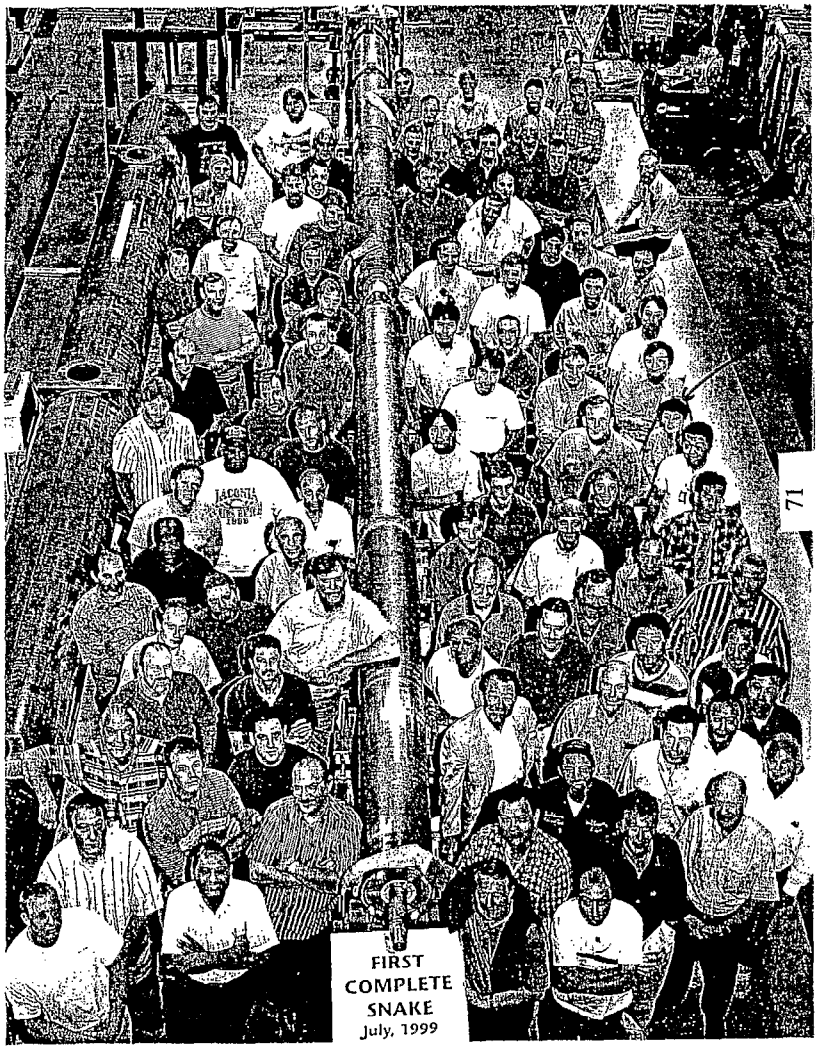

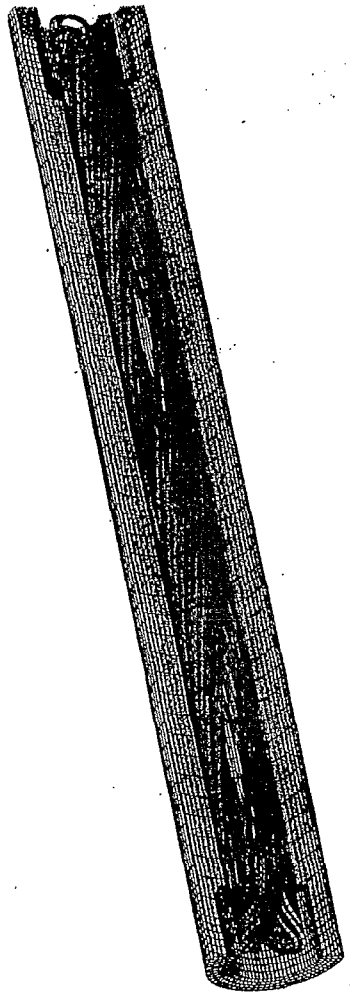

2. Brief Review to the Spin Dynamics

The evolution of spin vector of polarized proton in external electromagnetic fields is govern by Thomas[1927]- BMT [1959]equation:

$$\frac{d\bar{\mathbf{S}}}{dt} = -(\frac{e}{\gamma m})[(1+G\gamma)\bar{\mathbf{B}}_{\perp} + (1+G)\bar{\mathbf{B}}_{//}] \times \bar{\mathbf{S}} \qquad (1)$$

where the polarization vector $\bar{s}$ is expressed in the frame that moves with the particle. G = 1.7928 ,the anomalous magnetic moment of the proton. $\gamma = E/m_o c^2$.

At the same time, the velocity of the particle obeys Lorentz force equation:

$$\frac{d\bar{\mathbf{v}}}{dt} = -(\frac{e}{\gamma m})[\bar{\mathbf{B}}_{\perp}] \times \bar{\mathbf{v}} \qquad (2)$$

Compare with Eq. (1) and Eq.(2):

(1) In a pure vertical field, the spin rotates $G\gamma$ times faster than the orbital motion.

(2) We define: Spin Tune $\nu_{sp} = G\gamma$, the number of spin rotations in one revolution.

γG=477 at RHIC top energy.

- The spin depolarization due to resonances can be studied numerically by tracking the orbital and spin motion of protons in the ring.
- About 7.5×10^6 turns have to be tracked to see the behavior of the spin in RHIC during the acceleration.
- The key issue for such a long-term tracking is to keep the symplecticity for the orbital maps and to guarantee the unitarity for the spin matrices.

3. Symplectified orbit maps and unitary spin matrices of Siberian Snakes in RHIC

- Three dimensional spline function interpolation method is developed to describe the numerical field map including fringing field. Based on ¼ of a helical magnet field map, the magnetic field of each helical magnet is constructed and optimized to get spin rotation as complete as possible. See Figure 5 and Figure 6.
- Energy-dependent spin matrices, spin rotation angles and spin axis angles of the Snake are calculated around the central ray. The unitarity of spin matrices obtained in this way is checked and found the deviation from 1(unit) is about 10^{-8}. It is very close to unitarity as required. (see Table 1)
- TPSA (Truncated Power Series Algebra or Automatic Differentiation) is introduced. The TPSA approach makes possible to get an accurate map around an arbitrary ray (see Table 2).

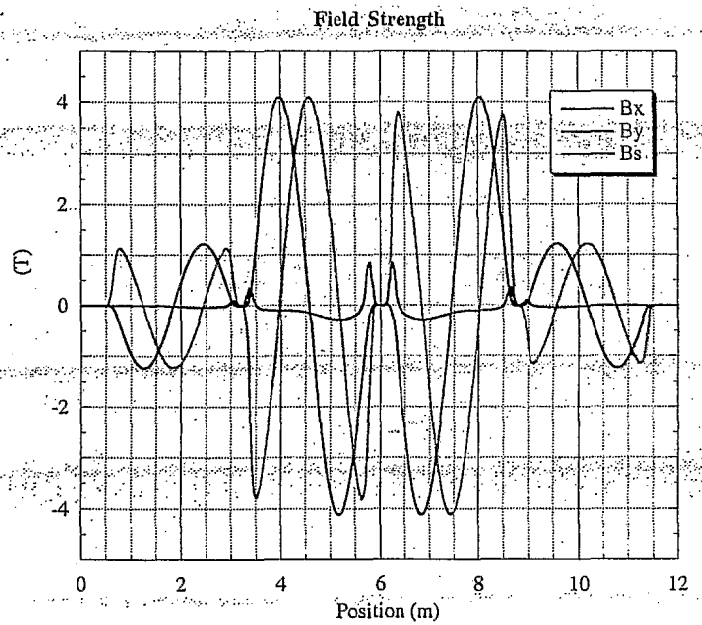

Fig 2.7 The magnetic field distribution of the Snake along the central ray

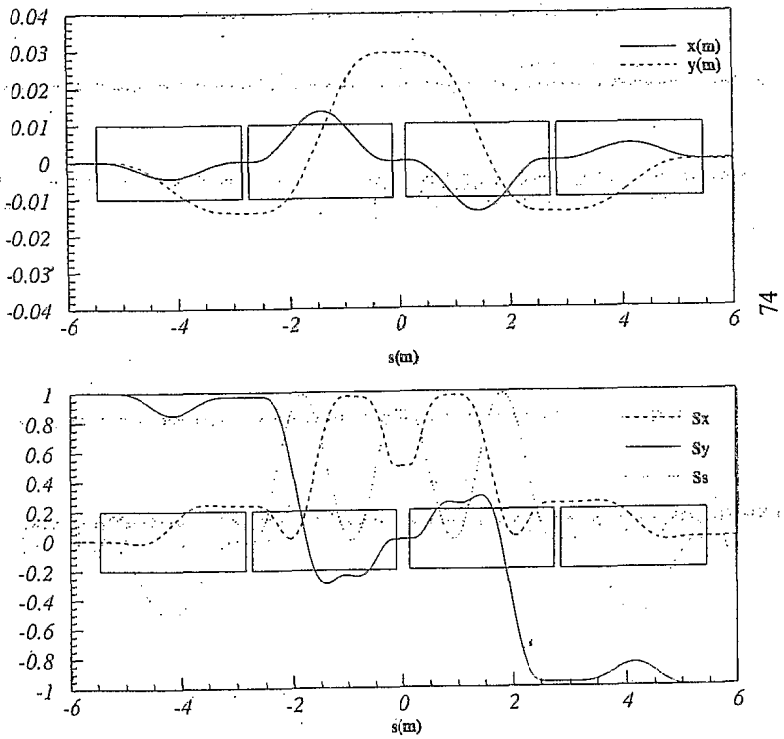

Fig 2.5 The trajectory of the central ray and its corresponding spin procession (25(a))

Table 2. 3 Spin matrices and the respective spin axis angles of Snake Type A and Snake Type B at high energy setting

	Siberian Snake Type A	Siberian Snake Type B
25 GeV	0.18349787 -0.03253694 0.98248149 0.03242783 -0.99870777 -0.03913085 0.98248510 0.03904017 -0.18220564	0.18405357 -0.03249902 -0.98237879 0.03235887 -0.99871114 0.03910192 -0.98238342 -0.03898551 -0.18276472
	$\phi = 50.27140023°, \theta = 0.00203346°$	$\phi = -50.28764491°, \theta = -0.00261130°$
50 GeV	0.07933313 -0.01336230 0.99675860 0.01334669 -0.99980629 -0.01446544 0.99675881 0.01445101 -0.07913942	0.07949613 -0.01342263 -0.99674480 0.01340345 -0.99980455 0.01453284 -0.99674506 -0.01451513 -0.07930068
	$\phi = 47.27255458°, \theta = -0.00030452°$	$\phi = -47.27721648°, \theta = -0.00037395°$
100 GeV	0.02920247 -0.00137924 0.99957257 0.00137767 -0.99999804 -0.00142008 0.99957257 0.00141855 -0.02920052	0.02926554 -0.00146810 -0.99957059 0.00145955 -0.99999779 0.00151146 -0.99957061 -0.00150316 -0.02926333
	$\phi = 45.83668095°, \theta = -0.00003128°$	$\phi = -45.83848502°, \theta = -0.00017071°$
150 GeV	0.01294584 0.00288311 0.99991204 -0.00288466 -0.99999157 0.00292069 0.99991204 -0.00292221 -0.01293742	0.01279645 0.00286726 -0.99991401 -0.00287433 -0.99999165 -0.00290427 -0.99991399 0.00291125 -0.01278811
	$\phi = 45.37076234°, \theta = -0.00003118°$	$\phi = -45.36648334°, \theta = -0.00014233°$
200 GeV	0.00485465 0.00507210 0.99997535 -0.00507410 -0.99997414 0.00509672 0.99997534 -0.00509871 -0.00482879	0.00479813 0.00511537 -0.99997541 -0.00512565 -0.99997365 -0.00513996 -0.99997535 0.00515019 -0.00477179
	$\phi = -45.13870744°, \theta = -0.00004041°$	$\phi = -45.13708133°, \theta = -0.00020778°$
250 GeV	0.00002865 -0.00640908 0.99997946 -0.00641177 -0.99995891 0.00[illegible]913 0.99997944 0.00640913 0.00001245	0.00007959 0.00643816 -0.99997927 0.00644504 -0.99995851 -0.00643751 -0.99997923 0.00644440 0.00012109
	$\phi = -45.00023181°, \theta = 0.00000941°$	$\phi = -44.99712530°, \theta = -0.00011464°$

The determinants of all the spin matrice are 1 ± 10^{-8}

Table 2.4a 6-D orbital maps of snakes with the variable ($x, p_x, y, p_y, -ct, p_t$) at high energy setting

E=25. GeV

0th order map	-0.1409555687180603E-03					
	0.3358052357261017E-06					
	-0.4801203199174461E-03					
	-0.7802012015377734E-04					
	-12.29079225657041					
	0.					
1st order map	0.99711713	12.27386124	0.00110738	-0.02550310	0.	0.00038444
	-0.00044143	0.99743369	0.00006690	-0.00503568	0.	-0.00000515
	-0.00382319	0.02406099	0.93356898	11.92552100	0.	0.00115692
	-0.00015083	0.00652518	-0.01067735	0.93474402	0.	0.00010906
	-0.00000215	0.00036189	-0.00011210	-0.00020649	1.0	0.02099824
	0	0.	0.	0.	0.	1.0

E=250GeV

Zeroth order map	0.6554569450470079E-08					
	-0.7465596586062003E-08					
	0.8642845640906037E-07					
	0.1595308597917521E-07					
	-12.28041065499392					
	0.0					
1st order map	0.99987402	12.27993881	0.00007164	-0.00029680	0.	0.00000018
	-0.00002035	0.99987606	-0.00000085	-0.00012853	0.	0.00000000
	-0.00002987	0.00014282	0.99947619	12.27772255	0.	0.00000012
	-0.00001740	-0.00013731	-0.00008627	0.99946440	0.	0.00000003
	0.	0.00000009	0.	-0.00000006	1.	0.00020931
	0.	0.	0.	0.	0.	1.

The second order coefficients are given as follows (E=250 GeV)

x_o^2	$x_o \cdot p_{xo}$	p_{xo}^2	$x_o \cdot y_o$
0.02303934	0.00973409	-0.61665107	-0.29190488
0.00069150	-0.02909934	-0.18357057	-0.04768163
-0.03238993	-0.43986280	-1.35570630	0.03756494
-0.00537809	-0.06730301	-0.19334167	0.01038820
-0.00003206	-0.00026759	-6.14121377	-0.00000009
0.	0.	0.	0.

+

$p_{xo} \cdot y_o$	y_o^2	$x_o \cdot p_{yo}$	$y_o \cdot p_{yo}$
-1.56633933	-0.03947694	-1.56646593	-9.62620884
-0.29365740	0.00017903	-0.29367107	-2.04001464
0.08352857	-0.00198998	0.08389846	0.02223569
0.08994011	-0.00013041	0.09001595	1.02120092
0.00013538	-0.00012640	0.00019041	0.00241431
0.	0.	0.	0.

+

$y_o \cdot p_{yo}$	$x_o \cdot p_{to}$	$p_{xo} \cdot p_{to}$	$y_o \cdot p_{to}$
0.00561049	0.00004287	-12.28015316	-0.00002543
0.08343674	-0.00001359	0.00004012	-0.00000009
-0.26890199	0.00016369	-0.00056972	0.00202648
0.00077952	0.00000003	-0.00004256	0.00024472
-0.00102856	0.	-0.00000078	0.00000023
0.	0.	0.	0.

+

p_{yo}^2	$p_{yo} \cdot p_{to}$	p_{to}^2
1.45429993	0.00087571	-0.00000061
0.50979 93	0.00012782	0.
-0.81574917	-12.26702986	-0.00000088
0.13924073	0.00203844	-0.00000012
-6.14288275	0.00000136	-0.00031398
0.	0.	0.

- The symplecticity violation of the orbital maps of the snakes directly calculated from a field map is found 5.47×10^{-4} . We introduce the exponential representation of Lie operators for a matrix, and then an iterative procedure is developed to symplectify the maps of Siberian Snakes up to the second order (see Table 3).

Symplectic Condition for the Linear Map of the Snake Obtained by TPSA

Take the linear map of the Snake for the particles of 250GeV, for example, to check the symplecticity violation

$$M_T = \begin{bmatrix} 0.99987402 & 12.27993881 & 0.00007164 & -0.00029660 & 0. & 0.00000018 \\ -0.00002035 & 0.99987606 & -0.00000085 & -0.00012853 & 0. & 0. \\ -0.00002987 & 0.00014282 & 0.99947619 & 12.27772255 & 0. & 0.00000012 \\ -0.00001740 & -0.00013731 & -0.00008627 & 0.99946440 & 0. & 0.00000003 \\ 0. & 0.00000009 & 0. & -0.00000006 & 1. & 0.00020931 \\ 0. & 0. & 0. & 0. & 0. & 1. \end{bmatrix}$$

Then,

$$M_T^T \cdot J \cdot M_T - J$$

$$= \begin{bmatrix} 0.00000000E+00 & -0.10447375E-08 & 0.16545028E-04 & 0.55258523E-04 & 0.00000000E+00 & 0.48549000E-11 \\ 0.10447375E-08 & 0.00000000E+00 & 0.55156686E-04 & \underline{0.54702027E-03} & 0.00000000E+00 & -0.17995693E-06 \\ -0.16545028E-04 & -0.55156686E-04 & 0.00000000E+00 & 0.60216855E-07 & 0.00000000E+00 & 0.29994791E-07 \\ -0.55258523E-04 & \underline{-0.54702027E-03} & -0.60216855E-07 & 0.00000000E+00 & 0.00000000E+00 & 0.18841908E-06 \\ 0.00000000E+00 & 0.00000000E+00 & 0.00000000E+00 & 0.00000000E+00 & 0.00000000E+00 & 0.00000000E+00 \\ -0.48549000E-11 & 0.17995693E-06 & -0.29994791E-07 & -0.18841908E-06 & 0.00000000E+00 & 0.00000000E+00 \end{bmatrix}$$

The maximum symplecticity violation: 5.4702027×10^{-4}.

The determinant deviation from 1(unit): 5.3169529×10^{-8}.

Maximum error of the magnetic field in Maxwell equations: 1.276×10^{-3}

The concept of symplectification

Suppose a symplectic map of phase space, $\bar{m}_\varepsilon(\bar{x},\bar{p})$. Let us assume that we expand this map in powers of ε to a specified order k and denote this map by $\bar{m}_\varepsilon^k$:

$$\bar{m}_\varepsilon^k = \bar{T}^0 + \bar{T}^1\varepsilon + \cdots + \bar{T}^k\varepsilon^k.$$

Two concepts:

- Symplectic Completion of the Taylor Coefficients $\bar{T}^j$

$$\bar{n}_\varepsilon^k = \bar{W}^0 + \bar{W}^1\varepsilon + \cdots + \bar{W}^k\varepsilon^k. \tag{3.2.2}$$

$$\bar{n}_\varepsilon^k + \Delta\bar{n}_\varepsilon^k = \sum_{j=0}^{k}(\Delta\bar{W}^j + \bar{W}^j)\varepsilon^j \tag{3.2.3}$$

- Symplectic completion of a map

Linear map is taken to do spin tracking

Exponential Representation of Lie Map for symplectifying the maps of Snakes

Construct a new map M_K, so that

$$M = D(\frac{L}{2}) \cdot M_K \cdot D(\frac{L}{2}),$$

L is the length of a Snake, $D(L/2)$ is the drift matrix. Then, the linear part of M_K is a matrix near identity.

A map near the identity can be expressed as follow:

$$M_K = \exp(\vec{F} \cdot \nabla) I_d$$

where I_d is identity map. $\vec{F} \cdot \nabla$ is Lie operator.

Poisson Bracket is defined as

$$:f: = \frac{\partial f}{\partial x} \cdot \frac{\partial}{\partial p_x} - \frac{\partial f}{\partial p_x} \cdot \frac{\partial}{\partial x} = \begin{pmatrix} \frac{\partial f}{\partial x} & \frac{\partial f}{\partial p_x} \end{pmatrix} \begin{pmatrix} 0 & 1 \\ -1 & 0 \end{pmatrix} \begin{pmatrix} \frac{\partial}{\partial x} \\ \frac{\partial}{\partial p_x} \end{pmatrix} = (\vec{\nabla} f)^T \cdot J \cdot \vec{\nabla} = -J\vec{\nabla} f \cdot \vec{\nabla}$$

If M_K is symplectic, then we obtain

$$\vec{F} \cdot \nabla = :f: = -J\vec{\nabla} f$$

$$f(\vec{z}) = \int_0^{\vec{z}} J \cdot \vec{F}(\vec{z}') \cdot d\vec{z}'$$

where $\vec{z} = (x,\ p_x,\ y,\ p_y,\ -c\Delta t,\ p_t)$

An iterative procedure to get $\vec{F}$:

$$M_K = \exp(\vec{F}_o \cdot \nabla) I_d \rightarrow \vec{F}_o$$

$$\text{do loop} \begin{cases} \exp(-\vec{F}_j \cdot \vec{\nabla}) M_K - I_d = \vec{m} \\ \Downarrow \\ \vec{F}_{j+1} = \vec{F}_j + \vec{m} \end{cases}$$

when $\vec{m}$ < converge error given

$$\downarrow$$

$$:f: = \vec{F} \cdot \vec{\nabla}$$

$$\downarrow$$

$$M_{K\_sym} = \exp(:f:) Id$$

$$\downarrow$$

$$M_{sym} = D(\frac{L}{2}) \cdot M_{k\_sym} \cdot D(\frac{L}{2})$$
$$= D(\frac{L}{2}) \cdot \exp(:f:) I_d \cdot D(\frac{L}{2})$$

Path length we used: diagonal of 6-D hypercube

$\vec{z}_o = (0, 0, 0, 0, 0, 0) \rightarrow \vec{z} = (x, p_x, y, p_y, -cdt, p_t)$

Table 3.1 The symplectified linear maps of a Snake and their symplecticity

E=25. GeV

Symplectified	0.99711554	12.27394059	-0.00375918	-0.02971225	0.	0.00038518
1st order Map	-0.00044179	0.99745011	-0.00005640	-0.00164909	0.	-0.00000146
	0.00085553	0.02774281	0.93337028	11.94264992	0.	0.00115408
	-0.00007184	0.00295773	-0.01069278	0.93456523	0.	0.00010818
	0.00000111	0.00040251	-0.00011334	-0.00021412	1.	0.02099825
	0.	0.	0.	0.	0.	1.0

$M^T \cdot J \cdot M - J =$

$$\begin{bmatrix} 0. & 0.27251E-08 & 0.47700E-13 & 0.41281E-11 & 0. & 0.35250E-14 \\ -0.27251E-08 & 0. & 0.54769E-11 & -0.31580E-11 & 0. & -0.18758E-11 \\ -0.47700E-13 & -0.54769E-11 & 0. & -0.61026E-10 & 0. & 0.39773E-12 \\ -0.41281E-11 & -0.31580E-11 & 0.61026E-10 & 0. & 0. & -0.35995E-12 \\ 0. & 0. & 0. & 0. & 0. & 0. \\ -0.35250E-14 & 0.18758E-11 & -0.39773E-12 & 0.35995E-12 & 0. & 0. \end{bmatrix}$$

The deviation of the determinant from 1: 0.26640723E-08

E=250.GeV

Symplectified	0.99987402	12.27993880	-0.00000235	-0.00036238	0.	0.00000013
1st order map	-0.00002035	0.99987606	-0.00000912	-0.00015614	0.	0.
	0.00004410	0.00020831	0.99947619	12.27772254	0.	0.
	-0.00000913	-0.00010970	-0.00008626	0.99946440	0.	0.00000001
	0.	0.00000013	-0.00000001	-0.00000018	1.0	0.00020931
	0.	0.	0.	0.	0.	1.0

$M^T \cdot J \cdot M - J =$

$$\begin{bmatrix} 0. & 0.22039E-08 & -0.34293E-13 & -0.46319E-12 & 0. & -0.47910E-19 \\ -0.22039E-08 & 0. & -0.37064E-12 & -0.12354E-11 & 0. & -0.70241E-16 \\ 0.34293E-13 & 0.37064E-12 & 0. & -0.42443E-08 & 0. & -0.34691E-16 \\ 0.46319E-12 & 0.12354E-11 & 0.42443E-08 & 0. & 0. & -0.84241E-16 \\ 0.0 & 0.0 & 0. & 0. & 0. & 0. \\ 0.47910E-19 & 0.70241E-16 & 0.34691E-16 & 0.84241E-16 & 0. & 0. \end{bmatrix}$$

The deviation of the determinant from 1: -0.20404467E-08

Table 3.2 The symplectified second order coefficients of a Snake's map for the protons with the energy of 250 GeV at high energy setting

$$\begin{bmatrix} x_a^2 & x_a \cdot p_{xa} & p_{xa}^2 & x_a \cdot y_a \\ 0.02303934 & 0.00976078 & -0.61646155 & -0.21619516 \\ 0.00069211 & -0.02908918 & -0.18351881 & -0.03537210 \\ -0.10809657 & -1.19092179 & -3.66103610 & 0.00128103 \\ -0.01768602 & -0.21820923 & -0.74449077 & 0.00704761 \\ -0.00000615 & -0.00005068 & -6.14011250 & -0.00000003 \\ 0. & 0. & 0. & 0. \end{bmatrix} +$$

$$\begin{matrix} p_{xa} \cdot y_a & y_a^2 & x_a \cdot p_{ya} & y_a \cdot p_{ya} \\ -1.19082535 & -0.00061269 & -1.19093263 & -7.32108631 \\ -0.21820515 & 0.00352144 & -0.21821168 & -1.48890894 \\ 0.05736501 & -0.00198868 & 0.05775346 & 0.98313234 \\ 0.08776228 & -0.00013115 & 0.08783942 & 1.02059284 \\ 0.00013923 & -0.00012372 & 0.00006173 & 0.00164540 \\ 0. & 0. & 0. & 0. \end{matrix} +$$

$$\begin{matrix} y_a \cdot p_{ya} & x_a \cdot p_{ta} & p_{xa} \cdot p_{ta} & y_a \cdot p_{ta} \\ 0.05808090 & 0.00020186 & -12.27930018 & -0.00013947 \\ 0.08780034 & -0.00001231 & 0.00019925 & -0.00000000 \\ -0.26888323 & 0.00006204 & -0.00060672 & 0.00204296 \\ 0.00077525 & 0.00000002 & -0.00002726 & 0.00024740 \\ -0.00099562 & 0. & -0.00000092 & 0.00000024 \\ 0. & 0. & 0. & 0. \end{matrix} +$$

$$\begin{matrix} p_{ya}^2 & p_{ya} \cdot p_{ta} & p_{ta}^2 \\ 0.49369955 & 0.00091557 & -0.00000046 \\ 0.51037486 & 0.00005009 & 0. \\ -0.81566519 & -12.26692037 & -0.00000073 \\ 0.13925737 & 0.00205491 & -0.00000012 \\ -6.14278991 & 0.00000163 & -0.00031398 \\ 0. & 0. & 0. \end{matrix}$$

4. Spin tracking with "real" Siberian Snakes in RHIC

- Upgrade the code SPINK for numerical spin tracking.
- Spin tracking with "real" Siberian Snakes in RHIC has been completed.

  with no closed orbit distortion (COD) (see Figure 7)

  with corrected COD of 0.2mm (Figure 8)

  0.5mm (Figure 9).

  Single particle:

  normalized emittances = 5πmm·mard,

  10πmm·mard,

  15πmm·mard,

  20πmm·mard.

  Acceleration: 25 GeV - 250GeV.

Single particle tracking shows that "real" Siberian Snakes can keep the polarization of the protons through the acceleration to more than 95% in a RHIC machine with no closed orbit distortion, and to more than 88% in a machine with corrected closed orbit distortion of 0.2mm(r.m.s) if the

polarized proton is extracted from a contour of 10πmm.mrad. But the polarization is only 38% when the polarized proton is extracted from a contour of 5πmm.mrad in the case that corrected closed orbit distortion is 0.5mm(r.m.s).

- Multi-particle tracking : 32 particles

  (1) Generated from the inside of the phase space volume randomly with a Gaussian distribution.

  (2) Acceleration: from 197.92 GeV ($G\gamma$=378.18)

  to 250.00 GeV ($G\gamma$= 477.67).

Multi-particle tracking shows that "real" Siberian Snakes can keep the polarization of the protons in RHIC through the acceleration in a machine with corrected closed orbit distortion about 0.2mm(r.m.s) to 73.00% (r.m.s.) (see Figure 10), if the polarized protons are extracted from a contour of 10πmm.mrad.

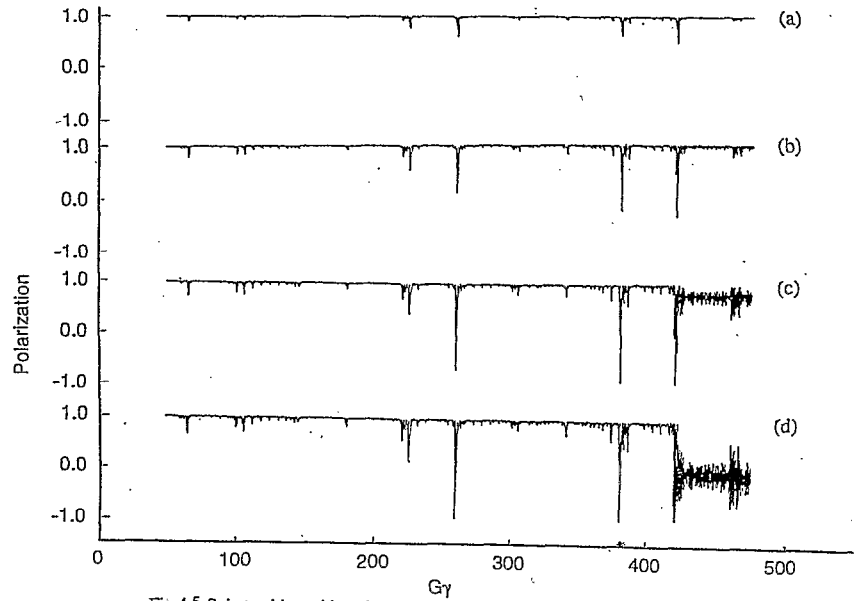

Fig 4.5 Spin tracking with real Snakes in RHIC, orbital tracking with the symplectified "transport" matrices from Code MAD
a. $\varepsilon_x = \varepsilon_y =$ 5πmm·mrad, *b.* $\varepsilon_x = \varepsilon_y =$ 10πmm·mrad,
c. $\varepsilon_x = \varepsilon_y =$ 15πmm·mrad, *d.* $\varepsilon_x = \varepsilon_y =$ 20πmm·mrad.

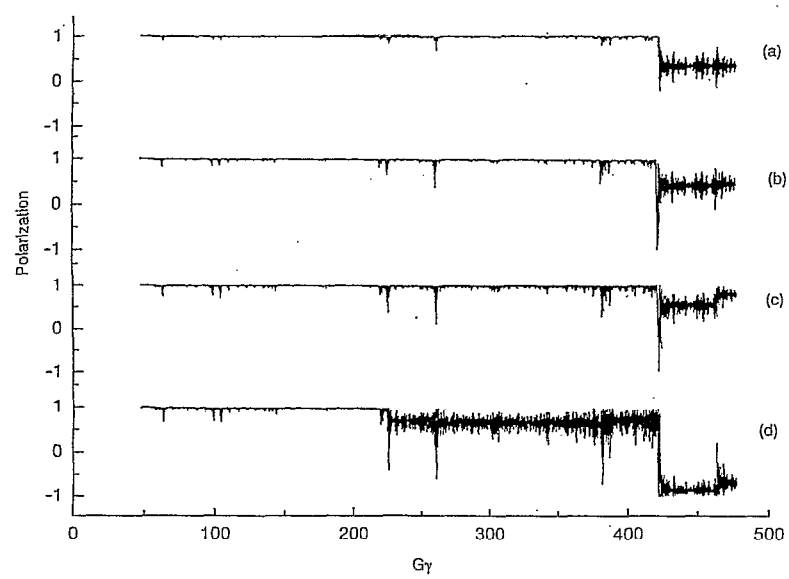

Fig 4.11 Spin tracking with real Snakes in RHIC, orbital tracking with the symplectified "transport" matrices from Code MAD
Misalignment randomly assigned, Corrected Closed Orbit Distortion ≈ 0.5 mm
a. $\varepsilon_x = \varepsilon_y =$ 5πmm·mrad, *b.* $\varepsilon_x = \varepsilon_y =$ 10πmm·mrad,
c. $\varepsilon_x = \varepsilon_y =$ 15πmm·mrad, *d.* $\varepsilon_x = \varepsilon_y =$ 20πmm·mrad

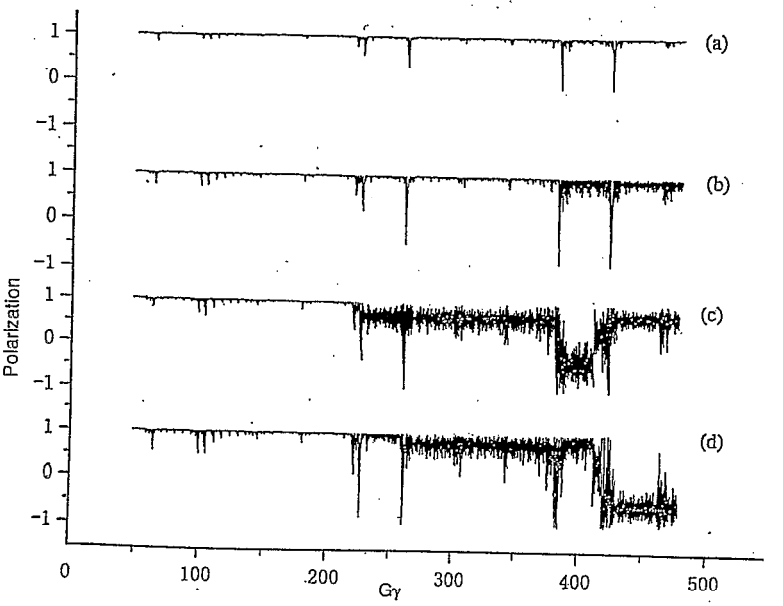

Fig 4.10 Spin tracking with real Snakes in RHIC, orbital tracking with the symplectified "transport" matrices from Code MAD
Misalignment randomly assigned, Corrected Closed Orbit Distortion ≈ 0.2 mm
a. $\varepsilon_x = \varepsilon_y =$ 5πmm·mrad, *b.* $\varepsilon_x = \varepsilon_y =$ 10πmm·mrad,
c. $\varepsilon_x = \varepsilon_y =$ 15πmm·mrad, *d.* $\varepsilon_x = \varepsilon_y =$ 20πmm·mrad.

94

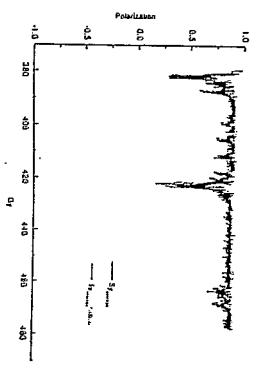

(a) With "perfect" Snakes in RHIC

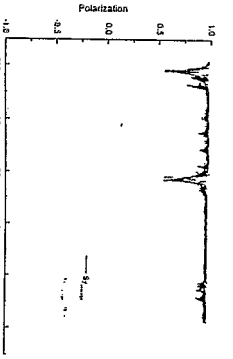

(b) With "real" Snakes in RHIC

Fig 4.12 The average results of polarization from 32 particles' tracking in RHIC with no misalignment and no field errors. Original emittance: 10πmm.mrad.

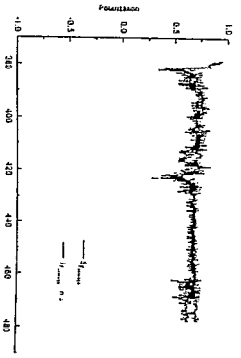

Fig 4.13 The average results of polarization from 32 particles' tracking in RHIC with r.m.s. misalignment of 2.5mm and corrected vertical closed orbit distortion of 0.185mm. Orginal emittance: 10πmm.mrad.

96

- Due to the presence of large longitudinal magnetic fields in "real" Snake, the coupling of horizontal and vertical betatron motions are found, and the vertical betatron tune is found to change from 29.22 at the injection energy 25 GeV to 29.18 at the top energy 250 GeV (see Figure 11). It means that the operation points cross many different resonances during the acceleration.

$\Delta Q_x = 0.01919$
$\Delta Q_y = 0.0306$ (2-G

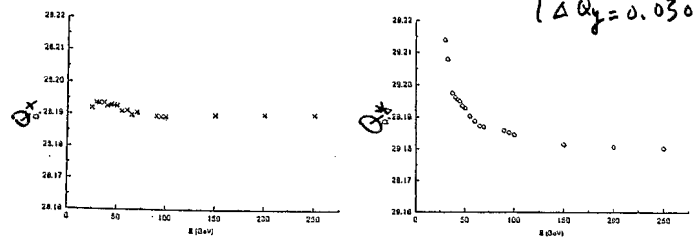

Fig 4.7 The transverse betatron tunes Q_x and Q_y shifts through the acceleration

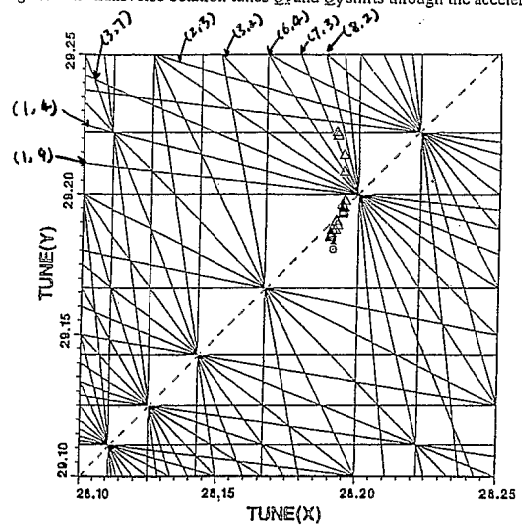

(n, m)
$nQ_x \pm mQ_y = p$
$n+m =$ order

Fig 4.8 Tune diagram showing the selected working point of RHIC at $Q_x = 28.19$ and $Q_y = 29.18$ (with symbol "o") with neighboring sum and difference resonances. The shifted working point due to the insertion of Snakes are shown with symbol "Δ" in the diagram.

5. Conclusion

We have solved the symplectic problem on the orbital motion in the Snake magnet, one of the key issues for spin tracking, and have performed the long term tracking of spin and orbital motion of polarized protons in RHIC. The simulated results show the necessity of high level correction of closed orbit distortion, and predict the "actual" operation conditions in RHIC.

Spin Flipping in RHIC

M. Bai, A. Lehrach, A. Luccio, W. W. MacKay, T. Roser, N. Tsoupas
Brookhaven National Laboratory, Upton, NY 11973, U.S.A

Abstract

At the Relativistic Heavy Ion Collider (RHIC), polarized protons will be accelerated and stored for spin physics experiments. Two full helical snakes will be used to eliminate the depolarization due to imperfection and intrinsic spin resonances. Since no resonances are crossed in RHIC, the beam polarization remains fixed through acceleration. However, in order to reduce systematic errors, the experiment often requires the polarization direction reversed. This paper presents a method of using an AC dipole to obtain a full spin flip in the presence of two full snakes. A similar method of using an rf solenoid for spin flip was tested at IUCF [1, 2].

References

[1] D.D.Caussyn et al., Phys.Rev. Lett. 73, 2857 (1994).
[2] B.B.Blinov et al., PRL 81, 2906 (1998).

Spin Flipping in RHIC

Mei Bai

Brookhaven National Laboratory

RSC2000, Oct. 13 ~ Oct. 14, 2000

BROOKHAVEN
NATIONAL LABORATORY

- Thomas-BMT equation

$$\frac{d\vec{S}}{dt} = \vec{\Omega} \times \vec{S} = -\frac{e}{\gamma m}\left[G\gamma B_{\perp} + (1+G)B_{//} + \left(G\gamma - \frac{\gamma}{\gamma^2 - 1}\right)\frac{\vec{E} \times \vec{\beta}}{c}\right] \times \vec{S}$$

S: spin vector in the particle's rest frame.
Ω: spin precession frequency.
G: anomalous gyromagnetic g-factor. For proton, G=1.7928474.
$\mathbf{B}_{\perp}$: transverse magnetic field in the laboratory frame.
$\mathbf{B}_{//}$: longitudinal magnetic field in the laboratory frame.
E: electric field.
β: the Lorentz factor.

In a flat circular accelerator. While the particle travels around the machine, its spin vector precesses around the guiding magnetic field, or vertical direction.

BROOKHAVEN NATIONAL LABORATORY

- Spin tune ν_s :
  number of spin precessions around the axis when the particle circulates one turn in the machine.

  For a perfect machine,

  spin tune $\nu_s = G\gamma$

  For RHIC,
  spin tune = $\frac{1}{\pi}|\phi_1 - \phi_2|$, ϕ_1 and ϕ_2 are the axis angles of the two snakes with snake axis set at (45°,-45°), the spin tune = 0.5.

BROOKHAVEN NATIONAL LABORATORY

– RHIC polarized proton acceleration layout

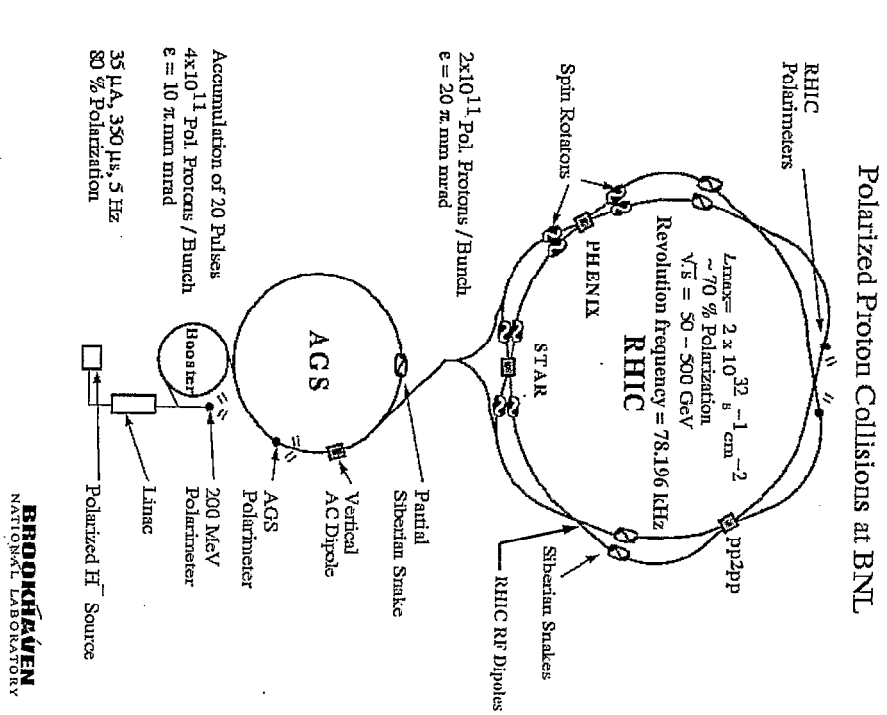

- Spin flipper -- use an RF dipole to induce a spin flip in the presence of full snake(s)

An RF dipole with horizontal oriented oscillating dipole field induces a spin resonance at

$$\nu_m = \frac{\textit{RF dipole field oscillation frequency}}{\textit{beam revolution frequency}}$$

Its strength is: $\varepsilon = \frac{1 + G\gamma}{4\pi} \frac{B_m L}{B\rho}$

To achieve more than 99% spin flip, the frequency ramping rate of the RF dipole has to satisfy:

$$\frac{P_f}{P_i} = 2e^{-\frac{\pi|\varepsilon|^2}{2\alpha}} - 1 \geq -0.99$$

BROOKHAVEN NATIONAL LABORATORY

– spin flipping

» tune the snakes axis so that the spin tune is away from 1/2

» adiabatically turn on the RF dipole field with its oscillation frequency away from the spin tune

» slowly ramp the RF dipole oscillation frequency across the spin tune so that an adiabatic spin flip is induced

» slowly turn off the RF dipole

» turn the snake axis back to 45°, so that the spin tune is back to 1/2

BROOKHAVEN NATIONAL LABORATORY

• A simple simulation of using an RF dipole as a spin flipper
» tracking model

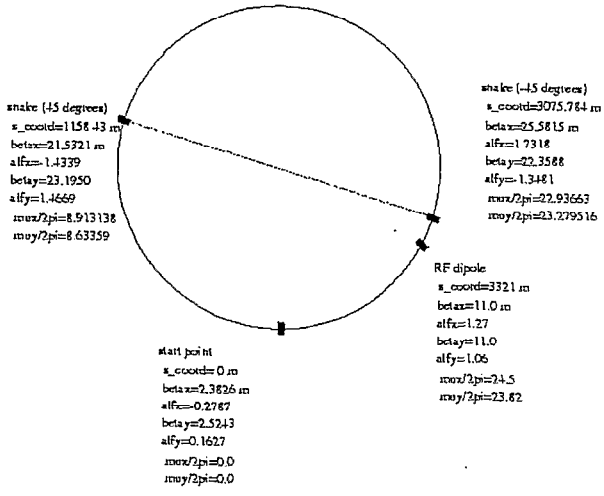

BROOKHAVEN NATIONAL LABORATORY

» RF dipole amplitude and tune profile

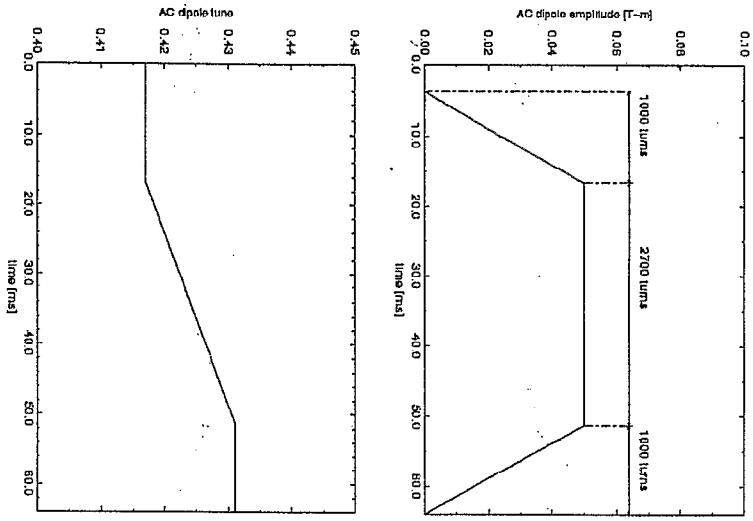

BROOKHAVEN NATIONAL LABORATORY

» tracking result with a beam of 1000 particles

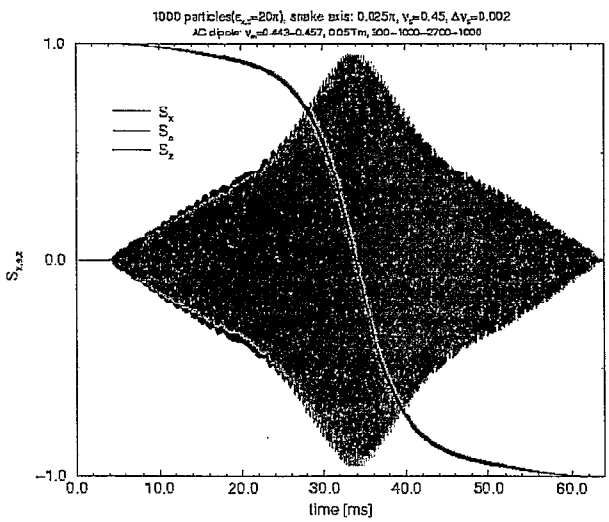

BROOKHAVEN NATIONAL LABORATORY

- RHIC AC dipoles

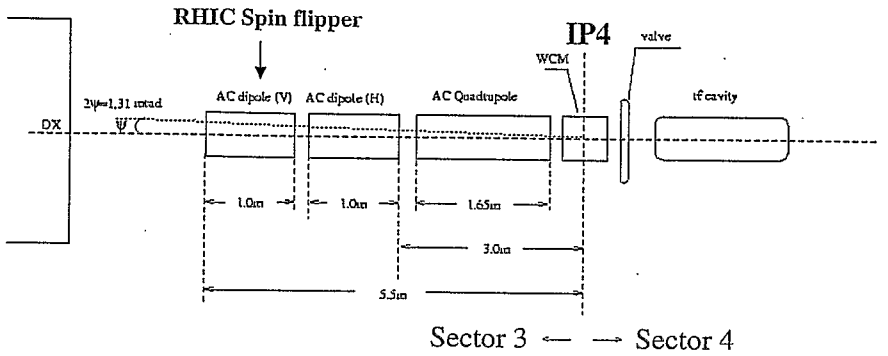

BROOKHAVEN NATIONAL LABORATORY

- Spin flipper for RHIC

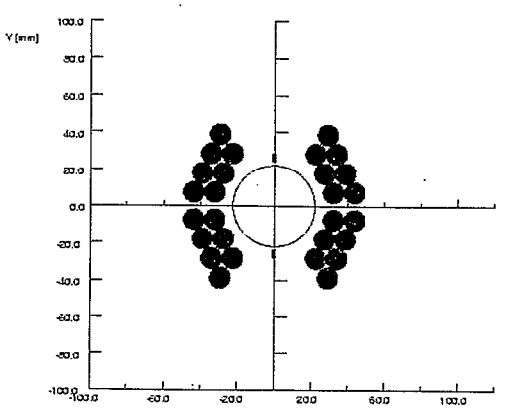

Magnet parameter:

length: 1.4m
Max field: 300 Gauss
frequency: 37.5kHz
tunning: 2.5kHz

BROOKHAVEN NATIONAL LABORATORY

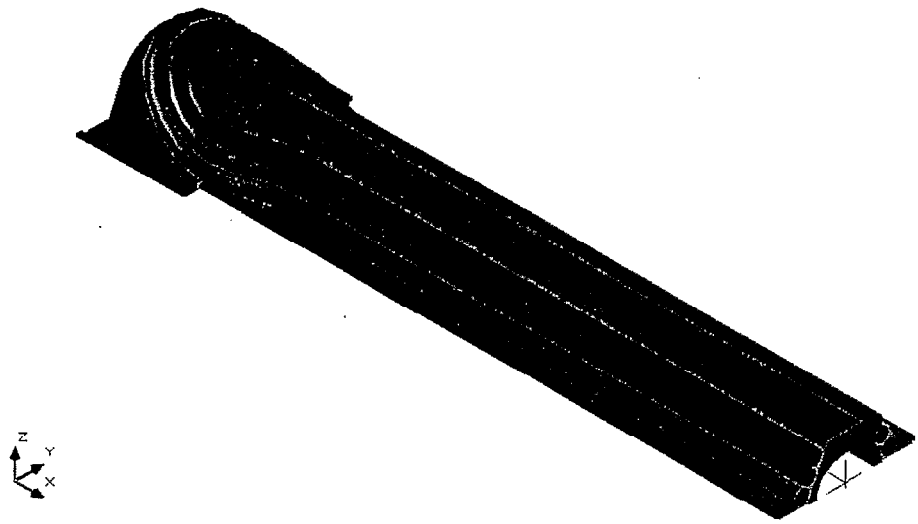

- Status and Plans

magnet status

– preliminary design completed
– 2 ceramic beam pipes are purchased and coated
– magnet stands are under machining.
– Designers are working on the detail mechanical drawings

Plans:

– the magnet stands will be installed in the ring along with the beam tubes in Jan. 2001.
– The parts for the coil is expected to be ready early Feb. 2001
– finish coil winding, assembly and testing in May 2001.
– For the 1st year, our goal is to reach ≥100 Gm at 37.5 kHz.

Overview of RHIC spin commissioning and plans

Thomas Roser

Overview of RHIC spin commissioning and plans

Summary of RHIC heavy ion commissioning and operation

Summary of RHIC spin commissioning

Plans for RUN2001

BROOKHAVEN NATIONAL LABORATORY

Thomas Roser
RSC 2000
October 13 - 14, 2000

Parameters and goals for RHIC RUN2000

- 60 bunches per ring ✓
- 5×10^{8} Au/bunch ✓
- Longitudinal emittance: 0.3 eVs/nucleon/bunch ✓
- Transverse emittance at storage: 15 π µm (norm, 95%) ✓
- Initial storage energy: γ = 70 [66 GeV/nucl.] ✓ (This energy is below the lowest quench of any DX magnet)
- Lattice at injection and acceleration: β^*= 3 m @ 2, 4, 8, and 12 o'clock
  β^*= 8 m @ 6 and 10 o'clock
- Lattice at storage and collision: β^*= 3 m @ 2, 4, 8, and 12 o'clock
  β^*=2- 8 m @ 6 and 10 o'clock
- Luminosity: 2×10^{25} cm^{-2} s^{-1} ✓
- Integrated luminosity: a few (µb)$^{-1}$ ✓

BROOKHAVEN NATIONAL LABORATORY

RF bunch merging in AGS

- 4 × 6 bunches injected from Booster
- Debunch / rebunch into 4 bunches at AGS injection
- Final longitudinal emittance: 0.3 eVs/nuc./bunch
- Achieved 4×10^{9} Au ions in 4 bunches at AGS extraction on 8/4/00

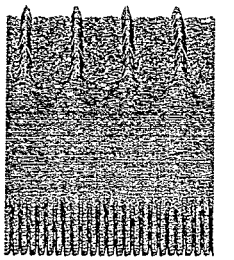

AGS circumference

BROOKHAVEN NATIONAL LABORATORY

RHIC beam measurements

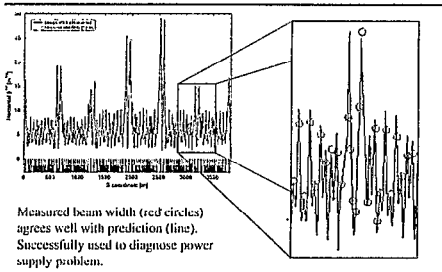

Measured beam width (red circles) agrees well with prediction (line). Successfully used to diagnose power supply problem.

BROOKHAVEN NATIONAL LABORATORY

Transition energy crossing

RHIC is first superconducting, slow ramping accelerator to cross transition energy:

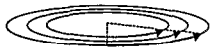

Slow and fast particles remain in step.
⇨ increased particle interaction (space charge)
⇨ short, unstable bunches

Cross unstable transition energy with radial energy jump:

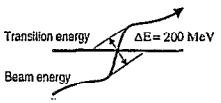

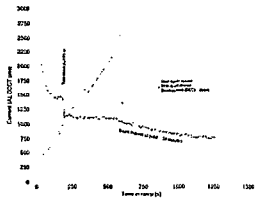

BROOKHAVEN NATIONAL LABORATORY

Bringing beams into collision

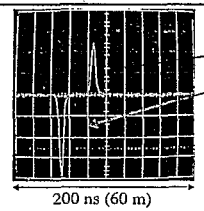

Beam in blue ring

Beam in yellow ring

200 ns (60 m)

Beams in collision at the interaction regions

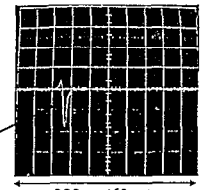

200 ns (60 m)

BROOKHAVEN NATIONAL LABORATORY

Ramp to first collision

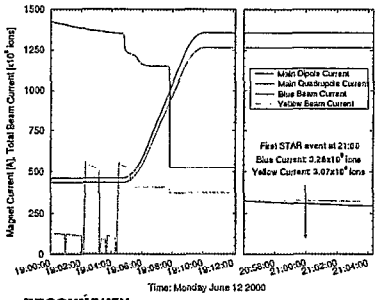

BROOKHAVEN NATIONAL LABORATORY

Collision rate at detectors

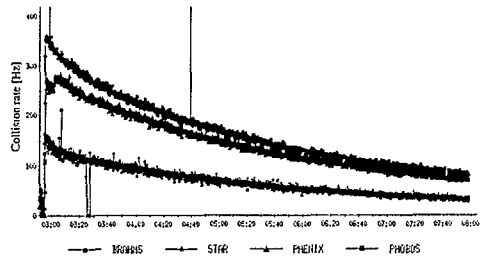

BROOKHAVEN NATIONAL LABORATORY

Specific luminosity

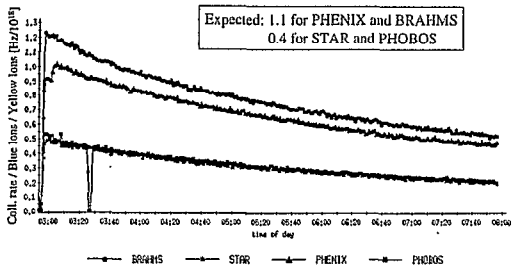

BROOKHAVEN NATIONAL LABORATORY

RUN2000 integrated Au-Au luminosity

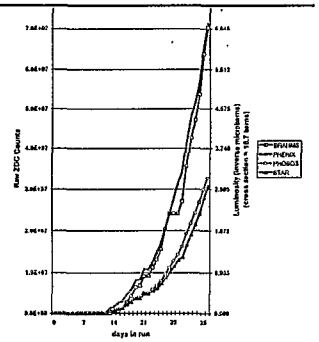

BROOKHAVEN NATIONAL LABORATORY

Parameters and goals for RHIC RUN2001

- Transition energy jump quadrupole power supplies installed
- 60 bunches per ring with 1×10^9 Au/bunch
- Storage energy: $\gamma = 107$ [100 GeV/nucl.]
- All bipolar power supplies installed:
  - Lattice at injection and acceleration: $\beta^* = 10$ m at all IR's
  - Lattice at storage and collision: $\beta^* = 2$-10 m at all IR's
- Luminosity goal: 2×10^{26} cm^{-2} s^{-1} (design luminosity)
- Availability: ≈ 75 %
- Machine efficiency: ≈ 50 %

BROOKHAVEN NATIONAL LABORATORY

Polarized proton collisions in RHIC

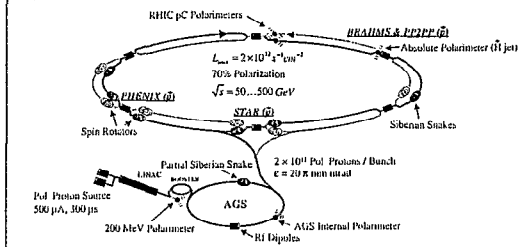

BROOKHAVEN NATIONAL LABORATORY

First Siberian Snake in RHIC Tunnel

Siberian Snake: 4 superconducting helical dipoles, 4Tesla,
2 m long with full 360° twist

⇨ Acceleration of spin polarized protons beams in RHIC

⇨ Beam studies in September 2000

Funded by RIKEN, Japan
Designed and constructed at BNL

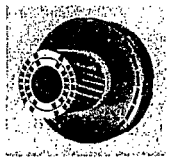

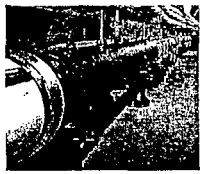

BROOKHAVEN NATIONAL LABORATORY

Single Snake in RHIC (E ≤ 100 GeV)

At E = 100.53 GeV: Gγ = 192 = 6 × 32
→ all IP's have same polarization
For snake axis at -52° → longitudinal polarization

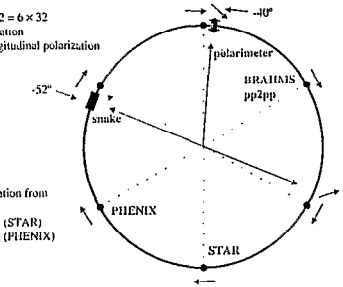

For Δp/p = ±0.001 max. deviation from long. polarization:
32 × Δp/p × 360° = ±12° [0.98] (STAR)
64 × Δp/p × 360° = ±24° [0.91] (PHENIX)

BROOKHAVEN NATIONAL LABORATORY

FY2000 commissioning plan

June-July 2000: (independent of RHIC operation)

- New pol. source (OPPIS) commissioned and beam transp. through linac: 65% polarization measured at 200 MeV polarimeter, 200 μA and 300 μs beam pulse (4×10^{11} polarized protons)

August 2000: (during RHIC Au stores)

- Accelerate single bunch (10^{11} pol. pr. / bunch) in Booster and AGS to Gγ = 46.5 (γ = 25.94) ✓
- Commission coupled spin resonance crossing using horizontal rf dipole ✓

September 2000: (dedicated RHIC operation)

- Inject 6 bunches (+ − + − + −) into RHIC blue ring with snake off. ✓
- Commission pC polarimeter and measure vertical polarization ✓
- Turn on snake and measure radial polarization ✓
- Accelerate and measure polarization ✓

BROOKHAVEN NATIONAL LABORATORY

Proton-Carbon CNI Polarimeter (AGS E950)

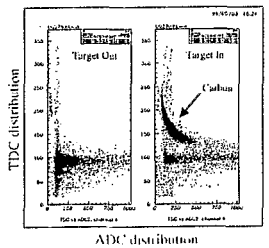

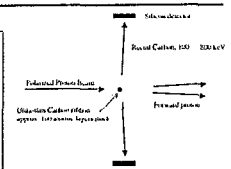

- 2-3% energy independent analyzing power for small-angle elastic scattering in the Coulomb-Nuclear Interference (CNI) region
- Slow recoil Carbon detected in between bunch crossings
- Fiber target allows for polarization profile measurement

BROOKHAVEN NATIONAL LABORATORY

Polarized proton injection into RHIC

Injection at $G\gamma = 46.5$ without snake: vertical polarization!

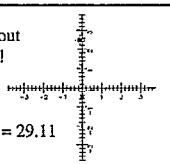

$\nu_y = 29.11$

Sensitive to betatron tune setting

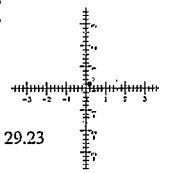

$\nu_y = 29.23$

BROOKHAVEN NATIONAL LABORATORY

Snake operating points

- Single snake RUN2000 B1 = B2
- Two snakes for RUN2001

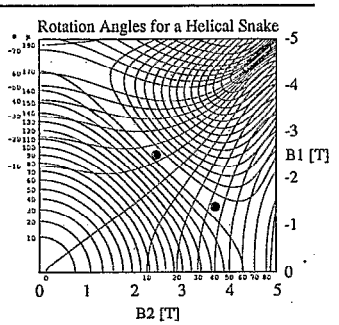

BROOKHAVEN NATIONAL LABORATORY

Spin commissioning with a single Snake

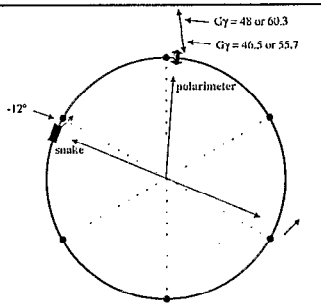

BROOKHAVEN NATIONAL LABORATORY

Acceleration with single snake

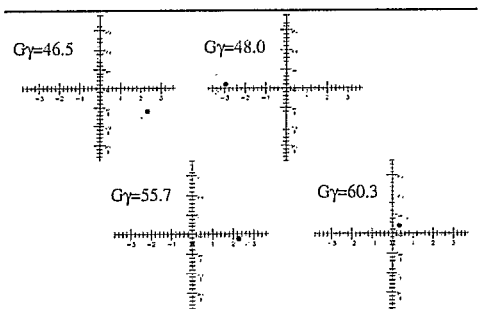

BROOKHAVEN NATIONAL LABORATORY

Measured RHIC asymmetries

RHIC asymmetries normalized to AGS (Preliminary)

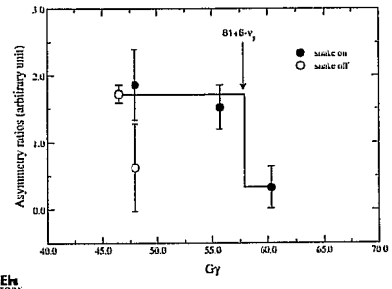

BROOKHAVEN NATIONAL LABORATORY

Spin resonances in RHIC (w/o Snakes)

Feb2000lattice $\nu_x = 28.23$ $\nu_y = 29.22$ and $\varepsilon_N = 10\pi$ mm-mrad

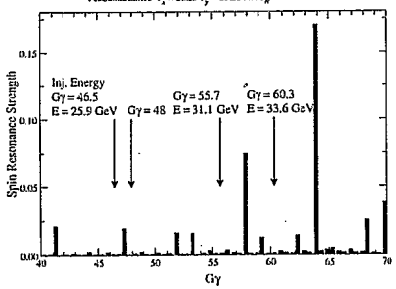

BROOKHAVEN NATIONAL LABORATORY

Polarized proton status and plans (1)

FY2000 run:

- Single Siberian snake and pC polarimeter installed in blue ring
- New polarized proton source: ~ 10^{12} pol. protons/pulse
- Goal: Accelerate polarized beam in blue ring

FY2001 run:

- All four Snakes and pC polarimeters installed in blue and yellow ring
- Goal: 100 GeV×100 GeV collision with long. pol. at interaction regions
  - Accelerate with two Snakes
  - Collide beams with one Snake per ring for longitudinal polarization
  - Polarization: ≥ 50 %
  - 10^{11} protons per bunch; 60 bunches; $\beta^* = 2$ m; $L = 5 \times 10^{30}$ cm^{-2} s^{-1}
  - Integrated luminosity per week : 1.5 (pb)$^{-1}$ (50% availability)
  - Accelerate polarized beam to 250 GeV

BROOKHAVEN NATIONAL LABORATORY

Polarized proton status and plans (2)

FY2002 run:

- All eight spin rotators installed
- Goal: 250 GeV×250 GeV collision with long. pol. at STAR and PHENIX

FY2003 run:

- Polarized hydrogen jet target for absolute polarimetry installed

BROOKHAVEN NATIONAL LABORATORY

Polarized Hydrogen Jet Target

- pC polarimeter is used as fast relative polarization monitor and was calibrated in AGS at 22 GeV to about 15 %.
- Polarized hydrogen jet target allows for absolute beam polarization measurement:

$$P_{\text{Beam}} = P_{\text{Target}} \frac{N_{\uparrow\uparrow\uparrow} - N_{\uparrow\downarrow\uparrow} + N_{\downarrow\uparrow\uparrow} - N_{\downarrow\downarrow\uparrow}}{N_{\uparrow\uparrow\uparrow} - N_{\uparrow\downarrow\uparrow} - N_{\downarrow\uparrow\uparrow} + N_{\downarrow\downarrow\uparrow}}$$

- Jet target thickness of 3×10^{11} cm^{-2} achievable (HERMES, PINTEX, NIKHEF)
- Jet polarization measurable to better than 3% using Stern-Gerlach method
- Collaboration started with Wisconsin, IUCF, and Amsterdam

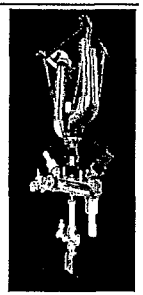

BROOKHAVEN NATIONAL LABORATORY

Pol. H jet target at Bates from NIKHEF

Summary

- Very successful first RHIC spin commissioning run:
  - RHIC Polarimeter commissioned
  - Single Siberian snake works
- With two snakes per ring and improved tune and orbit control during acceleration expect to preserve full beam polarization to 100 GeV
- Collisions of polarized protons are planned for FY 2001

BROOKHAVEN NATIONAL LABORATORY

Polarized Parton Distribution Functions with Estimate of Uncertainties

Y. Goto[1], N. Hayashi[2], M. Hirai[3], H. Kobayashi[2], S. Kumano[3], M. Miyama[4], T. Morii[5], N. Saito[1,2], T.-A. Shibata[6], and T. Yamanishi[7] (Asymmetry Analysis Collaboration)

[1]RIKEN BNL Research Center, Upton, NY 11973, U.S.A.

[2]Radiation Laboratory, RIKEN, Saitama 351-0198, Japan

[3]Department of Physics, Saga University, Saga 840-8502, Japan

[4]Department of Physics, Tokyo Metropolitan University, Tokyo 192-0397, Japan

[5]Faculty of Human Development, Kobe University, Kobe 657-8501, Japan

[6]Department of Physics, Tokyo Institute of Technology, Tokyo 152-8551, Japan

[7]Department of Management Science, Fukui University of Technology, Fukui 910-0028, Japan

Abstract

Experimental data on the structure function $g_1(x,Q^2)$ have been accumulated with the proton, deuteron and ^{3}He targets. We study parameterization of the polarized parton distributions (pol-PDFs) [1] in the leading order (LO) of α_s and in the next-to-leading order (NLO) with estimate of uncertainties.

The polarized distributions are provided with a number of parameters at Q^2=1 GeV^2 ($\equiv Q_0^2$). Considering the positivity condition and the helicity retention property following functional form is proposed for the pol-PDFs:

$$\Delta f_i(x,Q_0^2) = A_i x^{\alpha_i}(1+\gamma_i x^{\lambda_i}) f_i(x,Q_0^2), \tag{1}$$

where $\Delta f_i(x,Q_0^2)$ is an unpolarized parton distribution (GRV98). The subscript i denotes the type of the parton distribution $f_i \in (u_v, d_v, \bar{q}, g)$. The parameters A_i, α_i and λ_i are determined by fitting available experimental data on the inclusive spin asymmetry A_1 from experiments: EMC, SMC, SLAC (E130, E142, E143, E154, E155) and HERMES, where A_1 is expressed with the structure function g_1 and other known functions and g_1 is expressed as linear combination of pol-PDFs Δf_i. The first moments of Δu_v and Δd_v and are fixed by the semi-leptonic decay data by assuming the SU(3) symmetry, so that the number of free parameters is reduced from 16 to 14.

The χ^2 minimization is performed by using the CERN library subroutine MINUIT with the following definition,

$$\chi^2 = \sum (A_1^{data} - A_1^{calc})^2 / (\sigma_{A_1^{data}})^2 \tag{2}$$

comparing theoretical asymmetries with the experimental data weighted by square inverse of the error in each points. As a result, we obtain the minimumχ^2 : χ^2/d.o.f=322.6/359 for the LO and χ^2/d.o.f=300.4/359 for the NLO.

The uncertainties of pol-PDFs can be estimated from the errors of the parameters. However,

previous attempts to quantify the uncertainties on the pol-PDFs have been rather unsatisfactory. This is due to that extracting the uncertainties of pol-PDFs is not easy because there are strong correlations between pol-PDFs of different flavors and from different values of x and Q^2. We present preliminary results from an effort to quantify the uncertainties in polarized parton distribution functions.

[1] Y. Goto, N. Hayashi, M. Hirai, H. Horikawa, S. Kumano, M. Miyama, T. Morii, N. Saito,T.-A. Shibata, E. Taniguchi, and T. Yamanishi, hep-ph/0001046, Phys. Rev. D 62 34017 (2000).

RHIC-SPIN Collaboration Meeting in Kyoto

13 Oct 2000

Polarized Parton Distribution Functions with Estimate of Uncertainties

H. Kobayashi @ RIKEN

On behalf of

the Asymmetry Analysis Collaboration (AAC)

Y. Goto[1], N. Hayashi[2], H. Kobayashi[2], M. Hirai[3], S. Kumano[3], M. Miyama[4], T. Morii[5], N. Saito[1,2], T.-A. Shibata[6], T. Yamanishi[7]

[1]RIKEN BNL Research Center

[2]RIKEN

[3]Saga University

[4]Tokyo Metropolitan University

[5]Kobe University

[6]Tokyo Institute of Technology

[7]Fukui University of Technology

Contents

A talk about spin asymmetry data analysis

- Polarized Deep Inelastic Scattering
- What is the AAC Parameterization?
- Q^2 Evolution
- Fit Results
- Estimate of Uncertainties
- Summary

Polarized Deep Inelastic Scattering

Longitudinally Polarized Beam and Target

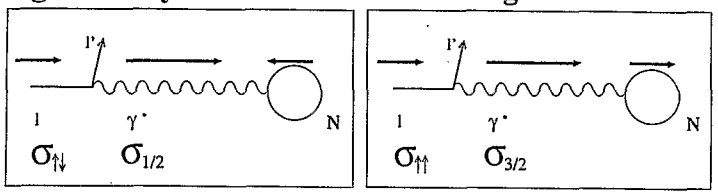

Cross Section of Polarized DIS

$$\sigma_{\uparrow\downarrow} = \overline{\sigma} + \frac{1}{2}\Delta\sigma, \qquad \sigma_{\uparrow\uparrow} = \overline{\sigma} - \frac{1}{2}\Delta\sigma$$

"Virtual Photon-Nucleon" Spin Asymmetry

$$A_1 = \frac{\sigma_{1/2} - \sigma_{3/2}}{\sigma_{1/2} + \sigma_{3/2}} \simeq \frac{1}{D}\frac{\sigma^{\uparrow\downarrow} - \sigma^{\uparrow\uparrow}}{\sigma^{\uparrow\downarrow} + \sigma^{\uparrow\uparrow}} = \frac{1}{D}\frac{\Delta\sigma}{2\overline{\sigma}} \simeq \frac{g_1(x,Q^2)}{F_1(x,Q^2)}$$

$$F_1(x,Q^2) = \frac{F_2(x,Q^2)}{2x\left[1 + R(x,Q^2)\right]}$$

Parton Model Analysis

$$\begin{aligned} g_1(x,Q^2) &= \frac{1}{2}\sum_{i=1}^{n_f} e_i^2 x\{\Delta C_q(x,\alpha_s) \otimes \left[\Delta q_i(x,Q^2) + \Delta\bar{q}_i(x,Q^2)\right] \\ &\quad + \Delta C_g(x,\alpha_s) \otimes \Delta g(x,Q^2)\} \end{aligned}$$

Convolusion $\quad f(x) \otimes g(x) = \int_x^1 \frac{dy}{y} f\left(\frac{x}{y}\right) g(y)$

What is the AAC Parameterization?

DGLAP Q^2 evolution

- $Q_0^2 = 1$ GeV^2.
- LO and NLO ($\overline{\text{MS}}$ scheme) analysis.

Computation Method

- χ^2 analysis using MINUIT.

$$\chi^2 = \sum \left(\frac{A_1^{\text{data}}(x,Q^2) - A_1^{\text{calc}}(x,Q^2)}{\delta A_1^{\text{data}}(x,Q^2)} \right)^2$$

  δA_1 includes both stat. and syst. errors.

- Functional form : $\frac{\Delta f_i(x,Q_0^2)}{f_i(x,Q_0^2)} = A_i x^{\alpha_i}(1 + \gamma_i x^{\lambda_i})$.
- Use GRV unpol PDF parameterization.
- Use $R(x,Q^2)$ parameterization from SLAC.
  $A_1(x,Q^2) = \frac{2xg_1(x,Q^2)}{F_2(x,Q^2)}\left[1 + R(x,Q^2)\right]$

Constraints & Conditions

- Positivity condition $\quad |\Delta f_i(x,Q_0^2)| \leq f_i(x,Q_0^2)$.
- SU(3) flavor symmetric sea at $Q_0^2 = 1$ GeV^2.
  $\Delta u_{sea}(x) = \Delta\bar{u}(x) = \Delta d_{sea}(x) = \Delta\bar{d}(x) = \Delta s(x) = \Delta\bar{s}(x)$
- First moments of Δu_v and Δd_v, constrained by axial charges for octet baryon.
  $\eta_{u_v} - \eta_{d_v} = F + D, \quad \eta_{u_v} + \eta_{d_v} = 3F - D$

Q^2 Evolution

Performance of the Q^2 Evolution Program

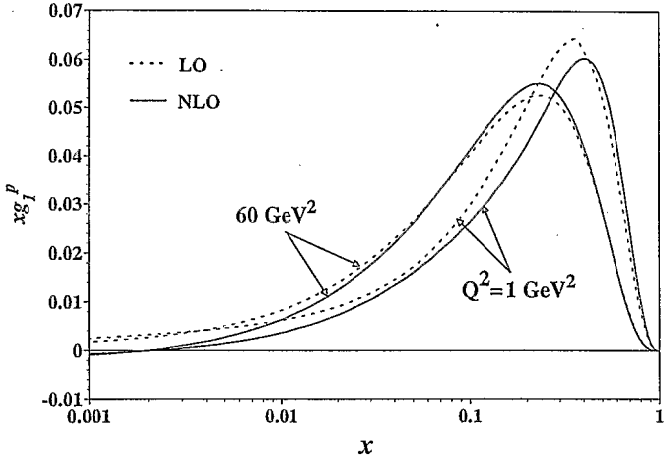

Q^2 Dependence of A_1 at $x = 0.117$

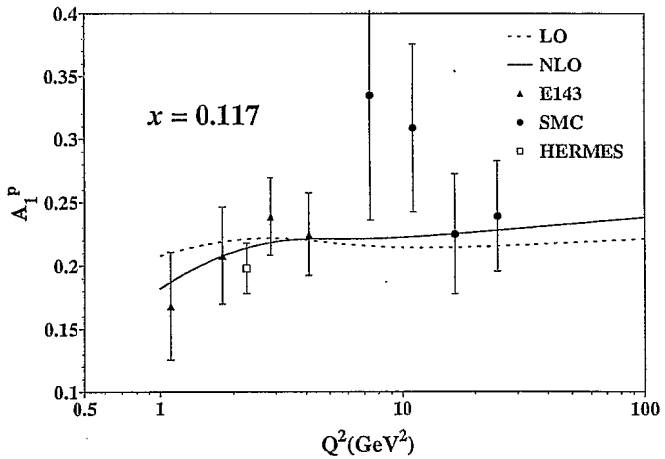

Fit Results of A_1 and Input 375 data points

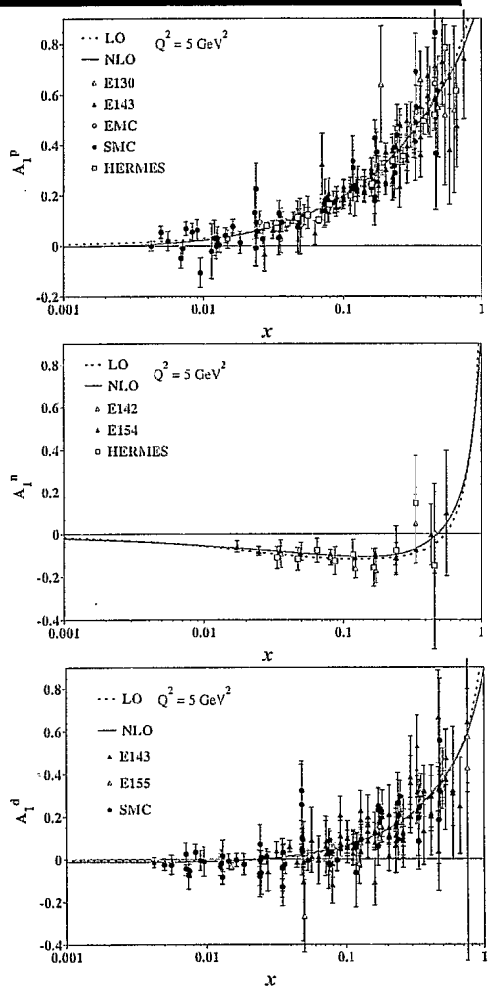

Fit Results : g_1

$g_1(x, Q^2)$ at $Q^2 = 1, 5, 20$ GeV^2

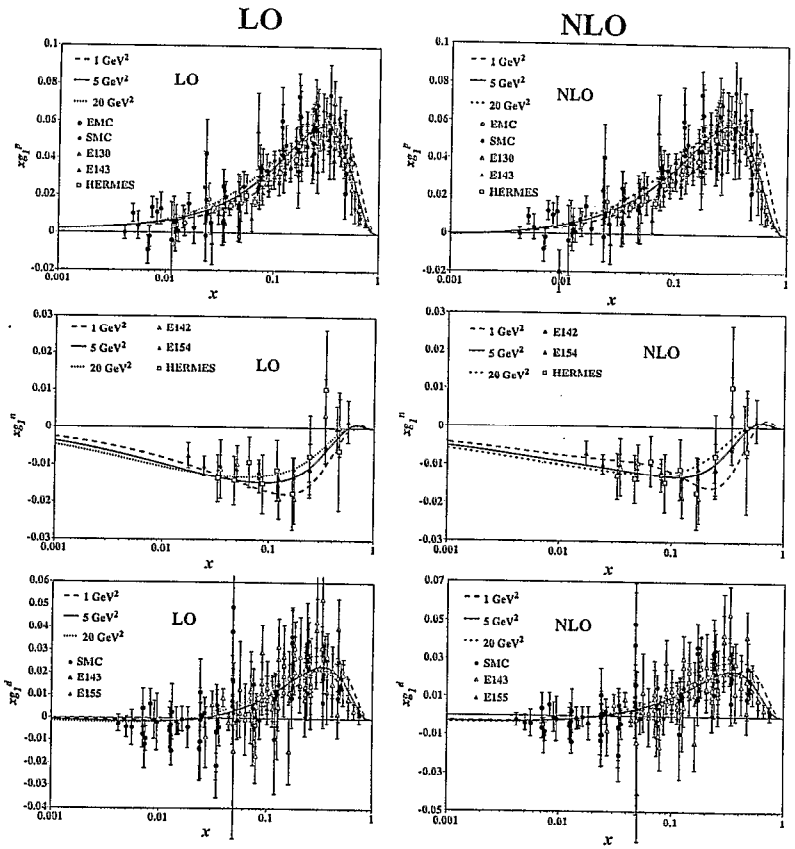

$\chi^2 = 322.6,$ $\chi^2 = 300.4$

375 points, 14 free parameters

Fit Results: Polarized PDF

Polarized PDF, $Q^2 = 1$ GeV^2

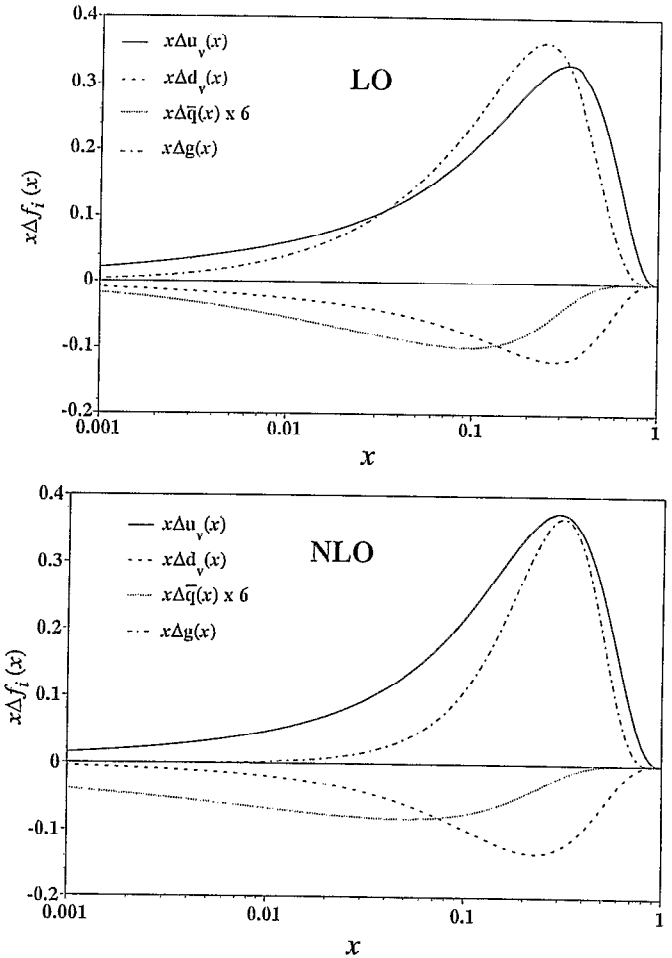

Spin Content $\Delta\Sigma$

$\Delta\Sigma = 0.201 \quad \Delta g = 0.831 \quad$ in the LO

$\Delta\Sigma = 0.051 \quad \Delta g = 0.532 \quad$ in the NLO

NLO analysis with fixed $\alpha_{\bar{q}}$ at $Q^2 = 1$ GeV^2

Distribution	$\alpha = 0.5$	$\alpha = 1.0$	$\alpha = 1.6$
$\Delta\bar{q}$	-0.077	-0.057	-0.051
Δg	0.550	0.533	0.294
$\Delta\Sigma$	0.123	0.241	0.276

$$\Delta\Sigma(x_{min}) = \int_{x_{min}}^{1} \Delta\Sigma(x)dx$$

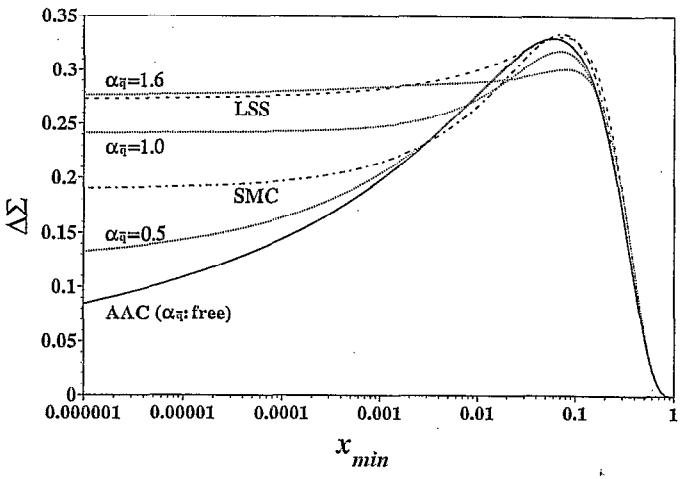

Exclusive Variation of Errors

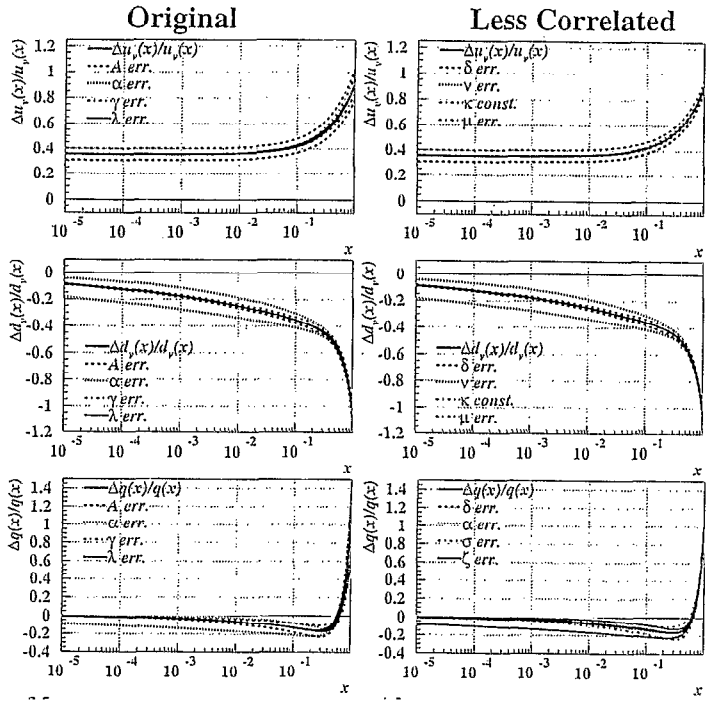

Practical Parameter Set

Originarl Parameter Set

$$h_i(x) = A_i x^{\alpha_i}(1+\gamma_i x^{\lambda_i})$$

$$A_i,\ \alpha_i,\ \gamma_i,\ \lambda_i : \text{variable}$$

Valence Quark : u_v, d_v

$$h_i(x) = \delta_i x^{\nu_i} - \kappa_i(x^{\nu_i} - x^{\mu_i})$$

$$\delta_i,\ \nu_i,\ \mu_i : \text{variable}, \quad \kappa_i : \text{fixed}$$

$$A_i = \delta_i - \kappa_i,\ \ \alpha_i = \nu_i,\ \ \gamma_i = \frac{\kappa_i}{\delta_i - \kappa_i},\ \ \lambda_i = \mu_i - \nu_i$$

Sea Quark and Gluon : $\bar{q}$, g

$$h_i(x) = \delta_i x^{\alpha_i} - \sigma_i \kappa_i'(x^{\alpha_i} - x^{\alpha_i \zeta_i}) x^{\alpha_i \zeta_i}$$

$$\delta_i,\ \alpha_i,\ \sigma_i,\ \zeta_i : \text{variable}, \quad \kappa_i' : \text{fixed}$$

$$A_i = \sigma_i \kappa_i',\ \ \alpha_i = \mu_i,\ \ \gamma_i = \frac{\delta_i}{\sigma_i \kappa_i'} - 1,\ \ \lambda_i = \frac{\mu_i}{\zeta_i}(1-\zeta_i)$$

TABLE II. Obtained parameters at $Q^2 = 1$ GeV^2 in the leading-order χ^2 analysis.

Distribution	A	α	γ	λ
Δu_v	0.404 ± 0.054	0.00 ± 0.01	1.47 ± 0.20	1.41 ± 0.46
Δd_v	-0.274 ± 0.056	0.00 ± 0.01	2.65 ± 0.54	1.25 ± 0.28
$\Delta \bar{q}$ LO	-0.680 ± 0.373	0.59 ± 0.94	-2.47 ± 0.82	4.06 ± 1.14
Δg	47.5 ± 4.1	1.44 ± 0.73	-0.986 ± 0.002	0.06 ± 1.05

TABLE III. Obtained parameters at $Q^2 = 1$ GeV^2 in the next-to-leading-order χ^2 analysis (set NLO-1).

Distribution	A	α	γ	λ
Δu_v	0.356 ± 0.047	0.00 ± 0.00	1.54 ± 0.20	0.889 ± 0.058
Δd_v	-0.502 ± 0.031	0.153 ± 0.065	0.992 ± 0.062	2.48 ± 0.27
$\Delta \bar{q}$ NLO-1	-0.269 ± 0.107	0.32 ± 0.22	-4.72 ± 1.48	3.20 ± 0.47
Δg	249.2 ± 8.3	2.15 ± 0.11	-1.0040 ± 0.0002	0.031 ± 0.152

TABLE V. Obtained parameters at $Q^2 = 1$ GeV^2 in the NLO χ^2 analysis with fixed $\alpha_{\bar{q}}$.

Distribution	χ^2	A	α	γ	λ
($\alpha_{\bar{q}} = 0.5$)	300.7				
Δu_v		0.357 ± 0.093	0.000 ± 0.001	1.55 ± 0.40	0.900 ± 0.335
Δd_v		-0.512 ± 0.098	0.159 ± 0.227	0.952 ± 0.181	2.65 ± 0.66
$\Delta \bar{q}$		-9.50 ± 10.07	0.5 (fixed)	-0.980 ± 0.060	0.0102 ± 0.0394
Δg		148.5 ± 7.4	2.11 ± 0.26	-1.0067 ± 0.0005	0.051 ± 0.337
($\alpha_{\bar{q}} = 1.0$)	305.8				
Δu_v		0.589 ± 0.055	0.120 ± 0.090	0.632 ± 0.059	1.62 ± 0.27
Δd_v		-0.279 ± 0.086	0.000 ± 0.001	2.58 ± 0.80	1.32 ± 0.31
$\Delta \bar{q}$ NLO-2		-47.7 ± 9.7	1.0 (fixed)	-1.0065 ± 0.0056	0.0204 ± 0.0707
Δg		173.8 ± 17.3	2.14 ± 0.19	-1.0058 ± 0.0007	0.045 ± 0.253
($\alpha_{\bar{q}} = 1.6$)	323.5				
Δu_v		1.356 ± 0.132	0.335 ± 0.120	-0.477 ± 0.046	0.313 ± 0.209
Δd_v		-0.321 ± 0.097	0.000 ± 0.000	2.12 ± 0.64	2.21 ± 0.17
$\Delta \bar{q}$		-119.6 ± 11.8	1.6 (fixed)	-0.9976 ± 0.0071	0.033 ± 1.304
Δg		176.6 ± 9.3	2.77 ± 0.38	-1.0057 ± 0.0004	0.057 ± 0.547

Error Estimate using Error Matrix

χ^2 definition

$$\chi^2 = (\mathbf{A} - \mathbf{f}(\mathbf{a}))^T \mathcal{E}_{\mathbf{a}}^{-1} (\mathbf{A} - \mathbf{f}(\mathbf{a})) \equiv S(\mathbf{a})$$

χ^2 minimum

$$\chi^2_{min} = S(\widehat{\mathbf{a}})$$

Expansion around χ^2 minimum

$$S(\mathbf{a}) = S(\widehat{\mathbf{a}}) + (\mathbf{a} - \widehat{\mathbf{a}})^T \mathcal{E}_{\widehat{\mathbf{a}}}^{-1} (\mathbf{a} - \widehat{\mathbf{a}})$$

Definition of 1-σ Error

$$S(\mathbf{a}) \leq S(\widehat{\mathbf{a}}) + 1$$

$$(\mathbf{a} - \widehat{\mathbf{a}})^T \mathcal{E}_{\widehat{\mathbf{a}}}^{-1} (\mathbf{a} - \widehat{\mathbf{a}}) \leq 1$$

$\mathcal{E}_{\widehat{\mathbf{a}}}$ is given by MINUIT

$$V_{ij} = (\mathcal{E}_{\widehat{\mathbf{a}}})_{ij}$$

Error Propagation to Function $F(\mathbf{a})$

$$(\delta F)^2 = \sum_i \sum_j \frac{\partial F}{\partial a_i} V_{ij} \frac{\partial F}{\partial a_j}, \qquad V_{ij}\text{: Covariance Matrix}$$

Summary

Features of the AAC parameterization

- Pol-DIS experiment A_1, 375 data points.
- DGLAP Q^2 evolution.
- Functional form : $\frac{\Delta f_i(x,Q_0^2)}{f_i(x,Q_0^2)} = A_i x^{\alpha_i}(1+\gamma_i x^{\lambda_i})$.
- Positivity condition $|\Delta f_i(x)| \leq f_i(x)$.
- SU(3) symmetric sea, 1st moments Δu_v, Δd_v fixed.
- One LO and two NLO parameter sets.

What was found?

- Q^2 dependence of A_1 at $Q^2 < 2$.
- χ^2 in NLO is smaller than that in LO.
- Small x behavior of the sea-quark distributions can not be uniquely determined.
- Spin contents, $\Delta\Sigma$ and Δg, are very sensitive to the variation of sea quark distribution.
- Spin contents :

$\Delta\Sigma = 0.201$	$\Delta g = 0.831$	LO
$\Delta\Sigma = 0.051$	$\Delta g = 0.532$	NLO-1
$\Delta\Sigma = 0.241$	$\Delta g = 0.533$	NLO-2 ($\alpha_{\bar{q}} = 1.0$)

- Detailed uncertainty analysis is on going.

Error Estimate using Error Matrix

χ^2 definition

$$\chi^2 = (\mathbf{A} - \mathbf{f}(\mathbf{a}))^T \mathcal{E}_{\mathbf{a}}^{-1} (\mathbf{A} - \mathbf{f}(\mathbf{a})) \equiv S(\mathbf{a})$$

χ^2 minimum

$$\chi^2_{min} = S(\widehat{\mathbf{a}})$$

Expansion around χ^2 minimum

$$S(\mathbf{a}) = S(\widehat{\mathbf{a}}) + (\mathbf{a} - \widehat{\mathbf{a}})^T \mathcal{E}_{\widehat{\mathbf{a}}}^{-1} (\mathbf{a} - \widehat{\mathbf{a}})$$

Definition of 1-σ Error

$$S(\mathbf{a}) \leq S(\widehat{\mathbf{a}}) + 1$$

$$(\mathbf{a} - \widehat{\mathbf{a}})^T \mathcal{E}_{\widehat{\mathbf{a}}}^{-1} (\mathbf{a} - \widehat{\mathbf{a}}) \leq 1$$

$\mathcal{E}_{\widehat{\mathbf{a}}}$ is given by MINUIT

$$V_{ij} = (\mathcal{E}_{\widehat{\mathbf{a}}})_{ij}$$

Error Propagation to Function $F(\mathbf{a})$

$$(\delta F)^2 = \sum_i \sum_j \frac{\partial F}{\partial a_i} V_{ij} \frac{\partial F}{\partial a_j}, \qquad V_{ij}\text{: Covariance Matrix}$$

Summary

Features of the AAC parameterization

- Pol-DIS experiment A_1, 375 data points.
- DGLAP Q^2 evolution.
- Functional form : $\frac{\Delta f_i(x,Q_0^2)}{f_i(x,Q_0^2)} = A_i x^{\alpha_i}(1+\gamma_i x^{\lambda_i})$.
- Positivity condition $|\Delta f_i(x)| \leq f_i(x)$.
- SU(3) symmetric sea, 1st moments Δu_v, Δd_v fixed.
- One LO and two NLO parameter sets.

What was found?

- Q^2 dependence of A_1 at $Q^2 < 2$.
- χ^2 in NLO is smaller than that in LO.
- Small x behavior of the sea-quark distributions can not be uniquely determined.
- Spin contents, $\Delta\Sigma$ and Δg, are very sensitive to the variation of sea quark distribution.
- Spin contents :

$\Delta\Sigma = 0.201$	$\Delta g = 0.831$	LO
$\Delta\Sigma = 0.051$	$\Delta g = 0.532$	NLO-1
$\Delta\Sigma = 0.241$	$\Delta g = 0.533$	NLO-2 ($\alpha_{\bar{q}} = 1.0$)

- Detailed uncertainty analysis is on going.

How well do we know the polarized parton densities in the nucleon at present ?

Elliot Leader[a], Aleksander V. Sidorov [b] and Dimiter B. Stamenov[c]
a)Birkbeck College, University of London, England
b)Bogoliubov Theoretical Laboratory, JINR, Dubna, Russia
c)Institute for Nuclear Research and Nuclear Energy, Sofia, Bulgaria

Abstract

We present a critical assessment of what can be learned about the polarized parton densities from the present data on inclusive and semi - inclusive polarized DIS. Although the quality of the data has significantly improved in the past few years, the uncertainty in determining the polarized strange sea quark and gluon densities is still very large. Bearing in mind the limited range in x and Q^2 and the accuracy of the present data, almost all QCD analyses supplement the DIS data with information stemming from low-Q^2 weak interaction reactions. We draw attention to some problems in the combined use of high-Q^2 deep inelastic scattering (DIS) data and low-Q^2 hyperon β decay data in the determination of the polarized parton densities. We explain why factorization schemes like the JET or AB schemes are the simplest in which to study the implications of the DIS parton densities for the physics of the low-Q^2 region. A new study of the sensitivity of the polarized parton densities to a breakdown of the SU(3) flavour symmetry treatment of the hyperon β decays is presented. It is demonstrated that except for the strange sea quarks and the gluons the other densities are essentially those determined by the SU(3) analysis of the data. It is important to stress that the singlet quark density, as well as its first moment, $\Delta\Sigma$ (the spin of the nucleon carried by the quarks), are virtually unchanged by the SU(3) breaking. The mean value of $\Delta\Sigma$ in the JET scheme ranges from 0.34 to 0.40 and within the errors is not far from the value 0.60 expected in low-Q^2 quark models.

Despite the great progress of the past few years, the two challenging questions concerning the parton spin structure of the nucleon are still the gluon polarization Δg and the flavour decomposition of the sea quarks. It is expected that the Spin Physics Program at RHIC, as well as the future DIS experiments (COMPASS at CERN, HERMES at DESY and the Jefferson Lab. Spin program) will answer these questions very soon.

- I think it is a good time (before the start of the **new** generation of the experiments with polarized particles: RHIC, COMPASS, HERMES, pHERA) to present a critical assessment of what can be learned about the **polarized** parton densities (PD) from the present data on polarized DIS.

- In this talk I will present a summary of our results of the QCD analysis of the world data on **inclusive** polarized DIS.

Phys. Rev. D58 (1998) 114028;
Phys. Lett. B445 (1998) 232;
B462 (1999) 189; B488 (2000) 283;
J. High Energy Physics 07 (2000) 029.

OUTLINE

- Difficulties, specific for the **polarized** case
  There are **NO** charged current (neutrino) DIS data

- What can deduce from the **present** inclusive and semi-inclusive DIS data, in principle and in fact ?

- Information from the low-Q^2 region - hyperon semi-leptonic β-decays.

- Method of analysis
  - A_1 rather than g_1 data
  - JET factorization scheme - why ?
  - Sensitivity of the polarized PD to the SU(3) symmetry breaking

- Results

- Conclusions

- As in the unpolarized case the main goal is:
  - to test QCD
  - to extract from the DIS data the **polarized** PD

$$\begin{aligned}\Delta q(x,Q^2) &= q_+(x,Q^2) - q_-(x,Q^2)\ ,\\ \Delta\bar{q}(x,Q^2) &= \bar{q}_+(x,Q^2) - \bar{q}_-(x,Q^2)\ ,\\ \Delta G(x,Q^2) &= G_+(x,Q^2) - G_-(x,Q^2)\end{aligned}$$

where "+" and "-" denote the helicity of the parton, along or opposite to the helicity of the parent nucleon, respectively.

- The knowledge of the polarized PD will help us:
  - to make predictions for other processes like polarized **hadron-hadron** reactions, etc.
  - more generally, to answer the question how the spin of the nucleon is divided up among its constituents:

$$\frac{1}{2} = \frac{1}{2}(\Delta u + \Delta d + \Delta s) + \Delta G + L_z$$

In the **NLO QCD** approximation the quark-parton decomposition of the spin-structure function $g_1(x,Q^2)$ has the following form:

$$g_1(x,Q^2) = \frac{1}{2}\sum_q^{N_f} e_q^2[(\Delta q + \Delta\bar{q}) \otimes (1 + \frac{\alpha_s(Q^2)}{2\pi}\delta C_q)$$

$$+ \frac{\alpha_s(Q^2)}{2\pi}\Delta G \otimes \delta C_G],$$

where
$\Delta q(x,Q^2), \Delta\bar{q}(x,Q^2)$ and $\Delta G(x,Q^2)$ are quark, anti-quark and gluon polarized densities which evolve in Q^2 according to the spin-dependent NLO DGLAP equations.

$\delta C_{q,G}$ are the NLO terms in the spin-dependent Wilson coefficient functions and the symbol $\otimes$ denotes the usual convolution in Bjorken x space.

N_f is the number of flavours.

• **DIFFICULTIES**, specific for the polarized case:

i) There are **NOT** and will **NOT** be **charged** current DIS neutrino data in a near future. Note that in the *unpolarized* case due to the neutrino data a good separation of the quark densities with different flavours, and especially, a decomposition into valence and sea parts, has been achieved.

In the **polarized** case $\Rightarrow$ $(\Delta q + \Delta \bar{q})$ and ΔG.

ii) *Semi-inclusive* measurements in DIS, in principle, could help out of this situation. In LO QCD:

$$A_1^h(x,z,Q^2) = \frac{\Sigma_{q,\bar{q}} e_q^2 \; \Delta q_i(x,Q^2) \; D_i^h(z,Q^2)}{\Sigma_{q,\bar{q}} e_q^2 \; q_i(x,Q^2) \; D_i^h(z,Q^2)}$$

- an extra uncertainty is presented in these processes: the quark-hadron fragmentation functions $D_q^h(z,Q^2)$. Unfortunately, these quantities are not well known at present and $D_q^h(z,Q^2)$ given in different papers differ **significantly** (in some cases more than 100%).

- due to the quality of these data at present, many additional assumptions had to be made in order to extract the polarized PD (*SMC, HERMES*).

iii) A good strategy would be to try to perform a more sophisticated combined analysis of the polarized inclusive and semi-inclusive DIS data.

D. de Florian, R. Sassot, hep-ph/0007068 -
a conventional combined analysis has been performed. However, **NO** errors are given !
E. Christova, E. Leader, hep-ph/0007303 -
a new strategy for the analysis of SIDIS is presented. In order to test it new and more accurate SIDIS data are needed.

iv) A lot of the present data are at low

$$Q^2 \approx 1 - 5 \; GeV^2.$$

The value of $\alpha_s(Q^2)$ in this region is big and the theoretical uncertainties are large !

- What can be deduced in principle and in fact from the inclusive (*neutral* current) DIS data ?

- from **experiment** $\Rightarrow$ data for two independent structure functions g_1^p and g_1^n (or g_1^d)
- from **QCD** $\Rightarrow$ different Q^2-evolution for the individual PD:

$$(\Delta q + \Delta\bar{q}) \quad (q = u, d, s) \text{ and } \Delta G.$$

One can prove that *perfect* data **uniquely** determine the *sum* of the polarized quark and antiquark densities $(\Delta q + \Delta\bar{q})$ and the gluon density ΔG.

However, bearing in mind the limited range in x and Q^2 and the precision of the present data, it is immediately clear that the separation of the polarized PD from each other will *not* be very clear-cut.

In other words, the unknown free parameters α_i attached to the input parton densities at $Q^2 = Q_0^2$ are correlated and *not* well determined from the fit to the inclusive DIS data **alone**.

- That is why our knowledge on the *first* moments of the polarized parton densities coming from the hyperon semi-leptonic decays is **conventionally** used in addition to fix some of the free parameters.

- **Information from the low Q^2 region**

$$a_3 = (\Delta u + \Delta\bar{u})(Q^2) - (\Delta d + \Delta\bar{d})(Q^2) = g_A \tag{1}$$

$$\begin{aligned} a_8 &= (\Delta u + \Delta\bar{u})(Q^2) + (\Delta d + \Delta\bar{d})(Q^2) \\ &- 2(\Delta s + \Delta\bar{s})(Q^2) = 3F - D\ , \end{aligned} \tag{2}$$

where a_3 and a_8 are the nonsinglet axial charges corresponding to the 3rd and 8th components of the axial vector Cabibbo current. In (2) F and D are the SU(3) parameters.

The Bjorken sum rule (1) reflects the isospin SU(2) symmetry, whereas the relation (2) is a consequence of the SU(3) flavour symmetry treatment of the hyperon β-decays.

- **Note** that the nonsinglet axial charges a_3 and a_8 are Q^2 **independent** and this is the fact which helps us to link the information from both high and low-Q^2 regions.

- In the SU(3) limit

$$a_8 = 3F - D = 0.579 \pm 0.025 \ . \qquad (3)$$

While isospin symmetry is well established, there is indication for a *breakdown* of the SU(3) symmetry and consequently of Eq. (3).

- So, we have performed a **NLO QCD** fit to the world data on the nucleon spin asymmetries $A_1^N(x, Q^2)$ using for the first moments of the quark densities the relations (1) and (2).

- The sensitivity of the polarized PD to the deviation of a_8 from its SU(3) symmetric value **(0.58)** has been also studied. The SU(3) symmetry breaking effects have been taken into account in a **model-independent** way.

METHOD OF ANALYSIS

$$A_1^N(x, Q^2) \cong (1+\gamma^2)\frac{g_1^N(x, Q^2)}{F_1^N(x, Q^2)}$$

$$= \frac{g_1^N(x, Q^2)}{F_2^N(x, Q^2)}\, 2x[1 + R(x, Q^2)]$$

where

$$\gamma^2 = \frac{4M_N^2 x^2}{Q^2}$$

It should be noted that in the SLAC and HERMES kinematic region γ cannot be neglected.

- **Why A_1 rather than g_1 ?**

- in order to **minimize** the higher twist contributions which are expected to partly cancel in the ratio g_1/F_1 allowing use of the data at low $Q^2 \approx 1 - 5\ GeV^2$.

- g_1 has been extracted from the A_1 data by the different experimental groups using a various parametrizations of the experimental data for F_2 and R.

- Input parton densities

$$\Delta f_i(x, Q_0^2) = A_i \; x^{\alpha_i} \; f_i^{MRST}(x, Q_0^2)$$

A_i, α_i - free parameters (6 parameters in our fit).

For the unpolarized parton densities $f_i(x, Q_0^2)$ the Martin-Roberts-Stirling-Torn parametrization, which account for the world **unpolarized** data, has been used.

- We have performed the fits to the data in different factorization schemes: $\overline{\text{MS}}$, AB and JET and the consistency between the results of the analysis in each scheme has been demonstrated (*Phys. Lett. B445 (1998) 232*).

  The results are presented in the **JET** scheme (all hard effects are absorbed in the Wilson coefficient functions).

  Carlitz, Collins, Mueller (1988);
  Efremov, Teryaev (1989); Müller, Teryaev (1997);
  Anselmino, Efremov, Leader (1995).

Why JET scheme ?

It is useful to recall the transformation rules relating the first moments of the singlet quark density, $\Delta\Sigma(Q^2)$, and the strange sea, $(\Delta s + \Delta\bar{s})(Q^2)$, in the JET and $\overline{\text{MS}}$ schemes:

$$\Delta\Sigma_{\text{JET}} = \Delta\Sigma_{\overline{\text{MS}}}(Q^2) + N_f \frac{\alpha_s(Q^2)}{2\pi} \Delta G(Q^2),$$

$$(\Delta s + \Delta\bar{s})_{\text{JET}} = (\Delta s + \Delta\bar{s})_{\overline{\text{MS}}}(Q^2) + \frac{\alpha_s(Q^2)}{2\pi} \Delta G(Q^2).$$

A remarkable property of the JET scheme is that $\Delta\Sigma(Q^2)$, as well as $(\Delta s + \Delta\bar{s})(Q^2)$, are $\mathbf{Q^2}$ **independent** quantities. Then, in the JET scheme it is meaningful to directly interpret $\Delta\Sigma$ as the contribution of the quark spins to the nucleon spin and to compare its value obtained from **DIS region** with the predictions of the different (constituent, chiral, etc.) quark models at **low** Q^2.

It is important to mention that the difference between the values of $(\Delta s + \Delta\bar{s})$, obtained in the $\overline{\mathrm{MS}}$ and JET schemes could be **large** due to the axial anomaly. To illustrate how large it can be, we present the values of $(\Delta s + \Delta\bar{s})$ at $\mathrm{Q}^2 = 1\ \mathrm{GeV}^2$ obtained in our recent analysis of the world DIS data in the $\overline{\mathrm{MS}}$ and JET schemes ($\Delta\mathrm{G} = 0.57$):

$$(\Delta s + \Delta\bar{s})_{\overline{\mathrm{MS}}} = -0.10 \pm 0.01$$
$$(\Delta s + \Delta\bar{s})_{\mathrm{JET}} = -0.06 \pm 0.01.$$

Note that if $\Delta\mathrm{G}$ is larger, then $(\Delta s + \Delta\bar{s})_{\mathrm{JET}}$ could be even zero in agreement with what is intuitively expected at low-Q^2 region ($Q^2 \approx 0$).

RESULTS OF ANALYSIS

- The results on the PD are given at $\mathrm{Q}^2 = 1\ \mathrm{GeV}^2$. The total (statistical and systematic) errors have been taken into account in quadrature.
- Quality of the **NLO QCD** fits
  - A very good description of the world data on A_1^N and g_1^N is achieved.
  - χ^2 coincide almost exactly in the JET, AB and $\overline{\mathrm{MS}}$ schemes.
- A good agreement between the values of the axial charge $\mathrm{a_0(Q^2)}$ at $Q^2 = 1\ GeV^2$ determined in the different schemes. Note that $a_0(Q^2)$ is **scheme independent** quantity.

Scheme	JET	AB	$\overline{MS}$
χ^2/DOF	0.828	0.828	0.835
$(\Delta s + \Delta\bar{s})$	- 0.06 ± 0.01	- 0.06 ± 0.01	- 0.10 ± 0.01
$\Delta\Sigma$	0.40 ± 0.04	0.41 ± 0.04	0.28 ± 0.04
a_0	0.26 ± 0.05	0.27 ± 0.05	0.28 ± 0.04

Sensitivity to SU(3) symmetry breaking

Let me discuss now how the deviation of the nonsinglet axial charge a_8 from its SU(3) symmetric value 3F-D=0.58 influences the results on the polarized PD.

a_8	χ^2/DOF	$\Delta u+\Delta\bar{u}$	$\Delta d+\Delta\bar{d}$	$\Delta s+\Delta\bar{s}$	$\Delta\Sigma$	ΔG
0.40	0.82	0.81±0.02	-0.45±0.02	-0.02±0.01	0.34±0.05	0.13±0.14
3F-D	0.83	0.86±0.02	-0.40±0.02	-0.06±0.01	0.40±0.04	0.57±0.14
0.86	0.82	0.90±0.02	-0.35±0.02	-0.15±0.02	0.40±0.06	0.84±0.30

- The values of χ^2 are practically insensitive to the change of a_8, which means that any of the solutions presented here cannot be excluded by the present data.
- $\Delta\Sigma$ is essentially **independent** of SU(3) breaking and within the errors is not far from the value 0.60 expected in low-Q^2 quark models.
- The non-strange quarks $(\Delta u+\Delta\bar{u})$ and $(\Delta d+\Delta\bar{d})$ change **slowly**.
- The strange quark and gluon polarizations are **strongly dependent** on the SU(3) symmetry assumption.

- The strange sea polarization $(\Delta s+\Delta\bar{s})$ changes **significantly** when SU(3) symmetry is broken - from **-0.02 to -0.15**.

  If $a_8=0.40$ (a strong breakdown of the SU(3) symmetry), $(\Delta s+\Delta\bar{s})$ is consistent with zero, in agreement with the usual assumption in low-Q^2 quark models.

- For the gluon polarization ΔG we have found that

  - ΔG is **positive**

  - the possible values of ΔG lie in the wide range **(0, 1.5)** if one takes into account the correlations and the sensitivity to the SU(3) symmetry breaking.

  - Our result on ΔG is in agreement with those obtained in other analyses.

SU(3) symmetry case ($Q^2=1$ GeV^2)

LSS: $\Delta G=0.57\pm0.31$ (sta + sys in quadrature)

SMC: $\Delta G=0.99\ ^{+1.17}_{-0.31}\ ^{+0.42}_{-0.22}\ ^{+1.43}_{-0.45}$

AAC: $\Delta G=0.53$ GRSV: $\Delta G=0.50$

Comments on the AAC result on $\Delta\Sigma$

(SU(3) symmetry case, $Q^2 = 1\ GeV^2$)

$\Delta\Sigma$ ($\overline{MS}$ scheme):

GRSV: 0.20 - F_1^{QCD} $\Leftrightarrow$ F_2^{QCD} and R^{QCD}

LSS: 0.28 ± 0.06 (sta + sys in quadrature) - F_1^{QCD}

SMC: 0.19 ± 0.05(sta) $\pm$ 0.04(sys)
[$R_{1990}(x \geq 0.1)$, $R_{NMC}(x < 0.1)$]

DeFS: 0.20 (F_2 as in AAC anal.) - $R_{1999}(x > 0.002)$

AAC: 0.05 (NLO-1 fit) - $R_{1990}(x \geq 0.1)$ $\Rightarrow x < 0.1$

I think that the rather small value of $\Delta\Sigma$ obtained by AAC is mainly an **R-effect**. R_{1990} used in the AAC analysis is NOT a good approximation at small x ($x < 0.1$) region, especially for Q^2 in the SMC region - the R data are lower than R_{1990} parametrization.

So, for small x : $R_{1990} > R_{1999}$

$$\Rightarrow \quad g_1^{AAC} < g_1^{DeFS} \quad \Rightarrow \quad \Delta\Sigma_{ACC} < \Delta\Sigma_{DeFS}$$

CONCLUSIONS

- Given the limited range and precision of present $g_1(x, Q^2)$ measurements, one would like

  a direct measurement of ΔG
  (*RHIC, COMPASS*)

- Inclusive DIS measurements are sensitive only to $(\Delta q + \Delta\bar{q})$ thus a new probe is needed to

  separate quark and anti-quark polarized PD
  (*HERMES, RHIC, COMPASS*)

- A **small** x-physics with **polarized** protons at *HERA* would be very important for our understanding of the spin properties of the nucleon.

Figure Captions

Fig. 1a. (1b.) Comparison of our NLO results in the JET scheme for $A_1^N(x, Q^2)$ with the experimental data at the measured x and Q^2 values. Errors bars represent the total error.

Fig. 1. Next-to-leading order polarized parton density $x(\Delta u + \Delta\bar{u})$ at $Q^2 = 1\ GeV^2$ (JET scheme). The solid, short-dashed and long-dashed curves correspond to the values 0.58 (SU(3) limit), 0.86 and 0.40 for the axial charge a_8, respectively. The error band accounts for the statistical and systematic uncertainties.

Fig. 2. Next-to-leading order polarized parton density $x(\Delta d + \Delta\bar{d})$ at $Q^2 = 1\ GeV^2$ (JET scheme). See caption to Fig. 1.

Fig. 3. Next-to-leading order polarized strange sea quark density $x(\Delta s + \Delta\bar{s})$ at $Q^2 = 1\ GeV^2$ (JET scheme). See caption to Fig. 1.

Fig. 4. Next-to-leading order polarized singlet quark density $x\Delta\Sigma$ at $Q^2 = 1\ GeV^2$ (JET scheme). See caption to Fig. 1.

Fig. 5. Next-to-leading order polarized gluon density $x\Delta G$ at $Q^2 = 1\ GeV^2$ (JET scheme). See caption to Fig. 1.

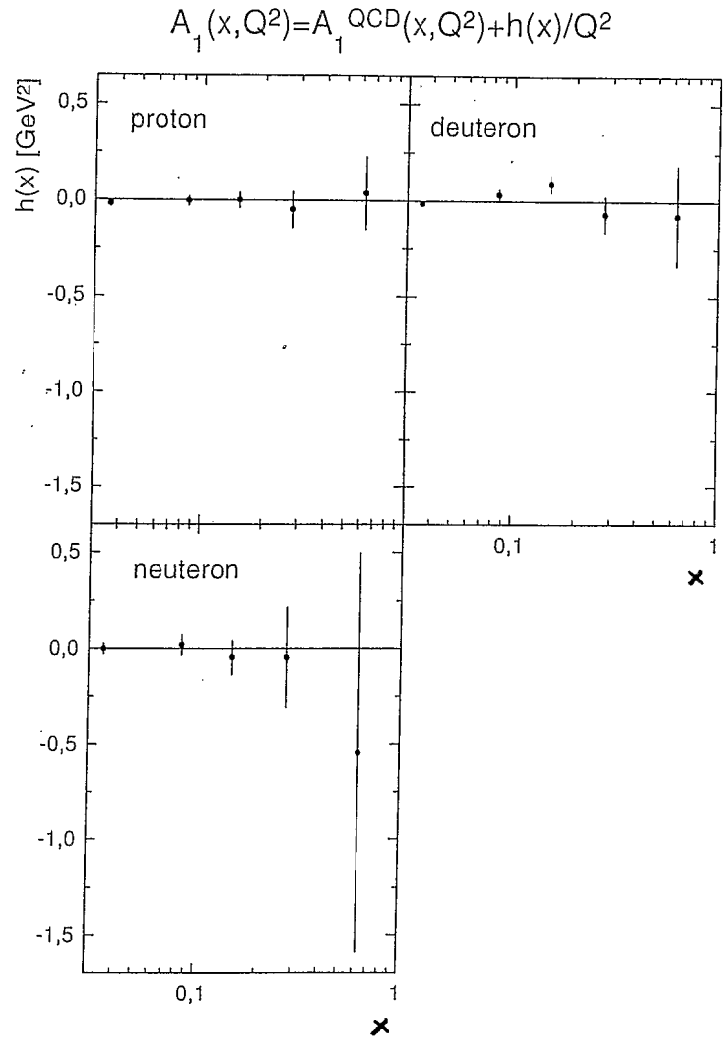

HT contributions

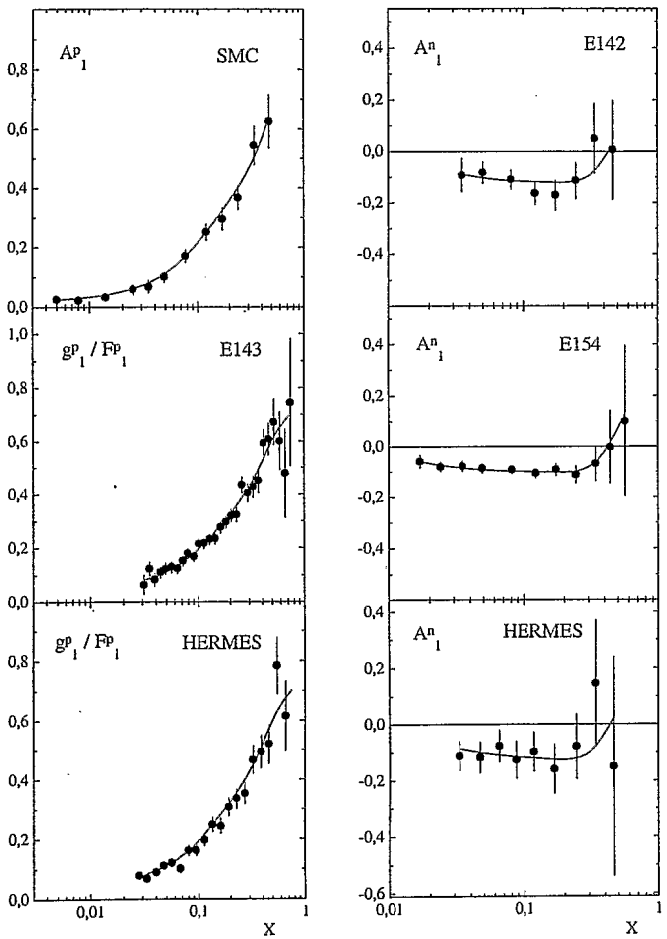
A^p_1
SMC
A^n_1
E142
g^p_1 / F^p_1
E143
A^n_1
E154
g^p_1 / F^p_1
HERMES
A^n_1
HERMES
X
X

Fig. 1a

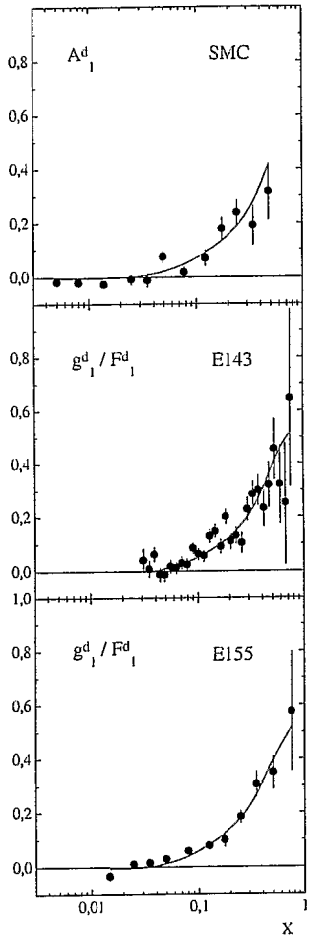
A^d_1
SMC
g^d_1 / F^d_1
E143
g^d_1 / F^d_1
E155
X

Fig. 1b

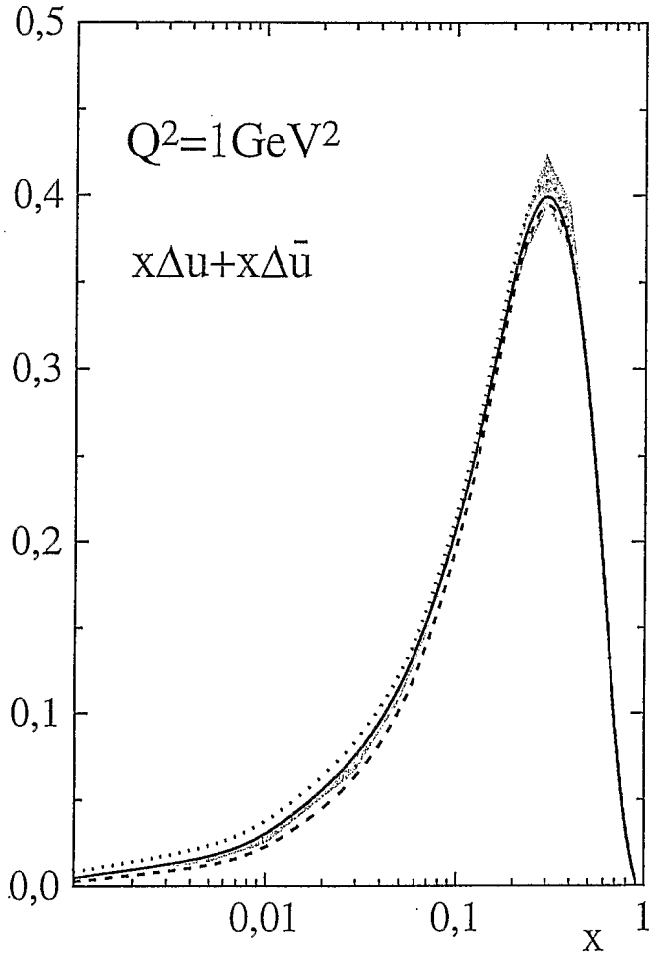
0,5
0,4
0,3
0,2
0,1
0,0
Q²=1GeV²
xΔu+xΔū
0,01
0,1
1
x

Fig. 1

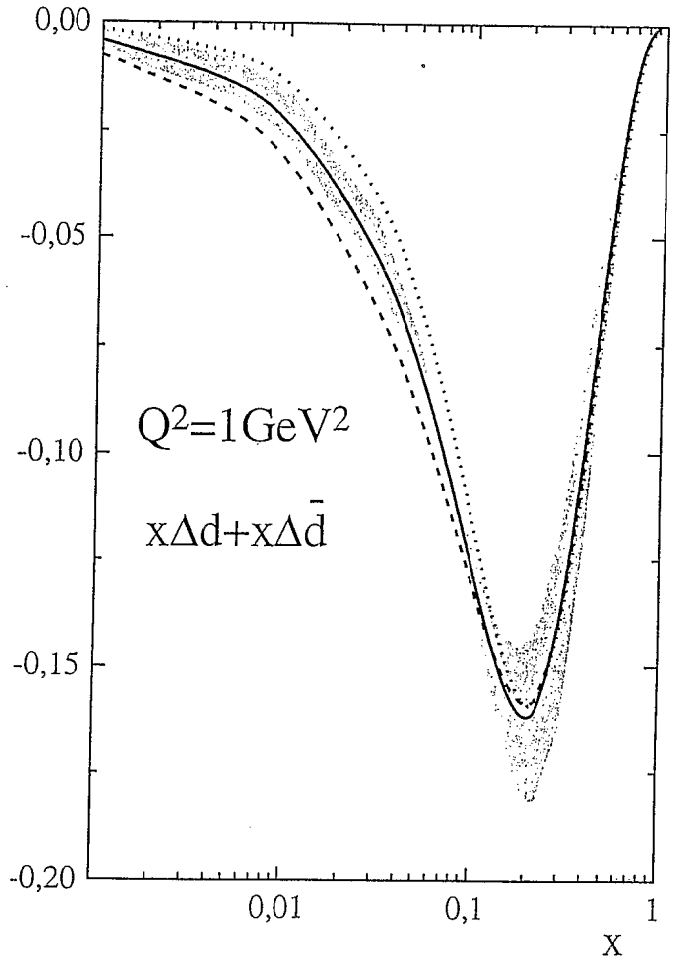
0,00
-0,05
-0,10
-0,15
-0,20
Q²=1GeV²
xΔd+xΔd̄
0,01
0,1
1
x

Fig. 2

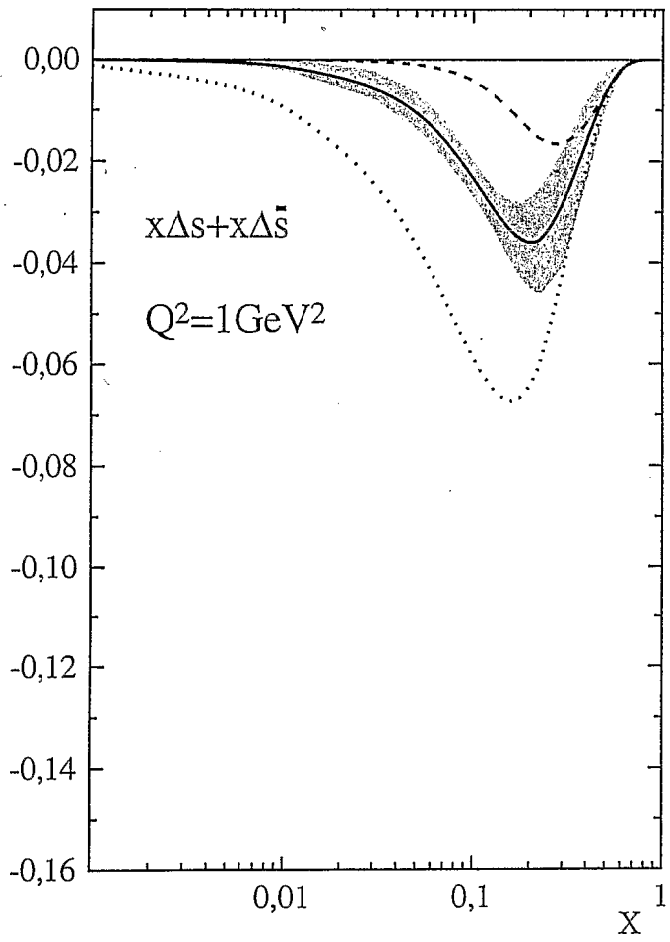
0,00
-0,02
-0,04
-0,06
-0,08
-0,10
-0,12
-0,14
-0,16
xΔs+xΔs̄
Q²=1GeV²
0,01
0,1
1
X

Fig. 3

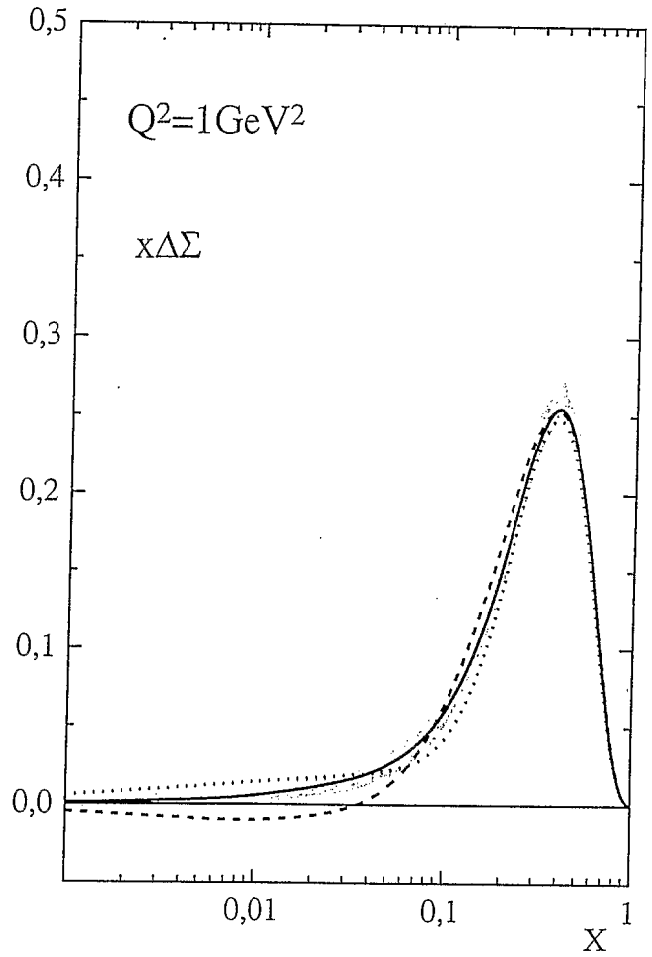
0,5
0,4
0,3
0,2
0,1
0,0
Q²=1GeV²
xΔΣ
0,01
0,1
1
X

Fig. 4

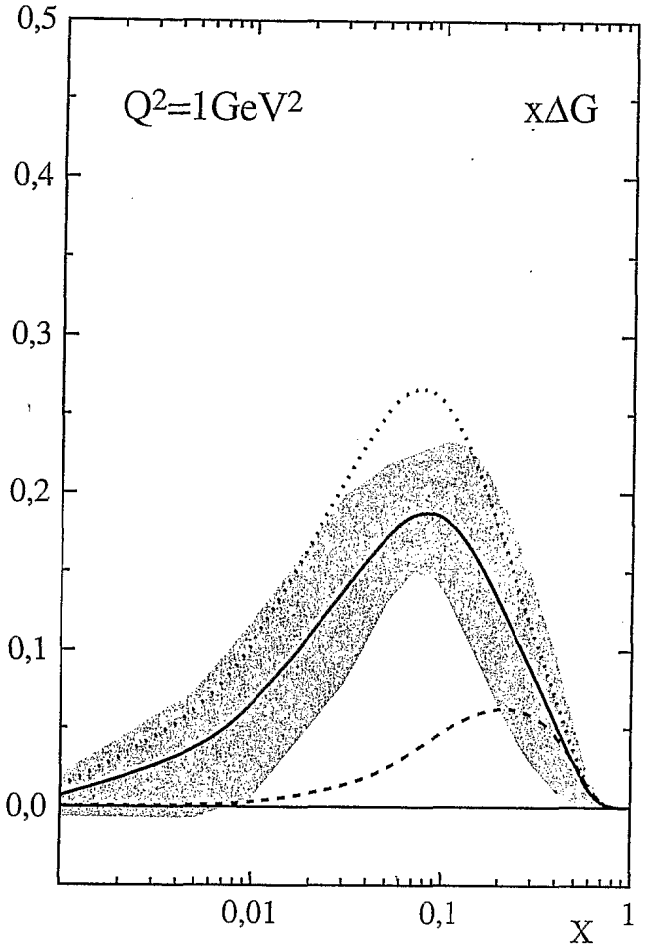

Fig. 5

Soft-gluon Effects in Polarized Prompt Photon Production

Werner Vogelsang (RIKEN-BNL Research Center)

Abstract

We parent a study of spin asymmetries for prompt photon production in collisions of Longitudinally polarized protons at BNL-RHIC. This reaction will be a key tool for Determining the gluon spin density in a polarized proton. We focus in particular on the role higher-order QCD corrections are expected to play in This context. Here, we address next-to-leading order corrections as well as all-order Soft –gluon resummations. We study theoretical uncertainties, such as the Dependence of the predictions on the factorization and renormalazation scales. We also address the issue of isolation cuts on the photon.

Soft-gluon Effects in Prompt-Photon Production

Werner Vogelsang

RIKEN BNL Research Center

RHIC Spin Meeting,
Kyoto, October 13, 2000

WORK WITH:
S. FRIXIONE; S. CATANI, M. MANGANO, P. NASON,
C. OLEARI; E. LAENEN, G. STERMAN

How to measure Δg ?

- Scaling violations in DIS,

$$\frac{d}{d\ln Q^2}\begin{pmatrix}\Delta\Sigma\\ \Delta g\end{pmatrix}=\frac{\alpha_s}{2\pi}\begin{pmatrix}\Delta P_{qq} & \Delta P_{qg}\\ \Delta P_{gq} & \Delta P_{gg}\end{pmatrix}\otimes\begin{pmatrix}\Delta\Sigma\\ \Delta g\end{pmatrix}$$

- to be viable, need large lever arm in Q^2 and/or high precision
  unpol. case: H1, ZEUS, NMC, ...
  pol. case: more difficult
  (so far, only fixed-target; pol. HERA?)

- more promising: study reactions which have gluon participation already at lowest order

Polarized gluon densities :
(Glück,Reya,Stratmann,WV; Gehrmann,Stirling)

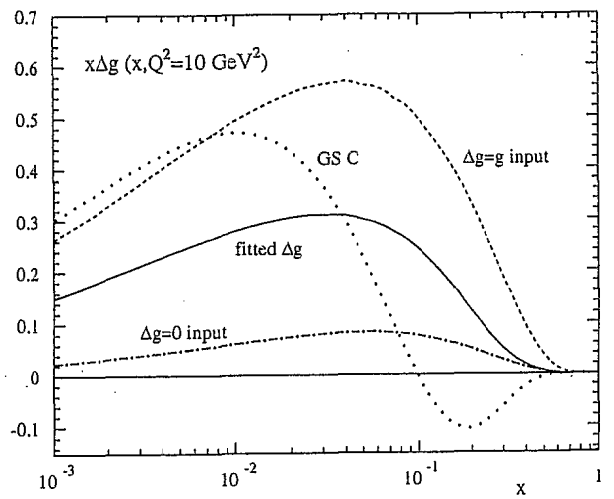

Fig. 1

What's so special about photons?

Prompt photons :
$\longrightarrow$ electromagnetic probe of hard scattering !

Lowest order ($\mathcal{O}(\alpha\alpha_s)$) :

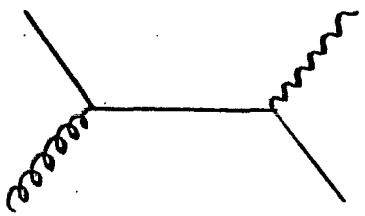

"Compton"

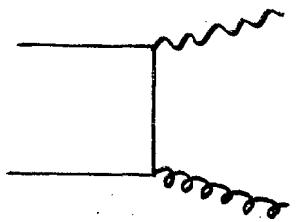

"Annihilation"

- "Direct" contributions $\longleftrightarrow$ 'clean' signal
- can be done at lower p_T and cms energies than jets
- qg process gives dominant contribution, in particular for pp or pN scattering

Spin asymmetry

$$A \equiv \frac{d\sigma_{++} - d\sigma_{+-}}{d\sigma_{++} + d\sigma_{+-}} \equiv \frac{d\Delta\sigma}{d\sigma}$$

Perturbative QCD / factorization theorem :

$$\begin{aligned} d\Delta\sigma^{dir} &= \sum_{a,b} \int dx_a dx_b \Delta f_a(x_a, M_F^2) \Delta f_b(x_b, M_F^2) \\ &\otimes \; d\Delta\hat{\sigma}_{ab\to\gamma x}(p_T^\gamma, \eta^\gamma, x_a, x_b, M_F^2, \mu_R^2) \end{aligned}$$

M_F, μ_R = fact. / renorm. scales

$\Delta\hat{\sigma}_{ab\to\gamma x}$ = subprocess cross sections ;
$\Delta\hat{\sigma}_{ab\to\gamma x} = \Delta\hat{\sigma}^{(0)}_{ab\to\gamma x} + \alpha_s \Delta\hat{\sigma}^{(1)}_{ab\to\gamma x} + \ldots$

- $\hat{\sigma}^{(1)}_{ab\to\gamma x}$: Aurenche et al.;
  Baer et al.;
  Gordon,WV
- $\Delta\hat{\sigma}^{(1)}_{ab\to\gamma x}$: Contogouris et al.;
  Gordon,WV; Frixione,WV

However, not *really* so clean ...

- Backgrounds from $\pi^0 \to 2\gamma$, ...
- "direct part" *not* the full story :
  "fragmentation" ("bremsstrahlung")

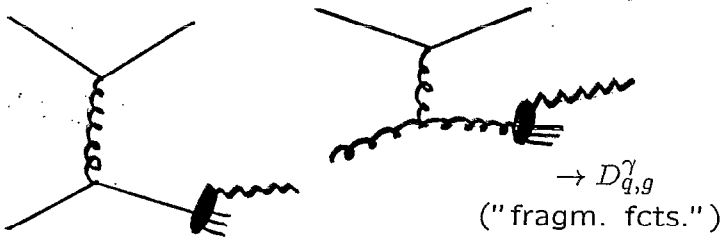

  - required by final-state collinear singularities at higher orders

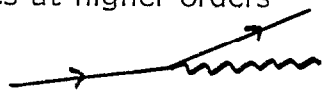

  - "photon $\longleftrightarrow$ vector meson"
  - should rise $\propto$ log of hard scale; $O(\frac{\alpha_{em}}{\alpha_s})$, driven by $q \to \gamma$ splitting
  - potentially important at low $x_T = 2p_T/\sqrt{s}$, and in particular in pp or pN scattering!

At RHIC, measure Δg through spin asymmetry

$$A_{LL} \equiv \frac{d\sigma_{++} - d\sigma_{+-}}{d\sigma_{++} + d\sigma_{+-}} \equiv \frac{d\Delta\sigma}{d\sigma}$$

(Frixione,WV)

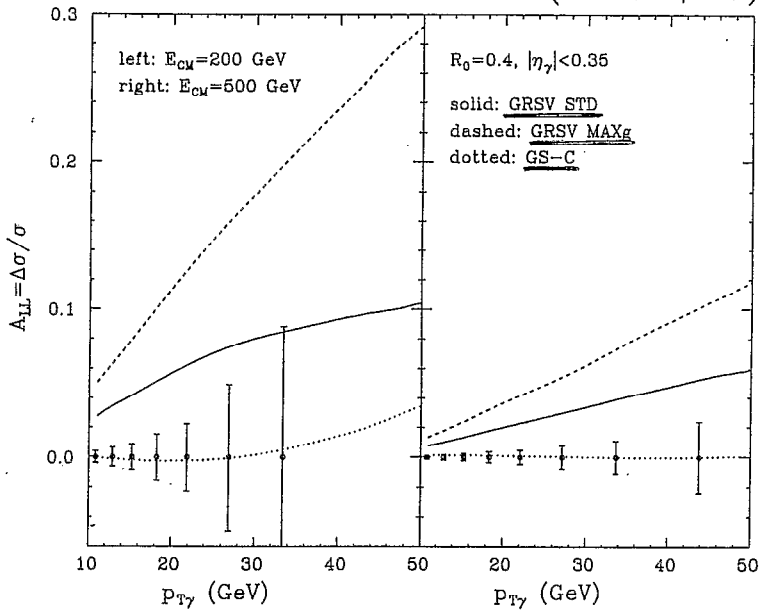

for all details, see :
G. Bunce, N. Saito, J. Soffer, WV,
Prospects for Spin Physics at RHIC (2000)

NLO: REDUCTION OF SCALE DEP.

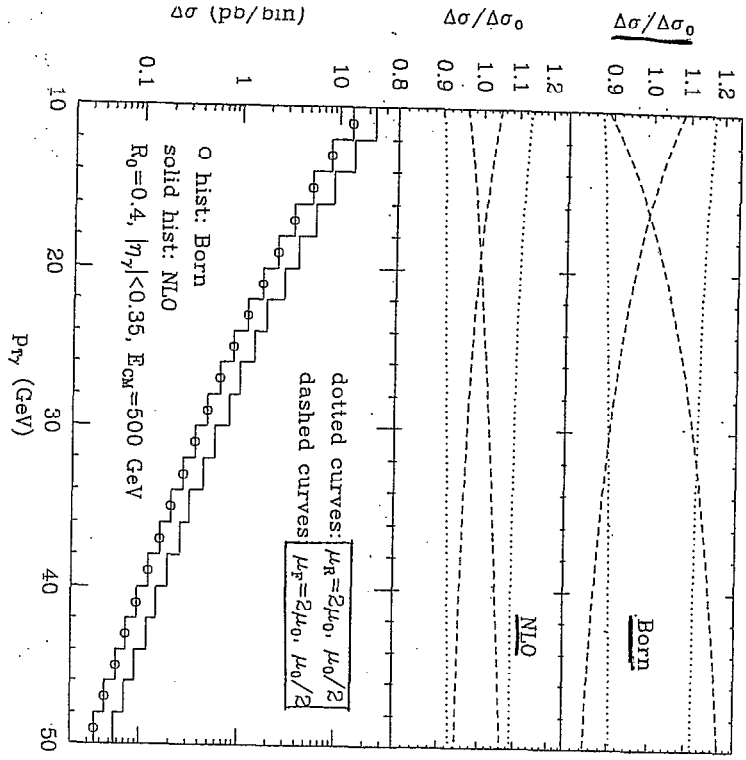

DOMINANCE OF qg SCATT.

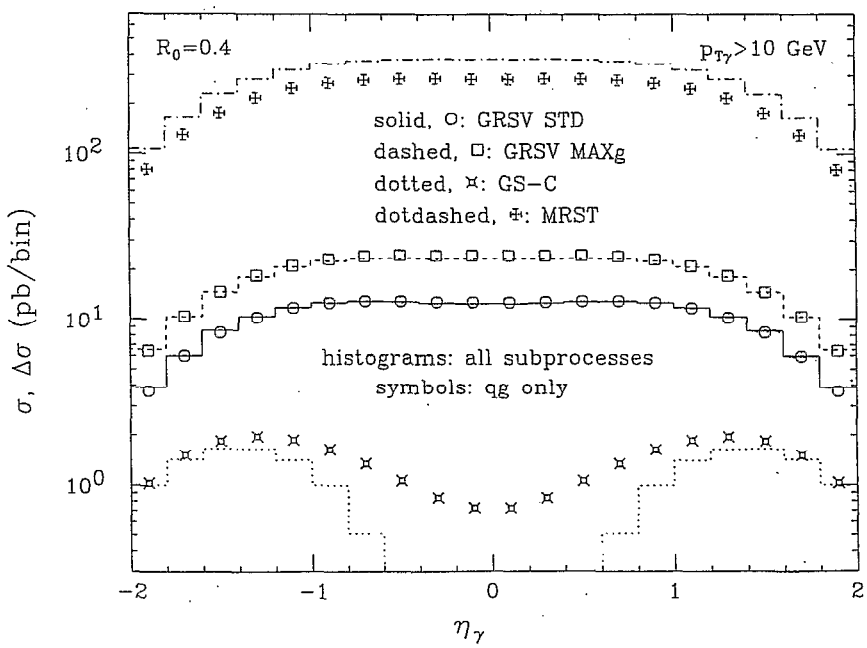

E 706

The trouble with prompt photons...

Unpolarized case :
comparison data $\longleftrightarrow$ NLO theory not satisfactory

- severe problems in fixed-target regime (E706, UA6)
- collider data : some difference (CDF, D0)
- not curable by changes of $g(x, Q^2)$

What to make of it ?

Theory :

- look for additional corrections beyond the NLO framework
- in particular, soft-gluon resummations (Laenen,Sterman,Oderda; Catani,Mangano,Nason,Oleari,WV; Kidonakis,Owens; Li Laenen,Sterman,WV)
- if this cures problems, need to apply in polarized case, too !
  - how are spin asymmetries affected ?
  - do effects cancel in asymmetry ?

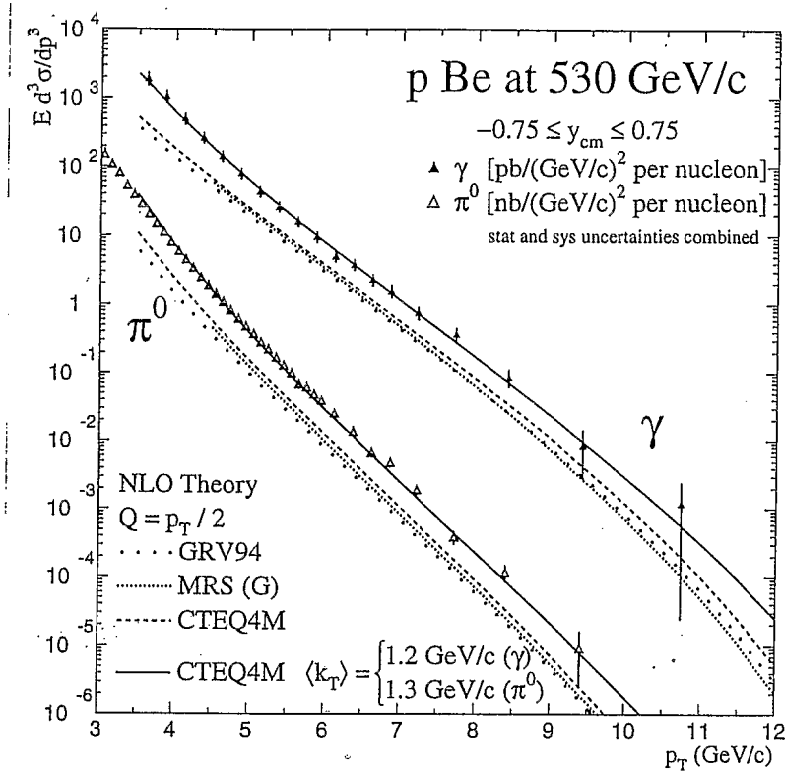

CDF, RUN 1B

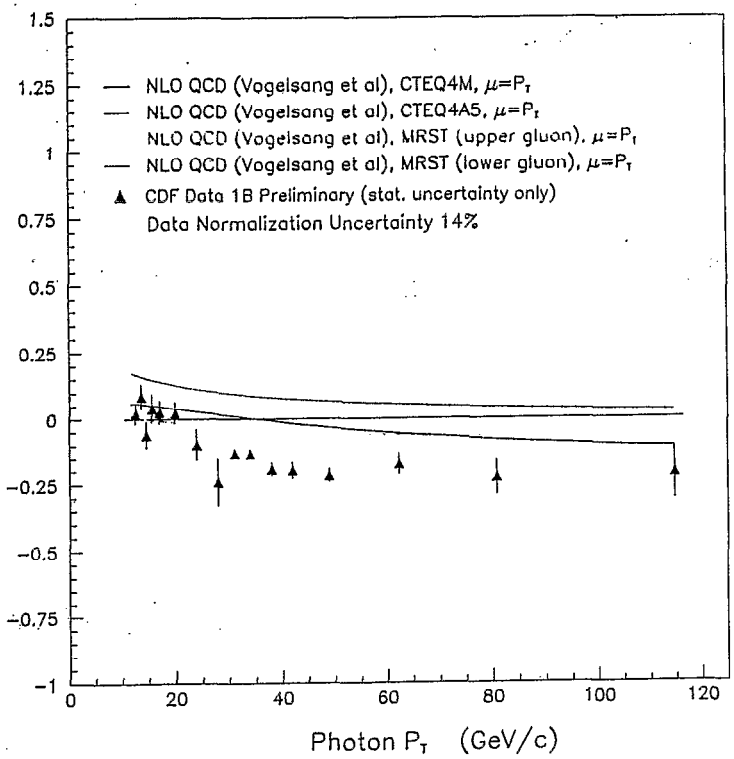

Threshold resummations

→ DY, Higgs, ...

Consider photon of given p_T^γ, η^γ :

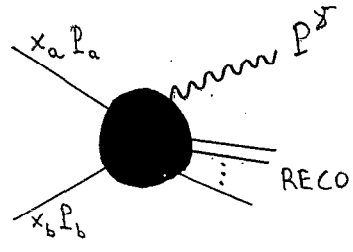

$s_4 = s + t + u$

$z = Q^2/s$

$z < 1$

$\frac{\ln(1-z)}{1-z}$

$s_4 \to 0$: partonic threshold

Partonic cross section for channel $ab \to \gamma x$ at Born level:

$$\frac{d^2\hat{\sigma}_{ab}}{dp_T^\gamma d\eta^\gamma} \propto \alpha_{em}\alpha_s \; \delta(s_4)$$

at higher orders : radiation inhibited for $s_4 \to 0$
cancellation of IR singularities leaves
(large) logarithmic remainders

k^{th} order in PT:

$$\frac{d^2\hat{\sigma}_{ab}^{(k)}}{dp_T^\gamma d\eta^\gamma} \propto \alpha_{em}\alpha_s \sum_{m=0}^{2k-1} A_{m,k}^{(ab)} \; \alpha_s^k \left[\frac{\ln^m(s_4/s)}{s_4}\right]_+$$

(defined under $\int ds_4$ in a distributional sense)

Effects of such terms become numerically important at "large" $p_T^\gamma / \sqrt{S}$ (because of steeply falling pdfs)

- Threshold resummation: these logs to all orders! (exponentiate in Mellin-moment space) 'NLL': Catani, Mangano, Nason; Laenen, Oderda, Sterman

- leads to moderate improvement in unpolarized case (fixed target regime) (Catani, Mangano, Nason, Oleari, WV; Sterman, WV; Kidonakis, Owens)

- presumably not so relevant at colliders

- nevertheless, 'toy' calculation : effects on spin asymmetry for 'fixed-target' kinematics, $E_{\text{beam}} = 530$ GeV, $3 < p_T < 11$ GeV

$$\tilde{\sigma}(N, \eta^\gamma) \equiv \int_0^s \frac{ds_4}{s} \left(1 - \frac{s_4}{s}\right)^{N-1} \frac{(p_T^\gamma)^3 d^2\tilde{\sigma}}{dp_T^\gamma d\eta^\gamma}$$

Here, logarithms occur as

$$\tilde{\sigma}^{(k)}(N, \eta^\gamma) \;\propto\; \alpha_{em}\alpha_s \sum_{m=0}^{2k-1} \tilde{A}_m(\eta^\gamma)\; \alpha_s^k \ln^{m+1}(N)$$

They *exponentiate* :

$$\tilde{\sigma}^{\text{res}}(N, \eta^\gamma) \;\propto\; \tilde{\sigma}^{\text{Born}}(\eta^\gamma) \exp\left[E(N, \eta^\gamma)\right]$$

$$E(N, \eta^\gamma) = \ln(N) \sum_{m=1}^{\infty} a_m \; \underbrace{(\alpha_s \ln(N))}_{\text{"EXPANSION PARAMETER!"}}{}^m + \sum_{m=1}^{\infty} b_m \; (\alpha_s \ln(N))^m + \ldots$$

a_m terms : "leading logs" (LL)
b_m terms : "next-to-leading logs" (NLL)
$\longrightarrow$ control over $\alpha_s^k \, [\ln(N)]^{\{2k, 2k-1, 2k-2\}}$ terms

(Catani, Mangano, Nason, Oleari, WV)

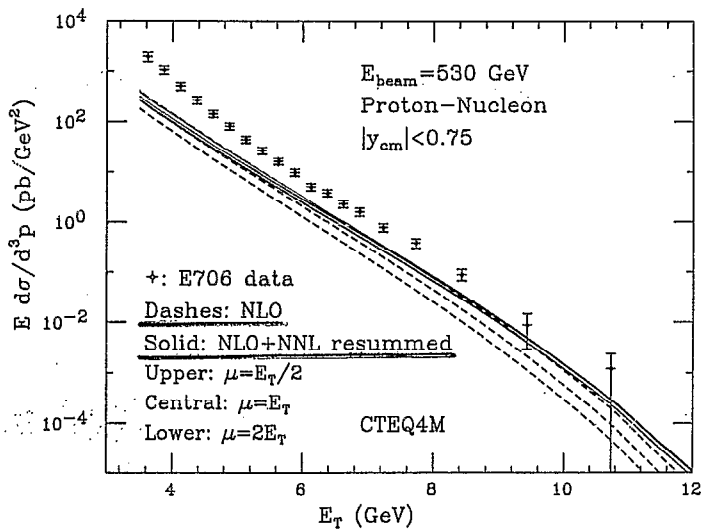

(STERMAI WV)

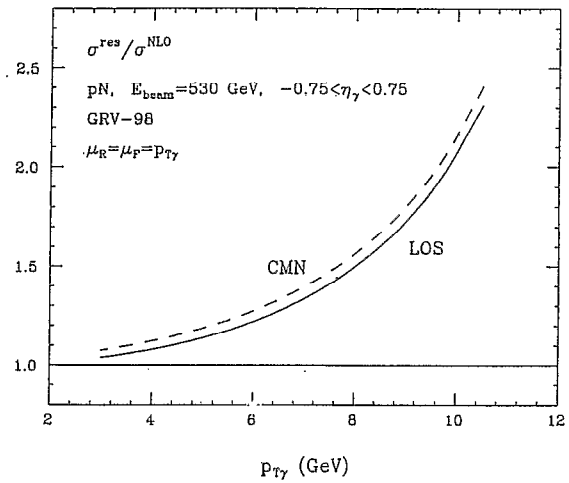

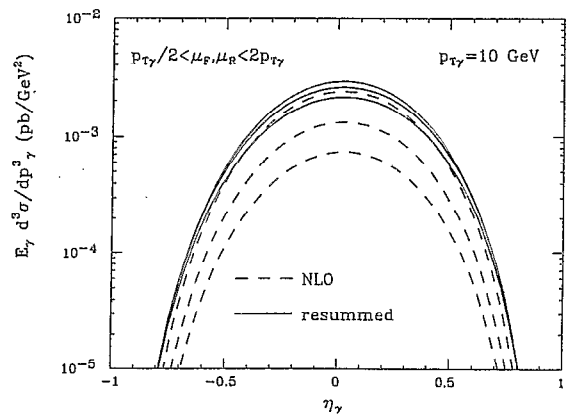

Spin asymmetry and threshold resummation :
(Sterman,WV)

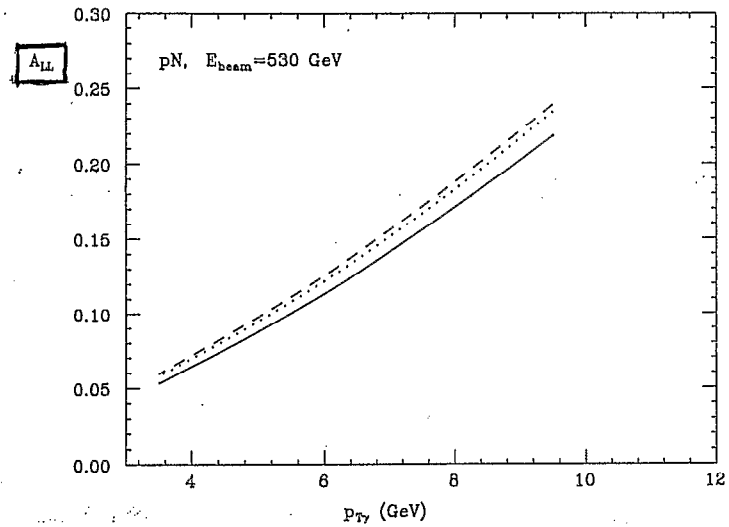

- dotted : LO
- dashed : NLO
- solid : threshold-resummed

'k_T / recoil effects'

Old idea: steeply falling cross section
$\longrightarrow$ hard scattering can produce photon more easily if initial partons have k_T

k_T "kick", "smearing", "broadening"

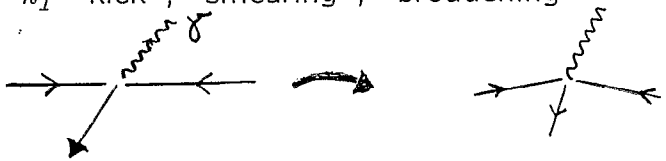

Phenomenological impact studied by :
E706; Apanasevich et al.; MRST; Baer,Reno

- Gaussian k_T distribution, multiplied to pdfs and folded into (LO) hard scattering
- guidance for $\langle k_T \rangle$ from measured values of $\langle p_T \rangle_{\text{pair}}$ for diphotons, dimuons, dijets
- nevertheless, what is k_T, what is $g(x, Q^2)$?
- physical origin thought of as initial-state gluon radiation; "effective description" of perturbative & non-pert. contributions
- remarkably successful, also for π^0 prod. $\langle k_T \rangle \approx 1.2$ GeV (E706) $\rightarrow$ 3.5 GeV (CDF)

APANASEVICH ET AL.
(BEGEL)

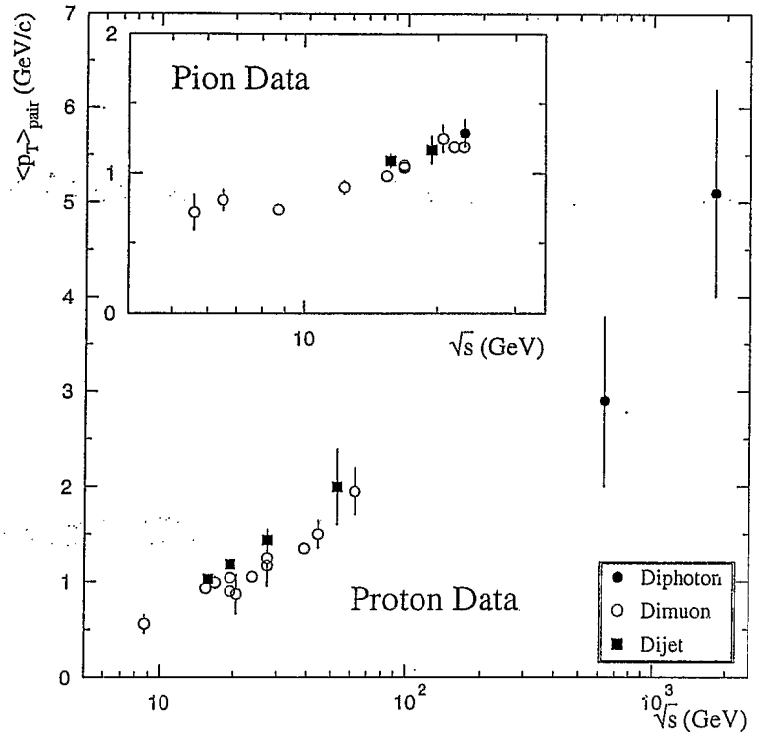

APANASEVICH
ET AL

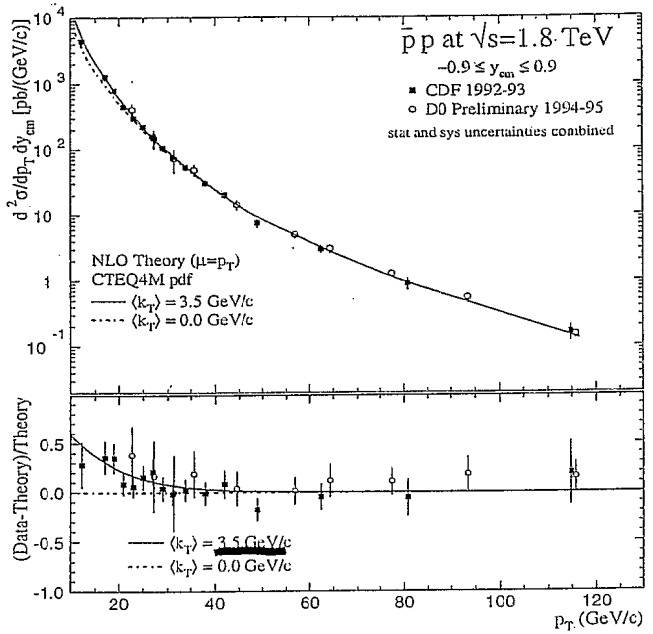

FIG. 2. Top: The CDF and DØ isolated direct-photon cross sections, compared to NLO theory without k_T (dashed) and with k_T enhancement for $\langle k_T \rangle = 3.5$ GeV/c (solid), as a function of p_T. Bottom: The quantity (Data−Theory)/Theory (for theory without k_T adjustment), overlaid with the expected effect from k_T enhancement for $\langle k_T \rangle = 3.5$ GeV/c. The error bars have experimental statistical and systematic uncertainties added in quadrature.

Theory basis ?
experience from Drell-Yan :

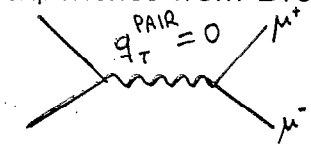

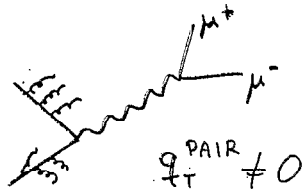

soft-gluon 'q_T logarithms'

$$\alpha_s^k \frac{\ln^{2k-1}(Q^2/q_T^2)}{q_T^2}, \quad \alpha_s^k \frac{\ln^{2k-2}(Q^2/q_T^2)}{q_T^2}, \quad \ldots$$

can be resummed (DDT; Parisi,Petronzio; Collins,Soper,Sterman; Altarelli et al.; Davies,Stirling,Webber; ... Ellis,Ross,Vesli; Balazs,Yuan; Stirling,Kulesza ...) (in q_T or b space). Accounts for observed q_T shape.

Prompt photon $d\hat{\sigma}/dp_T d\eta$:

- NLO terms do not show any $q_T \to 0$ sing.
- reason: q_T has been integrated over!
- "hidden logs of q_T" (Sterman)
- $d\hat{\sigma}/dp_T d\eta\, dq_T^2$ $\left[q_T = q_T^{\gamma+\text{jet}}\right]$ displays logs

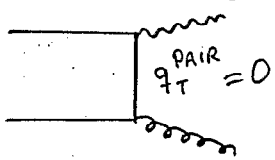

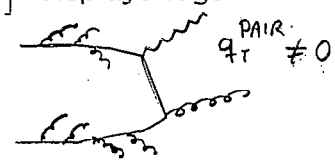

- q_T resummation possible; q_T corresponds to overall radiation $\sum k_T$ and produces recoil corrections in photon p_T spectrum

Laenen,Sterman,WV :

- reconsider threshold resummation and redistribute it over q_T of soft-gluon radiation $\to$ recoil correction to photon p_T spectrum
- exponentiation in threshold resummation results from factorization properties of partonic cross section in soft limit. Still works if transverse momenta of radiation are kept.
- conserve energy *and* transverse momentum
- usual collinear factorization $\Rightarrow$ usual pdfs !
- "joint threshold and k_T resummation"
- related ideas : Li

Drell-Yan near threshold and at low Q_T :

$$\frac{d\sigma_{ab\to V}}{Q^2 d^2 Q_T} = \sigma^{(0)}\; R_{a/a}(x_a, \mathrm{k}_a) \otimes R_{b/b}(x_b, \mathrm{k}_b) \otimes U_{ab}(w_s, \mathrm{k}_s)$$

transv. mom.

energy fraction

with convolutions satisfying

$$(1-x_a) + (1-x_b) + w_s \;=\; 1 - Q^2/S$$
$$\mathrm{k}_a + \mathrm{k}_b + \mathrm{k}_s = \mathrm{Q}_T$$

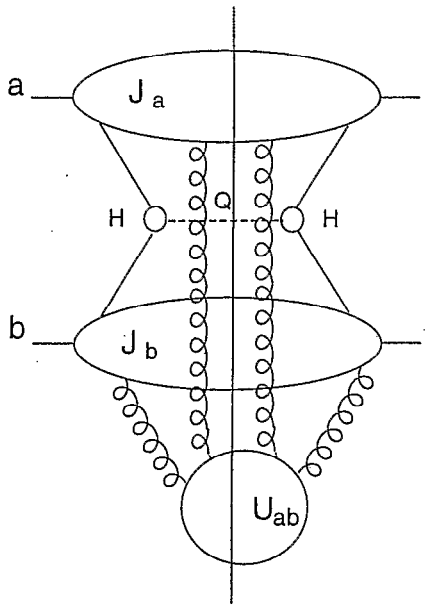

obtain

$$\frac{p_T^3 d\sigma^{(\mathrm{resum})}_{AB\to\gamma X}}{dp_T} = \sum_{ij} \frac{p_T^4}{8\pi S^2} \int_{\mathcal{C}} \frac{dN}{2\pi i}\, \tilde{\phi}_{i/A}(N,\mu)\tilde{\phi}_{j/B}(N,\mu)$$
$$\int_0^1 d\tilde{x}_T^2\, (\tilde{x}_T^2)^N \frac{|M_{ij}(\tilde{x}_T^2)|^2}{\sqrt{1-\tilde{x}_T^2}} \int \frac{d^2\mathrm{Q}_T}{(2\pi)^2}$$
$$\Theta(\bar{\mu} - Q_T) \left(\frac{S}{4\mathrm{p}_T'^2}\right)^{N+1} P_{ij}\left(N, \mathrm{Q}_T, \frac{2p_T}{\tilde{x}_T}, \mu\right)$$

where $\boxed{\mathrm{p}_T' = \mathrm{p}_T - \mathrm{Q}_T/2,}$

$$P_{ij}(N, \mathrm{Q}_T, Q, \mu) = \int d^2\mathrm{b}\, \mathrm{e}^{-i\mathrm{b}\cdot\mathrm{Q}_T} \exp\left[E_{ij\to\gamma h}(N, b, Q, \mu)\right],$$

$$E^{\mathrm{IS}}_{ij}(N, b, Q, \mu) = \sum_{l=i,j} \int_{Q\chi^{-1}(N,b)}^{\mu} \frac{d\mu'}{\mu'} A_l(\alpha_s(\mu'^2))\, 2 \ln \frac{\bar{N}\mu'}{Q}$$

with $\chi(N,b) = \bar{N} + bQ/2\mathrm{e}^{-\gamma_E}$, $\bar{N} = N\mathrm{e}^{\gamma_E}$. Note,

$$\int_{Q\chi^{-1}(N,b)}^{\mu} d\mu' = \int_{Q\chi^{-1}(N,b)}^{Q/\bar{N}} d\mu' + \underbrace{\int_{Q/\bar{N}}^{\mu} d\mu'}_{\text{pure thrshld. resumm.}}$$

- only initial state gives b dependence (Li, Lai)
- expd. to NLL in $\ln(\bar{N} + bQ/2\mathrm{e}^{-\gamma_E})$ and $\ln \bar{N}$
- new "minimal" way of doing b integration:

$$2J_0(z) = H_1(z) + H_2(z)$$

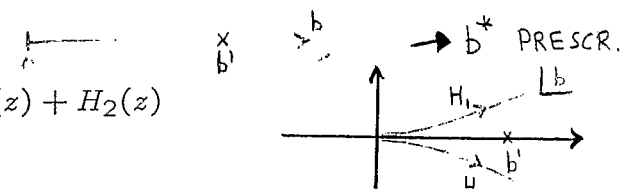

(Sterman,Laenen,WV)

PN , E = 530 GeV

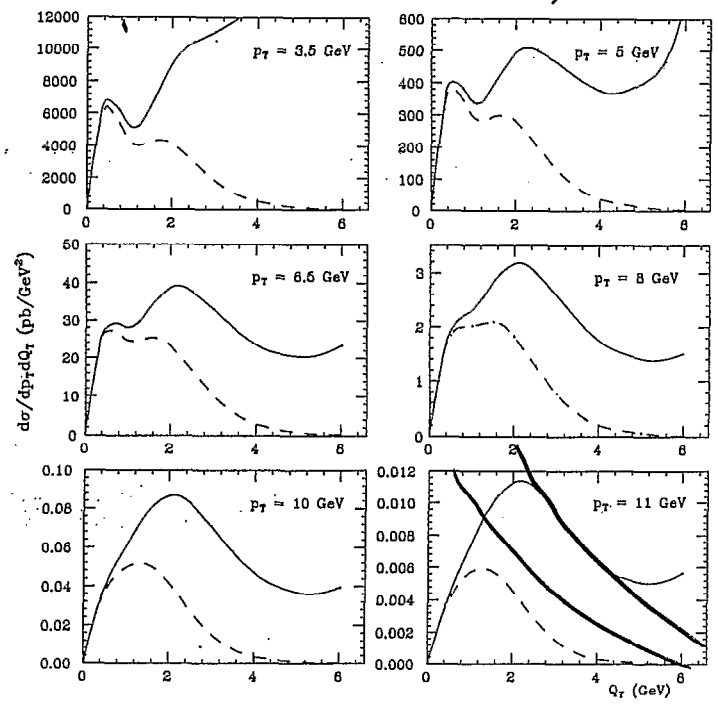

Laenen,Sterman,WV (PRL 84 (2000) 4296) :

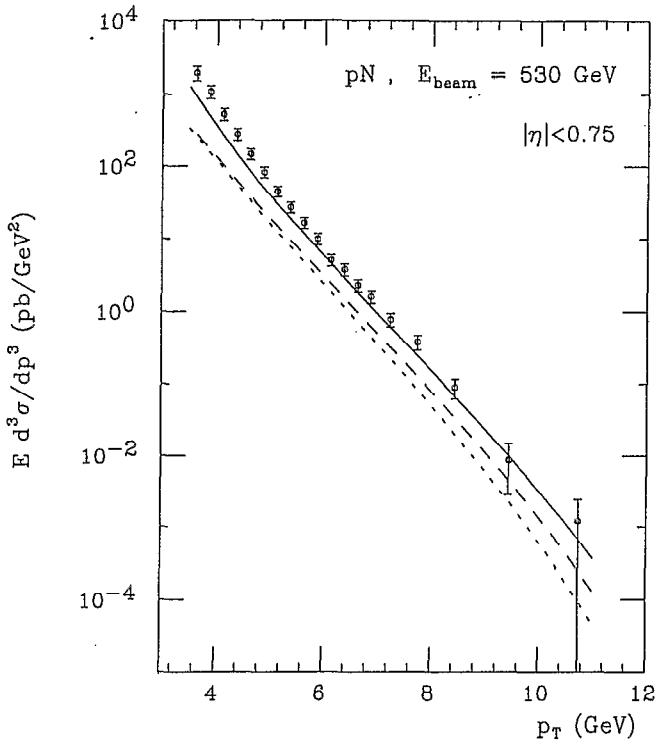

- dotted : NLO
- dashed : threshold-resummed
- solid : jointly resummed, "1st exploration"

STILL A LOT TO DO!

Conclusions

- prompt photons could give us desired information on $g(x, Q^2)$, in part. at large x
- however, still better understanding required
- much recent theory progress
- at RHIC, prompt photons will give first-hand information on Δg
  (need to learn from unpolarized case !)
- resummation effects generally small for A_{LL} ?
- final answer not yet in !

Future Transversity Measurement with PHENIX

Matthias Grosse Perdekamp, (RIKEN BNL Research Center)

Abstract

Hard lepton-nucleon and hadron-hadron scattering cross sections can be expressed with the help of three independent helicity amplitudes. Measurements of the nucleon structure functions $F_2(x, Q^2)$, helicity average, and $g_1(x, Q^2)$, helicity difference, have explored the helicity conserving part of the cross section with great experimental accuracy. In contrast, no information is presently available on the helicity flip amplitude. The absence of experimental measurements is a consequence of the chiral odd nature of the helicity flip amplitude and the related "transversity quark distributions", $\delta q(x, Q^2)$, which prevents the appearance of helicity flip contributions at leading twist in inclusive DIS experiments.

Transversity distributions were first discussed by Ralston and Soper [1] in doubly transverse polarized Drell-Yan scattering. In Drell-Yan processes the transverse double spin asymmetry, A_{TT}, is proportional to $\delta q \delta \bar{q}$ with even chirality. Unfortunately, a recent analysis [2] estimates $A_{TT} \approx 1 - 2\%$ with statistical errors comparable to the asymmetry itself for a projected measurement at RHIC.

Single spin asymmetries $A^{\perp}$ (e.g. unpolarized leptons on transversely polarized nucleon targets) in semi-inclusive DIS and pp scattering may offer an alternative way to observe helicity flip contributions at leading twist. This possibility relies on the presence of fragmentation functions, H, which are sensitive to the quark polarization in the final state and possess the necessary negative chirality. The asymmetries $A^{\perp}$ are proportional to $\Sigma_q \delta q \times \delta a_t^f \times H$, where a_t^f are the transversity dependent partonic initial-final-state asymmetries a_t^f of the struck quark which can be calculated from pQCD.

For example, Collins suggested that in semi inclusive single pion production the quark spin direction might be reflected in the azimuthal distribution of the final state pion [3]. Collins further demonstrated that the symmetry properties of the process do not require the proposed fragmentation function H_1 to be identical to zero.

The current interest in transversity distributions results from a recent Hermes result [4] which may suggest that Collins's function H_1 in fact is different from 0. Clearly the prospects are exciting to have a tool at hand which provides access to the complete helicity structure of hard scattering processes. At DESY a significant fraction (2 years) of the extended Hermes experimental program has been designated for the measurement of the transversity distributions.

Alternatively, Jaffe, Jin and Tang have proposed to utilize two meson interference fragmentation.

both in polarized pp scattering and DIS, [5] in order to access the transversity distributions. In this channel, it is essential to experimentally identify oppositely charged meson pairs coming from the invariant mass region of *S/P*-wave interference (e.g. the ρ/ω region). It is shown in the talk that the invariant mass resolution of the PHENIX detector is sufficient for this purpose. In addition it is demonstrated that rates are high and that it will be possible to analyze data in a fine binning of invariant mass and other kinematic variables. This will provide good control of systematic errors.

References

[1] J. Ralston, D.E. Soper, Nucl. Phys. B152, 109(1979).

[2] O. Martin et al., Phys. Rev. D60, 117502(1999).

[3] J.C. Collins, Nucl. Phys. B396, 161(1993).

[4] A. Airapetian et al., hep-ph/9910062.

[5] B. Jaffe et al., Phys. Rev. D57, 5920(1998), J. Tang, hep-ph/9807560 and J. Tang, Thesis, MIT(1999).

Transversity Measurements at RHIC

- Introduction
- Nucleon transversity through final state interaction in

$$p^{\uparrow} p \rightarrow \pi^{+}\pi^{-} + X$$

- Experimental issues

  Invariant Mass Resolution

  Rates

  Partron Kinematics

Proton Spin Structure at RHIC

Gluon Polarization: ΔG		$\frac{\Delta u}{u}, \frac{\Delta \bar{u}}{\bar{u}}, \frac{\Delta d}{d}, \frac{\Delta \bar{d}}{\bar{d}}$	Transverse Spin
π^0 Production $A_{LL}(gg, gq \to \pi^0 + X)$	STAR + PHENIX		Transversity h_1 :
Heavy Flavors $A_{LL}(gg \to c\bar{c}, b\bar{b} + X)$		W Production	π^+, π^- Interference Fragmentation $A_T(p_\perp p \to (\pi^+, \pi^-) + X)$
		$A_L(u\bar{d} \to W^+ \to l\nu_l)$	STAR +PHENIX+PHOBOS
Direct Photon $A_{LL}(gq \to \gamma + X)$		STAR +PHENIX	Single Pion Asymmetries :
Jet Photon $A_{LL}(gq \to \gamma + Jet + X)$			BRAHMS
Jet Jet $A_{LL}(gq \to Jet + Jet + X)$			

Helicity Amplitudes

Deep Inelastic Scattering

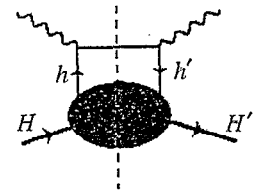

Proton Proton Scattering

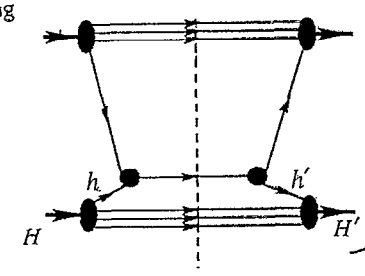

Three independent helicity amplitudes:

H	h		H'	h'
$\frac{1}{2}$	$\frac{1}{2}$	$\to$	$\frac{1}{2}$	$\frac{1}{2}$
$\frac{1}{2}$	$-\frac{1}{2}$	$\to$	$\frac{1}{2}$	$-\frac{1}{2}$

$\Rightarrow F_1, q(x)$ (helicity average)

$g_1, \Delta q(x)$ (helicity difference)

$\frac{1}{2}$	$-\frac{1}{2}$	$\to$	$-\frac{1}{2}$	$\frac{1}{2}$

$\Rightarrow \delta q$ helicity flip!

The transversity distributions $\delta q(x)$ remain the last unmeasured leading twist distribution functions

$H \equiv$ Proton helicity $h \equiv$ quark helicity

The transversity distribution $\delta q(x)$

Quark Distribution Functions:			Structure Functions:
$q(x)$	$\Leftrightarrow$	$\left(\frac{1}{2}\,\frac{1}{2} \to \frac{1}{2}\,\frac{1}{2}\right)+\left(\frac{1}{2}\,-\frac{1}{2} \to \frac{1}{2}\,-\frac{1}{2}\right)$	$\Leftrightarrow$ $F_1(x)=\frac{1}{2}\sum_{i=u,d,s} e_i^2 q_i(x)$ (unpol.)
$\Delta q(x)$	$\Leftrightarrow$	$\left(\frac{1}{2}\,\frac{1}{2} \to \frac{1}{2}\,\frac{1}{2}\right)-\left(\frac{1}{2}\,-\frac{1}{2} \to \frac{1}{2}\,-\frac{1}{2}\right)$	$\Leftrightarrow$ $g_1(x)=\frac{1}{2}\sum_{i=u,d,s} e_i^2 \Delta q_i(x)$ (long.pol.)
			Transversity Distributions
$\delta q(x)$	$\Leftrightarrow$	$\left(+\frac{1}{2}\,-\frac{1}{2} \to -\frac{1}{2}\,+\frac{1}{2}\right)$ $(H,h) \to (-H',-h')$	$\Leftrightarrow$ $h_1(x)\equiv\frac{1}{2}\sum_{i=u,d,s} e_i^2 \delta q_i(x)$ (trans.pol.) Helicity flip!

Probability that quark of flavor i and momentum fraction x contributes to the spin of a transversely polarized proton

$$\delta q_i(x,Q^2)=q_i^{\perp}(x,Q^2)-q_i^{\top}(x,Q^2)$$

The transversity distribution $\delta q(x)$

- For non-relativistic quarks: $\delta q(x,Q^2)=\Delta q(x,Q^2)$
  - ➡ Differences provides information on relativistic nature of quarks inside the proton

$\Delta\Sigma_{non-relativistic} = 1.0$

$\Delta\Sigma_{relativistic} \approx 0.2$

- Soffer's bound: $\left|2\delta q_i(x,Q^2)\right| \le q_i(x,Q^2)+\Delta q_i(x,Q^2)$
  - ➡ Not small! Possibly $|\delta q_i| \approx |\Delta q_i|$!
- $\delta q(x,Q^2)$ does not mix with gluons under evolution !
- First lattice QCD result: $\delta u+\delta d+\delta s=0.56\pm0.09$

  S. Aoki, M. Doui, T. Hatsuda and Y. Kuramashi Phys.Rev. D56 (1997)433
  More recently: S. Capitani et.al. Nucl. Phys. B (Proc. Suppl.) 79 (1999) 548

$$\Delta\Sigma=\Delta u+\Delta d+\Delta s\approx 0.2!$$

Transversity in DIS

Does not contribute in leading twist DIS!

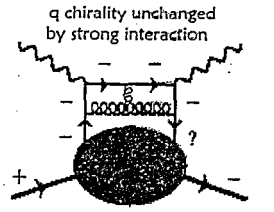

$+ \; - \; \rightarrow \; - \; - \quad ??$

Higher twist contributions are suppressed by $\approx O\left(1/Q^2\right)$

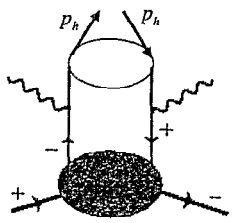

$+ \; - \; \rightarrow \; - \; + \quad !$

Transversity Measurements: DIS vs pp

Polarized pp	Polarized DIS
RHIC/BNL	HERA/DESY, SPS/CERN, e-RHIC, TESLA-N

STAR, PHOBOS, PHENIX

- π^+, π^- Interference Fragmentation: $A_T\left(p_\perp p \rightarrow (\pi^+, \pi^-) + X\right)$
- Drell-Yan: $A_{TT}(p_\perp p_\perp \rightarrow ll) \Leftrightarrow \delta q \cdot \delta \bar{q}$

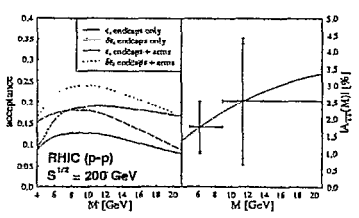

(O.Martin, A. Schafer, M. Stratmann and W. Vogelsang)

- Di-Jets: $A_{TT}(p_\perp p_\perp \rightarrow jet \cdot jet) \Leftrightarrow \delta q \cdot \delta \bar{q}$

(M. Stratmann and W. Vogelsang)

(Approved Transversity Programs)

HERMES, COMPASS

- Collins Effect: $A_T(lp_\perp \rightarrow e\pi^\uparrow + X)$
- π^+, π^- Interference Fragmentation: $A_T\left(lp_\perp \rightarrow l + (\pi^+, \pi^-) + X\right)$

Observables $\propto \delta q \cdot H$

(O $\propto$ distribution - func. $\times$ fragmentation func.)

➡ The transversity distribution δq only can be extracted from a combined analysis of different processes and experiments.

Nucleon transversity through final state interaction at RHIC

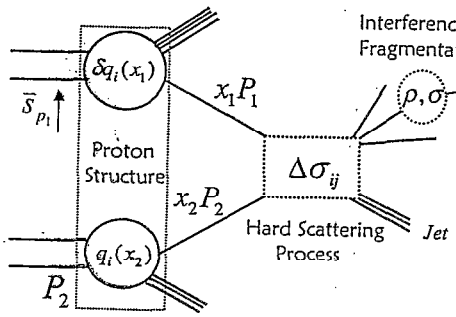

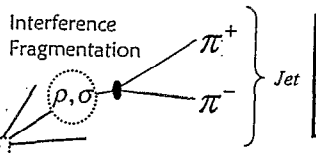

Jian Tang, Thesis MIT, June 1999
R. Jaffe, X.Jin, J. Tang Phys. Rev. D57 (1999)5920
X. Ji, Phys. Rev. D49 (1994)114
J. Collins, S. Heppelmann, G. Ladinsky, Nucl.Phys. B420 (1994)565

Experiment: $A_\perp = \frac{1}{P_{beam}} \frac{N^{\rightarrow} - N^{\leftarrow}}{N^{\rightarrow} + N^{\leftarrow}}$

Currently unknown: Model Calculations LEP Measurement(s)

measured parton dis.

pQCD

$$\frac{d^7\sigma_H(pp^\uparrow \to \pi^+\pi^- X)}{dx_1 dx_2 dt dz dm^2 d\cos\theta d\varphi} \propto \delta q(x_1)\cdot q(x_2) \times \frac{d^3\sigma(q_1 q_2 \to q_3 q_4)}{dx_1 dx_2 dt} \times \frac{d^2\mathcal{M}}{dz dm^2 d\cos\theta d\varphi}$$

Model Calculations

(RBRC Workshop on Future Transversity: Delphi, Jakob et.al., Polyakov, Weiss et.al. Leader et.al)

Interference fragmentation $\frac{d^2\mathcal{M}}{dz dm^2}$

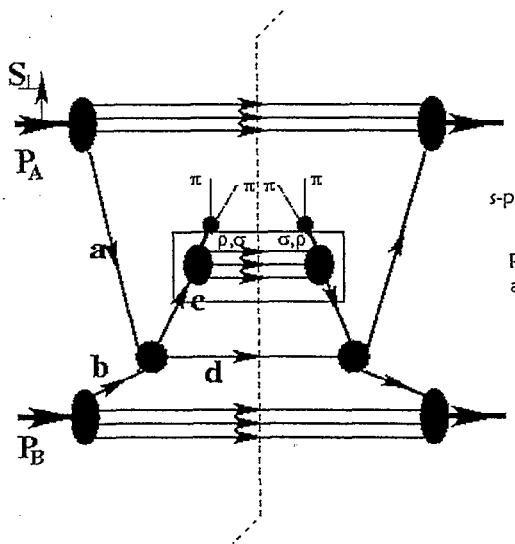

s-p wave interference fragmentation:

Parton emits ρ/σ followed by absorption of σ/ρ a forming a parton

Interference Fragmentation

$$\frac{d^2\mathcal{M}}{dzdm^2} \propto \sin\delta_0 e^{i\delta_0}\left(\kappa\cdot\hat{q}_I(z)+\lambda\cdot\delta\hat{q}_I(z)\right)\sin\delta_1 e^{-i\delta_1}+\ldots$$

s-wave

p-wave

Strong interaction π,π phase shifts

Where:
$\kappa = I\otimes\overline{\eta}_0,\ \lambda=\sigma_+\otimes\overline{\eta}_- + \sigma_-\otimes\overline{\eta}_+$
$\hat{q}_I(z), \delta\hat{q}_I(z)$: spin average and difference fragmentation functions

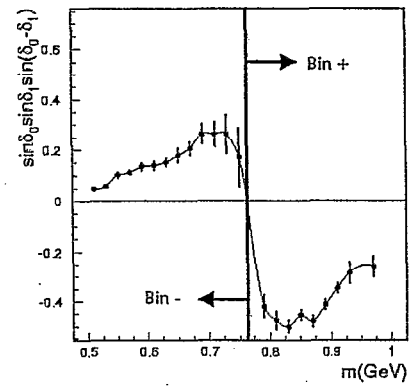

P. Estabrooks and A.D. Martin, Nucl. Phys. B79 (1974)301

Non-vanishing "support" only in the ρ mass region!

- Sufficient mass Resolution?
- Great for systematics!

Transverse Single Spin Asymmetry

(Tang, Thesis, MIT)

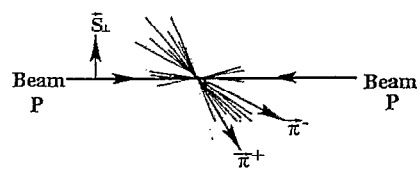

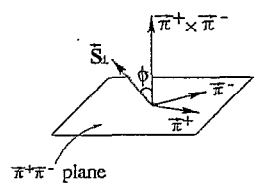

$N^{\rightarrow}$: Pion Pair Yield
$\sin\delta_i$: Two Pion Phase Shifts
$\delta q(x)$: Transversity quark DFs
$\delta\hat{q}(z)$: Pol. Fragmentation Func.

$$A_\perp = \frac{1}{P_{beam}}\frac{N^{\rightarrow}-N^{\leftarrow}}{N^{\rightarrow}+N^{\leftarrow}} = -\frac{\sqrt{6}\pi}{4}\boxed{\sin\delta_0\sin\delta_1\sin(\delta_0-\delta_1)\cdot\cos(\phi)}\cdot$$

$$\frac{[\delta q(x_1)\cdot G(x_2)\cdot\delta\hat{q}_I(z)]\delta\hat{\sigma}^{qg}_{qg}+\ldots}{\{[G(x_1)\cdot G(x_2)]\delta\hat{\sigma}^{q\bar{q}}_{gg}+\ldots\}\cdot[\sin^2\delta_0\hat{q}_0(z)+\sin^2\delta_1\hat{q}_1(z)]}$$

Maximum Asymmetry

$\eta=0, m_{\rho,\sigma}=0.83$ GeV, $\cos\phi=1$
$\delta\hat{q}_I^2 = 4\hat{q}_0\hat{q}_1/3,\ 2|\delta q|\le q+\Delta q$

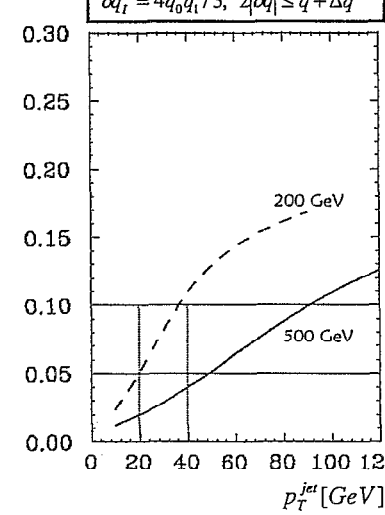

STAR

Momentum Resolution from TPC: 16 MeV
Jet Reconstruction Capability => Can estimate
Jet Energy and fraction of Jet Energy transferred
to the pion pair!

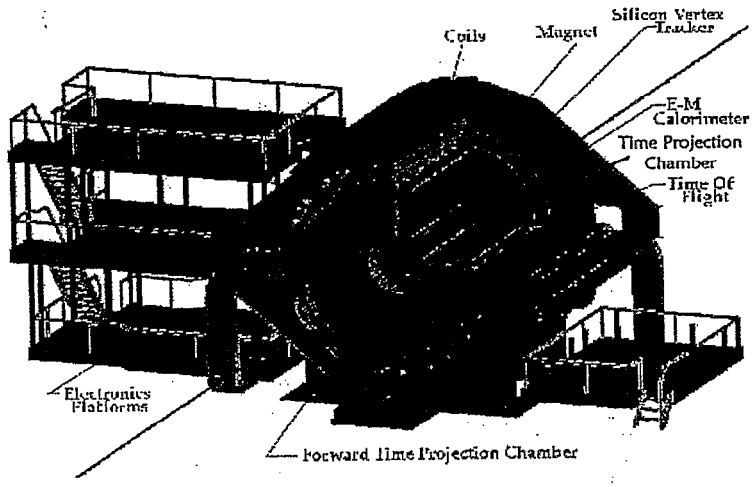

PHENIX-Measurement

Trigger: Tag $\pi^{+,-}$ in RICH and Jet Mul in EMCal

Reconstruct invariant mass of pion pairs

Form single spin asymmetry $A_{exp} = \frac{N^{\uparrow} - N^{\downarrow}}{N^{\uparrow} + N^{\downarrow}}$

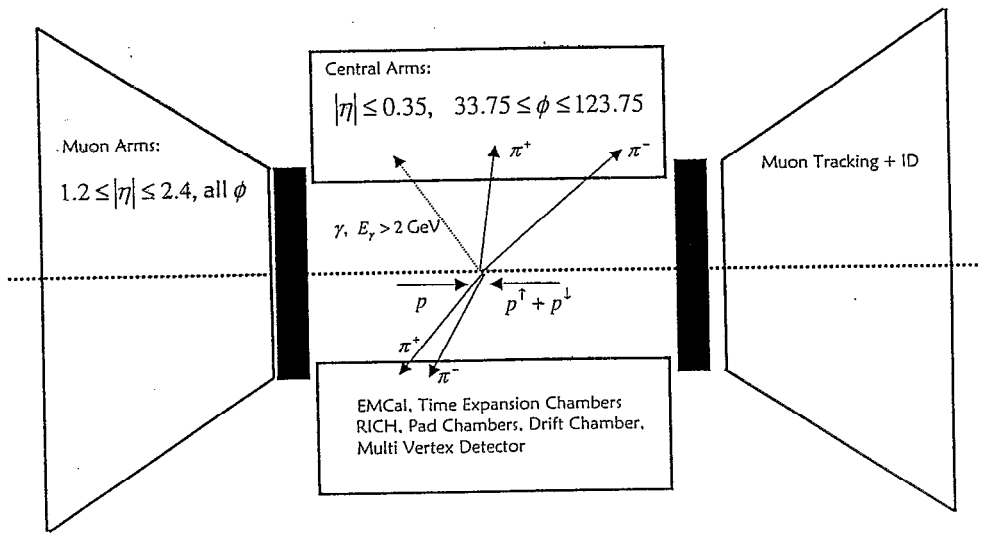

The PHENIX Detector

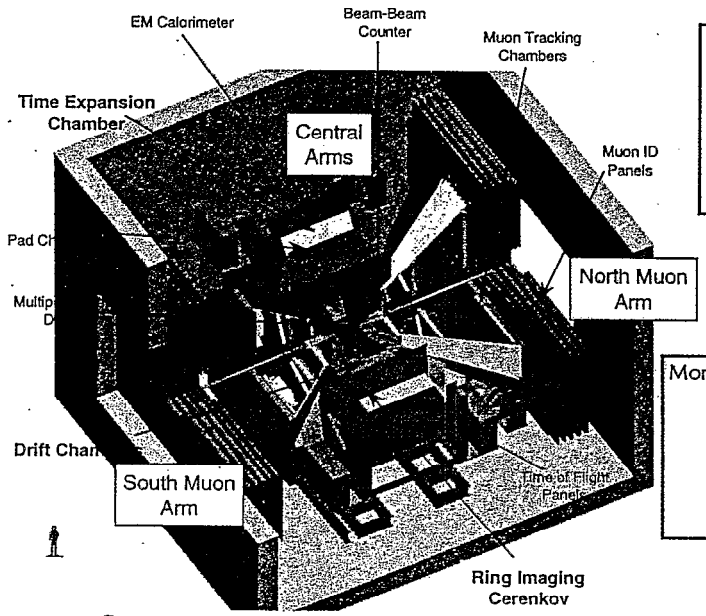

RICH Thresholds for different Species	
p-ID	p [GeV]
e	0.013
π	3.5
K	12.3
p	23.5

Momentum Resolution in the Central Arm	
p [GeV]	Δp [MeV]
1	6
3	36
5	90
10	200

PHENIX Momentum and Angular resolution

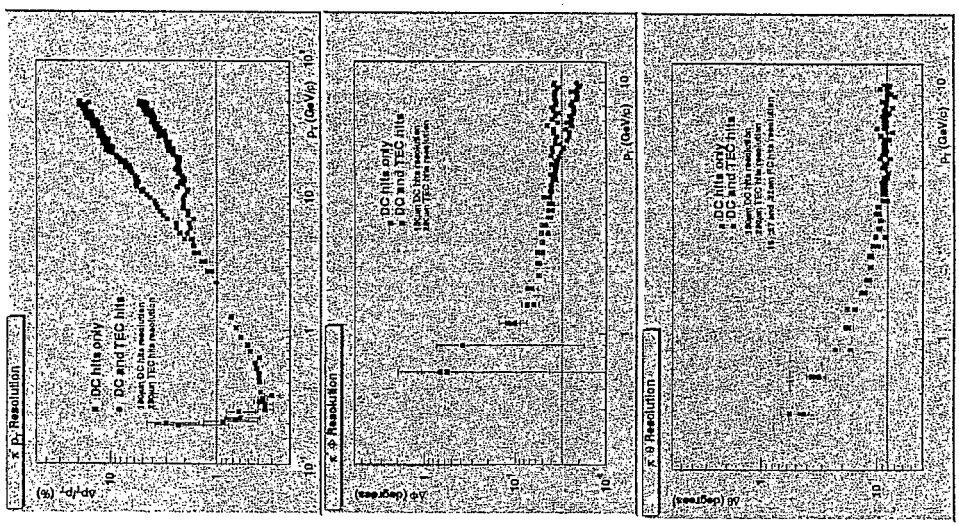

Invariant Mass Resolution in PHENIX

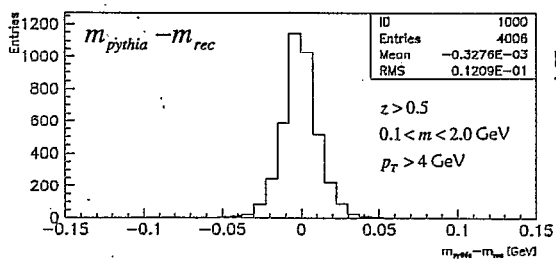

RMS=12 MeV

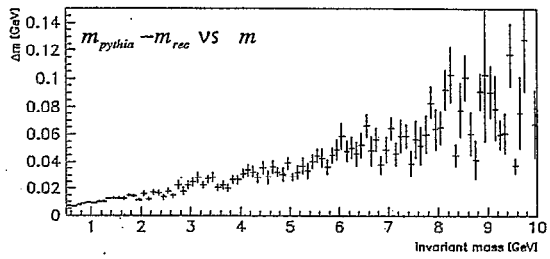

➡ Nice! (from Heavy Ion)

Expected Rate

Example:

$E_{\pi_1,\pi_2} > 4$ GeV
$\sqrt{p_{1T}^2 + p_{2T}^2} > 4$ GeV
800 MeV $< m <$ 950 MeV

} 5.2 Million events in 32 pb^{-1}
15% with pair after cuts

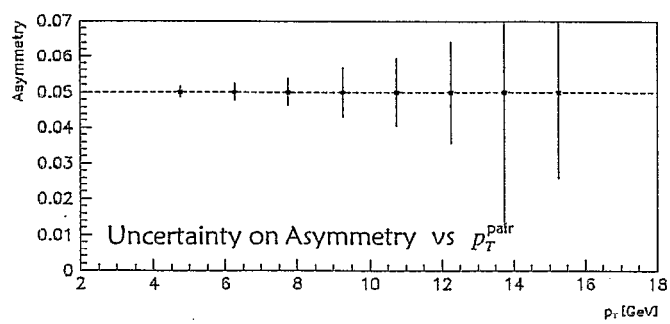

Kinematics

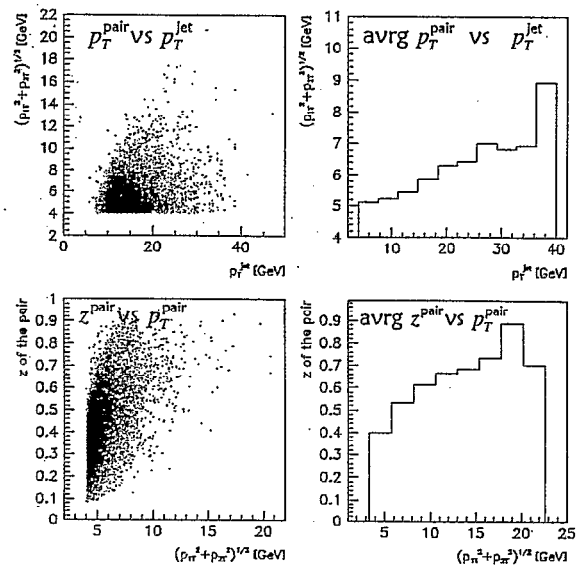

Cannot reconstruct Event Kinematics in PHENIX

-> STAR!

Projected Asymmetry

(For 1 week of running)

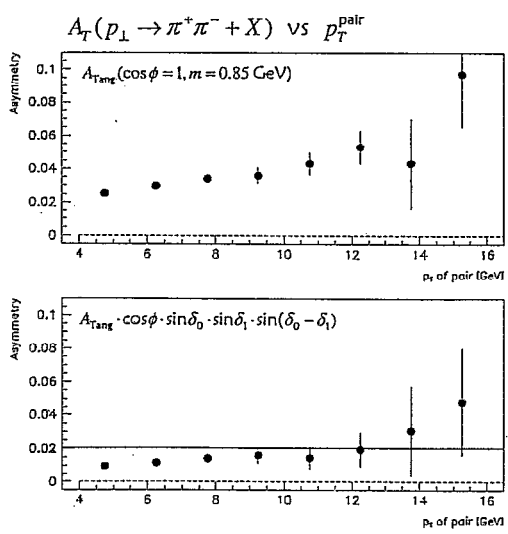

$\int Ldt = 32\,pb^{-1}$

$E_{\pi_1,\pi_2} > 4$ GeV

$\sqrt{p_{1T}^2 + p_{2T}^2} > 4$ GeV

800 MeV $< m <$ 950 MeV

Small aymmetry below 5% but good rate!

Conclusions

- $\delta q(x)$ remains last unmeasured leading twist distribution function
- Transversity can be probed using Interference Fragmentation Functions
- Momentum Resolution and Statistics are sufficient
- Good Control of Systematic Errors
- Fragmentation Functions are (currently) unknown

Short comment

Akiko Ogawa

STAR detector

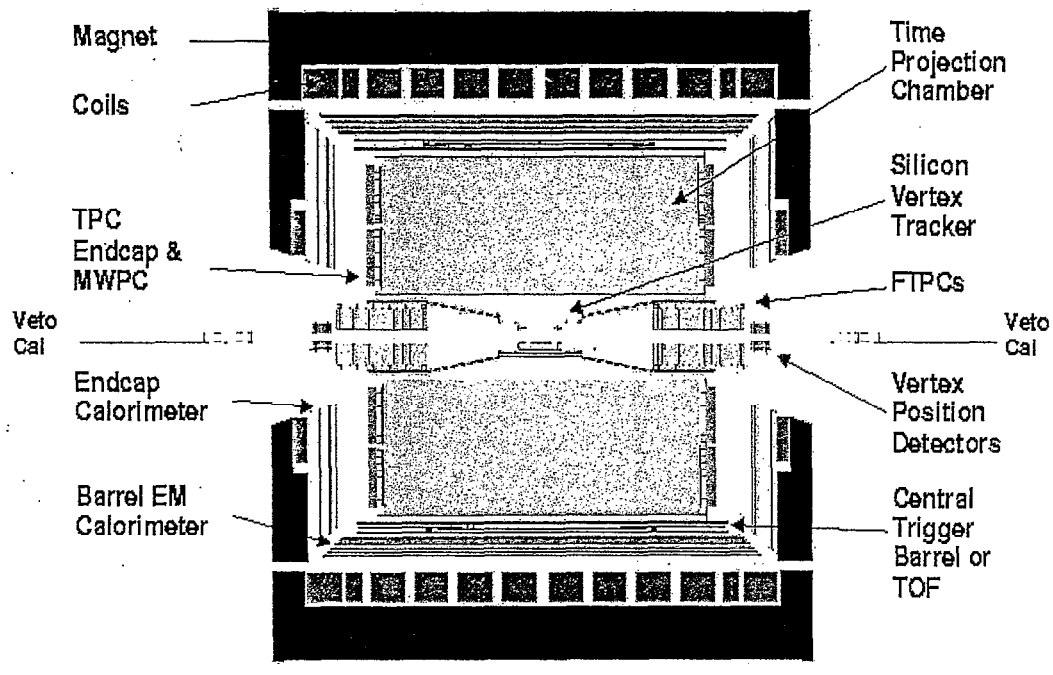

Two meson production

$$A=\frac{\sigma^{-\uparrow+}-\sigma^{+\uparrow-}}{\sigma+\sigma}=\frac{\sum\delta q\otimes q\otimes\delta\sigma\otimes\delta D}{\sum q\otimes q\otimes\sigma\otimes D}$$

$$=\frac{\sqrt{6}\pi}{4}\cos\phi\,\sin\delta_0\sin\delta_1\sin(\delta_0-\delta_1)\ \text{mass}$$

$$\otimes\frac{\sum_{qg\to qg,\bar{q}g\to\bar{q}g\ldots}\delta\hat{q}_0(z_1)\otimes\hat{q}_0(z_2)\otimes\delta\sigma\ \text{Pt},\eta\ \otimes\delta\hat{q}_I(z)\ z}{\sum_{gg\to q\bar{q},qg\to qg\ldots}\hat{q}_0(z_1)\otimes\hat{q}_0(z_2)\otimes\sigma\ \otimes\{\sin\delta_0\hat{q}_0(z)+\sin\delta_1\hat{q}_1(z)\}}$$

Phase Shift $\sin\delta_0\sin\delta_1\sin(\delta_0-\delta_1)$ is known

ρ,σ Fragmentation function $\hat{q}_0(z),\hat{q}_1(z)$

Interference fragmentation function $\delta\hat{q}_I(z)$ } unknown

Schwartz Inequality $\delta\hat{q}_I(z)=\frac{3}{4}\hat{q}_0(z)\hat{q}_1(z)$

$\hat{q}_0(z)=\hat{q}_1(z)$

A scenario

Year 2002 or 2003
L = 8 10^31 /cm^2/sec
1 week run, 50% machine time 32/pb

L0 (EMC Jet) Trigger with threshold ~ 10GeV
Only using north/south (not top/bottom)
With L3 data size reduction ~15Hz to tape

	Hz	300K sec Total		
Jet Events	15	4.5M	Beam Polarization	0.7
pt<10		2M	cosϕ integral	0.5
10<pt<20		2M	⟶ dilution factor	0.35
20<pt		0.5M	82K events = 1% error on A	

Study dependence on cosϕ, mass , z, Pt_jet , h _jet

Transversity (via 2 pions) in year 2?

Year 2001 L = 1.25 10^30 /cm^2/sec Polarization 50%
2 week run, 50% machine time
CTB multiplicity trigger
Only using north/south (not top/bottom) 30Hz(?)
(L3 event selection on Jets / high z ? /mass ?) ~10Hz to tape(?)

	Hz	600K sec Total	dA	Wild guess / Tang's Asym
Min bias	30			
Jet Events	~3	1.8 M		
5< pt<10	~2.5	1.8 M	0.3 %	
10<pt<20	~0.4	240K	0.8 %	0.6% / 4%
20<pt	~0.02	12K	3%	

Single spin & transverse spin / false asym free / EMC is not must
If we measure non-zero, it's already something
We should start looking at it, when we get collisions

But require good polarization & luminosity to have "real" physics data
Not in year 2

Sudakov Suppression of Azimuthal Spin Asymmetries

D. Boer (RIKEN-BNL Research Center)

Abstract

We will demonstrate that transverse momentum dependent azimuthal spin asymmetries, like the Collins effect asymmetry, generally suffer from suppression due to Sudakov factors. This means that tree level estimates of such asymmetries tend to overestimate the magnitude. This observation will be illustrated by two examples, which are relevant for present day studies. In these examples the inclusion of Sudakov factors cause suppression by at least an order of magnitude compared to the tree level result. Moreover, this suppression increases with energy approximately as a fractional power, numerically found to be $a \approx 0.3$.

The first example [1] is a helicity non-flip double transverse spin asymmetry in vector boson production, relevant for instance for the polarized proton-proton collisions to be performed at RHIC. In this case, the Sudakov suppression (on top of a kinematical suppression) implies that the asymmetry will be negligible for Z or W production at RHIC. On the other hand, this opens the way towards studies of physics beyond the Standard Model using the spin observable A_{TT}^{W}.

The second example is a Collins effect driven $\cos(2\phi)$ asymmetry in electron-positron annihilation into two almost back-to-back pions [2], which in principle can
be determined from existing LEP data. Such a determination of the Collins effect fragmentation function would be useful for the extraction of the transversity distribution function. However, the Sudakov suppression casts some doubt on the actual determination [3] of the Collins fragmentation function from LEP data. The same does not hold for a similar determination of the interference fragmentation functions
from LEP data which is therefore much more promising.

[1] D. Boer, hep-ph/0004217, to appear in Phys. Rev. D.
[2] D. Boer, R. Jakob, P.J. Mulders, Phys. Lett. B 424 (1998) 143.
[3] A.V. Efremov, O.G. Smirnova, L.G. Tkachev, Nucl. Phys. B (Proc. Suppl.) 74(1999) 49.

Sudakov Suppression of Azimuthal Spin Asymmetries

Daniël Boer
RIKEN-BNL Research Center

- Transverse momentum dependent azimuthal asymmetries
- Effects of Sudakov factors in two explicit examples:
  - Double transverse spin asymmetry in vector boson production
  - Collins effect asymmetry in electron-positron annihilation
- Implications and conclusions

Transverse momentum in asymmetries

Transverse momentum dependent azimuthal asymmetries can be described using transverse momentum dependent distribution and fragmentation functions

Leads to many azimuthal asymmetries, even unpolarized ones

Example 1: $H_1 H_2 \to V(q_T) \to \ell \ell' X$
Example 2: $e^+ e^- \to V(q_T) \to h_1 h_2 X$

The vector boson V has a transverse momentum q_T compared to the two hadrons

Tree level DY: Ralston & Soper, NPB 152 (1979) 109
Tangerman & Mulders, PRD 51 (1995) 3357

Beyond tree level: include gluon emission corrections; if $q_T^2 \ll Q^2$, perform resummation, yields Sudakov factors

Collins, Soper & Sterman, NPB 250 (1985) 199 [DY]
Collins & Soper, NPB 193 (1981) 381 [e^+e^-]

Transverse Momentum Dependence

Transverse momentum dependent distribution functions:

Pictorially:

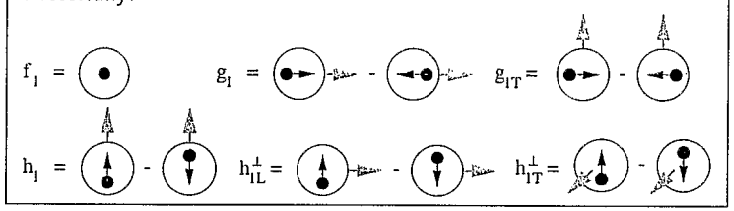

E.g., $g_{1T}(x, p_T^2)$ is the distribution of longitudinally polarized quarks (with nonzero transverse momenta) inside a transversely polarized hadron

g_{1T} is h^{LT} in Ralston & Soper, NPB 152 (1979) 109

$$\Phi(x, p_T) = \frac{M}{2} \left\{ f_1(x, p_T^2) \frac{\not{p}}{M} - \frac{(p_T \cdot S_T)}{M} g_{1T}(x, p_T^2) \frac{\not{p}\gamma_5}{M} + \ldots \right\}$$

One can show that (m=0)

$$\int d^2 p_T \frac{p_T^2}{2M^2} g_{1T}(x, p_T^2) \overset{WW}{=} x\, g_T(x)$$

Example: A_{TT}^V

Double transverse spin asymmetries in vector boson production (D.B., hep-ph/0004217, to appear in PRD)

Most well-known: the transversity double spin asymmetry

$$A_{TT} = \frac{\sigma(p^\uparrow p^\uparrow \to \ell\,\ell'\,X) - \sigma(p^\uparrow p^\downarrow \to \ell\,\ell'\,X)}{\sigma(p^\uparrow p^\uparrow \to \ell\,\ell'\,X) + \sigma(p^\uparrow p^\downarrow \to \ell\,\ell'\,X)}$$

$$= \frac{\sin^2\theta\cos 2\phi_S^\ell}{1+\cos^2\theta}\,\frac{\sum_{a,\bar{a}} e_a^2\, h_1^a(x_1)\,\overline{h}_1^a(x_2)}{\sum_{a,\bar{a}} e_a^2\, f_1^a\,\overline{f}_1^a}$$

It arises from a term $\propto \cos(\phi_{S_1}^\ell + \phi_{S_2}^\ell)$ in the cross section
Averaging over the lepton plane eliminates this contribution

Not present for W production

Helicity non-flip A_{TT}^V

Consider the cross section differential in the transverse momentum of V (angle and/or magnitude) ($q_T^2 \equiv Q_T^2 \ll Q^2$)

In the cross section there is a term proportional to $\cos(\phi_{S_1}^\ell - \phi_{S_2}^\ell)$, which does not depend on the lepton scattering plane

We find

$$A_{TT}^V(Q_T) = \frac{d\sigma(p^\uparrow p^\uparrow \to V\,X) - d\sigma(p^\uparrow p^\downarrow \to V\,X)}{d\sigma(p^\uparrow p^\uparrow \to V\,X) + d\sigma(p^\uparrow p^\downarrow \to V\,X)}$$

$$= -\frac{\sum_{a,\bar{a};b,\bar{b}} K_1^{ab}(y)\,\mathcal{F}\left[\boldsymbol{p}_T\cdot\boldsymbol{k}_T\, g_{1T}\overline{g}_{1T}\right]}{2M_1M_2\,\sum_{a,\bar{a};b,\bar{b}} K_1^{ab}(y)\,\mathcal{F}\left[f_1\,\overline{f}_1\right]}$$

For W production: $K_1^{ab}(y) = |V_{ab}|^2$

For neutral bosons, $K_1^{ab}(y) \propto \delta^{ab}$ is a dimensionless function of y and Q^2

Ralston & Soper, NPB 152 (1979) 109 (tree level and $V = \gamma^*$)

Helicity non-flip A_{TT}^V

Tree level (intrinsic transverse momentum only):

$$\mathcal{F}[f\bar{f}] \equiv \int d^2p_T\, d^2k_T\, \delta^2(p_T + k_T - q_T) f^a(x_1, p_T^2) \bar{f}^b(x_2, k_T^2)$$

Resummation of soft gluons into Sudakov form factors results in a replacement (Collins, Soper & Sterman)

$$\mathcal{F}[f\bar{f}] = \frac{1}{2\pi} \int_0^\infty db\, b\, J_0(bQ_T)\, e^{-S(b)} \tilde{f}^a(x_1, b)\, \tilde{\bar{f}}^b(x_2, b)$$

$$S(b, Q) = \int_{b_0^2/b^2}^{Q^2} \frac{d\mu^2}{\mu^2} \left[A(\alpha_s(\mu)) \ln \frac{Q^2}{\mu^2} + B(\alpha_s(\mu)) \right]$$

Collins (NPB 396 (1993) 161): "*The effect [of Sudakov form factors] is to broaden the transverse momentum distribution as Q increases, but in a spin-independent way: the broadening is due to recoil against the transverse momentum of soft gluon emission. This will have the effect of diluting the spin asymmetry [...].*

Sudakov form factors in polarized scattering: Weber (NPB 382 (1992) 63; NPB 403 (1993) 545)

Estimating the effect

Assume Gaussian transverse momentum dependence:

$$g_{1T}(x, p_T^2) = g_{1T}(x)\, \frac{R^2}{\pi}\, \exp\left(-R^2 p_T^2\right)$$

Also: $g_{1T}^{WW}(x) = x g_T^{WW}(x)\, 2M^2R^2 \approx x g_1(x)\, 2M^2R^2$

$$A_{TT}(Q_T) = \frac{\sum_{a,\bar{a};b,\bar{b}} K_1^{ab}(y)\, x_1 g_1^a(x_1)\, x_2 \bar{g}_1^b(x_2)}{2\sum_{a,\bar{a};b,\bar{b}} K_1^{ab}(y)\, f_1^a(x_1)\, \bar{f}_1^b(x_2)}\, \mathcal{A}(Q_T)$$

where

$$\mathcal{A}(Q_T) \equiv M^2 \frac{\int_0^\infty db\, b^3\, J_0(bQ_T)\, \exp\left(-S(b_*) - S_{NP}(b)\right)}{\int_0^\infty db\, b\, J_0(bQ_T)\, \exp\left(-S(b_*) - S_{NP}(b)\right)}$$

With usual b regulator $b_* = b/\sqrt{1 + b^2/b_{\max}^2}$, $b_{\max} = 0.5\ \text{GeV}^{-1}$

For the nonperturbative contribution S_{NP} we use the parameterization of Ladinsky-Yuan (PRD 50 (1994) R4239), with $x_1 x_2 = 10^{-2}$:

$$S_{NP}(b) = 1.98\ \text{GeV}^2\, b^2 \quad \text{at } Q = 80\ \text{GeV}$$
$$S_{NP}(b) = 0.77\ \text{GeV}^2\, b^2 \quad \text{at } Q = 10\ \text{GeV}$$

Estimating the effect

(Q_T)

$^2 = 80^2$ GeV^2

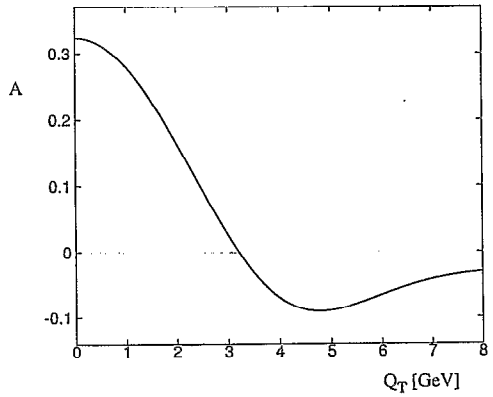

(Q_T)

$^2 = 10^2$ GeV^2

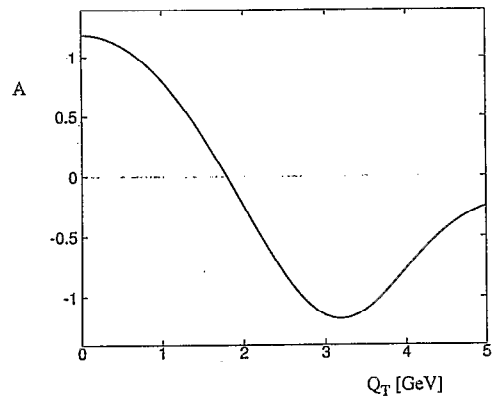

Implications

The total asymmetry $A_{TT}(Q_T)$ at $Q = M_W$ is expected to be below the percent level, if one assumes that on average $x_1 = 0.4$ and $x_2 = 0.07$ for W production at RHIC

The asymmetry oscillates, so an incomplete integration over Q_T –for instance due to imposed cuts– will not lead to a significant asymmetry either

$A^V_{TT}(Q_T)$ is mainly of interest at lower energies ($V = \gamma^*$)

$A(Q_T = 0) \sim 1/\log^2 Q$

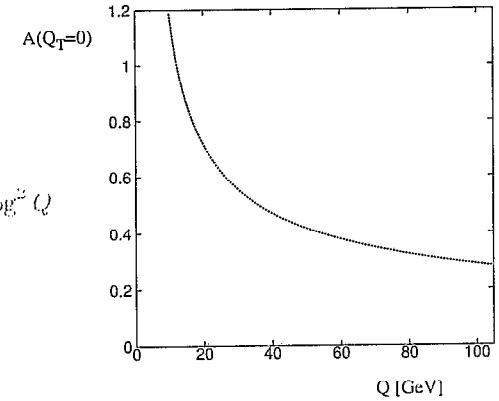

Comparison to tree level

omparing the resulting asymmetry with the tree level asymmetry,

$$A_{TT}(Q_T=0) = M^2R^2\,\frac{\sum_{a,\bar{a}}\,K_1^a(y)\,x_1 g_1^a(x_1)\,x_2\overline{g}_1^a(x_2)}{\sum_{a,\bar{a}}\,K_1^a(y)\,f_1^a(x_1)\,\overline{f}_1^a(x_2)}$$

ads to a comparison of $\mathcal{A}(Q_T=0)$ and $2M^2R^2$

a tree level analysis $R^2 = 1/\langle p_T^2\rangle$ with $R^2 \approx 2-11\,\mathrm{GeV}^{-2}$, i.e. $p_T^2\rangle \approx (300-700\,\mathrm{MeV})^2$

his shows that $\mathcal{A}(Q_T=0, Q=80)$ is at least an order of magnitude smaller

lence, tree level estimates tend to overestimate transverse momentum dependent azimuthal asymmetries

Beyond the SM

Standard Model A_{TT}'s (all small at RHIC)

$$\begin{aligned}
A_{TT}^{Z/\gamma^*} &\propto \cos(\phi_{S_1}^\ell + \phi_{S_2}^\ell)\,h_1^a(x_1)\,\bar{h}_1^a(x_2)\\
A_{TT}^{V} &\propto \cos(\phi_{S_1}^\ell - \phi_{S_2}^\ell)\,\frac{M_1M_2}{Q^2}\,g_T\,\overline{g}_T\\
A_{TT}^{V}(Q_T) &\propto \cos(\phi_{S_1}^\ell - \phi_{S_2}^\ell)\,\mathcal{F}\left[\boldsymbol{p}_T\cdot\boldsymbol{k}_T\,g_{1T}\overline{g}_{1T}\right]
\end{aligned}$$

The Sivers effect or soft gluon pole contributions may give rise to $\sin(\phi_{S_1}^\ell - \phi_{S_2}^\ell)$ asymmetries, but these also suffer from Sudakov suppression or power suppression

Therefore: is A_{TT}^W the perfect place to search for physics beyond the standard model?

For instance, Rykov's T-odd asymmetry (hep-ex/9908050)

$$A_{TT}^{\perp} \propto \sin(\phi_{S_1}^\ell + \phi_{S_2}^\ell)$$

which would arise due to CP-violating vector couplings of the quarks to the W (not $V-A$ anymore, but some complex linear combination of V and A). This is expected to be of order M_W^2/Λ^2 (unless from SM CP violation)

Lepton plane orientation

The asymmetries that depend on the lepton plane orientation:

$A_{TT} \propto \cos(\phi^\ell_{S_1} + \phi^\ell_{S_2})$ and $\propto \sin(\phi^\ell_{S_1} + \phi^\ell_{S_2})$ are transverse spin asymmetries at the parton level also: $\hat{a}_{TT}$, therefore will have to go with $h_1\,\overline{h}_1$

Bad news for $A^\perp_{TT}$

[$h_1 h_1$ contribution in $p^\uparrow p^\uparrow \to 2\,\text{jets}\,X$ small for other reasons]

The asymmetries that don't depend on the lepton plane orientation:

$A_{TT} \propto \cos(\phi^\ell_{S_1} - \phi^\ell_{S_2})$ and $\propto \sin(\phi^\ell_{S_1} - \phi^\ell_{S_2})$ are $\hat{a}_{UU}$, $\hat{a}_{UL}$ or $\hat{a}_{LL}$

Sudakov and/or power suppressed

Fragmentation functions

Collins & Soper, NPB 194 (1982) 445

$$\Delta_{ij}(k) = \sum_X \int \frac{d^4 z}{(2\pi)^4}\, e^{ik\cdot z} \langle 0|\psi_i(x)|P,S;X\rangle\langle P,S;X|\overline{\psi}_j(0)|0\rangle$$

The unpolarized fragmentation correlation function $\Delta(z)$ is parameterized as

$$\Delta(z) = D_1(z)\,\frac{\gamma^+}{4}$$

and $\Delta(z, k_T)$ as [Collins (NPB 396 (1993) 161)]

$$\Delta(z, k_T) = D_1(z, k_T)\,\frac{\gamma^+}{4} + iH_1^\perp(z, k_T)\,\frac{\not{k}_T\gamma^+}{4}$$

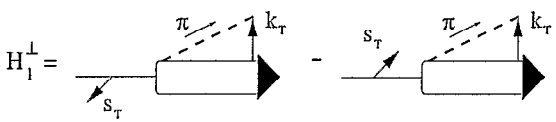

Apart from experimental indications that the Collins effect is nonzero at low energies (HERMES, SMC) and that it can account for the $p\,p^\uparrow \to \pi\,X$ SSA, there is also LEP data...

Collins effect in $e^+ e^- \to \pi^+ \pi^- X$

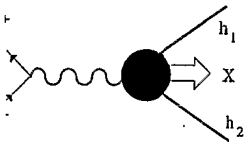

$e^+ + e^- \to \pi^+ + \pi^- + X$

$\cos(2\phi_1)\rangle \propto (H_1^\perperp)^2$

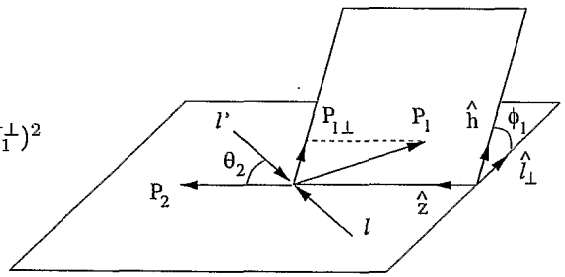

B., Jakob & Mulders, NPB 504 (97) 345; PLB 424 (98) 143

confirmation of this asymmetry would confirm the Collins effect, thout the need of polarization

first indication of a nonzero correlation comes from a preliminary alysis of the 91-95 LEP1 data (DELPHI) by Efremov, Smirnova & atchev, NPB (Proc. Suppl.) 79 (1999) 554

Collins effect in $e^+ e^- \to \pi^+ \pi^- X$

Problem is that the asymmetry expression used is the tree level result

$$\frac{d\sigma(e^+e^- \to \pi^+\pi^- X)}{d\Omega dz_1 dz_2 d^2 q_T} \propto \{1 + \cos(2\phi_1) A(q_T)\}$$

with $(q_T^2 \equiv Q_T^2 \ll Q^2)$

$$A(q_T) \equiv \frac{B(y) \sum_a c_2^a \mathcal{F}\left[(2\, q_T \cdot p_T\; q_T \cdot k_T - q_T^2 p_T \cdot k_T)\, H_1^\perp \overline{H}_1^\perp\right]}{Q_T^2 M_1 M_2\, A(y) \sum_a c_1^a \mathcal{F}\left[D_1 \overline{D}_1\right]}$$

$$A(y) = \left(\frac{1}{2} - y + y^2\right) \stackrel{cm}{=} \frac{1}{4}\left(1 + \cos^2\theta_2\right)$$

$$B(y) = y\,(1-y) \stackrel{cm}{=} \frac{1}{4}\sin^2\theta_2$$

$$c_1^a = \left(g_V^{a\,2} + g_A^{a\,2}\right)$$

$$c_2^a = \left(g_V^{a\,2} - g_A^{a\,2}\right)$$

Estimating the asymmetry

Tree level:

$$\mathcal{F}\left[D\overline{D}\right] \equiv \int d^2k_T\, d^2p_T\, \delta^2(p_T + k_T - q_T) D^a(z_1, k_T^2)\overline{D}^a(z_2, p_T^2)$$

Inclusion of the Sudakov form factor leads to

$$\mathcal{F}\left[D\overline{D}\right] = \frac{1}{2\pi}\int_0^\infty db\, b\, J_0(bQ_T)\, e^{-S(b)}\tilde{D}(z_1, b)\,\tilde{\overline{D}}(z_2, b)$$

Assume again Gaussian transverse momentum dependence

We find

$$A(q_T) \equiv \frac{B(y)\ \sum_a c_2^a\, H_1^{\perp a}(z_1)\, \overline{H}_1^{\perp a}(z_2)}{4M^4R^4\, A(y)\ \sum_a c_1^a\, D_1^a(z_1)\, \overline{D}_1^a(z_2)}\, \mathcal{A}(Q_T)$$

where

$$\mathcal{A}(Q_T) \equiv M^2\, \frac{\int_0^\infty db\, b^3\, J_2(bQ_T)\, \exp\left(-S(b_*) - S_{NP}(b)\right)}{\int_0^\infty db\, b\, J_0(bQ_T)\, \exp\left(-S(b_*) - S_{NP}(b)\right)}$$

$$S_{NP}(b) = 2.05\, b^2 \qquad \text{at } Q = 90\,\text{GeV}$$

We restrict to S_{LL}

Implications

$$\mathcal{A}(Q_T) \equiv M^2\, \frac{\int_0^\infty db\, b^3\, J_2(bQ_T)\, \exp\left(-S(b_*) - S_{NP}(b)\right)}{\int_0^\infty db\, b\, J_0(bQ_T)\, \exp\left(-S(b_*) - S_{NP}(b)\right)}$$

$\mathcal{A}(Q_T)$

$Q^2 = M_Z^2$

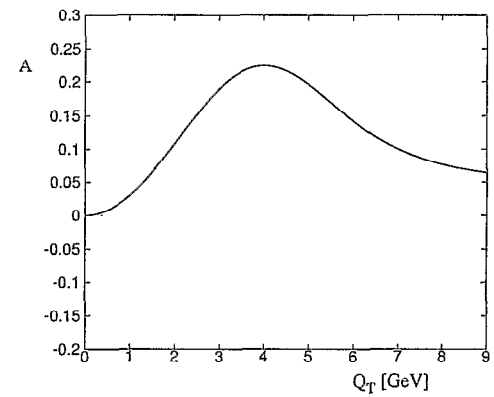

Features:

- Kinematic zero at $Q_T = 0$ as expected
- Maximum of 0.22 at $Q_T = 4$ GeV

Comparison to tree level

Efremov *et al.* NPB (Proc. Suppl.) 74 (99) 49; 79 (99) 554

$$\frac{d\sigma}{d\cos\theta_2 d\phi_1} \propto \left(1 + \frac{6}{\pi}\left[\frac{H_1^{q\perp}}{D_1^q}\right]^2 \frac{v_q^2 - a_q^2}{v_q^2 + a_q^2} \frac{\sin^2\theta_2}{1+\cos^2\theta_2}\cos(2\phi_1)\right)$$

$$\frac{d\sigma}{d\cos\theta_2 d\phi_1} \propto \left(1 + A\left[\frac{H_1^{\perp a}(z_1)}{D_1^a(z_1)}\right]^2 \frac{g_V^{a\,2} - g_A^{a\,2}}{g_V^{a\,2} + g_A^{a\,2}} \frac{\sin^2\theta_2}{1+\cos^2\theta_2}\cos(2\phi_1)\right)$$

Note: numerator and denominator have separate $\sum_a$

$$\left.\begin{array}{rcl} A^{\text{efr}} & = & 6/\pi \\ A^{(0)} & = & 1/(2M^2R^2) \end{array}\right\} \Longrightarrow \left\{\begin{array}{rcl} R^2 & \sim & 13\,\text{GeV}^{-2} \\ \langle p_T^2\rangle & \sim & (270\,\text{MeV})^2 \end{array}\right.$$

$$A^{\text{sud}} = 0.07$$

If $A^{\text{efr}} = 6/\pi$ yields $\overline{|H_1^\perp/D_1|} = 6\% \pm 2\%$,

then $A^{\text{sud}} = 0.07$ yields $\overline{|H_1^\perp/D_1|} = 30\% \pm 10\%$ [too large?]

Conclusions

- Leading twist factorization at $Q_T^2 \ll Q^2$ requires distribution and fragmentation functions as a function of transverse momentum
- Sudakov factors need to be included – important at high Q^2
- In the example of the double transverse spin asymmetry $A_{TT}^V(Q_T)$ Sudakov suppression was demonstrated, implying:
  - $A_{TT}^W(Q_T)$ is negligible at RHIC
  - $A_{TT}^V(Q_T)$ is mainly of interest at lower energies ($V = \gamma^*$)
- In the Collins effect $\cos(2\phi)$ asymmetry in $e^+e^- \to \pi^+\pi^- X$ a strong suppression due to Sudakov factors was demonstrated
- This is relevant at $Q \sim M_Z$ and casts some doubt on the actual determination of the Collins fragmentation function from LEP data
- Tree level estimates tend to overestimate transverse momentum dependent azimuthal asymmetries

NEW PROSPECTS FOR POLARIZED FRAGMENTATION FUNCTIONS

Jacques SOFFER (Centre de Physique Th'eorique CNRS)

Abstract

The knowledge of hadron fragmentation functions gives a deeper understanding of the hadron structure and of the *hadronization* mechanism for inclusive production. Here we are concerned about the $\Lambda(\overline{\Lambda})$ hyperons and we will review the present status of their unpolarized and polarized fragmentation functions.

We first recall the results of a QCD analysis of the data for inclusive $\Lambda(\overline{\Lambda})$ production in e^+e^- collisions in the energy range $14 \leq \sqrt{S} \leq 91.2\ GeV$, which yields the first simple and reliable parametrization of the unpolarized fragmentation functions $D_f^{\Lambda,\overline{\Lambda}}(z,Q^2)$. The observed longitudinal polarization of the Λ's produced at LEP on the Z resonance, leads to some inaccurate information on the spin-dependent fragmentation functions $D_f^{\Lambda,\overline{\Lambda}}(z,Q^2)$. As we will see, several theoretical models have been proposed for these polarized fragmentation functions which are, so far, badly constrained by the existing data. Some predictions can be made for the spin transfer in polarized deep inelastic scattering, but one gets no definite conclusion by comparing them with the present very poor data from HERMES at DESY and E665 at FNAL. We also stress the importance of the $\Lambda(\overline{\Lambda})$ production in neutrino (antineutrino) deep inelastic scattering, which allows a clean flavor and spin separation. New data will be soon available from NOMAD at CERN.

We will also give the prospects from pp collisions with polarized protons at BNL RHIC, because there are recent interesting suggestions for measuring the helicity (and transversity) transfer asymmetry in the process $p\vec{p} \to \overline{\Lambda}X$. From its dependence on the rapidity of the Λ, it is possible to discriminate easily between the various theoretical models, thanks to the high luminosity and the small statistical errors.

SUMMARY

PRESENT SITUATION

$D_q^\Lambda(z, Q^2)$ KNOWN BUT NEED BETTER FLAVOR SEPARATION

$\Delta D_q^\Lambda(z, Q^2)$ POORLY KNOWN NEED BETTER ACCURATE DATA TO TEST SEVERAL SCENARIOS AND DIFF. MODELS

FUTURE PROSPECTS

POL. SIDIS : HERMES, COMPASS, HERA SHOULD LEAD TO SOME IMPROVEMENTS

$\vec{e}\, p \to \nu(\bar{\nu})\, \Lambda^\uparrow X$ AT HERA (?)

pp COLLISIONS

RHIC A POWERFUL FACILITY TO STUDY D_q^Λ, ΔD_q^Λ AND $\Delta_T D_q^\Lambda$

WILL ALLOW TO DISCRIMATE BETWEEN DIFF. MODELS DUE TO HIGH STATISTICS

DON'T FORGET OTHER BARYONS

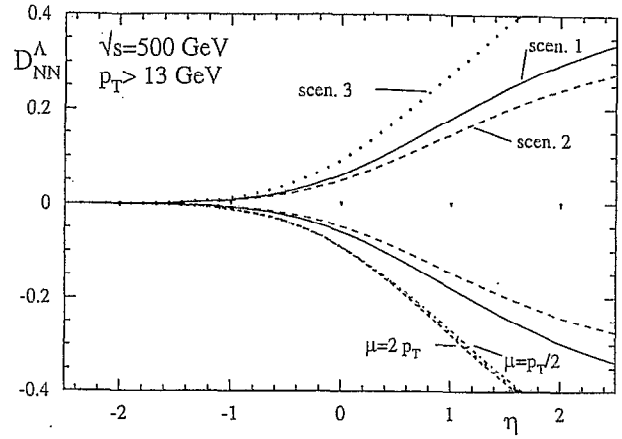

Fig. 2. Upper bounds for the spin-transfer asymmetry D_{NN}^Λ according to Eqs. (7) and (8), as functions of the rapidity of the produced Λ at RHIC energies, using saturated positivity bounds in (1) and (3) for the $\Delta_T q$ and for the three sets of transversity fragmentation functions $\Delta_T D_q^\Lambda$, respectively, as defined in the text. The "error bars" correspond to the expected statistical accuracy for such a measurement at RHIC and have been calculated according to (15) and as discussed in the text. For "scenario 3" we also illustrate the typical theoretical uncertainty induced by a variation of the hard scale μ in (8) in the range $p_T/2$ to $2p_T$.

THEORETICAL ESTIMATE

$\sigma^{pp \to \Lambda X}(p_T > 13\ \mathrm{GeV}) \sim 3\ \mathrm{mb}$

$-0.5 \le \eta \le 0.5$

$$R_q(z,Q^2) = \frac{2\,\Delta_T D_q^{\Lambda}(z,Q^2)}{D_q^{\Lambda}(z,Q^2) + \Delta D_q^{\Lambda}(z,Q^2)}$$

D. de Florian et al. / Physics Letters B 439 (1998) 176–182

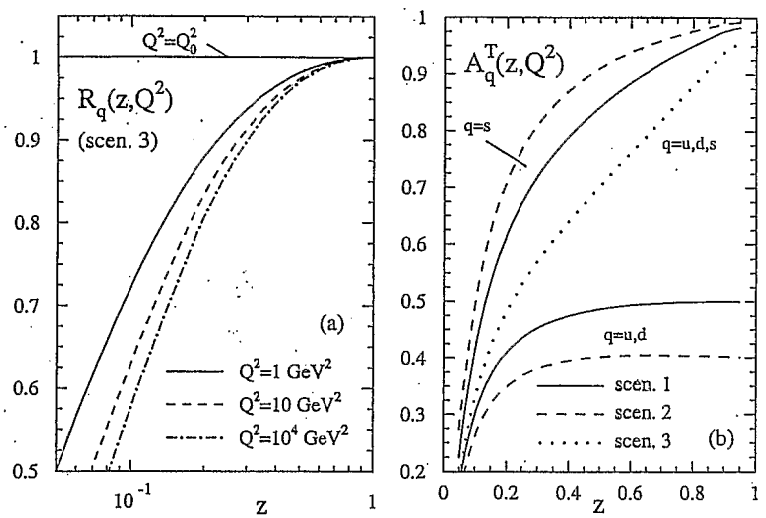

$R_q(z,Q^2)$ as defined in (14) for various different values of Q^2 using scenario 3 for the transv
$R_d = R_s$). The results for the other two scenarios are very similar. (b) The ratio $A_q^T \equiv \Delta_T D_q^{\Lambda}/D_q^{\Lambda}$
sets of transversity Λ fragmentation functions $\Delta_T D_q^{\Lambda}$. The unpolarized D_q^{Λ} in A_q^T are taken frc

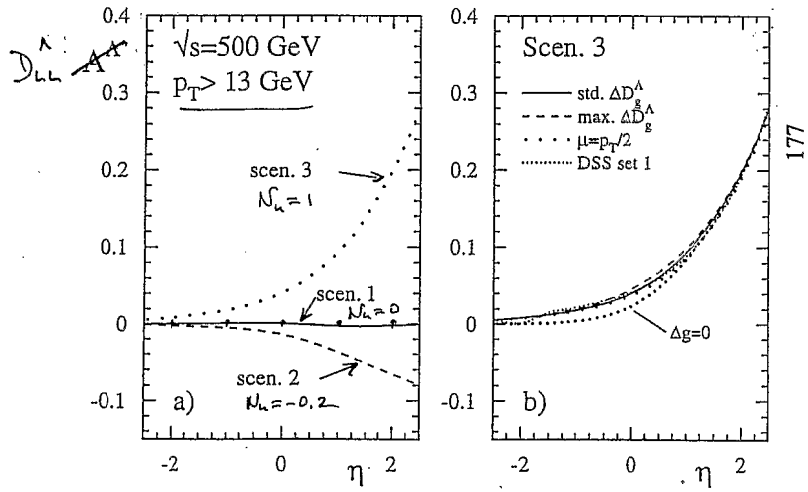

D. de FLORIAN, M. STRATMANN and W. VOGELSANG
Phys. Rev. Lett. 81 (1998) 530
Fig. 1

+ ERRORS ASSUME $\int \mathcal{L} = 800\ \mathrm{pb}^{-1}$ AND $P = 80\%$

POLARIZED F.F. IN pp COLLISIONS

i) HELICITY TRANSFERT IN $\vec{p}p \to \vec{\Lambda} X$

WE CONSIDER THE FOLLOWING SPIN OBSERVABLE

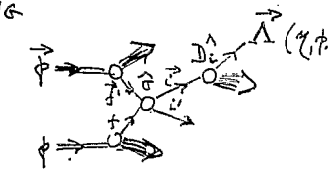

$$D_{LL}^{\Lambda}(\sqrt{s}, \eta, p_T) = \frac{\sigma(++) - \sigma(+-)}{\sigma(++) + \sigma(+-)}$$

($\eta > 0$ ALONG THE DIRECTION OF $\vec{p}$)

$$D_{LL}^{\Lambda} \sim \frac{\sum_f f^p(x_1, Q^2)\, \Delta f'^p(x_2, Q^2)\, \Delta D_i^{\Lambda}(z, Q^2)\, \Delta\hat{\sigma}(ff' \to \vec{i}\, i')}{\sum_f f^p(x_1, Q^2)\, f'^p(x_2, Q^2)\, D_i^{\Lambda}(z, Q^2)\, \hat{\sigma}(ff' \to i i')}$$

CAN MAKE PREDICTIONS FOLLOWING THE THREE SCENARIOS

- SIGN AND MAGNITUDE OF D_{LL}^{Λ} FOLLOWS FROM N_4
- LITTLE EFFECTS FROM ΔD_f^{Λ}

ii) TRANSERVE SPIN ASYMMETRY

CONSIDER D_{NN} SIMILAR TO D_{LL}

NEED TO REPLACE IN NUM $\Delta f'^p \to h_1^{f'}$, $\Delta D_i^{\Lambda} \to \Delta_T D_i^{\Lambda}$

AND $\Delta\hat{\sigma} \to \Delta_T\hat{\sigma}$

HOWEVER $\Delta_T D_i^{\Lambda}$ IS <u>NOT</u> KNOWN BUT IN ANALOGY TO THE POSITIVITY BOUND FOR h_1^f i.e. $2|h_1^f| \leq f + \Delta f$ WE WILL USE $2|\Delta_T D_f^{\Lambda}| \leq D_f^{\Lambda} + \Delta D_f^{\Lambda}$

- WE HAVE CHECKED THAT IT SURVIVES FROM Q^2 EVOLUTION
- WE HAVE OBTAINED BOUNDS FOR D_{NN} FROM THE THREE SCENARIOS

B.Q. MA, I. SCHMIDT, J.S., J.J. YANG
hep-ph 0012159 (Euro Phys. J. (2000) in press)

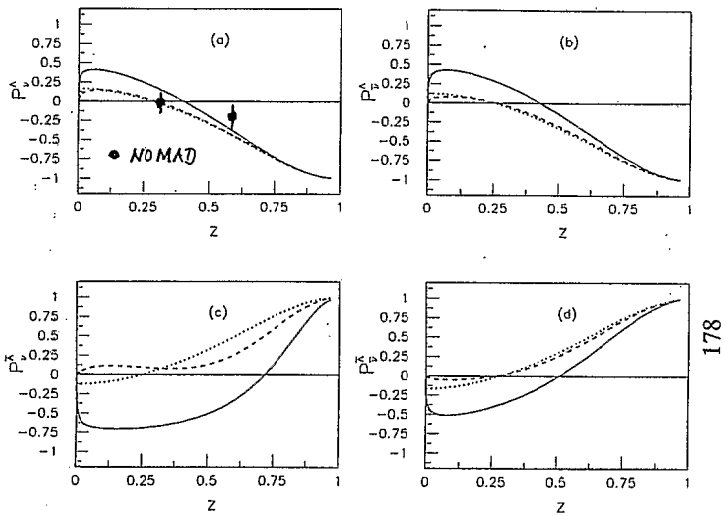

Figure 5: The z-dependence of the Λ and $\bar{\Lambda}$ polarizations for the neutrino (antineutrino) DIS processes. The dotted curve corresponds to pure valence quark contributions. The solid and dashed curves are with the contributions of sea quarks for scenario I and scenario II, respectively (see section 4). Note that the dashed and dotted curves in (a) and (b) almost overlap. x and y are integrated in the ranges [0.02, 0.1] and [0, 1], respectively.

BY ASSUMING u AND d SYMMETRY AND ALSO MATTER ANTIMATTER SYMMETRY GET FOR BOTH D AND ΔD

$$D_q^{\Lambda}(z) = D_u^{\Lambda}(z) = D_d^{\Lambda}(z) = D_{\bar{u}}^{\bar{\Lambda}}(z) = D_{\bar{d}}^{\bar{\Lambda}}(z)$$

$$D_{\bar{q}}^{\Lambda}(z) = D_{\bar{u}}^{\Lambda}(z) = D_{\bar{d}}^{\Lambda}(z) = D_u^{\bar{\Lambda}}(z) = D_d^{\bar{\Lambda}}(z)$$

SO TWO UNPOL. F.F. AND TWO POL. F.F. WE CAN SOLVE WITH THE FOUR EQS.

NOMAD IS WORKING ON THE ANALYSIS OF A FEW THOUSANDS EVENTS

A. KOTZINIAN, A. BRAVAR and D. von HARRACH
EUR. PHYS. J. C2 (1998) 329

(ν)

(ν̄)

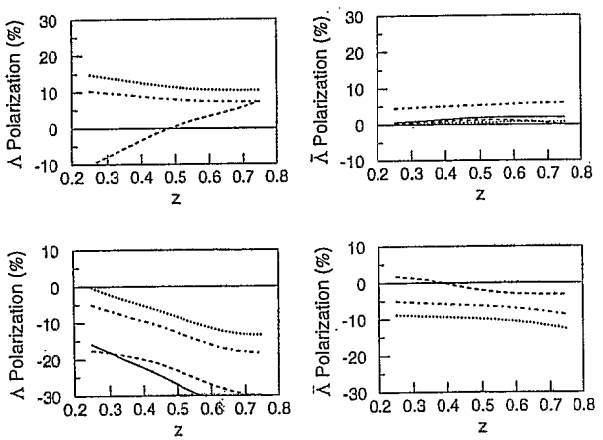

Figure 9: $\Lambda/\overline{\Lambda}$ polarization in the current fragmentation region in ν–DIS (upper plots) and $\overline{\nu}$–DIS (lower plots): solid line - *NQM*, dashed - *BGH*, dotted - *BJ-I*, and dot-dashed - *BJ-II*.

QUARK FLAVOR SEPARATION IN ν AND ν̄ DIS
(BO-QIANG MA, J.S., PRL 82 (1999) 2250)

ν (ν̄) DIS PROVIDES A SOURCE OF POLARIZED QUARKS WITH SPECIFIC FLAVOR

From the charged current quark transitions, for neutrino induced reactions

$$\begin{aligned} &\nu\, d \to \mu^- u; && \nu\, d \to \mu^- c; \\ &\nu\, \overline{u} \to \mu^- \overline{d}; && \nu\, \overline{u} \to \mu^- \overline{s}; \\ &\nu\, s \to \mu^- c; && \nu\, s \to \mu^- u, \end{aligned} \tag{2}$$

and for antineutrino induced reactions

$$\begin{aligned} &\overline{\nu}\, u \to \mu^+ d; && \overline{\nu}\, u \to \mu^+ s; \\ &\overline{\nu}\, \overline{d} \to \mu^+ \overline{u}; && \overline{\nu}\, \overline{d} \to \mu^+ \overline{c}; \\ &\overline{\nu}\, \overline{s} \to \mu^+ \overline{c}; && \overline{\nu}\, \overline{s} \to \mu^+ \overline{u}, \end{aligned} \tag{3}$$

the expressions for the Λ and $\overline{\Lambda}$ longitudinal polarizations in the beam direction are, for Λ and $\overline{\Lambda}$ produced in the current fragmentation,

$$P_\nu^\Lambda(x,y,z) = -\frac{d(x)\Delta D_u^\Lambda(z) - (1-y)^2\overline{u}(x)\Delta D_{\overline{d}}^\Lambda(z)}{d(x)D_u^\Lambda(z) + (1-y)^2\overline{u}(x)D_{\overline{d}}^\Lambda(z)} \quad for \quad \nu N \to \mu^- \overrightarrow{\Lambda} X; \tag{4}$$

$$P_{\overline{\nu}}^\Lambda(x,y,z) = -\frac{(1-y)^2 u(x)\Delta D_d^\Lambda(z) - \overline{d}(x)\Delta D_{\overline{u}}^\Lambda(z)}{(1-y)^2 u(x)D_d^\Lambda(z) + \overline{d}(x)D_{\overline{u}}^\Lambda(z)} \quad for \quad \overline{\nu}N \to \mu^+ \overrightarrow{\Lambda} X; \tag{5}$$

$$P_\nu^{\overline{\Lambda}}(x,y,z) = -\frac{d(x)\Delta D_u^{\overline{\Lambda}}(z) - (1-y)^2\overline{u}(x)\Delta D_{\overline{d}}^{\overline{\Lambda}}(z)}{d(x)D_u^{\overline{\Lambda}}(z) + (1-y)^2\overline{u}(x)D_{\overline{d}}^{\overline{\Lambda}}(z)} \quad for \quad \nu N \to \mu^- \overrightarrow{\overline{\Lambda}} X; \tag{6}$$

$$P_{\overline{\nu}}^{\overline{\Lambda}}(x,y,z) = -\frac{(1-y)^2 u(x)\Delta D_d^{\overline{\Lambda}}(z) - \overline{d}(x)\Delta D_{\overline{u}}^{\overline{\Lambda}}(z)}{(1-y)^2 u(x)D_d^{\overline{\Lambda}}(z) + \overline{d}(x)D_{\overline{u}}^{\overline{\Lambda}}(z)} \quad for \quad \overline{\nu}N \to \mu^+ \overrightarrow{\overline{\Lambda}} X. \tag{7}$$

NEGLECT CABIBBO SUPPRESSED PROCESSES AND SMALL STRANGE QUARK CONTRIBUTION IN p.

MA, SCHMIDT, J.S., YANG
Phyl. Rev. D62, 114OXX (2000)

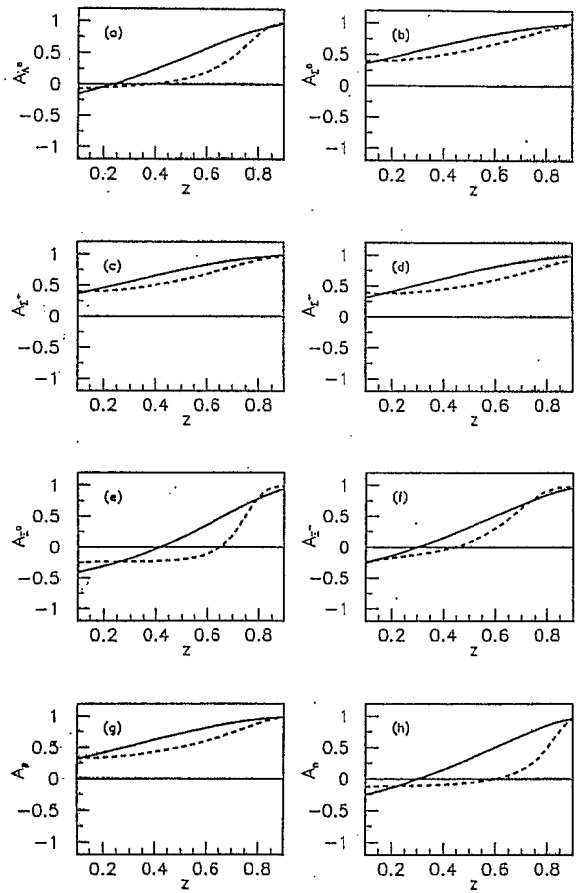

Figure 2: The predictions of the z-dependence for the *hadron* spin transfer in polarized charged lepton DIS process for the octet baryons. We adopt the CTEQ5 set quark distributions [44] for the target proton at $Q^2 = 2.5$ GeV^2 with the Bjorken variable x integrated over $0.02 \to 0.4$. The corresponding input fragmentation functions adopt the Ansatz Eq. (1) from valence quark distributions in the pQCD based analysis (solid curves) and the quark-diquark model (dashed curves).

MA, SCHMIDT, J.S., YANG
Phyl. Rev. D62, 114OXX (2000)

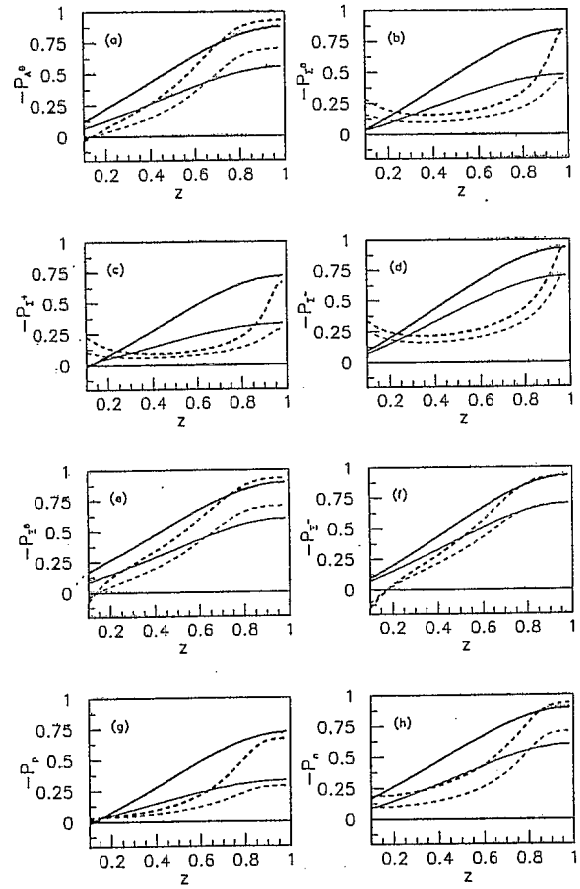

Figure 1: The prediction of the longitudinal hadron polarizations for the octet baryons in e^+e^--annihilation at two energies: LEP I at Z resonance $\sqrt{s} \approx 91$ GeV (thick curves) and LEP II at $\sqrt{s} \approx 200$ GeV (thin curves), with input fragmentation functions adopting the Ansatz Eq. (1) from valence quark distributions in the pQCD based analysis (solid curves) and the quark-diquark model (dashed curves).

(SU(6) QUARK SPECTATOR - DIQUARK MODEL))

7 September 2000

PHYSICS LETTERS B

ELSEVIER

Physics Letters B 488 (2000) 254–260

www.elsevier.nl/locate/npe

The quark-antiquark asymmetry of the nucleon sea from Λ and $\bar{\Lambda}$ fragmentation

Bo-Qiang Ma [a,b,c], Ivan Schmidt [d], Jacques Soffer [e], Jian-Jun Yang [d,f]

[a] Department of Physics, Peking University, Beijing 100871, China [1]
[b] CCAST (World Laboratory), P.O. Box 8730, Beijing 100080, China
[c] Institute of Theoretical Physics, Academia Sinica, Beijing 100080, China
[d] Departamento de Física, Universidad Técnica Federico Santa María, Casilla 110-V, Valparaíso, Chile
[e] Centre de Physique Théorique, CNRS, Luminy Case 907, F-13288 Marseille Cedex 9, France
[f] Department of Physics, Nanjing Normal University, Nanjing 210097, China

Received 24 May 2000; accepted 28 July 2000
Editor: R. Gatto

21 September 2000

PHYSICS LETTERS B

ELSEVIER

Physics Letters B 489 (2000) 293–299

www.elsevier.nl/locate/npe

The quark–antiquark asymmetry of the nucleon sea from Λ and $\bar{\Lambda}$ fragmentation

Bo-Qiang Ma [a,b,c], Ivan Schmidt [d], Jacques Soffer [e], Jian-Jun Yang [d,f]

[a] Department of Physics, Peking University, Beijing 100871, China [1]
[b] CCAST (World Laboratory), P.O. Box 8730, Beijing 100080, China
[c] Institute of Theoretical Physics, Academia Sinica, Beijing 100080, China
[d] Departamento de Física, Universidad Técnica Federico Santa María, Casilla 110-V, Valparaíso, Chile
[e] Centre de Physique Théorique, CNRS, Luminy Case 907, F-13288 Marseille Cedex 9, France
[f] Department of Physics, Nanjing Normal University, Nanjing 210097, China

Received 24 May 2000; accepted 28 July 2000
Editor: R. Gatto

Abstract

We present a general analysis of the spin transfer for Λ and $\bar{\Lambda}$ production in deep-inelastic scattering of polarized charged leptons on the nucleon, and find that the pattern of different behaviors of Λ and $\bar{\Lambda}$ production observed by the E665 Collaboration suggests the possibility of quark–antiquark asymmetries either in the quark to Λ fragmentation functions and/or in the quark and antiquark distributions of the target proton. We also point out that the strange-antistrange asymmetry of the nucleon sea may produce an observable contribution to the different behaviors of Λ and $\bar{\Lambda}$ production. We find that a softer $\bar{s}(x)$ than $s(x)$ as predicted by the light-cone baryon-meson fluctuation model of intrinsic quark–antiquark pairs of the nucleon sea might lead to a reasonable picture. However, the magnitude is still too small to explain the E665 data and the conclusion has also strong model-dependence. This may suggest the importance of quark–antiquark asymmetry in the quark to Λ fragmentation functions, provided that the E665 data are confirmed. © 2000 Elsevier Science B.V. All rights reserved.

PACS: 14.20.Jn; 12.38.Bx; 13.87.Fh; 13.88.+e

..... PURE VALENCE QUARKS
—— SEA QUARKS SCE. I
- - - - " " SCE. II

(E665 μ^+ 470 GeV/c)
EJPC in press $\vec{\mu} p \to \mu \vec{\Lambda} X$

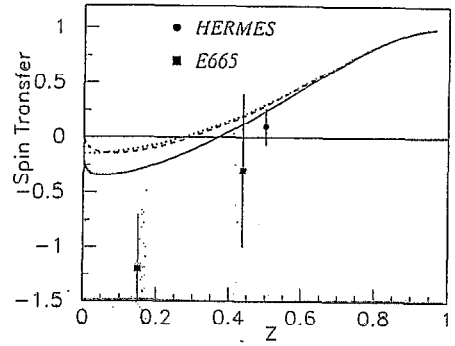

Figure 1: The z-dependence of the Λ spin transfer in electron or positron (muon) DIS. The dotted curve corresponds to pure valence quark contributions. The solid and dashed curves are with the contributions of sea quarks for scenario I and scenario II, respectively (see section 1). Note that for HERMES data the Λ polarization is measured along the virtual-photon momentum, whereas for E665 it is measured along the virtual-photon spin. The averaged value of the Bjorken variable is chosen as $x = 0.1$ (corresponding to the HERMES averaged value) and the calculated result is not sensitive to a different choice of x in the small x region (for example, $x = 0.005$ corresponding to the E665 averaged value).

(750 Λ)

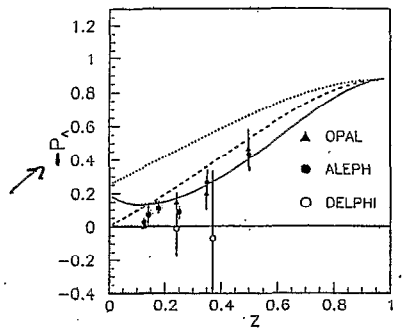

Figure 5: The comparison of the experimental data [28, 29, 30] for the longitudinal Λ-polarization P_Λ in e^+e^--annihilation process at the Z-pole with the theoretical calculations in the the pQCD analysis with three different cases: (a) case 1: the SU(6) quark-model spin distributions for the quark helicities, Eq. (36) (dotted curves); (b) case 2: the Burkardt-Jaffe values for the quark helicities, Eq. (37) (dashed curves); (c) case 3: the canonical form of quark distributions, Eq. (42) (solid curves).

B.Q MA, I. SCHMIDT, J.J. YANG
PHYS. REV. D61, 034017 (2000)

A pQCD BASED MODEL (B.Q.MA, I. SCHMIDT, J.S., J.J. YANG hep-ph 001259)
EURO. PHYS. J. (2000) in press

USE THE RECIPROCITY RELATION PROPOSED BY GRIBOV - LIPATOV

$$D_q^h(z) \sim q_h(x) \qquad \text{FOR } x, z \to 1$$

PURE VALENCE CASE

$$u_v^\uparrow(x) = d_v^\uparrow(x) = \frac{1}{x^{\alpha_v}}\left[A_{u_v}(1-x)^3 + B_{u_v}(1-x)^4\right]$$

$$u_v^\downarrow(x) = d_v^\downarrow(x) = \frac{1}{x^{\alpha_v}}\left[C_{u_v}(1-x)^5 + D_{u_v}(1-x)^6\right]$$

$$s_v^\uparrow(x) = \frac{1}{x^{\alpha_v}}\left[A_{s_v}(1-x)^3 + B_{s_v}(1-x)^4\right]$$

$$s_v^\downarrow(x) = \frac{1}{x^{\alpha_v}}\left[C_{s_v}(1-x)^5 + D_{s_v}(1-x)^6\right]$$

$\alpha_v \sim 1/2$ AND 8 PARAMETERS DETERMINED WITH SOME CONDITIONS i.e. $\Delta s = 0.7$ $\Delta u = -0.1$ + e^+e^- DATA

POSSIBLE SEA QUARK CONTRIBUTIONS

$$q_s^\uparrow(x) = \frac{1}{x^{\alpha_s}}\left[A_{q_s}(1-x)^5 + B_{q_s}(1-x)^6\right]$$

$$q_s^\downarrow(x) = \frac{1}{x^{\alpha_s}}\left[C_{q_s}(1-x)^7 + D_{q_s}(1-x)^8\right]$$

$$\bar{q}^\uparrow(x) = \frac{1}{x^{\alpha_s}}\left[A_{\bar{q}}(1-x)^5 + B_{\bar{q}}(1-x)^6\right]$$

$$\bar{q}^\downarrow(x) = \frac{1}{x^{\alpha_s}}\left[C_{\bar{q}}(1-x)^7 + D_{\bar{q}}(1-x)^8\right]$$

$\alpha_s \sim 1.12$

SOME CONDITIONS FOR CONVERGENCE i.e. $A_q + B_q = C_q + D_q$

(I) ASYMMETRIC SEA $\Delta q_s = -0.3$, $\Delta\bar{q} = 0.2$

(II) SYMMETRIC SEA $\Delta q_s = \Delta\bar{q} = -0.05$

EUR. PHYS. J. C2 (1998) 329

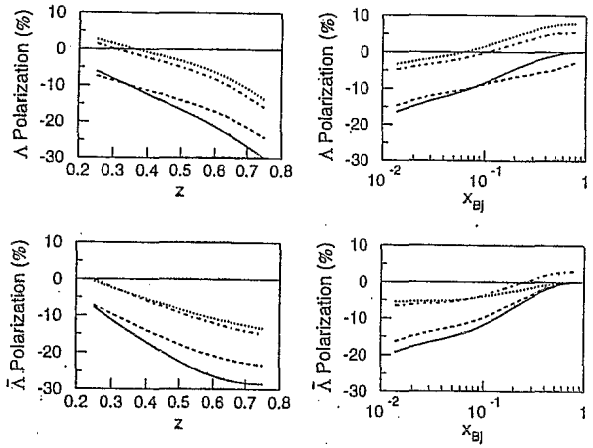

Figure 3: Λ and $\overline{\Lambda}$ longitudinal polarization in the current fragmentation region for DIS of polarized μ^+'s on an unpolarized target for different mechanisms of spin transfer: solid line - *NQM*, dashed - *BGH*, dotted - *BJ-I*, and dot-dashed - *BJ-II*.

only val. quarks pol.

sea quarks and antiquarks polarized

BGH

BJ-I

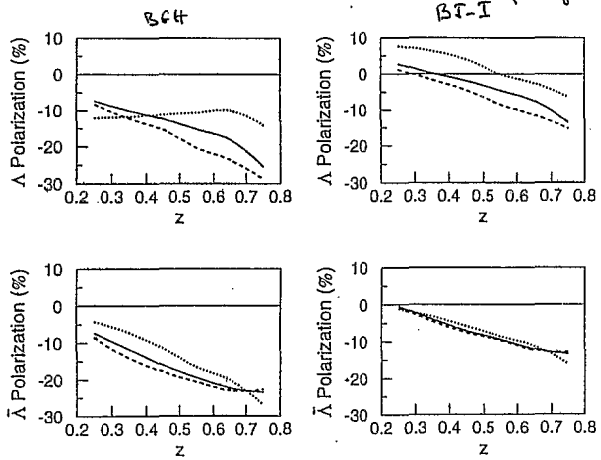

ENERGY DEPENDENCE

Figure 4: Λ and $\overline{\Lambda}$ longitudinal polarization for three different beam energies using the *BGH* (left plots) and the *BJ-I* (right plots) spin transfer mechanism: solid line - E_μ = 200 GeV, dashed - E_μ = 500 GeV, and dotted - E_{el} = 30 GeV.

DIFFERENT THEORETICAL MODELS IN
A. KOTZINIAN, A. BRAVAR and D. von HARRACH
EUR. PHYS. J. C2 (1998) 329

NQM $\quad A_u = A_d = 0 \quad A_s = 1$

BGH (Bigi, Gustafson, Häkkinen) $\quad A_u = A_d \quad A_s = 0.8$

BJ (Burkardt, Jaffe)

(I) $\quad A_u = A_d = -0.2 \quad A_s = 0.6 \quad (\bar{q}=0)$

(II) $\quad A_u = A_d = -0.14 \quad A_s = 0.66 \quad (\bar{q}=-$

$D^{\Lambda}_{LL'}$ = LONGITUDINAL SPIN TRANSFER FROM γ^* TO Λ

$\vec{e}p \to e\vec{\Lambda}X$

$\int \mathcal{L}dt = 500\,pb^{-1}$

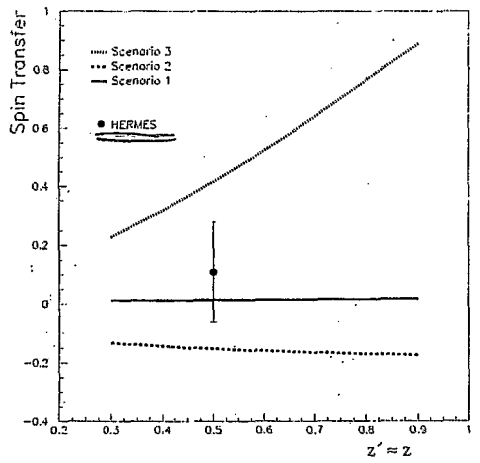

$\vec{e}+$ 27.5 GeV

Fig. 2. Spin transfer $D^{\Lambda}_{LL'}$ as a function of $z' = \frac{E_\Lambda}{E_N(1-z)}$. The curves correspond to different models for the Λ spin structure: the naive QPM (scenario 1), the SU(3) flavor symmetric model (scenario 2) and a model with equal contributions of all light quark flavors to the Λ polarization (scenario 3) and are explained in the text.

- 2237 events ($0.2 < z < 0.7$, $0.02 < x < 0.4$, $1 < Q^2 < 10\ GeV^2$)
- quantization axis along $\vec{p}_\Lambda$

$D^{\Lambda}_{LL'} = 0.11 \pm 0.17\,(stat.) \pm 0.03\,(sys.)$

(if quantization axis along γ^*
$D^{\Lambda}_{LL'} = 0.03 \pm 0.17\,(stat.) \pm 0.03\,(sys.)$)

(SCEN. 1 FAVORS ??)

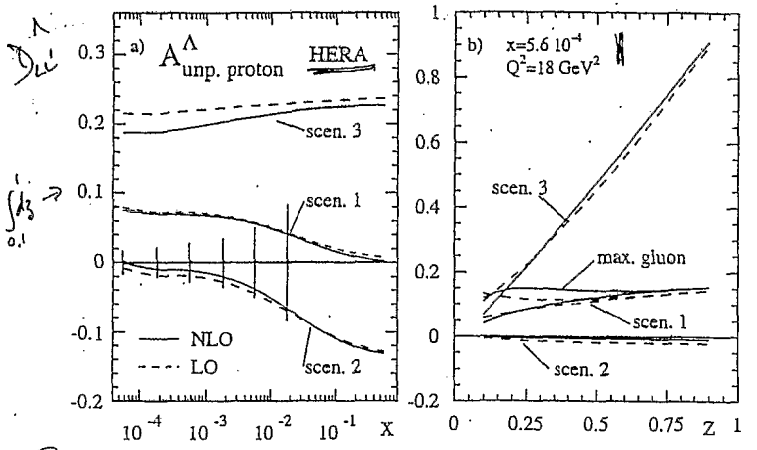

Fig. 7

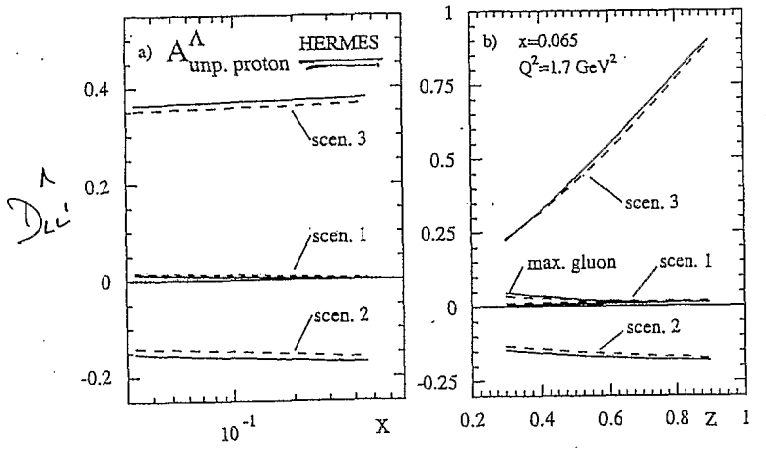

FIG. 8. The same as in Fig. 7, but now for HERMES kinematics.

POLARIZED (e AND μ) SEMI-INCLUSIVE DIS

$$\vec{e}\, p \to e' \vec{\Lambda} X$$

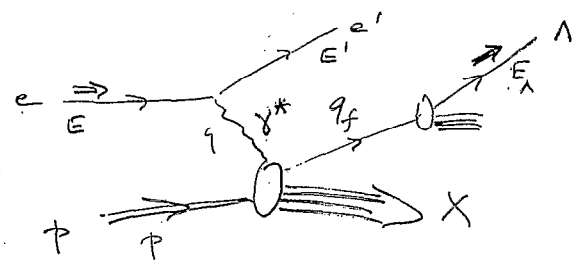

$Q^2 = -q^2$

$\nu = E - E'$

$x = Q^2/2M\nu$, $y = \nu/E$, $z = E_\Lambda/\nu$

Bjorken variable

$$P_\Lambda(x,y,z) = P_B\, D(y)\, D^\Lambda_{LL'}(x,z)$$

P_B BEAM POLARIZATION

$$D(y) = \frac{1-(1-y)^2}{1+(1+y)^2}$$ γ^* DEPOLARIZATION FACTOR

$$D^\Lambda_{LL'}(x,z) = \frac{\sum_f e_f^2 \left[q_f^N(x,Q^2)\, \Delta D^\Lambda_{q_f}(z,Q^2) + (q \to \bar{q}) \right]}{\sum_f e_f^2 \left[q_f^N(x,Q^2)\, D^\Lambda_{q_f}(z,Q^2) + (q \to \bar{q}) \right]}$$

LONG. SPIN TRANSFER

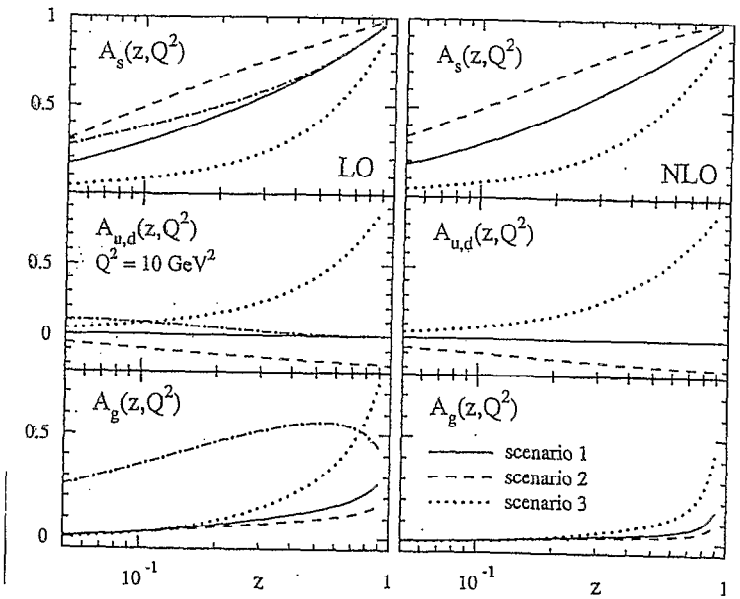

$$A_f = \frac{\Delta D_f^\Lambda}{D_f^\Lambda}$$

—·—·— EFFECT FROM ASSUMED MAX POL. GLUON ON SCENARIO 1
$\Delta D_g(\mu^2) = D_g(\mu^2)$ AND NOT $\Delta D_g(\mu^2) = 0$

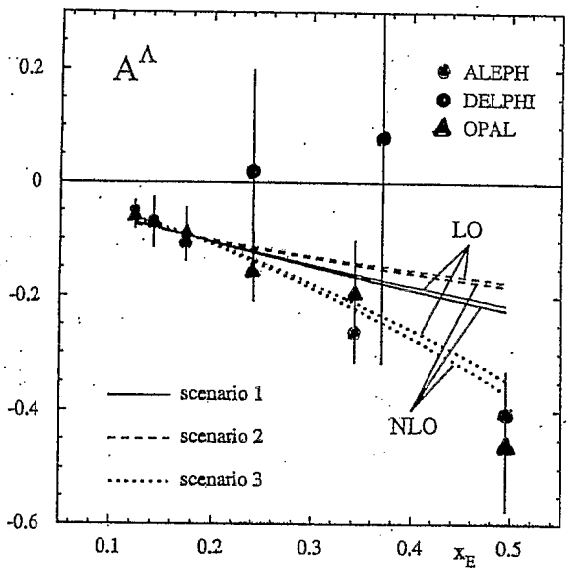

FIG. 4. Comparison of LEP data [10–12] and our LO and NLO sults for the asymmetry A^Λ in Eq. (26), using the three different

$x_E = \frac{2p_H \cdot q}{q^2} = 2E_H/\sqrt{s}$ $(q^2 = q_0^2 = s)$

- ALEPH AND OPAL PRETTY CONSISTENT AND $A^\Lambda < 0$
- DELPHI $A^\Lambda \sim 0$

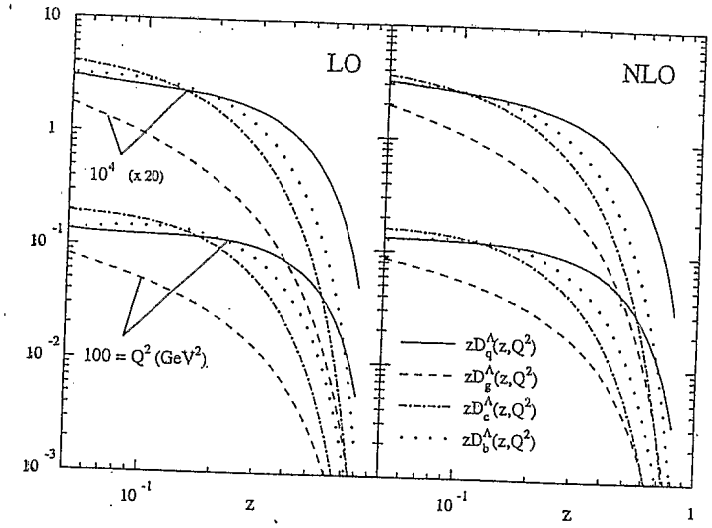

PHYS. REV. D 57 (1998) 5811

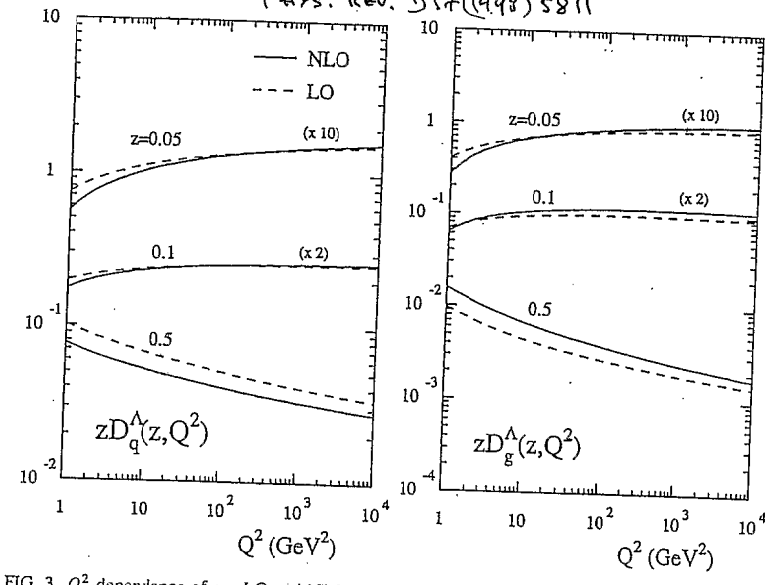

FIG. 3. Q^2-dependence of our LO and NLO q and g fragmentation functions at fixed $z=0.05$, 0.1, 0.5.

DE FLORIAN, STRATMANN, VOGELSANG
PHYS. REV. D57 (1998) 5811

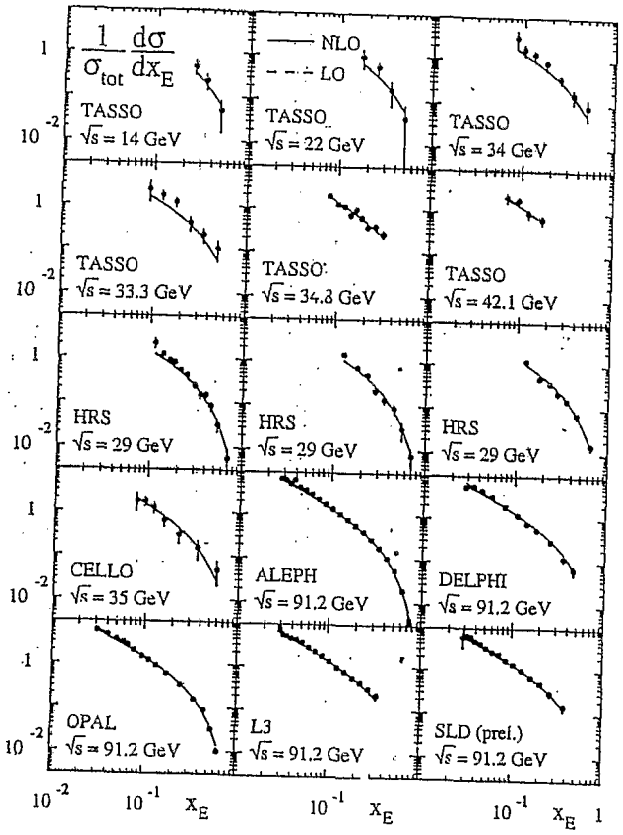

FIG. 1. Comparison of our LO and NLO results for $(1/\sigma_{tot})d\sigma/dx_E$ according to Eq. (5) with all available data on unpolarized Λ production in e^+e^- annihilation [2,3]. Note that only data points with $x_E \geq 0.1$ have been included in our fit (see text).

- THREE SCENARIOS

① NRQM : ONLY STRANGE QUARK CAN CONTRIBUTE TO POL. F.F. $\Rightarrow$ $N_u = 0$

② BASED ON BURKARDT - JAFFE MODEL (PRL 70 (1993) 2537)

IN NRQM WE HAVE FOR THE POL. P.D. IN A Λ

$$\Delta u_\Lambda = \Delta d_\Lambda = 0 \quad \text{AND} \quad \Delta s_\Lambda = 1$$

BY MAKING USE OF SU(3) FLAVOR OCTET AXIAL CHARGES CAN RELATED $I_\Lambda = \int_0^1 dx\, g_1^{e\Lambda}(x)$ TO $I_p = \int_0^1 dx\, g_1^{ep}(x)$ AND USING THE DATA ON I_p GET ALL VALUES PUSHED DOWN (LIKE IN PROTON CASE)

$$\Delta u_\Lambda = \Delta d_\Lambda = -0.20 \quad \text{AND} \quad \Delta s_\Lambda = 0.60$$

BY TRANSPOSING THIS TO THE TIME-LIKE CASE $(\Delta q_\Lambda \sim \Delta D_q^\Lambda)$ LEADS TO $N_u = -0.2$

③ ALL POL. F.F. ARE EQUAL, VERY EXTREME CASE $N_u = 1$

- SHOW THE RESULTS ON THE FIG FOR A^Λ AT LEP ONCE MORE VERY LITTLE DIFF. BETWEEN LO AND NLO AND ③ SEEMS TO BE FAVORED AT HIGH x_E ALTHOUGH MIGHT NEED TO BREAK $SU_f(3)$ TO GET LARGER A^Λ WITH $D_s^\Lambda > D_{u,d}^s$?

FOR THE DIFFERENT PARTONS $u = d$, s AND g GET $A_f = \frac{\Delta D_f^\Lambda}{D_f^\Lambda}$

- CAN BE USED TO MAKE PREDICTIONS FOR SIDIS (AT HERA AND HERMES) $\vec{e}p \to e\vec{\Lambda}X$

$$D_{LL} \sim \sum_q e_q^2\, q(x,Q^2)\, \Delta D_q^\Lambda(z,Q^2) \Big/ \sum_q e_q^2\, q(x,Q^2)\, D_q^\Lambda(z,$$

(SEE FIG.)

ALSO $\neq$ PREDICTIONS FROM ANOTHER APPROACH: USE $\neq$ SETS OF P.D.

QCD ANALYSIS (LO AND NLO) FOR D_f^Λ AND ΔD_f^Λ

i) D_f^Λ

- THE DETERMINATION WILL BE BASED ON ALL AVAILABLE DATA IN e^+e^- WHICH DOES NOT SEPARATE Λ^0 FROM $\bar{\Lambda}^0$. SO WILL CALL $D_f^\Lambda \equiv D_f^{\Lambda^0} + D_f^{\bar{\Lambda}^0}$ AN IMPORTANT SIMPLIFYING ASSUMPTION
- SECOND WILL MAKE THE CRUDE APPROXIMATION BASED ON $SU_f(3)$

$$D_u^\Lambda \equiv D_d^\Lambda \equiv D_s^\Lambda \equiv D_{\bar{u}}^\Lambda \equiv D_{\bar{d}}^\Lambda \equiv D_{\bar{s}}^\Lambda \quad \text{CALLED} \quad D_q^\Lambda$$

- BUT WILL INCLUDE HEAVY QUARK (c, b) AND GLUON

USE A STANDARD PARAMETRIZATION AT INITIAL SCALE μ^2

$$D_f^\Lambda(z,\mu^2) = N_f\, z^{\alpha_f}(1-z)^{\beta_f} \qquad \left(\begin{array}{l}\mu_{LO}^2 = 0.23\ \text{GeV}^2 \\ \mu_{NLO}^2 = 0.34\ \text{GeV}^2\end{array}\right)$$

WITH $N_c = N_b = N_q$. SO TEN FREE PARAMETERS ARE DETERMINED BY (LO AND NLO) QCD Q^2 EVOLUTION AND FIT OF WORLD DATA FOR $14\ \text{GeV} < \sqrt{s} < 91.2\ \text{GeV}$ (SEE FIG.)

- ALMOST NO DIFF. BETWEEN LO AND NLO
- HQ COMPARABLE TO LQ FOR SMALL z BUT GLUON SMALLER
- NOTE THAT CONTRIBUTION TO MOM. S.R. IS ONLY 2-3% OF π, K

ii) ΔD_f^Λ

- DATA IS FROM LEP AT THE Z BOSON MASS (SEE FIG)
- NOTE THAT A^Λ DEPENDS ONLY ON VALENCE PART OF POL. F.F. i.e. $\Delta D_f^\Lambda - \Delta D_{\bar{f}}^\Lambda$ (NON-SINGLET)
- ONE USUALLY MAKES THE SIMPLE ASSUMPTION

$$\Delta D_f^\Lambda(z) = C_f^\Lambda(z)\, D_f^\Lambda(z)$$

AT A GIVEN SCALE (CANNOT HOLD IN GENERAL IN QCD) (C_f^Λ SPIN TRANSFER COEFFICIENTS)

- WILL NEGLECT HQ AND GLUON AND ASSUME $u = d$

SO WILL INTRODUCE ONLY TWO NEW PARAMETERS α, N_u AT μ^2

$$\Delta D_s^\Lambda = z^\alpha D_s^\Lambda \qquad \Delta D_u^\Lambda = \Delta D_d^\Lambda = N_u\, \Delta D_s^\Lambda$$

A PARTON DISTRIBUTION $f_H(x, Q^2)$

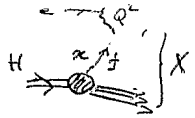

OBTAINED IN DIS FOR $Q^2 < 0$ SPACE-LIKE, HAS A COUNTERPART FOR $Q^2 > 0$ TIME-LIKE

THE FRAGMENTATION FUNCTION $D_f^H(z, Q^2)$

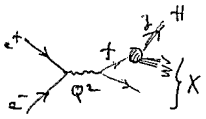

OBTAINED e.g. IN e^+e^- ANNIHILATION

PROBABILITY AT MASS SCALE Q TO FIND HADRON H WITH FRACTION z OF PARTON f MOMENTUM

LIKE P.D. FOR THE F.F., QCD PREDICTS THE Q^2 EVOLUTION AND THEY ARE PROCESSES INDEPENDENT i.e. UNIVERSAL

CAN BE MEASURED IN

- $e^+e^- \to (\gamma, Z) \to HX$ (SIA) LEP
- $lp \to l'HX$ (SIDIS) HERA (HERMES), CERN (COMPASS), FNAL (E665)
- $pp \to HX$ (HC) FNAL, RHIC, HERA-$\vec{N}$

SO FAR BEST KNOWN ARE THOSE OF LIGHT MESONS D_f^π, D_f^K

LET'S SEE WHAT CAN BE SAID ON $D_f^\Lambda(z, Q^2)$ AND SINCE Λ IS A SPIN-½ OBJECT

$$\Delta D_f^\Lambda(z, Q^2) \equiv D_{f(+)}^{\Lambda(+)}(z, Q^2) - D_{f(+)}^{\Lambda(-)}(z, Q^2)$$

FOR LONG. POL. Λ AND LONG. POL. PARTON f (D IS THE SUM)

AND ALSO FOR TRANS. POL. CASE

$$\Delta_T D_f^\Lambda(z, Q^2)$$

NEW PROSPECTS FOR POLARIZED FRAGMENTATION FUNCTIONS (T. SOFFER)

(KYOTO WORKSHOP 13-16 OCT. 2000)

* MOTIVATIONS
  WHY FRAG. FUNCT. ? WHY POL. FRAG. FUNCT. ?
  WILL EMPHASIZE Λ's

* e^+e^- COLLISIONS
  A QCD ANALYSIS (LO AND NLO) FOR
  Λ's F.F. D_f^Λ AND POL. F.F. ΔD_f^Λ (3 SCENARIOS)

* POLARIZED (e AND μ) SEMI-INCLUSIVE DIS
  THE LONGITUDINAL SPIN TRANSFER
  SEVERAL THEORETICAL MODELS
  EXTENSION TO OTHER BARYONS (Σ, Ξ, p, ...)

* ν ($\bar{\nu}$) DIS
  QUARK FLAVOR SEPARATION

* pp COLLISIONS
  LONGITUDINAL POL. $\Rightarrow$ ΔD_f^Λ
  TRANSVERSE POL. $\Rightarrow$ $\Delta_T D_f^\Lambda$

* SUMMARY

Polarized Λ_c^+ Production at RHIC

Kazumasa OHKUMA (Kobe University)

Abstract

To extract information about the polarized gluon distribution in the nucleons, we propose Λ_c^+ productions in polarized pp scattering which will be observed at RHIC experiment. For this process, we have calculated the spin correlation differential cross section, and the spin correlation asymmetry. We have found that the spin correlation asymmetry is sensitive to the polarized gluon distribution in the nucleon and thus the process is promising for testing the polarized gluon distribution.

International Workshop on Polarized Partons at High Q^2 region

Polarized Λ_c^+ Production at RHIC

Kazumasa OHKUMA (Kobe Univ.)

2000/OCT./13, KYOTO

Based on

K.O, K. Sudoh and T. Morii,

hep-ph/0009004.

(*to appear in Phys. Lett. B*)

I. Introduction
II. Λ_c^+ Production in pp reaction
III. Numerical Calculation
IV. Summary

I. Introduction

Proton Spin Puzzle

$$\frac{1}{2} = \frac{1}{2}\Delta\Sigma + \Delta g + < L >_{q+g}$$

$\Delta\Sigma$: Quark spin $\qquad$ Δg : Gluon spin

$< L >_{q+g}$: Orbital angular momentum of Quarks and Gluons

Experimental results : $\Delta\Sigma \sim 0.3$

$\Rightarrow$ Naive quark model does not work

$\Rightarrow$ need more information about polarized partons in the proton

— The knowlege of the polarized gluons is still poor !! —

To extract the imfomation about the polarized gluons, we propose one such process:

$$\vec{P} + P \longrightarrow \vec{\Lambda}_c^+ + X.$$

property of Λ_c^+ baryon

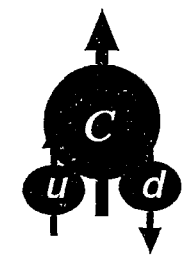

♣ Λ_c^+ baryon is composed of heavy c quark and antisymmetrically combined light u and d quarks.

$\Rightarrow$ Spin of Λ_c^+ baryon $\approx$ Spin of c quark

♣ c quarks are not the main constituents of the proton

$\Rightarrow$ gluon-gluon fusion process is dominant for c quark production in pp scattering.

$\Rightarrow$ There is relation between the gluon spin and produced c quark spin.

$\Downarrow$

observation of the spin of the produced Λ_c^+ gives us information about the polarized gluons in the proton.

II. Λ_c^+ production in pp reaction

$\vec{p} + p \rightarrow \vec{\Lambda}_c^+ + X$

Subprocess

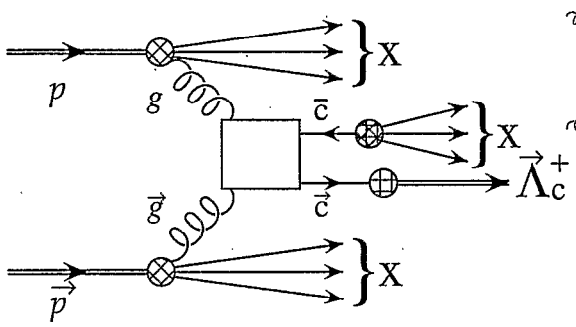

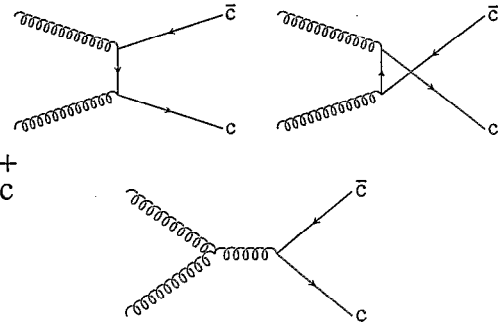

This process can be measured by forthcoming RHIC experient.

To extract the information about polarized gluon distribution in the proton, we calculated two observables using parton model.

1 : <u>the spin correlation differential cross section</u>

$$\frac{d\Delta\sigma}{dp_T} \equiv \frac{d\sigma(++) - d\sigma(+-) + d\sigma(--) - d\sigma(-+)}{dp_T}$$

p_T : Transverse momentum of Λ_c^+

$d\sigma(+,-)/dp_T$: Spin dependent differential cross section with the positive helicity of the target proton and the negative helicity of the produced Λ_c^+

2 : <u>the spin correlation asymmetry</u>

$$A_{LL} \equiv \frac{d\sigma(++) - d\sigma(+-) + d\sigma(--) - d\sigma(-+)/dp_T}{d\sigma(++) + d\sigma(+-) + d\sigma(--) + d\sigma(-+)/dp_T} = \frac{d\Delta\sigma/dp_T}{d\sigma/dp_T}.$$

Proton–proton center of mass frame

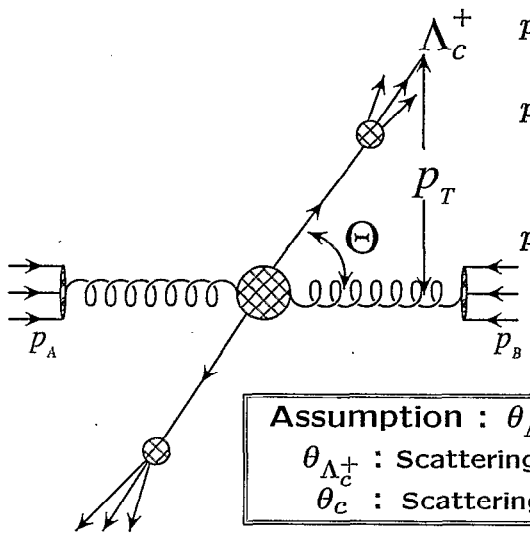

$$p_{A/B} = \frac{\sqrt{s}}{2}(1, \pm\beta, \vec{0}) \ , \ \beta \equiv \sqrt{1 - \frac{4m_p^2}{s}}$$

$$p_{\Lambda_c} = (E_{\Lambda_c}, p_L, p_T) = \left(\sqrt{m_{\Lambda_c}^2 + (p_T \csc\Theta)^2}, p_T \cot\Theta, p_T\right)$$

$$p_{a,b} = x_{a,b} p_{A,B} \quad , \quad p_c = \frac{p_{\Lambda_c}}{z}$$

Assumption : $\theta_{\Lambda_c^+} \simeq \theta_c \equiv \Theta$

$\theta_{\Lambda_c^+}$: Scattering angle of the produced Λ_c^+ in final state

θ_c : Scattering angle of the c quark in the subprocess

The spin correlation differential cross section

$$\frac{d\Delta\sigma}{dp_T} \equiv \int_{\Theta^{\min}}^{\Theta^{\max}} \int_{x_a^{\min}}^{1} \int_{x_b^{\min}}^{1} G_{g_a/p_A}(x_a, Q^2) \Delta G_{\vec{g}_b/\vec{p}_B}(x_b, Q^2) \times \frac{d\Delta\hat{\sigma}}{d\hat{t}} \Delta D_{\vec{\Lambda}_c^+/\vec{c}}(z) \mathcal{J} d\Theta dx_a dx_b$$

$G_{g_a/p_A}(x_a, Q^2)$: Unpolarized gluon distribution function

$\Delta G_{\vec{g}_b/\vec{p}_B}(x_b, Q^2)$: Polarized gluon distribution function

$d\Delta\hat{\sigma}/d\hat{t}$: Spin correlation differential cross section for subprocess

$\Delta D_{\vec{\Lambda}_c^+/\vec{c}}(z)$: Spin dependent fragmentation function

$\mathcal{J}$: Jacobian which transform the variables z and $\hat{t}$ into Θ and p_T

III. Numerical Calculation

Gluon Distribution Function of the proton

For unpolarized gluon distribution : $G_{g/p}(x, Q^2)$

- GRV95

  M. Glück, *et al* Z. Phys. C67 (1995), 433.

For polarized gluon distribution : $\Delta G_{\vec{g}/\vec{p}}(x, Q^2)$

- GS96-setA andB

  T. Gehrmann, *et al* Phys. Rev. D53 (1996), 6100.

- GRSV96

  M. Glück,*et al* Phys. Rev. D53 (1996), 4775.

Fragmentation Function : $(\Delta)\mathrm{D}(z)$

- Peterson Fragmentation Function

  C. Peterson *et. al* Phys. Rev. D27 (1983), 105.

p_T distribution of Spin correlation differential cross section

$$\frac{\pi}{6} \leq \Theta \leq \frac{5\pi}{6}$$

$\sqrt{s}$=200GeV

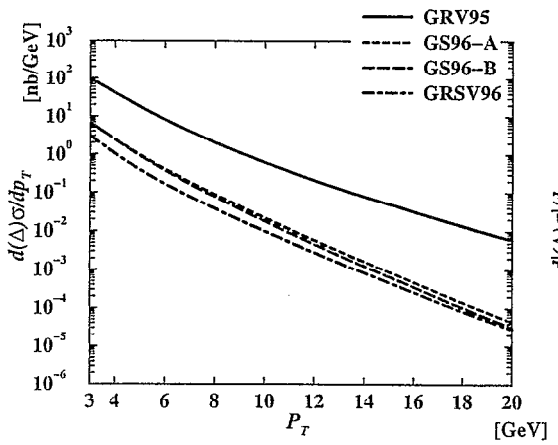

$\sqrt{s}$=500GeV

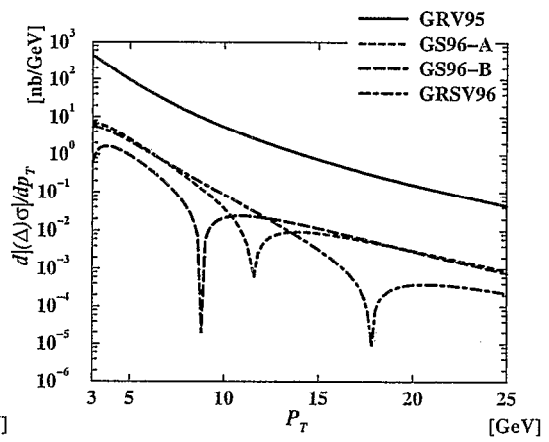

$$\frac{d\Delta\sigma}{dp_T} \equiv \int_{\Theta^{\min}}^{\Theta^{\max}} \int_{x_a^{\min}}^{1} \int_{x_b^{\min}}^{1} G_{g_a/p_A}(x_a, Q^2)\Delta G_{\vec{g}_b/\vec{p}_B}(x_b, Q^2)$$

$$\times \frac{d\Delta\hat{\sigma}}{d\hat{t}} \Delta \mathrm{D}_{\vec{\Lambda}_c^+/\vec{c}}(z)\mathcal{J}\, d\Theta dx_a dx_b$$

a sign of the $\frac{d\Delta\sigma}{dp_T}$ is determined by the sign of $\frac{d\Delta\hat{\sigma}}{d\hat{t}}$ because all the other variables are positive for all kinematical region.

$\Downarrow$

$$\frac{d\Delta\hat{\sigma}}{d\hat{t}} = \frac{\pi\alpha_s^2}{\hat{s}}\left[\frac{m_c^2}{24}\left\{\frac{9\hat{t}-19\hat{u}}{\hat{t}\hat{u}} + \frac{3}{\hat{u}^2}\right\} + \frac{\hat{s}}{6}\left\{\frac{\hat{t}-\hat{u}}{\hat{t}\hat{u}}\right\} - \frac{3}{8}\left\{\frac{2\hat{t}}{\hat{s}} + 1\right\}\right]$$

the sign of $\frac{d\Delta\hat{\sigma}}{dp_T}$ mainly originates from the second term, because both $\hat{t}$ and $\hat{u}$ are negative and smaller than $\hat{s}$ in magnitude.

$\Downarrow$

$$\hat{t} - \hat{u} = x_b\sqrt{s}\left\{x_a\sqrt{s} - \frac{2}{z}\left(\sqrt{m_{\Lambda_c^+}^2 + p_T^2 \mathrm{cosec}^2\Theta} + p_T \cot\Theta\right)\right\}$$

$$x_a^{\min} \simeq \frac{\sqrt{m_{\Lambda_c^+}^2 + {p_T}^2 \mathrm{cosec}^2\Theta} + p_T \cot\Theta}{\sqrt{s} - \left(\sqrt{m_{\Lambda_c^+}^2 + {p_T}^2 \mathrm{cosec}^2\Theta} - p_T \cot\Theta\right)}$$

x_a becomes very small in large $\sqrt{s}$ and small p_T region. For vary small x_a, $\hat{t} - \hat{u}$ can be negative. $\rightarrow d\Delta\hat{\sigma}/d\hat{t} < 0$

$\Downarrow$

$$\frac{d\Delta\sigma}{dp_T} \equiv \int_{\Theta^{\min}}^{\Theta^{\max}} \int_{x_a^{\min}}^{1} \int_{x_b^{\min}}^{1} G_{g_a/p_A}(x_a, Q^2)\Delta G_{\vec{g}_b/\vec{p}_B}(x_b, Q^2)$$

$$\times \frac{d\Delta\hat{\sigma}}{d\hat{t}} \Delta \mathrm{D}_{\vec{\Lambda}_c^+/\vec{c}}(z)\mathcal{J}\, d\Theta dx_a dx_b$$

Vary small x_a leads to large values of the gluon distributions and negative values of $d\Delta\hat{\sigma}/d\hat{t} \rightarrow d\Delta\sigma/dp_T < 0$

Spin correlation asymmetry

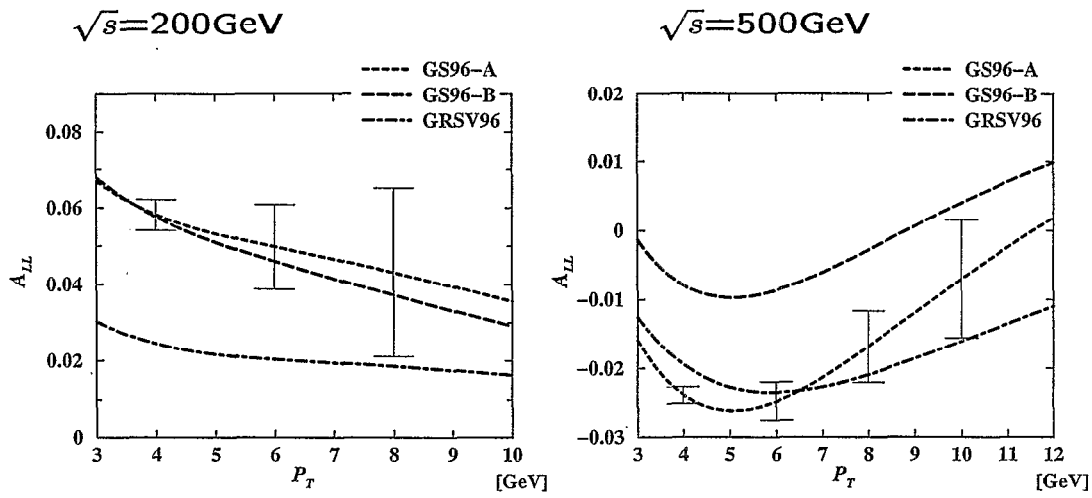

Error bar :the statistical sensitivity for $T = 100$-day experiments

IV.Summary

♣ The spin correlation differential cross section, $\frac{d\Delta\sigma}{dp_T}$, and asymmetry, A_{LL}, has been calculated for $\sqrt{s} = 200$ GeV and 500 GeV. ⇐ RHIC experiment can measured these observables.

Both $\frac{d\Delta\sigma}{dp_T}$ and A_{LL} shows considerable difference in behaviors for these two energies.

A_{LL} is sensitive to polarized gluon distribution.

FUTURE

Study of higher order corrections needed !!!

Large momentum transfer electroproduction of mesons

Hanwen Huang (Kobe University)

Abstract

Assuming the proton's light-cone wave function to be dominated by small parton virtualities and small intrinsic transverse momenta, we show that the electro-production amplitudes at large momentum transfer factorize into parton-level subprocess amplitudes and form factors representing $1/x$-moments of skewed parton distributions. On the basis of a wave function overlap model for the form factors we present detailed predictions for the electro-production cross sections. We also comment on large momentum transfer photo-production.

Large momentum transfer electroproduction of mesons

Han-Wen Huang (Kobe Univ.)

2000/OCT./13, KYOTO

Based on
H.W.Huang and P.Kroll (Wuppertal univ.)
hep-ph/0005318.

I. Introduction
II. The soft mechanism
III. The form factors and the meson distribution amplitudes
IV. Potoproduction of mesons
V. Electoproduction of mesons
VI. Summary

I. Introduction

In hard scattering, nonperturbative information is parameterized in terms of hadronic matrix elements of operators.

- Inclusive: diagonal matrix elements of bi-local operators $\Rightarrow$ parton distribution functions (PDFs).
- Exclusive: non-diagonal matrix elements of local combinations of operators $\Rightarrow$ hadron form factors.

non-diagonl matrix elements of bi-local products of operators $\Rightarrow$ skewed parton distributions (SPDs), combine properties of PDFs and form factors.

- Large Q^2, small $|t|$: deeply virtual compton scattering (DVCS) and deeply virtual electroproduction of mesons (DVEM) factorize into hard photon-parton scattering and SPDs.
- Large $|t|$, small Q^2: $|t| \to \infty$, perturbative dominate; $|t|$ accessible in current experiments, in compton scattering, soft contribution dominate, factorize into hard subprocess and new form factors representing $1/x$ moments of SPDs (M.Diehl, *et al.*, hep-ph/9811253).

$\Downarrow$

Apply to large angle electroproduction of mesons.

II. The soft mechanism

Kinematical region: $s = (p+q)^2, \quad -t = -\Delta^2, \quad -u = -(p-q')^2$ are large ($\gg \Lambda^2_{QCD}$), Q^2 is not considered as a large scale. Work in symmetric frame

$$p = \left[p^+, \frac{m^2 - t/4}{2p^+}, -\frac{1}{2}\Delta_\perp\right], \quad p' = \left[p^+, \frac{m^2 - t/4}{2p^+}, \frac{1}{2}\Delta_\perp\right]$$

$\Delta^+ = \Delta^- = 0$, $t = -\Delta_\perp^2$, $\zeta = -\frac{\Delta^+}{p^+} = 1 - \frac{p'^+}{p^+}$

Parton momenta $x_i = k_i^+/p^+$, $x_i' = k_i'^+/p'^+$, $\mathrm{k}_{\perp i}$ and $\mathrm{k}'_{\perp i}$.

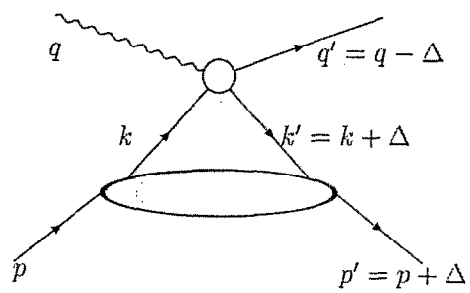

The arguments of the light-cone wave function

$$\tilde{x}_i = x_i\,, \quad \tilde{\mathrm{k}}_{\perp i} = \mathrm{k}_{\perp i} + x_i\,\Delta_\perp/2\,.$$
$$\hat{x}' = x_i' \quad \hat{\mathrm{k}}'_{\perp i} = \mathrm{k}'_{\perp i} - x_i'\,\Delta_\perp/2.$$

<u>The crucial hypothesis in the soft physics approach</u>: soft proton wave functions dominated by $|k_i^2|, |k_i'^2| \lesssim \Lambda^2$ and intrinsic transverse parton momenta $\tilde{\mathrm{k}}^2_{\perp i}/x_i, \hat{\mathrm{k}}'^2{}_{\perp i}/x_i' \lesssim \Lambda^2$.

$\hat{s} = (k+q)^2$ *and* $\hat{u} = (k'-q)^2$ are equal to s *and* u up to corrections of order $\Lambda^2(t \pm Q^2)/t$

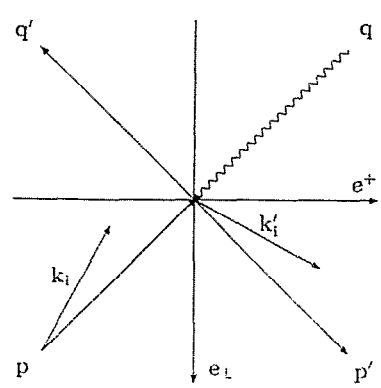

The physical situation is that of a hard parton-level subprocess ($\hat{s}, -t, -\hat{u} \gg \Lambda^2$) and a soft proton matrix element describing the soft emission and reabsorption of a parton by the proton.

$$\begin{aligned}
\mathcal{M}^{M(q)}_{\mu'\nu',\mu\nu} &= \sum_a e e_a B^M_a \int d^4k\, \theta(k^+) \int \frac{d^4z}{(2\pi)^4} e^{ik\cdot z} \\
&\times \Big[\langle p'\nu' | T\overline{\psi}_{a\alpha}(0)\psi_{a\beta}(z) | p\nu \rangle H^{M(q)\alpha\beta}_{\mu'\mu}(k',k) \\
&+ \langle p'\nu' | T\overline{\psi}_{a\alpha}(z)\psi_{a\beta}(0) | p\nu \rangle H^{M(q)\alpha\beta}_{\mu'\mu}(-k,-k') \Big]
\end{aligned}$$

Active parton is on shell, collinear with parent proton $\Rightarrow$ integration over k^- and $k_\perp$ leaving an integral $\int dk^+ \int dz^- \Rightarrow z \to \bar{z} = [0, z^-, 0_\perp]$.

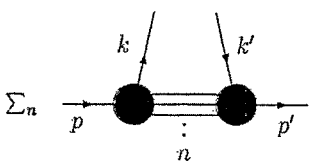

$$\begin{aligned}
\overline{\psi}_\alpha(0)\,\psi_\beta(\bar{z}) &\to \left(\frac{1}{2k^+}\right)^2 \sum_{\lambda,\lambda'} \left(\overline{\psi}(0)\gamma^+ u(k',\lambda')\right) \\
&\times \left(\bar{u}(k,\lambda)\gamma^+\psi(\bar{z})\right)\, \bar{u}_\alpha(k',\lambda')\, u_\beta(k,\lambda)
\end{aligned}$$

Define

$$\mathcal{H}^{M(q)}_{\mu'\lambda',\mu\lambda} = \bar{u}(k',\lambda')\, H^{M(q)}_{\mu',\mu}(k',k)\, u(k,\lambda)\,,$$

$$\begin{aligned}
\mathcal{M}^{M(q)}_{0+,\mu+}(s,t) &= \frac{e}{2}\Big\{ \mathcal{H}^{M(q)}_{0+,\mu+}(s,t)\,[R^M_V(t) + R^M_A(t)] \\
&\quad + \mathcal{H}^{M(q)}_{0-,\mu-}(s,t)\,[R^M_V(t) - R^M_A(t)] \Big\}\,,
\end{aligned}$$

Form factor decomposition

$$\begin{aligned}
&\int_0^1 \frac{dx}{x} p^+ \int \frac{dz^-}{2\pi} e^{ixp^+z^-} \left\langle p'\nu' \middle| \overline{\psi}_a(0)\gamma^+\psi_a(\bar{z}) + \kappa_M \overline{\psi}_a(\bar{z})\gamma^+\psi_a(0) \middle| p\nu \right\rangle \\
&= R^{Ma}_V(t)\, \bar{u}(p',\nu')\gamma^+ u(p,\nu) + R^{Ma}_T(t) \frac{i}{2m}\, \bar{u}(p',\nu')\sigma^{+\beta}\Delta_\beta u(p,\nu)\,, \\
&\int_0^1 \frac{dx}{x} p^+ \int \frac{dz^-}{2\pi} e^{ixp^+z^-} \left\langle p'\nu' \middle| \overline{\psi}_a(0)\gamma^+\gamma_5\psi_a(\bar{z}) - \kappa_M \overline{\psi}_a(\bar{z})\gamma^+\gamma_5\psi_a(0) \middle| p\nu \right\rangle \\
&= R^{Ma}_A(t)\, \bar{u}(p',\nu')\gamma^+\gamma_5 u(p,\nu)\,.
\end{aligned}$$

$$\mathcal{H}^{M(q)}_{0+,\mu+} = 2\pi\alpha_s(\mu_R) f_M \frac{C_F}{N_c} \int_0^1 d\tau \phi_M(\tau) f^{(q)}_\mu(\tau)$$

Large Q^2, small $|t|$ (DVEM):
$\mathcal{H}^{M(q)}_{0+,0+} \propto 1/\tau$ moment;
$\mathcal{H}^{M(q)}_{0+,\pm+} \propto 1/\tau^2,\ 1/\bar{\tau}^2 \Rightarrow$ the break-down of factorization for transversally photons.

For flavor-neutral vector meson production, gluons contribute.

$$\begin{aligned}\mathcal{M}^{V(g)}_{0+,\mu+}(s,t) &= \frac{e}{2}\Big[\mathcal{H}^{V(g)}_{01,\mu 1}(s,t)\left(R^{V(g)}_V(t) + R^{V(g)}_A(t)\right) \\ &+ \mathcal{H}^{V(g)}_{0-1,\mu-1}(s,t)\left(R^{V(g)}_V(t) - R^{V(g)}_A(t)\right)\Big],\end{aligned}$$

The form factors are related to SPDs at zero skewedness

$$R^g_V(t) = \int_0^1 \frac{dx}{x^2}\mathcal{F}^g_{\zeta=0}(x,t) \quad , R^g_A(t) = \int_0^1 \frac{dx}{x^2}\mathcal{G}^g_{\zeta=0}(x,t)$$

are still called $1/x$-moments of SPDs.

III. the form factors and the meson distribution amplitudes

	R^M_i	R^{Vg}_i
ρ^0, π^0	$\frac{1}{\sqrt{2}}[e_u R^{Mu}_i - e_d R^{Md}_i]$	$\frac{1}{\sqrt{2}}[e_u - e_d] R^g_i$
ω, η_q	$\frac{1}{\sqrt{2}}[e_u R^{Mu}_i + e_d R^{Md}_i]$	$\frac{1}{\sqrt{2}}[e_u + e_d] R^g_i$
ϕ, η_s	$e_s R^{Ms}_i$	$e_s R^g_i$

In Compton scattering, the sum runs over all flavors, here the sum is over the valence quarks of the produced mesons.
$\omega - \phi$ mixing is small and ignored. $\eta - \eta'$ mixing is taken into account.

$$\begin{aligned}\eta &= \cos\phi_P\, \eta_q - \sin\phi_P\, \eta_s\,, \\ \eta' &= \sin\phi_P\, \eta_q + \cos\phi_P\, \eta_s\,,\end{aligned}$$

take $\phi_P = 39.2°$.
In a frame $\Delta^+ = 0$, SPDs can be represented as overlaps of light-cone wave functions summed over all Fock states.

Assuming a single Gaussian $\tilde{k}_{i\perp}$-dependence of the soft Fock state wave functions

$$\Psi_{N\beta}(x_i, \tilde{k}_{\perp i}) \;\propto\; \exp[-a_N^2 \sum_{i=1}^{N} \frac{\tilde{k}_{\perp i}^2}{x_i}],$$

The form factors for individual flavors ($a = u, d, s$):

$$\begin{aligned}
R_V^{Va}(t) &= \int_0^1 \frac{dx}{x} \exp\left[\frac{1}{2}\hat{a}^2 t \frac{1-x}{x}\right] \{q_a(x) + \bar{q}_a(x)\}\,, \\
R_V^{Pa}(t) &= \int_0^1 \frac{dx}{x} \exp\left[\frac{1}{2}\hat{a}^2 t \frac{1-x}{x}\right] \{q_a(x) - \bar{q}_a(x)\}\,, \\
R_V^{g}(t) &= \int_0^1 \frac{dx}{x} \exp\left[\frac{1}{2}\hat{a}^2 t \frac{1-x}{x}\right] g(x)\,.
\end{aligned}$$

three lowest Fock state contribution $q_a^{(N=3,4,5)}(x)$ are evaluated from the light-cone wave functions (with $a_3 = a_4 = a_5 = 0.75\,\mathrm{GeV}^{-1}$), higher Fock states is estimated by setting ($a_N = 1.3\,a_3$ for $N > 5$)

$$\sum_{N>5} q_a^{(N)}(x) \;=\; q_a(x) - \sum_{N=3,4,5} q_a^{(N)}(x),$$

$q_a(x)$ are taken from the GRV parameterization.

Form factors, scaled by t^2, evaluated from the overlap model

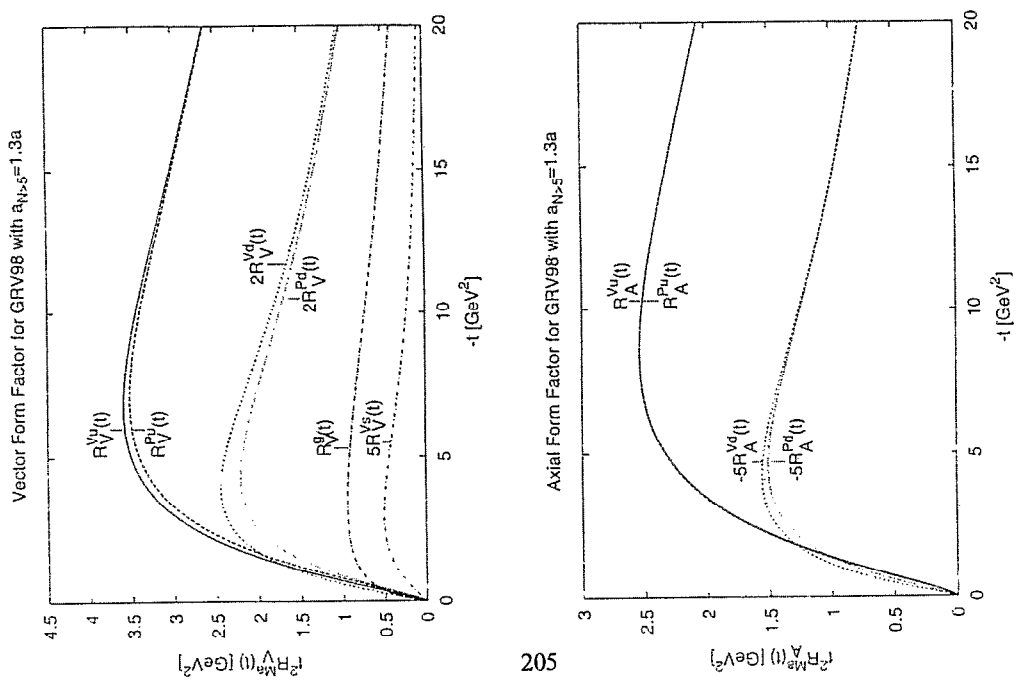

They approximately behave as $1/t^2$ in the momentum transfer region from about 5 to $15\,\mathrm{GeV}^2$. With increasing $|t|$ the form factors for u and d quarks gradually turn into the soft physics asymptotic $\propto 1/t^4$

The form of the meson's distribution amplitude

$$\phi_{\mathrm{AS}}(\tau) \;=\; 6\tau(1-\tau)\,.$$

For the meson decay constants

$$\begin{aligned} f_\pi &= 132\,\mathrm{MeV}\,, \quad f_\rho = 216\,\mathrm{MeV}\,, \\ f_\omega &= 195\,\mathrm{MeV}\,, \quad f_\phi = 237\,\mathrm{MeV}\,, \end{aligned}$$

for the decay constants of the states η_q and η_s

$$f_q = 141\,\mathrm{MeV}\,, \quad f_s = 177\,\mathrm{MeV}\,.$$

Soft physics contribution to photoproduction of π^0 scaled by s^7

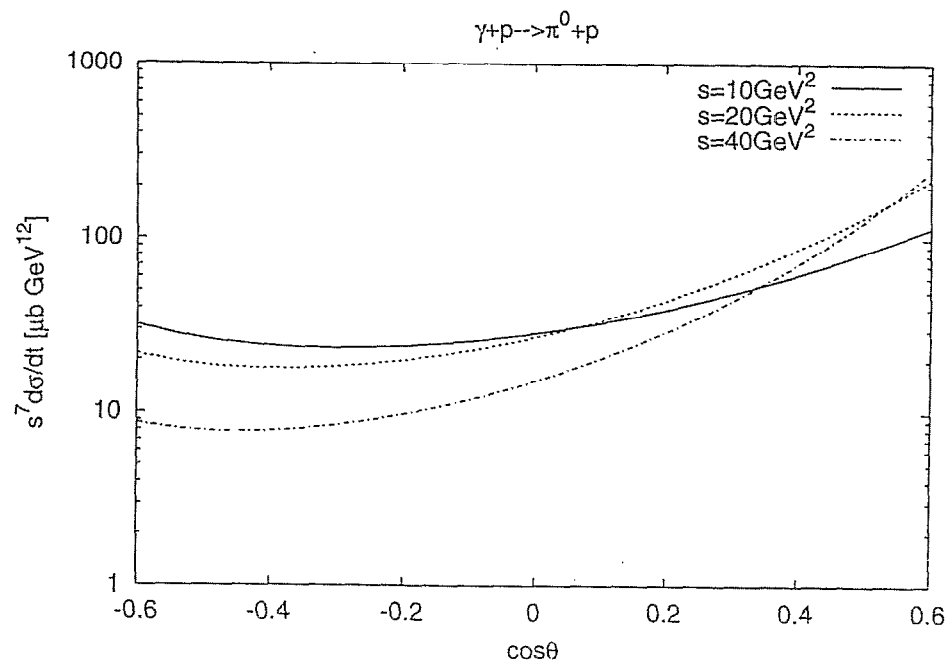

IV. Photoproduction of mesons

Photoproduction cross section of pseudoscalar mesons

$$\frac{d\sigma_P}{dt} = \frac{1}{2}\alpha_{\rm em}\left[\pi\alpha_s(\mu_R) f_P \langle 1/\tau\rangle_P \frac{C_F}{N_C}\right]^2 \times \frac{-t}{u^2 s^4}\left\{(s-u)^2 \left(R_V^P(t)\right)^2 + t^2 \left(R_A^P(t)\right)^2\right\}.$$

As compared to experiment (at $s \simeq 10\,\mathrm{GeV}^2$) the soft physics contributions are too small by orders of magnitude.
Another dynamical mechanism (hadronic component of photon) is at work here. Vector meson dominance (VMD) estimate of the photoproduction cross section

$$\frac{d\sigma}{dt}(\gamma p \to \rho^0 p) = \alpha_{\rm em}\frac{\pi f_\rho^2}{m_\rho^2}\left[\frac{d\sigma}{dt}(\pi^+ p \to \pi^+ p) + \frac{d\sigma}{dt}(\pi^- p \to \pi^- p)\right].$$

I. Electroproduction of mesons

$$\frac{d^4\sigma^M}{ds dQ^2 dt d\varphi} = \frac{\alpha_{\rm em}\, s}{16\pi^2 E_L^2 m^2 Q^2 (1-\epsilon)} \times \left(\frac{d\sigma_T^M}{dt} + \epsilon\frac{d\sigma_L^M}{dt} + 2\epsilon\cos 2\varphi \frac{d\sigma_{TT}^M}{dt} + \sqrt{2\epsilon(1+\epsilon)}\cos\varphi \frac{d\sigma_{LT}^M}{dt}\right)$$

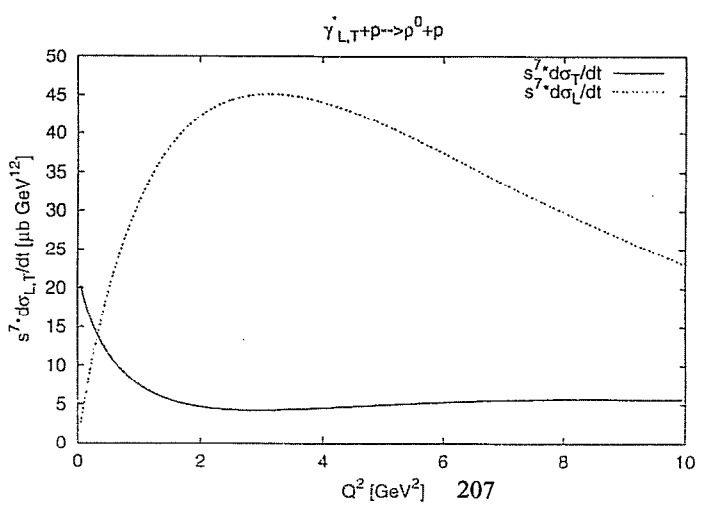

The partial cross sections for ρ^0 mesons ($\sqrt{s}$=20Gev)

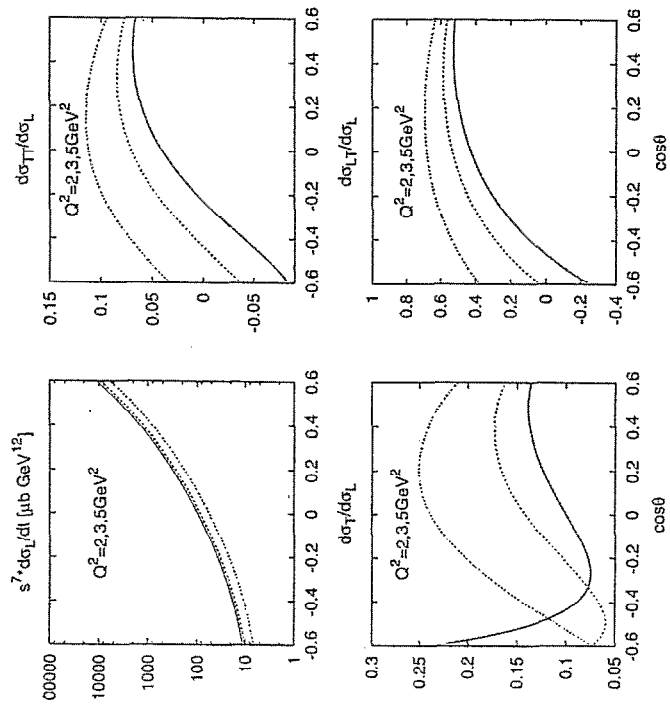

The partial cross sections for ρ^0 mesons ($\sqrt{s}$=40Gev)

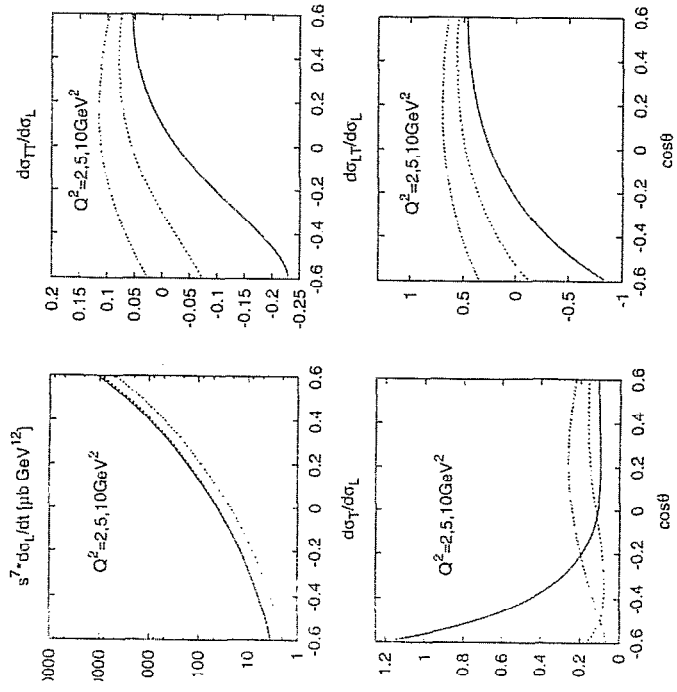

$s = 20\ \mathrm{GeV}^2$ and $Q^2 = 3\ \mathrm{GeV}^2$

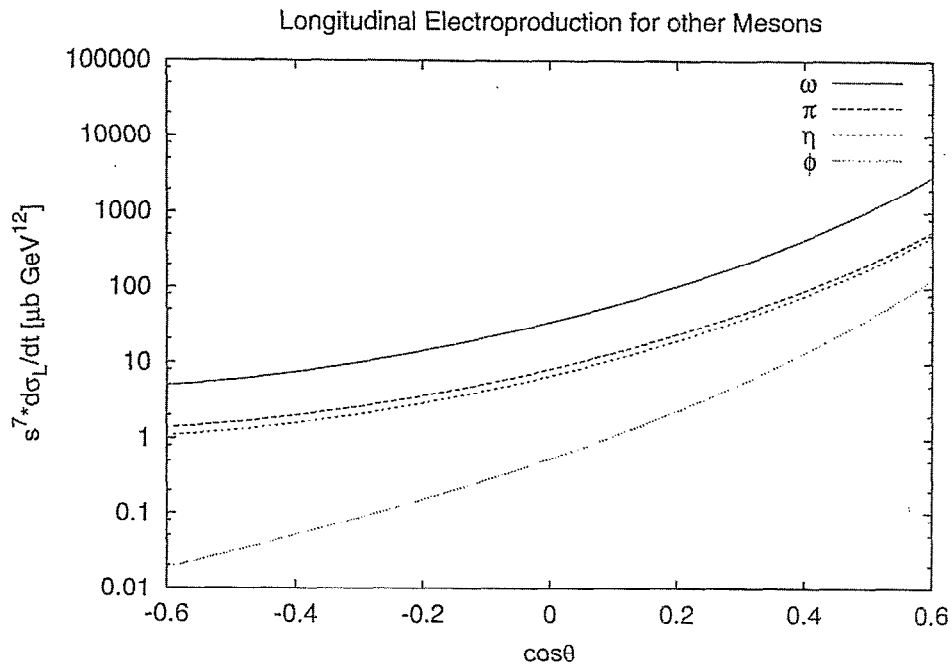

I. Summary

- The soft contribution to electroproduction amplitudes factorize in hard subprocess and soft proton matrix elements described by the same type as in Compton scattering, representing $1/x$-moments of SPDs.
- The new form factors, can be extracted from experiment, provide information on the large momentum transfer behavior of the proton SPDs.
- Based on a LCWF overlap model, predictions for electroproduction of mesons at moderately large photon virtuality are presented. The kinematical region in which the soft physics approach is applicable to electroproduction, is accessible to experiments at the TJlab, ELFE, and EPIC.

PHENIX Detector Commissioning and Prospects for Polarized Proton Running

Kenneth N. Barish for the PHENIX Collaboration (University of California)

Abstract

The Relativistic Heavy Ion Collider (RHIC) at Brookhaven National Laboratory will accelerate highly polarized proton beams and collide them at a center of mass energy up to $\sqrt{S}$=500 GeV. PHENIX is one of the major detector systems at RHIC, consisting of two central arms ($|\eta|$ <0.35 and 2 X 90°ϕ coverage) and two muon arms (1.2<$|\eta|$< 2.4). The first spin run is expected in 2001.

The RHIC Heavy-Ion program began earlier this year. In this running period, PHENIX successfully commissioned at least in part 12 subsystems, and first physics from PHENIX have recently been presented at the JPS and DNP meetings. In this talk, I will give an overview of the Heavy-Ion physics run with a particular focus on the detector needs and schedule for spin physics running.

PHENIX Detector Commissioning and Prospects for Polarized Proton Running

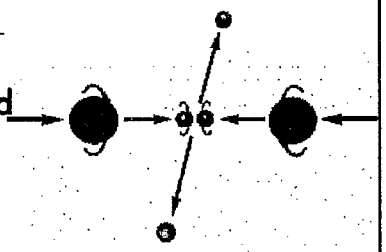

Kenneth N. Barish
UC Riverside
RSC'2000, Oct 2000

The show's just beginning ...

PHENIX

K. Barish
UC Riverside
14 Oct. 2000

PHENIX Physics Program

Relativistic Heavy Ion Program

Characterize nuclear matter at high temperatures

- Understand transitions between phases

Or

Excite vacuum and see what happens:

- Deconfinement
- Chiral symmetry restoration

Spin Physics Program

~~ΔG, $\Delta q/q$,~~ δq, physics beyond standard model

PHENIX

K. Barish
UC Riverside
14 Oct. 2000

PHENIX Spin Physics channels

Central Arms			Muon Arms		
Physics	Process	Trigger	Physics	Process	Trigger
ΔG	Direct Photon	EMC, h.T.	ΔG	Heavy flavor	Mu-Id based
	π^0 asymmetries	EMC, h.T.		J/ψ	Mu-Id based
	$\pi^+\pi^-$ asymmetries	EMC, l.T. Mul.			
	O. Heavy flavor	EMC*RICH, l.T.			
	J/ψ	EMC*RICH, l.T.			
$\Delta q/q$	W-production	EMC, h.T.	$\Delta q/q$	W-production	Mu-Id based
δq	π^- asymmetries	EMC, l.T., Mul.			
all	Trigger bias	EMC, RICH pre-scaled	*all*	Trigger bias	Mu-Id pre-scaled

PHENIX

K. Barish
UC Riverside
14 Oct. 2000

PHENIX Spin Run Plan

Spin Year	□φ	Energy	Physics
S μ arm Channels			
1	32 pb^{-1} A_{LL}#	200 GeV	π^0 (e, $\pi^{+/-}$)
2	290 pb^{-1} A_{LL}	200 GeV	γ, $\pi^{0/+/-}$, e, μ, μμ, eμ, J/ψ
N & S μ arms 2	32 pb^{-1} A_{TT}	200 GeV	$\pi^{+/-}$
3	800 pb^{-1} A_{LL}	800 GeV	W + above

#Discussion on a short A_{TT} run in spin year-1 ongoing.

PHENIX

K. Barish
UC Riverside
14 Oct. 2000

The PHENIX Detector

A complex apparatus to measure
- » Hadrons
- » Muons
- » Electrons
- » Photons

Executive summary:
- » *High* resolution
- » *High* granularity
- » Superb PID

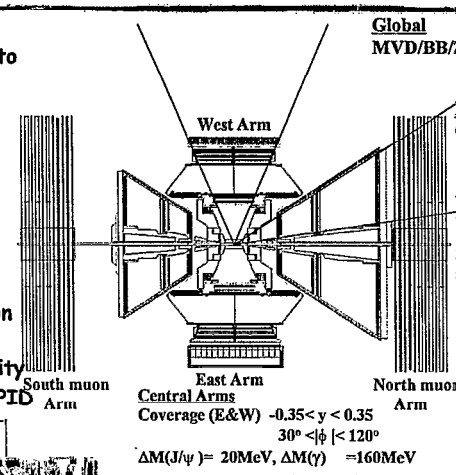

PHENIX

K. Barish
UC Riverside
14 Oct. 2000

The PHENIX Detector

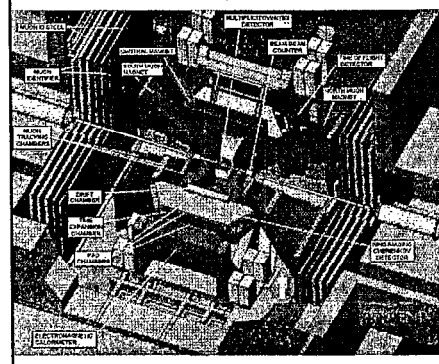

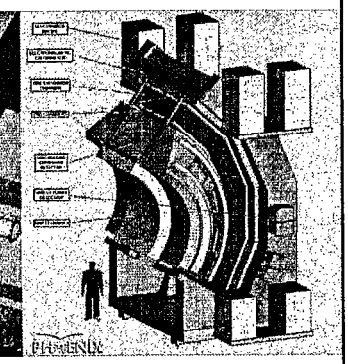

The PHENIX Detector

One "Central Arm"

PHENIX

K. Barish
UC Riverside
14 Oct. 2000

Requirements for Spin Channels

Physics	Trigger	Detectors (Required/Helpful)	Approx □φdt
Direct γ	EMC	EMC, DCH, PAD	300 pb^{-1}
π^0 Asymmetry	EMC	EMC, DCH, PAD	10 pb^{-1}
$\pi^{+/-}$ Asymmetry	EMC/RICH	EMC, DCH, PAD, RICH, TEC	10 pb^{-1}
e	EMC/RICH	EMC, DCH, PAD, RICH, TEC, MVD	25 pb^{-1}
$e\mu$	EMC/RICH	EMC, DCH, PAD, RICH, TEC, MVD, 1 μ arm	300 pb^{-1}
μ	μ-ID		300 pb^{-1}
$\mu\mu$	μ-ID	1 μ arm	300 pb^{-1}
J/ψ □ ee	EMC/RICH	1 μ arm	300 pb^{-1}
J/ψ □ $\mu\mu$	μ-ID	EMC, DCH, PAD, RICH, TEC	300 pb^{-1}
W □ eν	EMC/RICH	1 μ arm	800 pb^{-1}
W □ $\mu\nu$	μ-ID	EMC, DCH, PAD, RICH, TEC	800 pb^{-1}
Drell-Yan (e)	EMC/RICH	2 μ arms	300 pb^{-1}
Drell-Yan (μ)	μ-ID	EMC, DCH, PAD, RICH, TEC 1 μ arm	300 pb^{-1}

PHENIX

K. Barish
UC Riverside
14 Oct. 2000

Year-1 Configuration

PHENIX in Year-1

- » 12 subsystems at least partially commissioned.
- » Over 200,000 channels

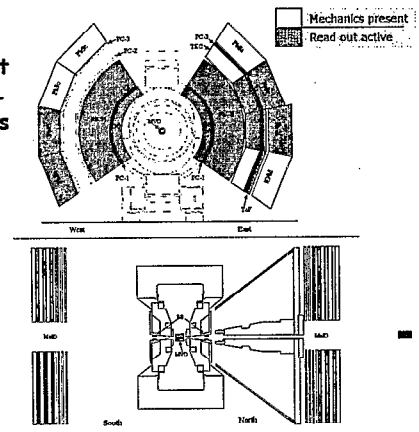

PHENIX

K. Barish
UC Riverside
14 Oct. 2000

Run/Luminosity Progress In Year2000

March thru June

- » RHIC Machine studies
- » Detector Commissioning

June 15, 2000

- » First collisions (γ=30)

Initial Operation (γ=70, 6 bunches)

- » 500,000 Minimum-bias triggers

Final Operation (γ=70, 55 bunches)

- » 45,000,000 Min-bias triggers (4.1 mb^{-1})

5 Million Events Taped

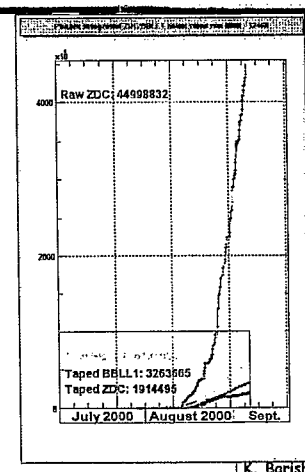

PHENIX

K. Barish
UC Riverside
14 Oct. 2000

Reading out the Same Event!

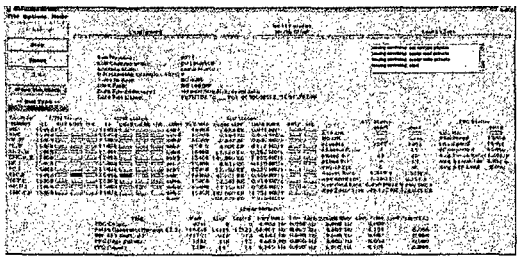

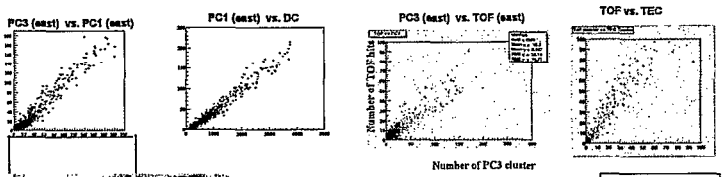

PHENIX

K. Barish
UC Riverside
14 Oct. 2000

BB and ZDC Counters

- Tungsten/quartz fiber hadron calorimeter
  - only forward neutrons
- Luminosity monitoring, min. bias triggering
- ZDC's the <u>same</u> for all intersection regions

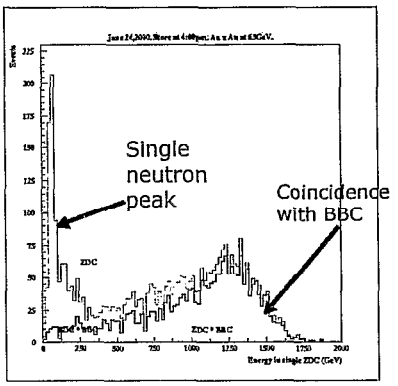

PHENIX

K. Barish
UC Riverside
14 Oct. 2000

Beam Beam Counters

BBC (beam-beam counter)

» start timing, vertex location

» multiplicity

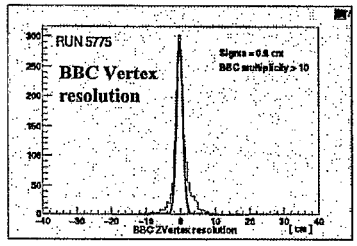

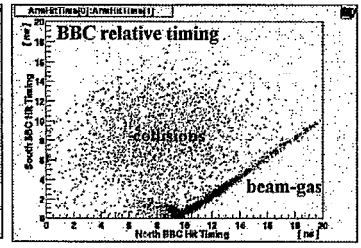

PHENIX

K. Barish
UC Riverside
14 Oct. 2000

Correlations with ZDC

Peripheral Collisions
Large fragments, small number of forward neutrons

Central Collisions
Mostly participants, small number of forward neutrons

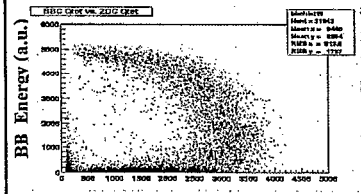

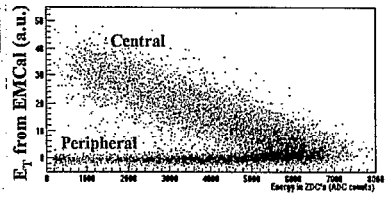

PHENIX

K. Barish
UC Riverside
14 Oct. 2000

Tracking and Alignment

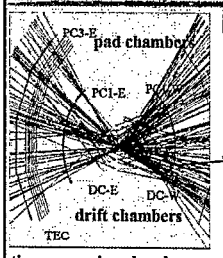

Event projected into xy plane

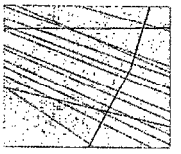

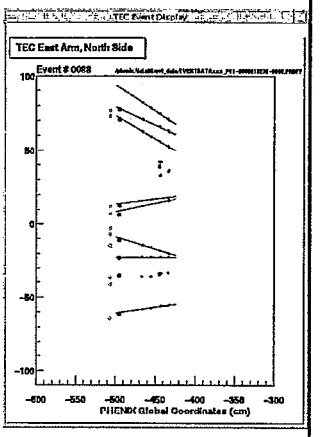

PC vs BB vertex

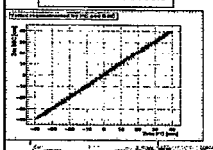

TEC points back to vertex

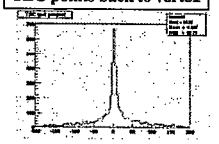

PHENIX

K. Barish
UC Riverside
14 Oct. 2000

Multiplicity Distributions

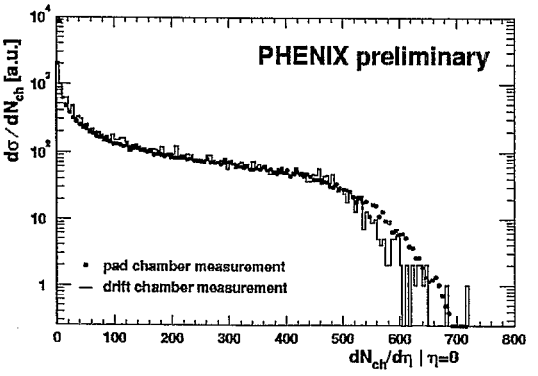

PHENIX

K. Barish
UC Riverside
14 Oct. 2000

E_T Analysis from Calorimetry

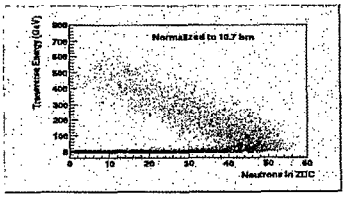

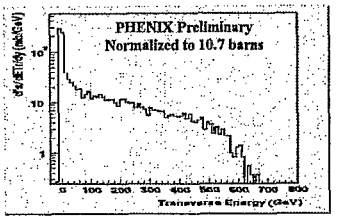

One-fourth of azimuthal coverage used for this analysis
- » Corresponds to 5184 5x5 cm^2 towers
- » Minimum-bias trigger includes 7.2b strong, 3.7b mutual-Coulomb dissociation

Energy scale and $e/\pi/p$ response checked at AGS & CERN, 1-70 GeV

Upper left shows correlation of E_T with E_{ZDC}, expressed as # neutrons

Upper right is $d\sigma/dE_T$ for minimum-bias trigger

$dE_T/d\eta$, $\eta=0$, is 570 GeV +/- 10% for 2% most central

PHENIX

K. Barish
UC Riverside
14 Oct. 2000

Particle Identification using Time Of Flight

Time of Flight array
- » 1024 slats, PMT each end
- » Covers 1 EMCal sector
- » Presently <120ps resolution
  - Amplitude-slewing not corrected

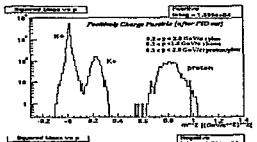

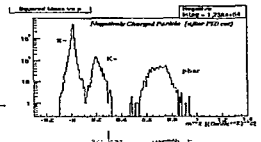

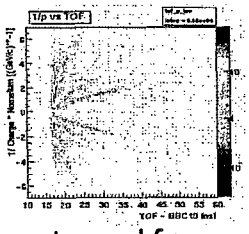

Tracking system used for momentum reconstruction
- » Track association and momentum resolution still improving

Resulting spectrum shows
- » Both charge signs $e/\pi/K/p$
- » Separation to ~2 GeV/c
- » Good signal/background!!

PHENIX

K. Barish
UC Riverside
14 Oct. 2000

Identified Charged-Hadron m_T-m_0 Spectra

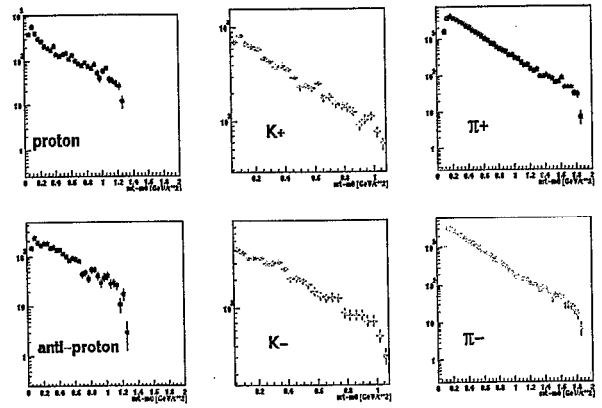

Raw distributions; acceptance and efficiency corrections yet to be applied !

PHENIX

K. Barish
UC Riverside
14 Oct. 2000

π^0 Identification and p_T

Two photon invariant mass spectrum analyzed as function of pair p_T

Observe expected peak at π^0 mass

- » width all due to resolution
- » centroid and width stable with p_T
- » magnitudes as expected from Monte Carlos study of detector response using PISA (PHENIX Integrated Simulation Algorithm) and HIJING event generator

Can see pairs in RHIC Au+Au !!!

Future p_T reach thus governed by statistics, i.e. integrated luminosity

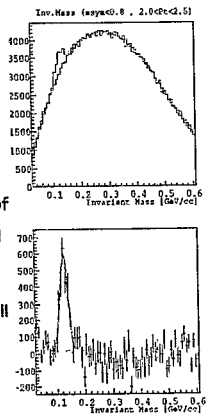

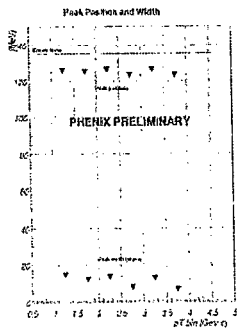

PHENIX

K. Barish
UC Riverside
14 Oct. 2000

p_T Spectra of π^0 and EM Clusters

Inclusive EM clusters shown on left side ("almost photons")

p_T spectra of π^0 on right for minimum-bias collisions

- » compared to WA98 π^0 spectra for 10% most central collisions
- » WA98 is 17 GeVA Pb+Pb

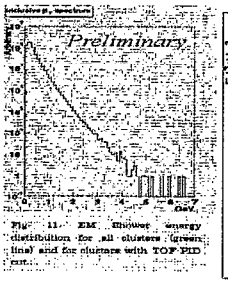

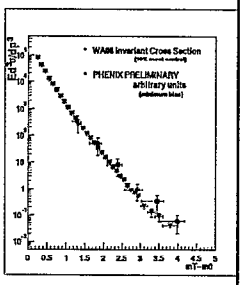

- » PHENIX inverse slopes larger, already for minimum-bias events
- » PHENIX finds T=303 ±11 (stat) ± 67 (syst) MeV for π^0 slope parameter
- » WA98 value is 180 MeV for low- p_T, rising to 260 MeV for large p_T

PHENIX

K. Barish
UC Riverside
14 Oct. 2000

Electrons via RICH

RICH for electron tagging

- » Field-off runs, look for converted γ, results in 2 overlapped rings
- » Rings and tracks found aligned
- » Pulse height as expected from test beam data with RICH

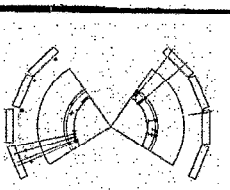

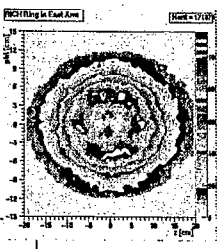

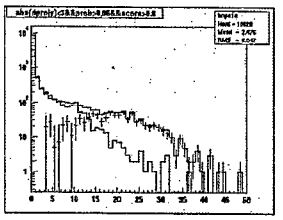

PHENIX

K. Barish
UC Riverside
14 Oct. 2000

PHENIX Spin Readiness

Detector

Fully instrumented Central arm and South Muon arm should be commissioned before spin run

Trigger

Central Arms – Upgrade needed to do spin physics

EMCal based trigger made possible by EMCal Trigger Cards

RICH/EMCal trigger needed electron and hadron triggger.

Muon Arms – Low L era ok/ High L under study

DAQ

Should evolve to 12.5KHz for next year

Start Time/Luminosity Monitor Needed

Beam-beam good enough?

ZDC, MVD, or EMCal?

New large coverage counter?

PHENIX

K. Barish
UC Riverside
14 Oct. 2000

Year-1 of Spin

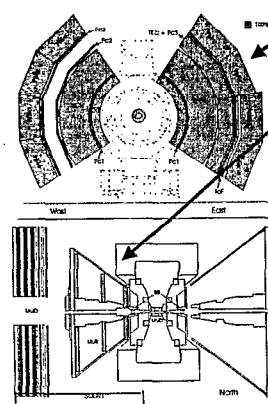

Full instrumentation at midrapidity

- full e, γ and hadron program

South muon arm

PHENIX

K. Barish
UC Riverside
14 Oct. 2000

μID Commissioning

Limited Configuration
- South Arm
- 3 layers (out of 5)
- 29 channels/layer (out of 634)

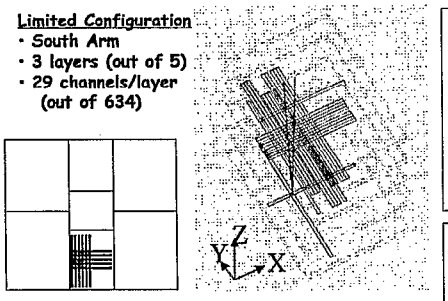

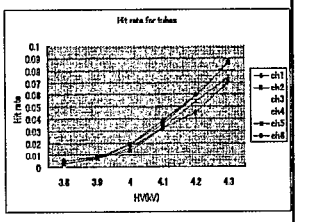

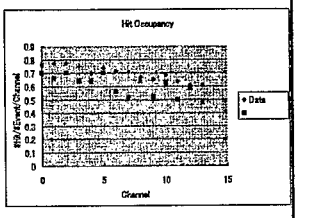

- Chambers are working well
- Hit rate is consistent with simulation
- Tracks are reconstructed

PHENIX

K. Barish
UC Riverside
14 Oct. 2000

Multiplicity and Vertex Detector

MVD installed July 13, 2000

Silicon strips and pads
Centrality selection and
event by event fluctuations
$-2.5 < dN_{ch}/dh < 2.5$

Several MCM's put into main data
Stream at end of run

PHENIX

K. Barish
UC Riverside
14 Oct. 2000

Triggering Needs

The PHENIX trigger was designed for Heavy Ions:

» For Heavy-Ion, data reduction done in Level-2

$\sqrt{s} = 200$ GeV,
$\sigma = 6$ barn, $\Rightarrow$ Raw Rate $= 1.2$ KHz
$L = 2 \cdot 10^{26}$ cm^{-2}s^{-1}

» But in proton-proton interaction rate will be high

$\sqrt{s} = 500$ GeV,
$\sigma = 60$ mbarn, $\Rightarrow$ Raw Rate $= 12$ MHz
$L = 2 \cdot 10^{32}$ cm^{-2}s^{-1}

» Expected Level-1 DAQ Bandwidth is 12kHz

» Need to be shared among 10 different physics channels

- A rejection factor of 10,000 is needed in Level-1 to fully utilize beam

PHENIX

K. Barish
UC Riverside
14 Oct. 2000

EMCal Trigger

Threshold on EMCal can be used to trigger on high p_T photons and electrons.

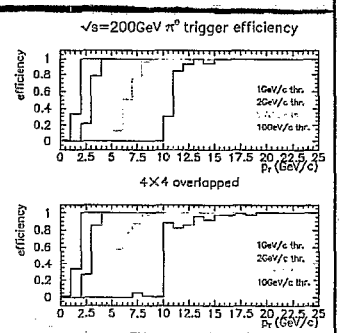

event type	trigger	p_T threshold 1GeV/c	2GeV/c	5GeV/c	10GeV/c
prompt photon	SM non-overlap	1.7Hz	0.43Hz	0.023Hz	0.0015Hz
	4x4 overlap	1.7Hz	0.43Hz	0.023Hz	0.0015Hz
QCD jet	SM non-overlap	1.4kHz	58Hz	0.79Hz	0.016Hz
	4x4 overlap	1.3kHz	53Hz	0.44Hz	0.008Hz

PHENIX

K. Barish
UC Riverside
14 Oct. 2000

π^0 and direct γ Production

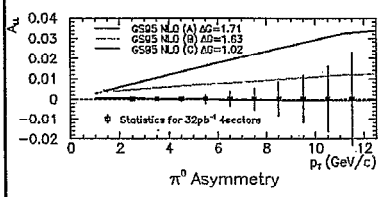

π^0 Asymmetry

π^0 p_T	$\sqrt{s} = 200$ GeV Yield	δA_{LL}
2 – 3 GeV/c	3.3×10^8	1.1×10^{-4}
3 – 4 GeV/c	4.3×10^7	3.1×10^{-4}
4 – 5 GeV/c	8.8×10^6	6.9×10^{-4}
5 – 6 GeV/c	2.3×10^6	1.3×10^{-3}
6 – 7 GeV/c	7.4×10^5	2.4×10^{-3}
7 – 8 GeV/c	3.5×10^5	3.4×10^{-3}
8 – 9 GeV/c	1.3×10^5	5.6×10^{-3}
9 – 10 GeV/c	6.8×10^4	7.8×10^{-3}
10 – 11 GeV/c	3.1×10^4	1.2×10^{-2}
11 – 12 GeV/c	2.1×10^4	1.4×10^{-2}

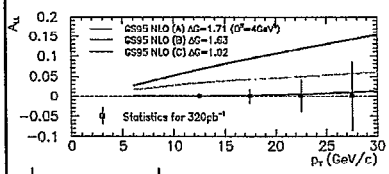

Photon p_T	$\sqrt{s} = 200$ GeV Yield	Errors on A_{LL}	$\Delta G/G$
10 – 15 GeV/c	100000	0.0062	0.046
15 – 20 GeV/c	13000	0.0168	0.089
20 – 25 GeV/c	2700	0.0376	0.171
25 – 30 GeV/c	590	0.0799	0.309

PHENIX

K. Barish
UC Riverside
14 Oct. 2000

EMCal/RICH Trigger

EMCal and RICH detectors can be used to form a powerful central arm electron and hadron trigger

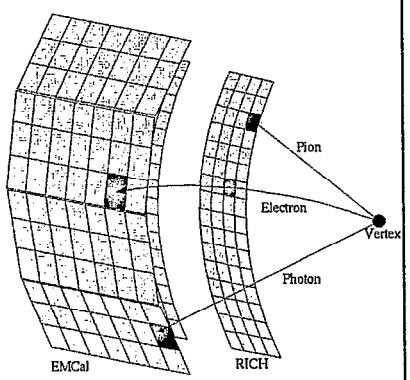

PHENIX

K. Barish
UC Riverside
14 Oct. 2000

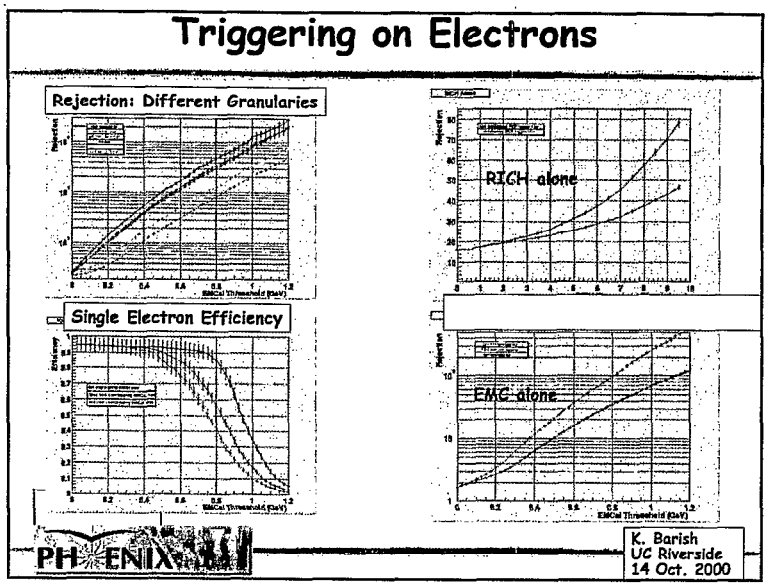
Triggering on Electrons
Rejection: Different Granularies
RICH alone
Single Electron Efficiency
EMC alone
PHENIX
K. Barish
UC Riverside
14 Oct. 2000

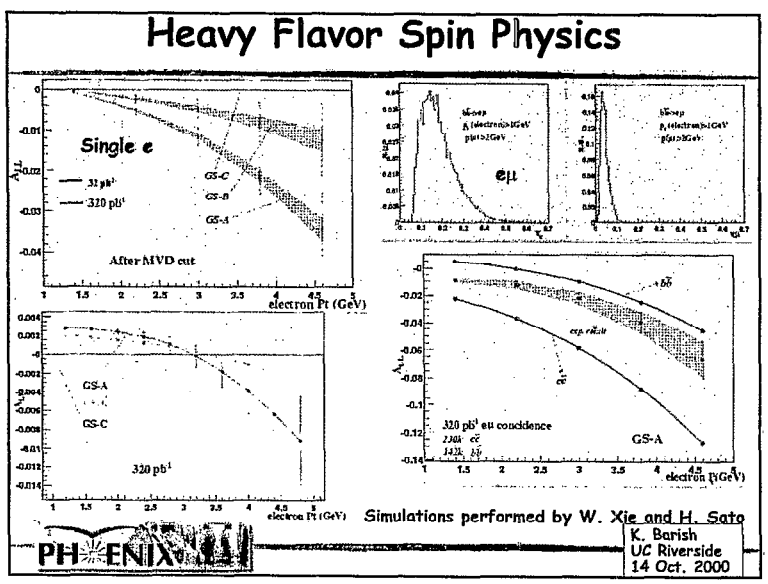
Heavy Flavor Spin Physics
Single e
31 pb⁻¹
320 pb⁻¹
GS-C
GS-B
GS-A
After MVD cut
electron Pt (GeV)
eμ
GS-A
GS-C
320 pb⁻¹
320 pb⁻¹ eμ coincidence
GS-A
electron P(GeV)
Simulations performed by W. Xie and H. Sato
PHENIX
K. Barish
UC Riverside
14 Oct. 2000

Heavy Flavor Spin Physics

Heavy Flavor Production:

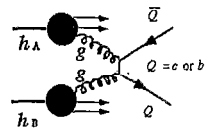

$$A_{LL} \propto \frac{\Delta G(x_A)}{G(x_A)} \otimes \frac{\Delta G(x_B)}{G(x_B)} \otimes a_{LL}^{gg \to q\bar{q}}$$

Tag as: single e, e-mu, e-D coincidence

Most Events Below 2 GeV!

For $\int dL = 32 pb^{-1}$

$6.8 \times 10^6 e$ from $c\bar{c}$

$0.6 \times 10^6 e$ from $b\bar{b}$

with $p_T > 0.9$ GeV

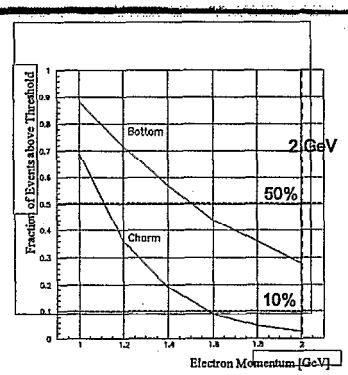

PHENIX

K. Barish
UC Riverside
14 Oct. 2000

Triggering on Hadrons

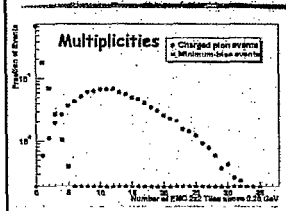

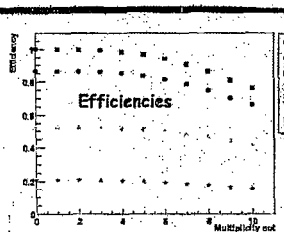

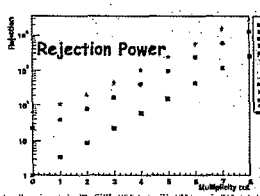

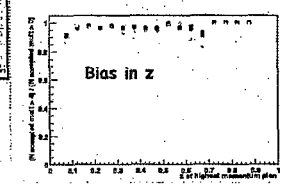

Simulations performed by B. Lillie and W. Xie

PHENIX

K. Barish
UC Riverside
14 Oct. 2000

Charged Pion Asymmetries

Trigger Requirements:

Jets with high z pions:

- o High EMC Multiplicities at low threshold
- o RICH hit

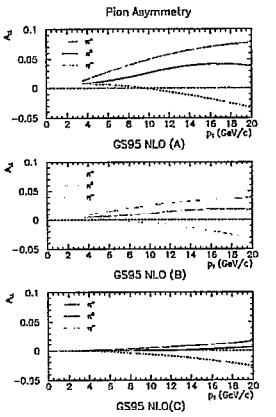

Simulations performed by Y. Goto

PHENIX

K. Barish
UC Riverside
14 Oct. 2000

Transversity Measurement

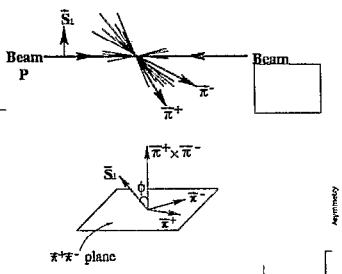

Trigger Requirements:

Jets with high z pions:

- o High EMC Multiplicities at low threshold
- o RICH hit

Projected Asymmetry

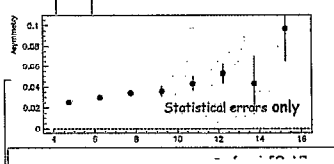

Talk by M. Grosse Perdekamp

PHENIX

K. Barish
UC Riverside
7 Oct. 2000

Trigger on Muons

- **Required rejection factors:**

$\sqrt{s}$ (GeV)	$\mathcal{L}$ ($cm^{-2}s^{-1}$)	σ (mb)	Rate (Hz)	Rejection Factor Required
200	8×10^{31}	50	4×10^{6}	320
500	2×10^{32}	60	12×10^{6}	960
500	7×10^{32}	60	42×10^{6}	3360

- **Estimated rejection factors:**

Depth	Width ±	Logical OR	Triggers/ Number Events	Rejection Factor
5	2,2,2,2	No	185/59960	1020
5	2,2,2,2	Yes	194/59960	975

PHENIX

K. Barish
UC Riverside
14 Oct. 2000

Single μ

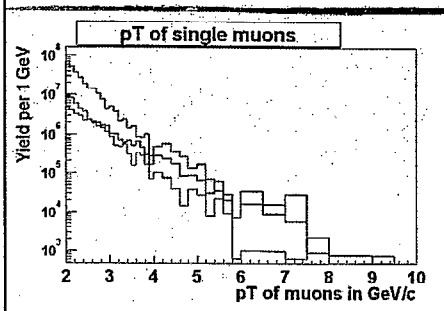

p_T^{min}	2GeV/c	4GeV/c	6GeV/c
charm	4×10^{6}	6×10^{4}	2×10^{3}
δA_{LL}	10^{-3}	0.01	0.05
bottom	4×10^{6}	2×10^{5}	2×10^{4}
δA_{LL}	10^{-3}	4×10^{-3}	0.015

PHENIX

K. Barish
UC Riverside
14 Oct. 2000

Flavor Decomposition by W

Muon with p_T>20 GeV/c dominated by W

	W^-	W^+
acceptance for muon w/ $p_T > 20$ GeV/c	14%	4%
yield (both muon arms)	5100	5600
ΔA_L (statistical only)	2%	2%
rapidity average	0.78±0.34	0.71±0.41
background from Z-decay	1095(21.5%)	984(17.6%)

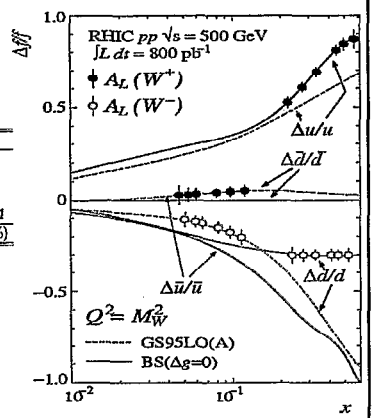

K. Barish
UC Riverside
14 Oct. 2000

Conclusions

This is a very exciting time
- » Year 2000 Heavy-ion run smashing success
- » Central arm tracking electrons will be complete for 2001 Spin run
- » South μ arm currently being installed
- » Trigger system undergoing upgrade for spin physics
- » Remaining spin-specific detector/software issues will be addressed

PHENIX will be ready to take advantage of the Year-2001 polarized proton run
- » Expect to make ΔG measurement in π^0 channel

K. Barish
UC Riverside
14 Oct. 2000

The STAR Level-3 Trigger System - Year 0 Experiences

Jens Soeren Lange (Frankfurt University)

Abstract

The level-3 trigger system at the STAR experiment performs full online event reconstruction for Au+Au and p+p collisions at RHIC, using processor farms of 432 Intel i960 processors for xyz hit determination and 12 (later 48) ALPHA processors for track finding. Moreover, the system provides a hard- ware-accelerated event display, which has been used about 1.5 million STAR events in 3 months data taking. As a preliminary benchmark, high multiplicity central Au+Au events (130.000 hits, 6000 tracks) could be reconstructed in t<160 ms (including online dE/dx). For the next years, several trigger on rare events are proposed, such as heavy fragments (e.g. anti-alpha), high-pT hadrons (hard scattering) or lepton pair production (J/ψ e^+e^- and Π e^+e^-).

The STAR Level-3 Trigger Year-0 Experiences

Jens Sören Lange
(Frankfurt University)
for the STAR L3 group

- What is L3 ?
- Year-0 experiences

  - L3 cluster finder
  - L3 track finder
  - "real" Year-0 L3 Triggers
    - z vertex in central Au+Au,
    - cosmic reject for peripheral Au+Au

  - some L3 events:
    pile-up, beam-pipe interactions, jets ...

- Year-1 prospects
  (what about L3 + pp/spin ?)

  - L3 + EMC
  - pile-up filter (raw data reduction)

STAR L3 Group

Clemens Adler, Jens Berger, Thomas Dietel, Dominik Flierl, Jens Sören Lange, Reinhard Stock, Christof Struck

Univ. Frankfurt

Pablo Yepes, Martin DeMello

Rice Univ., Houston, Texas

Tonko Llubicic, Jeff Landgraf, Mike LeVine

BNL DAQ group

John Nelson

Univ. Birmingham

Jan Balewski

Univ. Indiana

Dieter Röhrich, Anders Vestbo

Univ. Bergen

Aya Ishihara, Joe Schambach

Univ. Austin, Texas

What is L3 ?

- existing DAQ CPUs for (online) cluster finder
- fast CPUs

  ALPHA 466 MHz
  (faster than same clock Pentium factor ~1.7)

  12 + 12 + 12 + 1

- fast network

  MYRINET

  transfer rate (12 x sl3 -> gl3)
  R≤ 74 MB/s (32 bit)
  R≤ 90 MB/s (64 bit)
  for Au+Au track data, for p+p hit+track data

  12+12+12+2 PCI adapters (ALPHA)
  12 PMC adapters (VME)

  different from GB eth:
  data transfers = DMA (background)
  (CPU usage <12%, free for track finder)

Experiences in Year 0

- 1st test in 03/00: find cosmics in L0 random ✓
- L3 running permanently for event display
  42" plasma screen, 3 months, ~1.500.000 events

L3 Cluster Finder

- **CPU:** 432 x Intel i960 / VxWorks
  (existing DAQ mezzanines)
- fast **algorithm:**

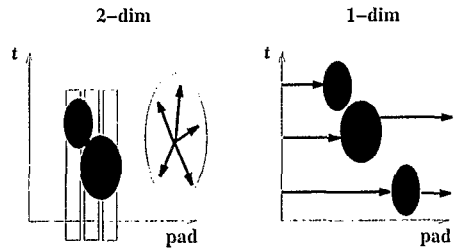

> deconvolution ON (CPU time Δt+=6%)

- **timing:** t=17-32 ms / ~130.000 cluster

Experiences in Year 0

L3 Track Finder

- **CPU:** 12(36) x ALPHA 466 MHz / Linux
- **algorithm:** conformal map NIM A 380(1996)582
- vertex-constraint
  conformal space **yes**, real space **no**
  (-> find all secondaries)
- **timing:**

  t=130 ms (Au+Au central, 2 TPC sectors)

- straight tracks OK (see B=0 events at γ_{beam}=30)
- dE/dx truncated mean (t=8 ms VENUS)
  straight line approx. across pad
- floating point exception (tan λ>1) "blocked"
  > no DAQ crash
- $\Delta p_T/p_T$~7% (FWHM) @ p_T=500 MeV/c
  Year 0 magnet @ half field B=0.25 T
  less curvature, shorter track length, more ExB distortion
  rule of thumb: $\Delta p_T/p_T$ ~ factor 2.
- ALPHA temperature goes up ΔT=3 K
- ALPHAs survive power dips
  (e.g. thunderstorm 09/02, 13:32, RHIC outage)

Experiences in Year 0 cont'd

Global L3

- **timing** (Au+Au central)

  t=13 ms
  t=23 ms + track ID assign to cluster
  t=44 ms + fill histo
  t=129 ms + track merging
  t=155 ms + helix extrapolation to DCA

- **Application #1: z vertex trigger (central events in TPC center)**

  R_{input} ~ 8-12 Hz @ ZDC rate 75-140 Hz
  L3 yes/no: $|z_{vertex}| < 80$ cm
  rejection factor ~2
  ~ 3 days, ~ 100k events

- **Application #2: xyz vertex + nTrack trigger (cosmic reject for peripheral Au+Au)**

  $R_{input} \leq 50$ Hz (topological L0, no ZDC)
  L3 yes/no:
  x_{vertex}, $y_{vertex} \leq 15$ cm, $z_{vertex} \leq 2$ m, $N_{track} \leq 100$
  rejection factor ~20
  ~ few hours, ~ 20k events

- **pp pile-up filter**
  TPC 40 μs drift @ high luminosity pp:
  $\sqrt{s}$=500 GeV, ~700 bunch X, N_{track}~2000

  idea: don't tape ADC raw data of unwanted tracks
  (z_{DCA} cut, helix -> EMC match)
  filter: developed + MC tested (J. Balewski)
  technical implementation:
  difficult, requires *backward* mapping
  (track -> hits -> clusters -> all ADC values)
  estimate 1 man•year
  easier solution:
  don't tape L3 hits of unwanted tracks (on gl3)
  (i.e. don't tape any ADC raw data at all)

  but: are L3 hits good enough ?

  > hit comparison L3 vs. offline (>70% hits Δz<200 μm)
  > L3 hit "gap" @ z=0 sensitive to wheather

L3 and pp/spin ?

- **L3+RICH**
  L3 helix extrapolation ✓ (RICH online event display)
- **L3+SVT** (work in progress)
  different L3 cluster finder (bi-polar in *t* direction)
- **L3+EMC** = extra L3 tasks/CPUs
  - EMC cluster finder (but only N_{hit}^{EMC}~30/event)
  - z_{DCA}
  - helix extrapolation TPC track -> EMC surface
- **L3+L0+TPC**

  i.e. what happened on 09/03 ?
  (Dave Underwood's email to starspin)

  - Au+Au central, typical L0 R~4 Hz
  - begin of spill, L3 z vertex cut switched on
  - if L3 no > event not taped
  - DAQ busy released earlier
  - next L0 earlier (rejection factor ~2, L0 R~8 Hz)
  - gating grid opens more frequently
  - TPC charge goes up ~ factor 5
  - TPC experts (already) worried
    (space charge, anode aging)

  > What about higher L0 rates for spin/pp ?

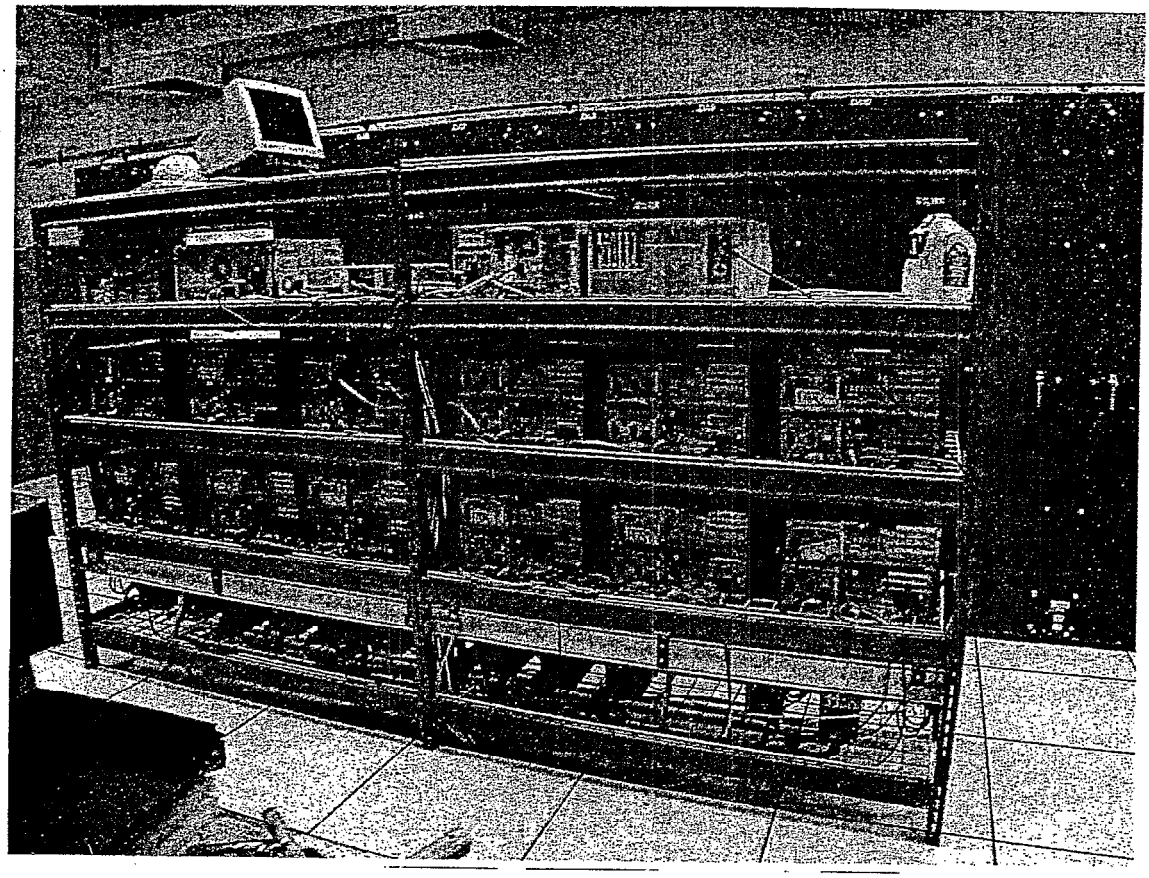

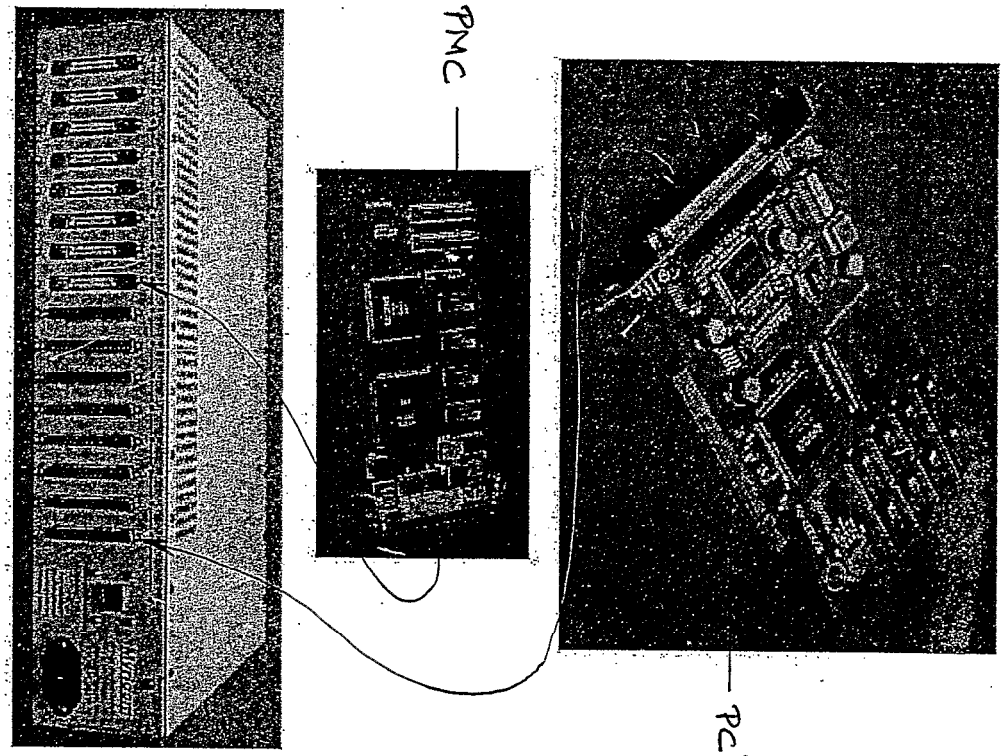
PMC
PCI
MYRINET

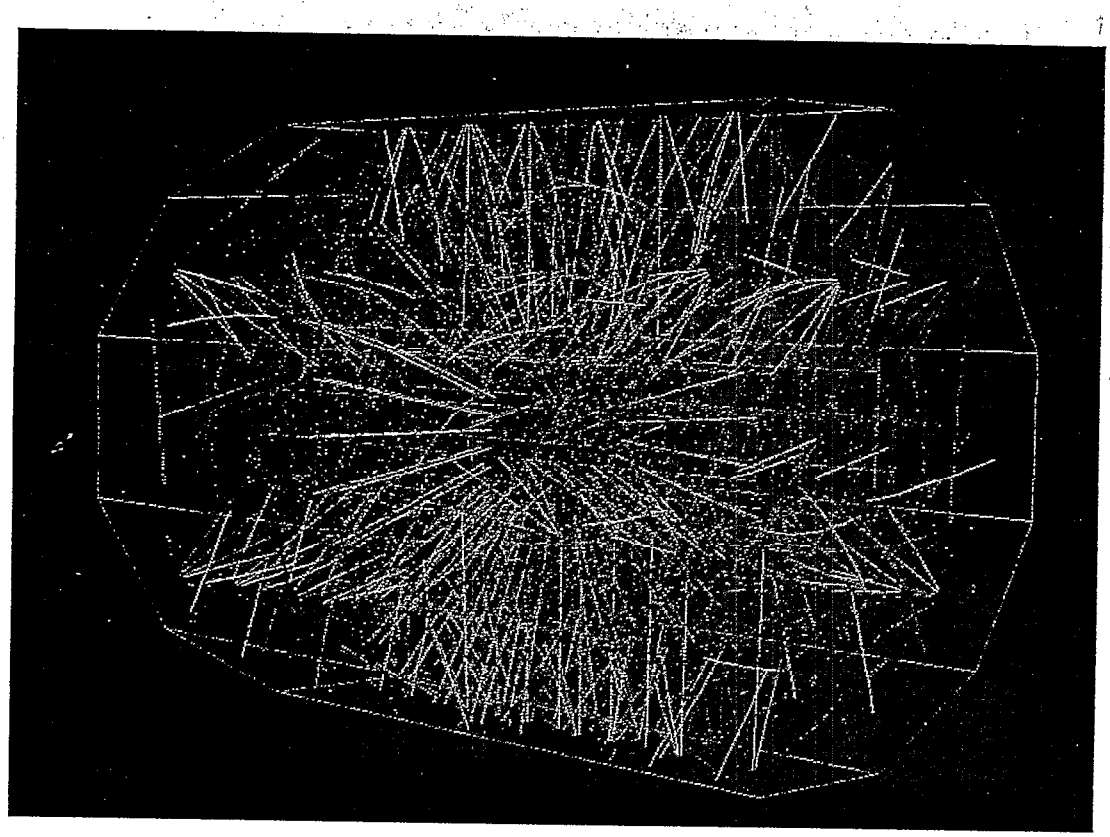

STAR LEVEL-2 LASER

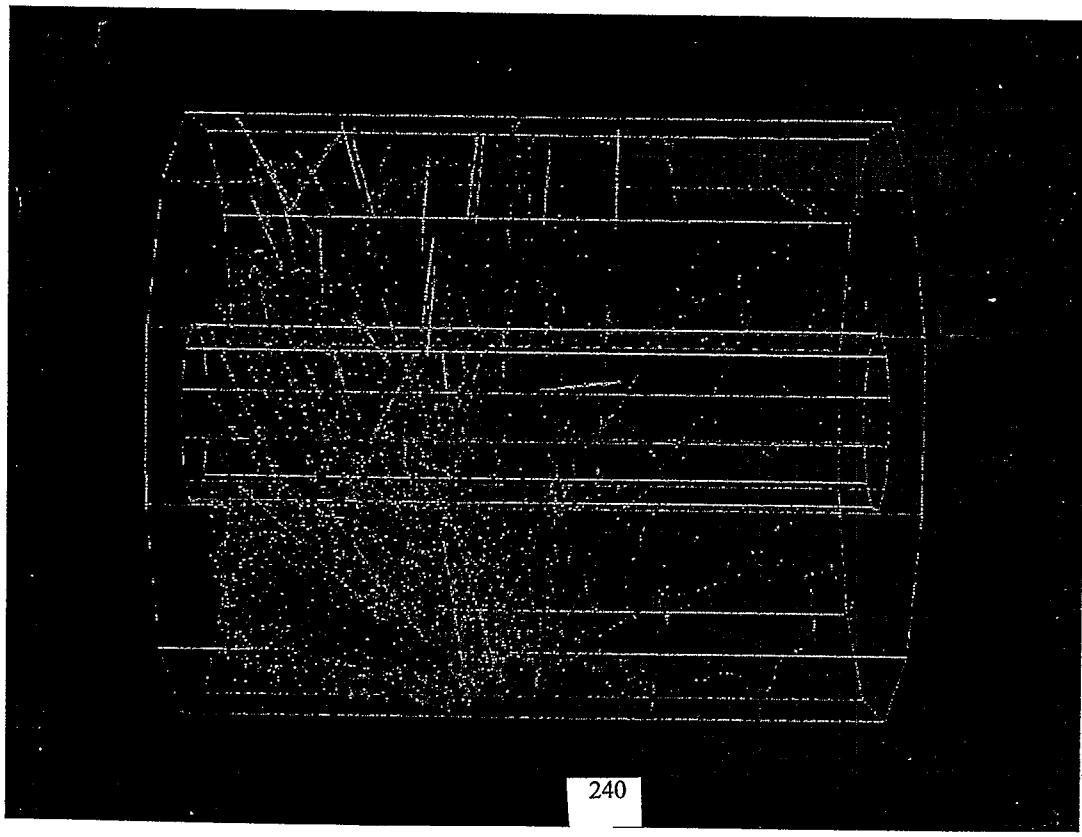

STAR LEVEL-3 COSMIC, LØ HIGH MULTIPLICITY

Trigger on Event Vertex Pos

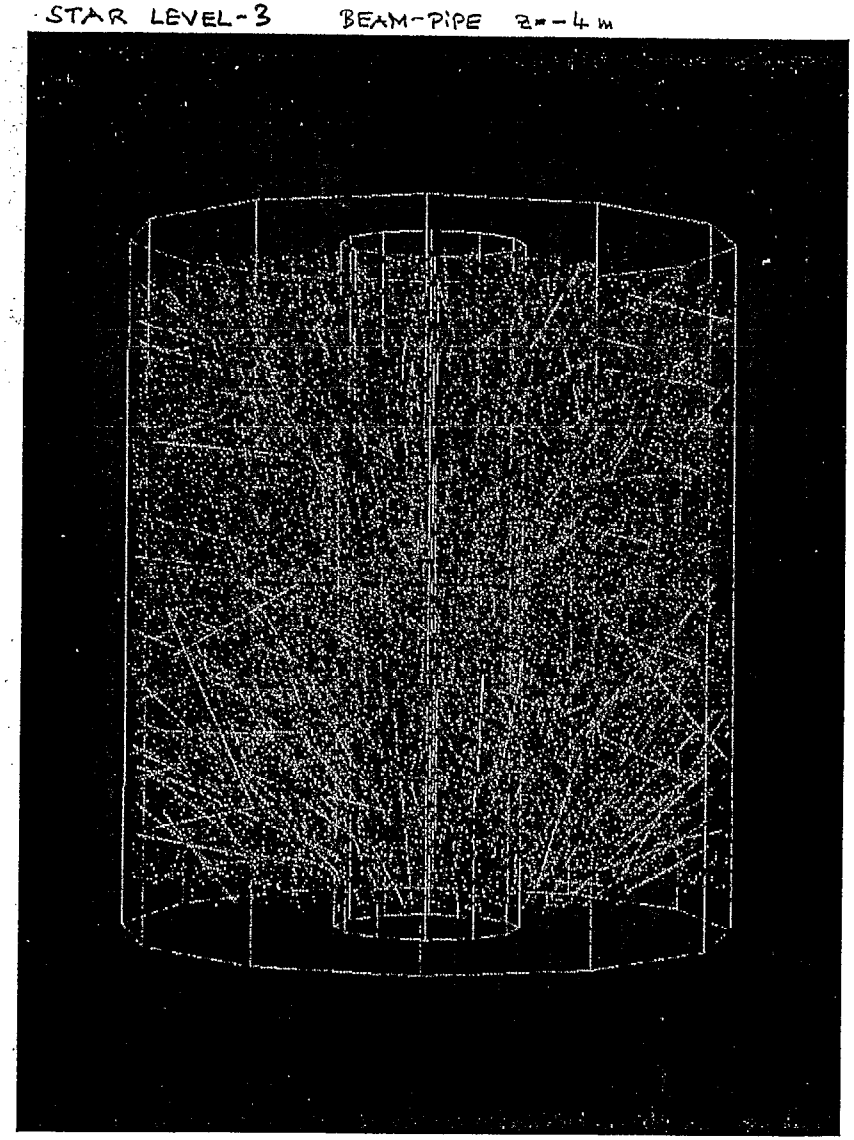

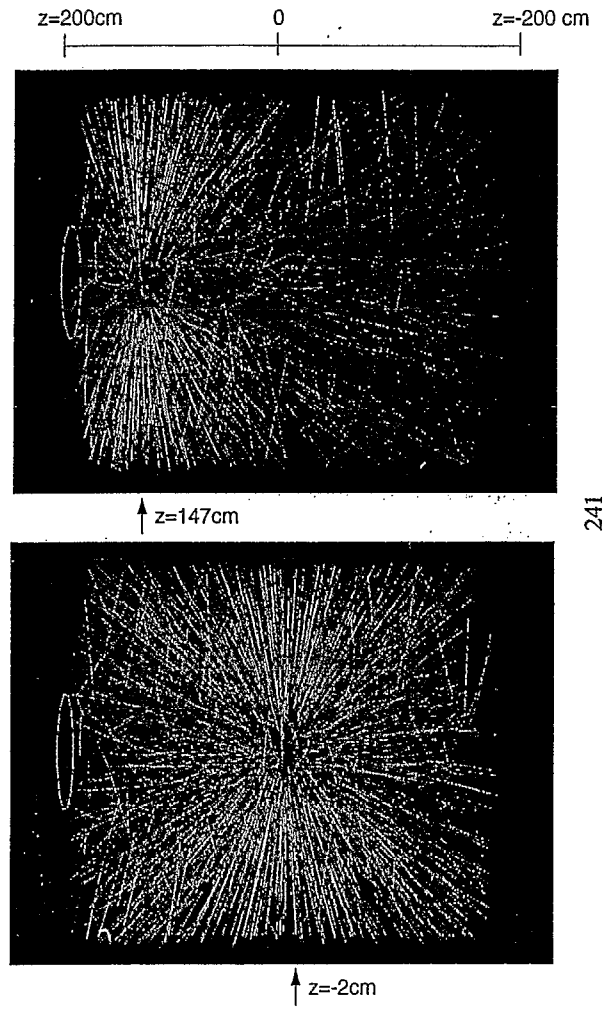

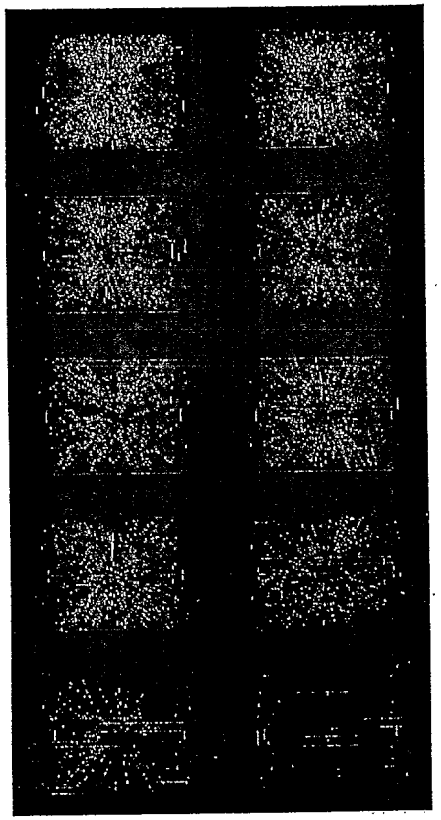

$|z| \leq 5$ cm

STAR LEVEL-3 FAKE (0,0,0) TRACKS (η/φ SLICES)

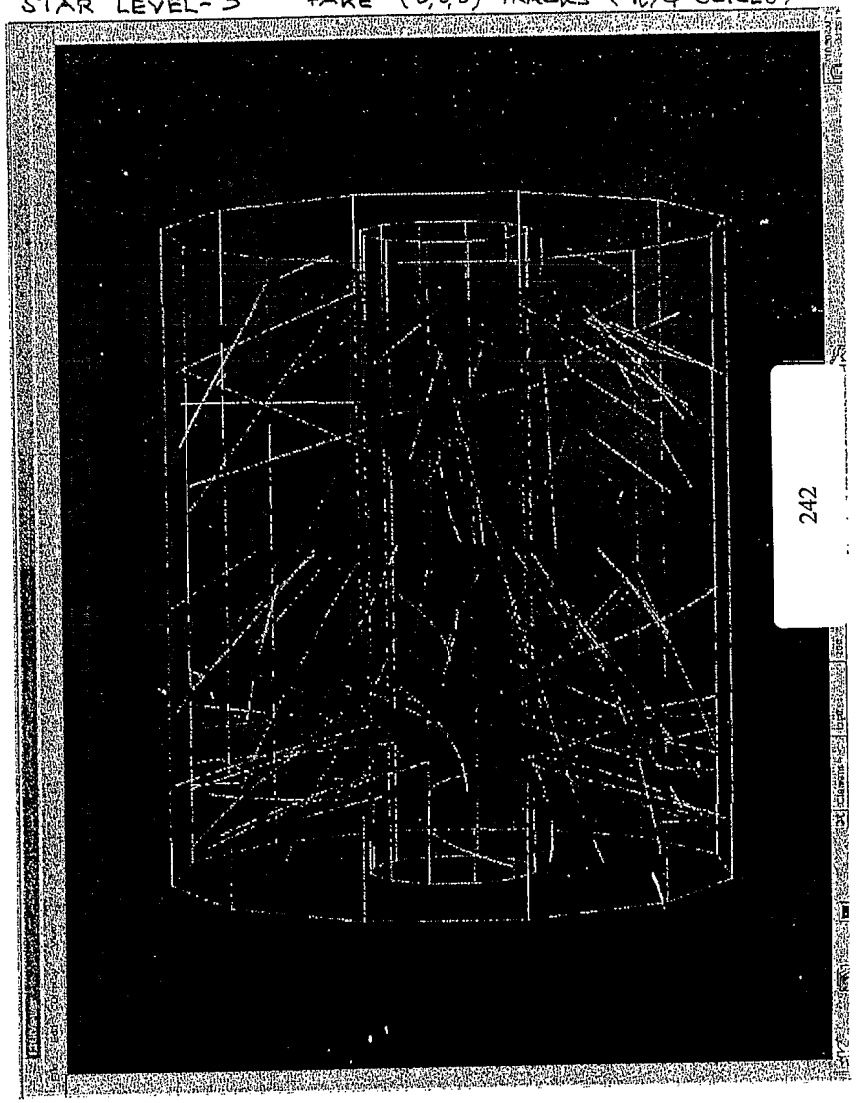

L3 Tracks

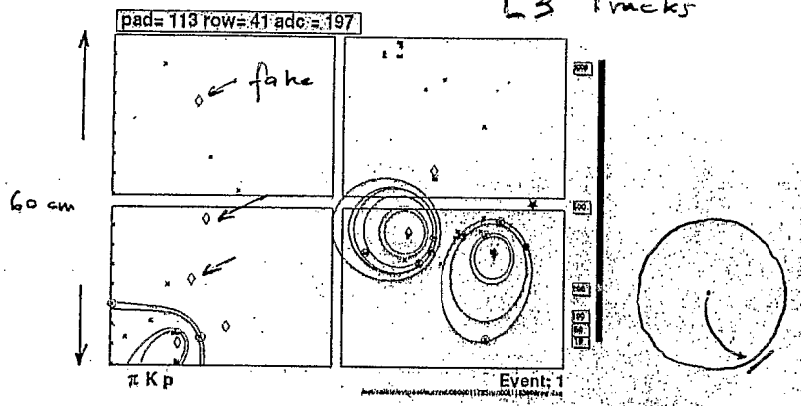

RICH Online (Jon Gans, Jamie Dunlop)
Helix extrapolation

Offline Tracks

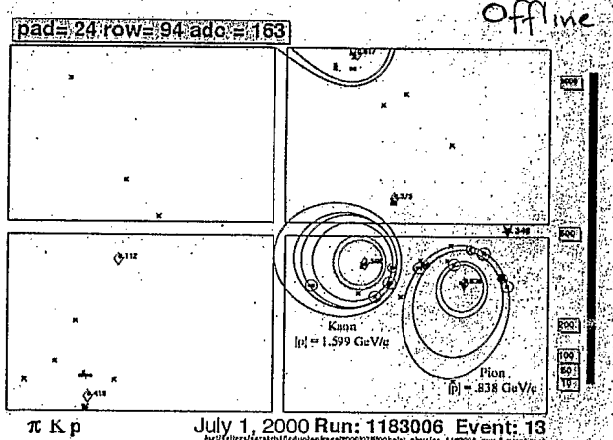

Dominik

L3Clufi versus Tcl

Overall : Tcl clusters in Green and L3Clufi clusters in Blue

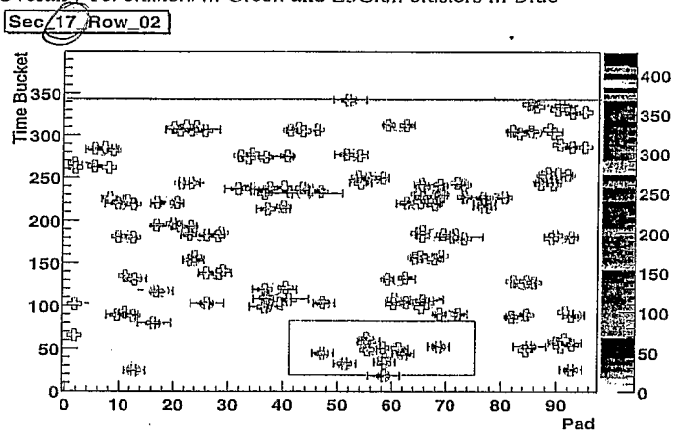

and in more detail :

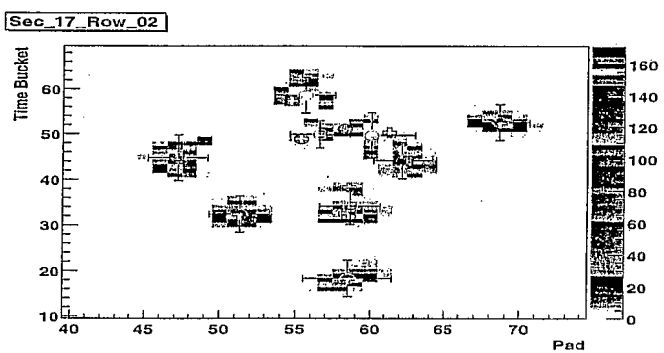

Dominik Flierl, Frankfurt University

Dominik

(offline)

L3-Tcl Matching

Tcl clusters found : 51123
L3Clufi clusters found : 49631
Loop over Tcl clusters and find match in 3 cm spacial distance -> found matches : 89%

deconvolution!

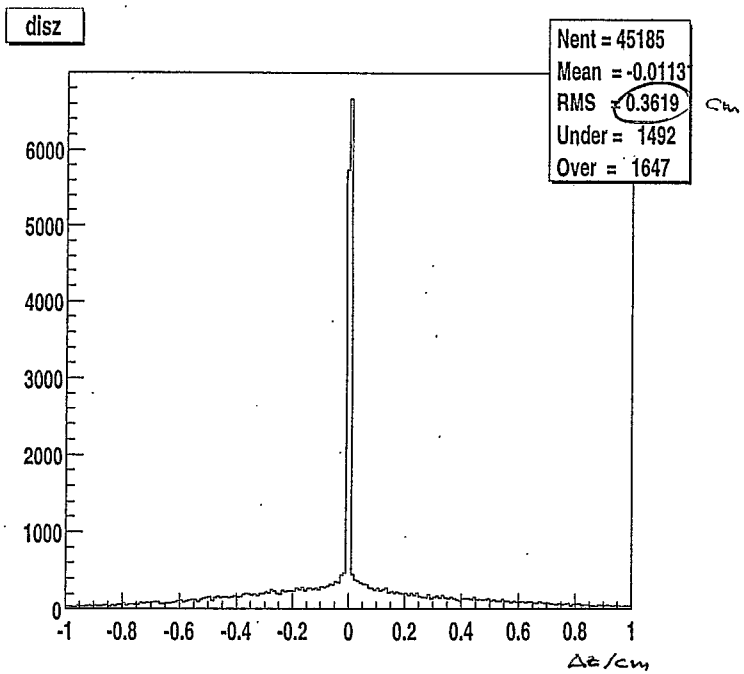

Noisy 13

Since we don't want to die from to much noise

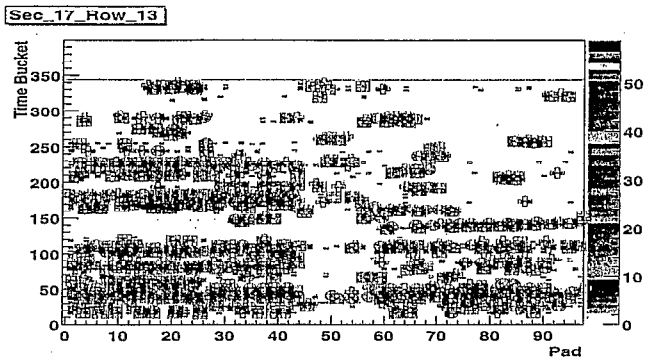

apply minimum charge cut.

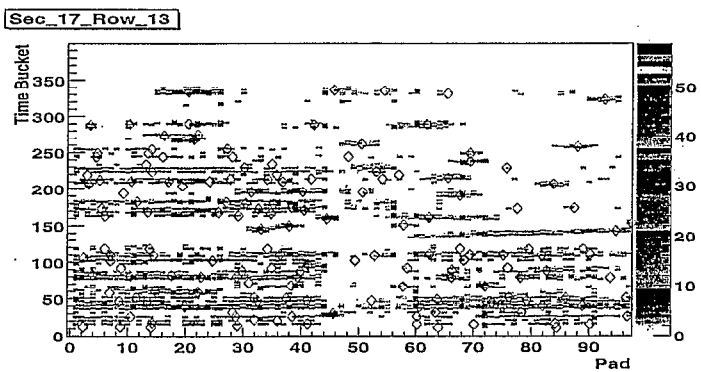

STAR LEVEL-3 Au+Au CENTRAL GAP @ z=0

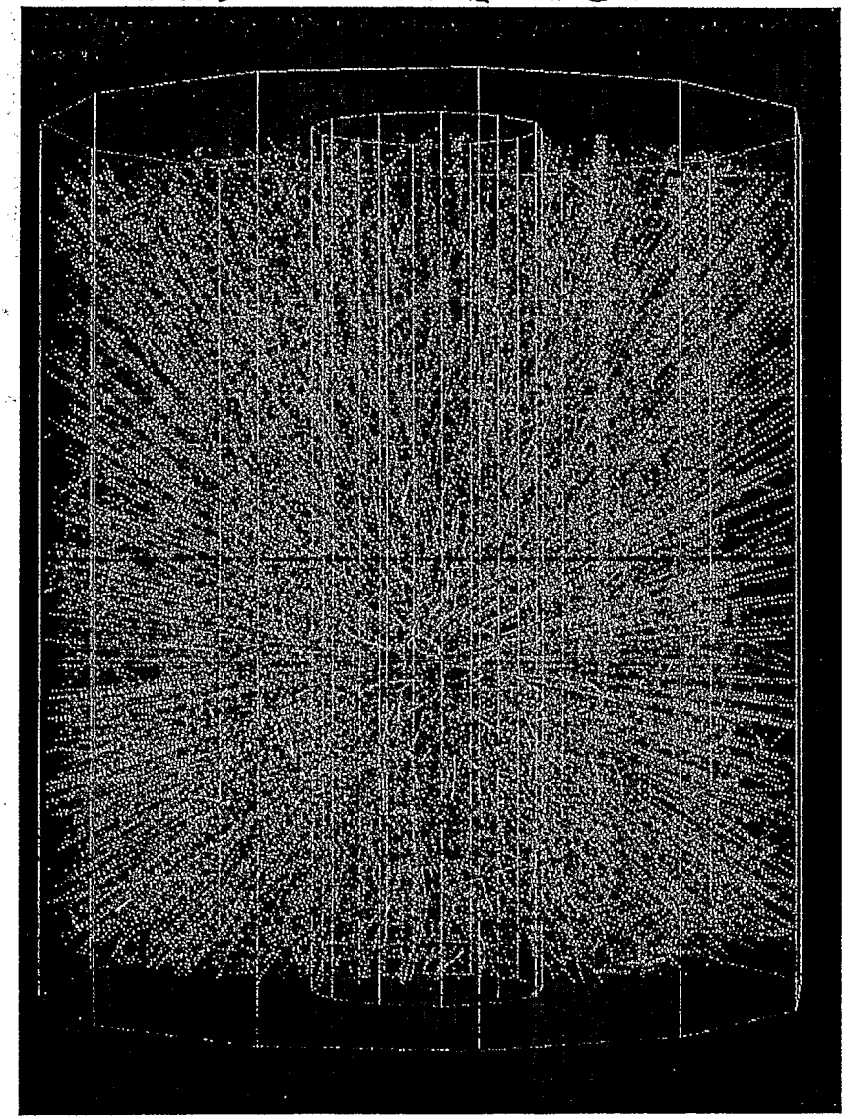

$V_{DRIFT} = 5.5$ cm/μs

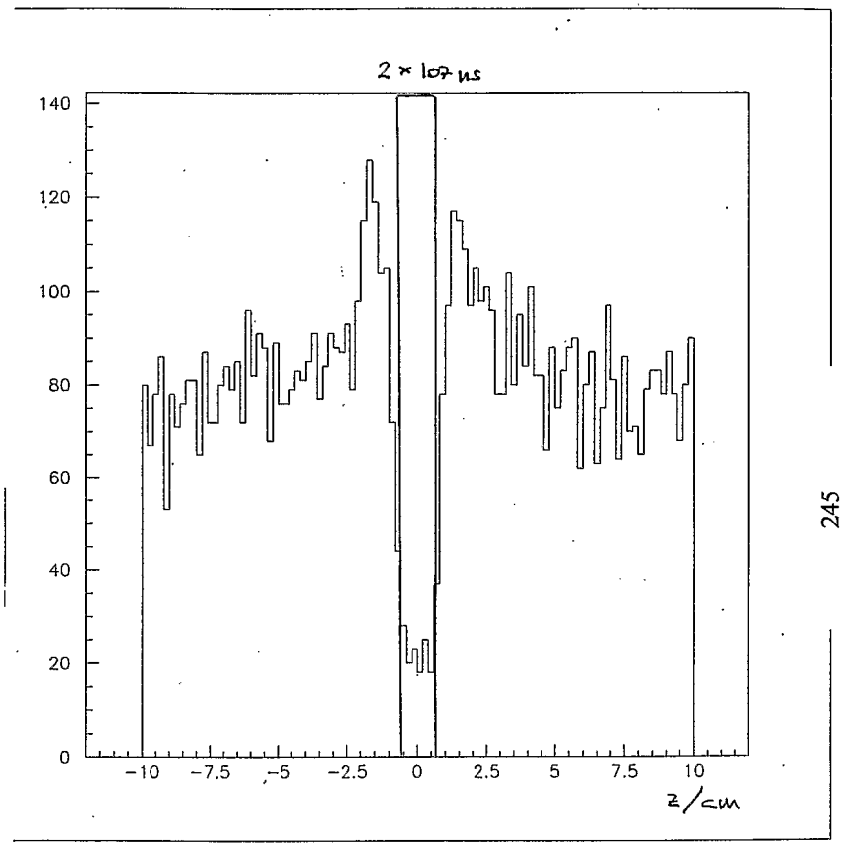

RHIC clock "bunch hop"
August 11, 2000

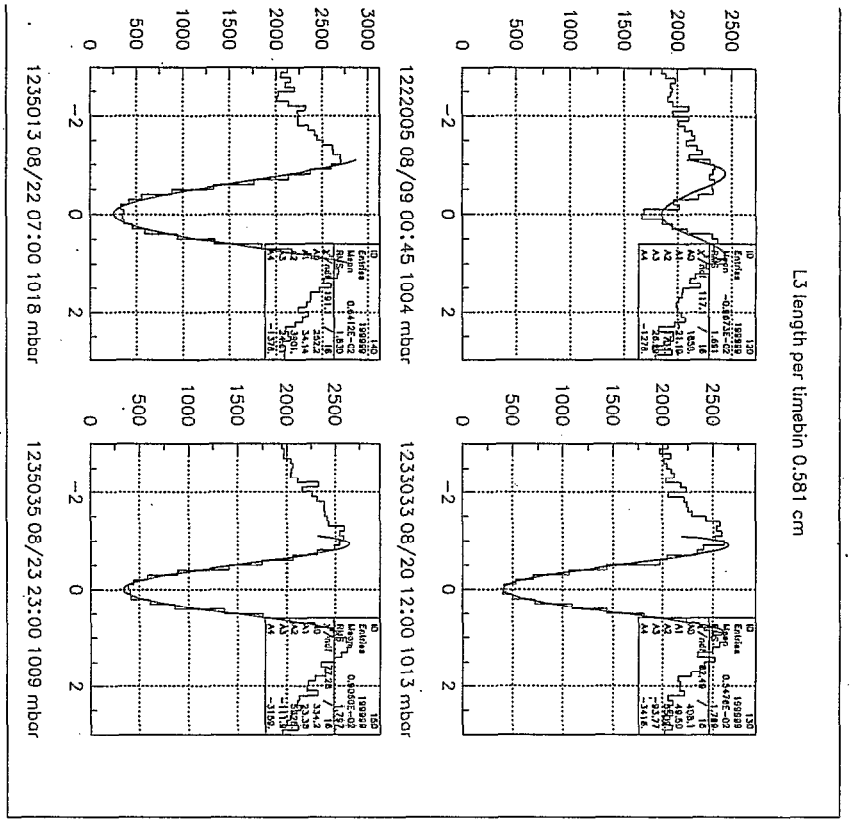

Bill Love, Aleksei Lebedev

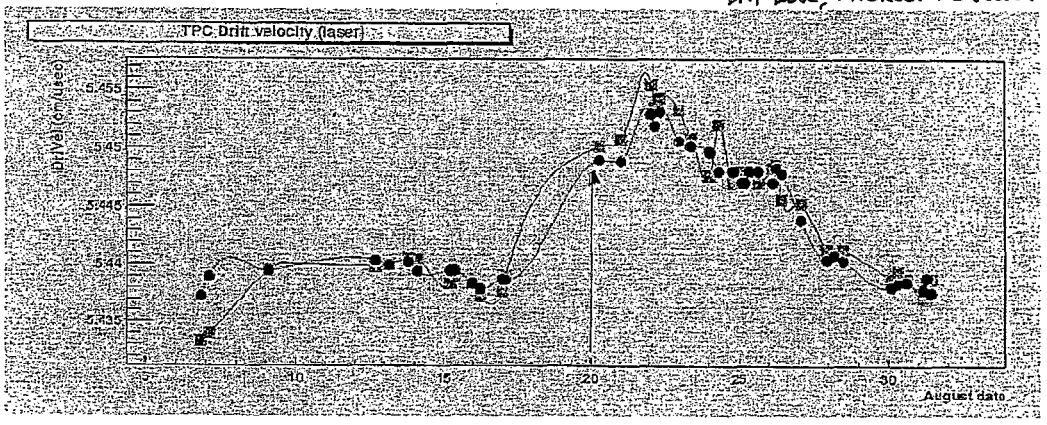

STAR LEVEL-3 Au+Au PERIPHERAL PILE-UP

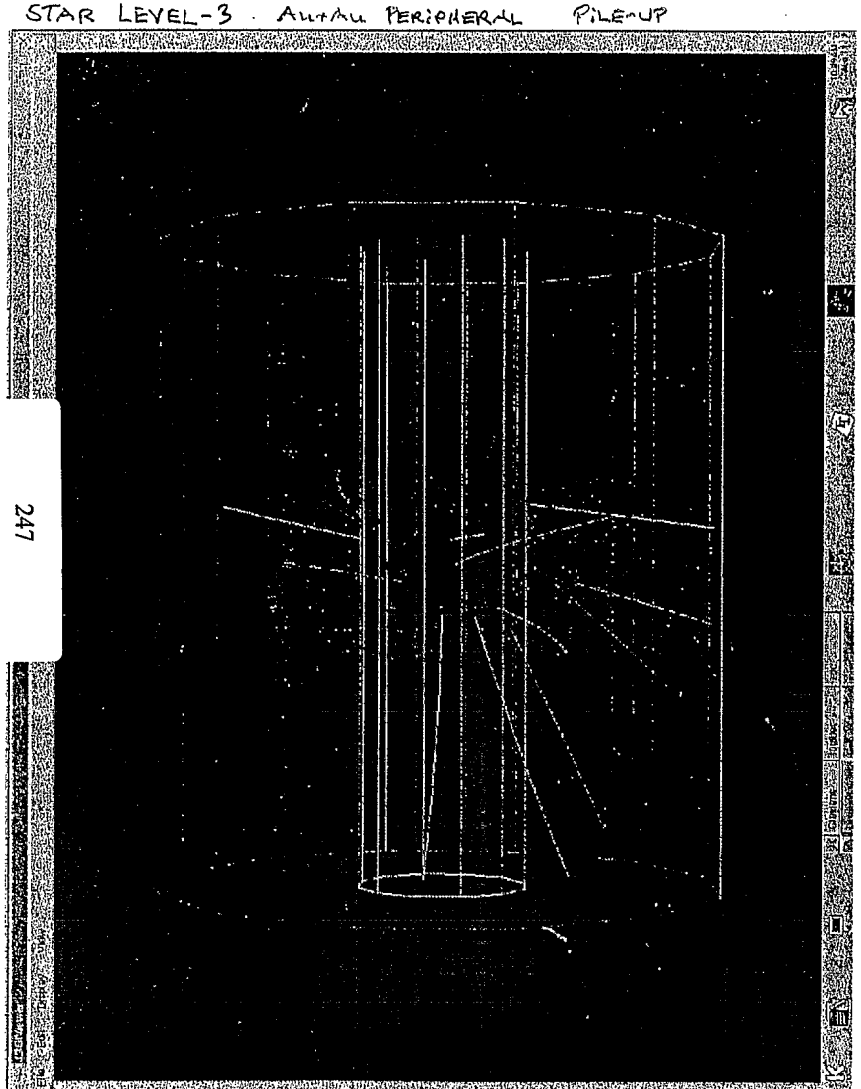

STAR LEVEL-3 Au+Au PERIPHERAL PILE-UP

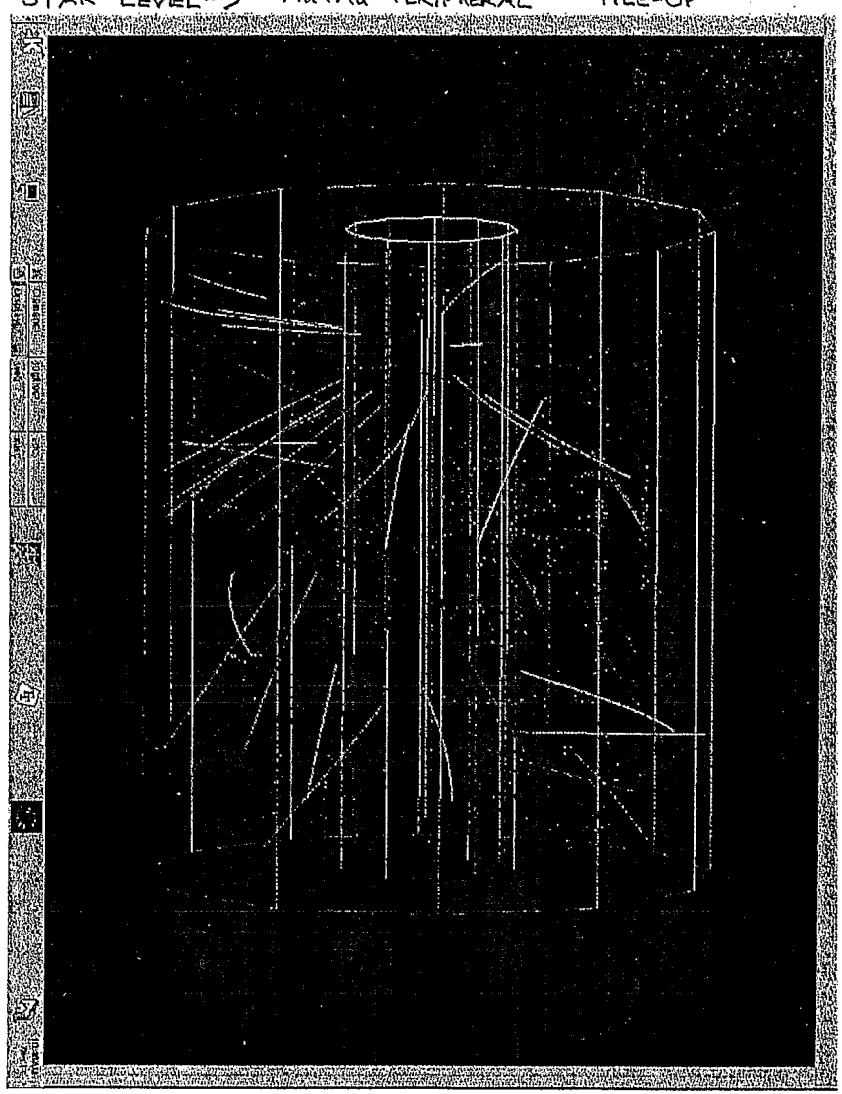

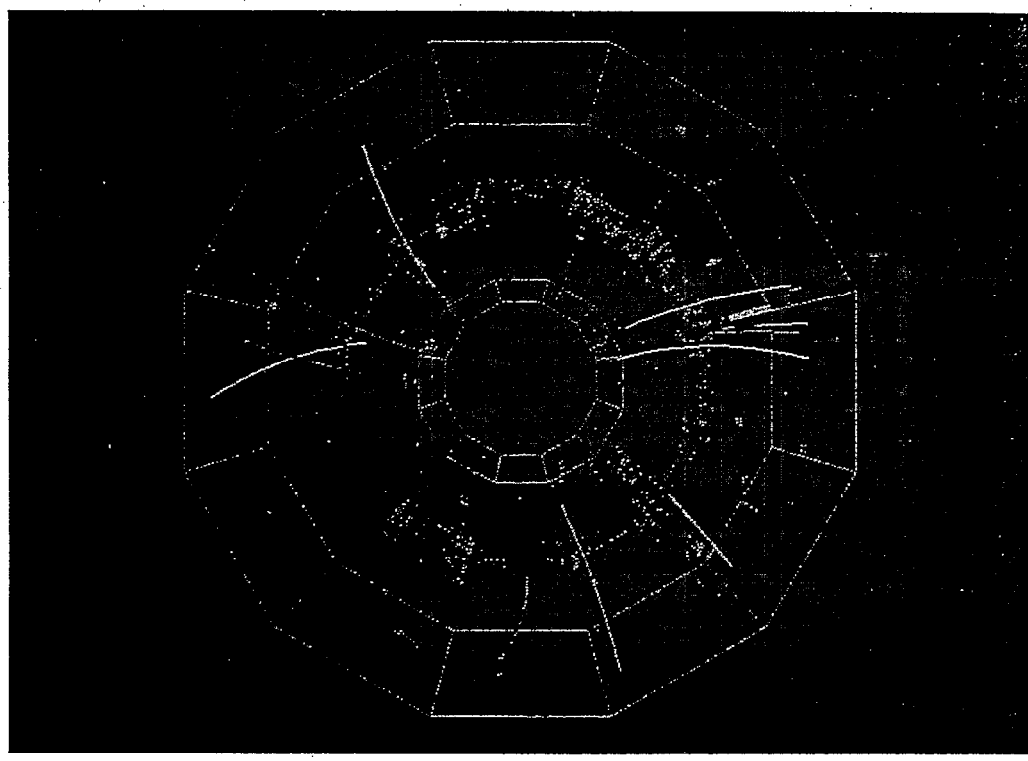

STAR LEVEL-3 Au+Au PERIPHERAL 2 Jet

Short comment

A.Ogawa

Coherent Interactions

Relativistic heavy ions are strong source of fields

$$A + A \rightarrow A + A + X$$

EM field

$$L_{\gamma\gamma} \propto Z^4 = 4 \cdot 10^7 \text{ (Au + Au)}$$

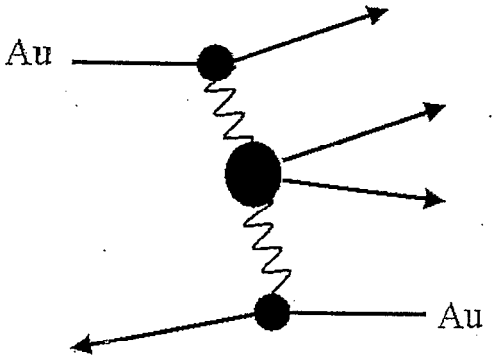

Colorless strong force field (mesons/Pomerons)

$$L_{\gamma(M/P)} \propto Z^2 A^{2 or 4/3}$$

Exclusive reaction
Large Impact parameter

Low multiplicity	= 2, 4 or 6
Low	$p_T < 1/R \approx 30 MeV$
Energy	$E_\gamma^{Max} < \gamma / R \approx 3 GeV$

Summer 2000 STAR trigger

L0 : Look at CTB/ZDC at every bunch crossing ~ 9M Hz
CTB worked fine — resolution down to 1 MIP
Flexible DSM — Topological cuts/coincidence/vetoing

CTB North-South coincidence with 0< ADC < 4 MIP each — Require back-to-back low multiplicity
CTB Top & Bottom veto — Cut cosmic
Software "discriminator" — Avoid triggering on tail
Close to "Jet trigger without EMC" for early spin runs

L1/2 : Abort events before/during TPC digitization — Not yet implemented
L2.5 (abort after TPC digitization) has been tested

L3: Full track reconstruction, vertex finding & more
Tracks go closer than 10cm to beam — Cut cosmic
Tracks go cross beam at |z| < 2m — Cut beam-gas
of "good" tracks < 15 — Cut beam-gas/pile ups

Trigger Detectors

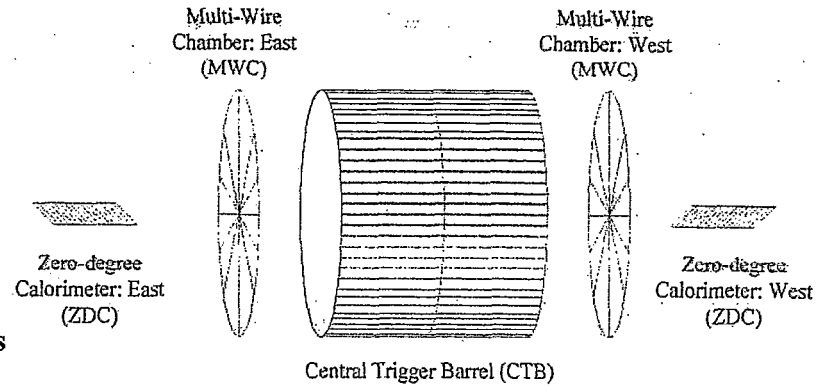

Level 0 Analysis

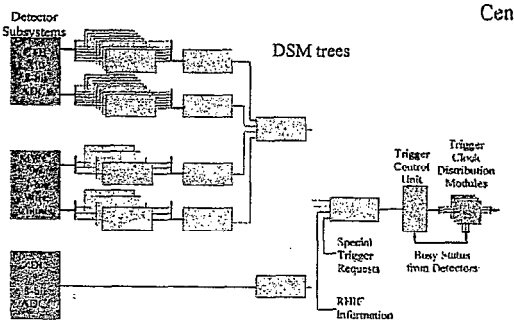

EMC will be in the same tree once instaled

Overlapped (pile up) AuAu high multiplicity event on top of triggered low multiplicity event from summer 2000 run

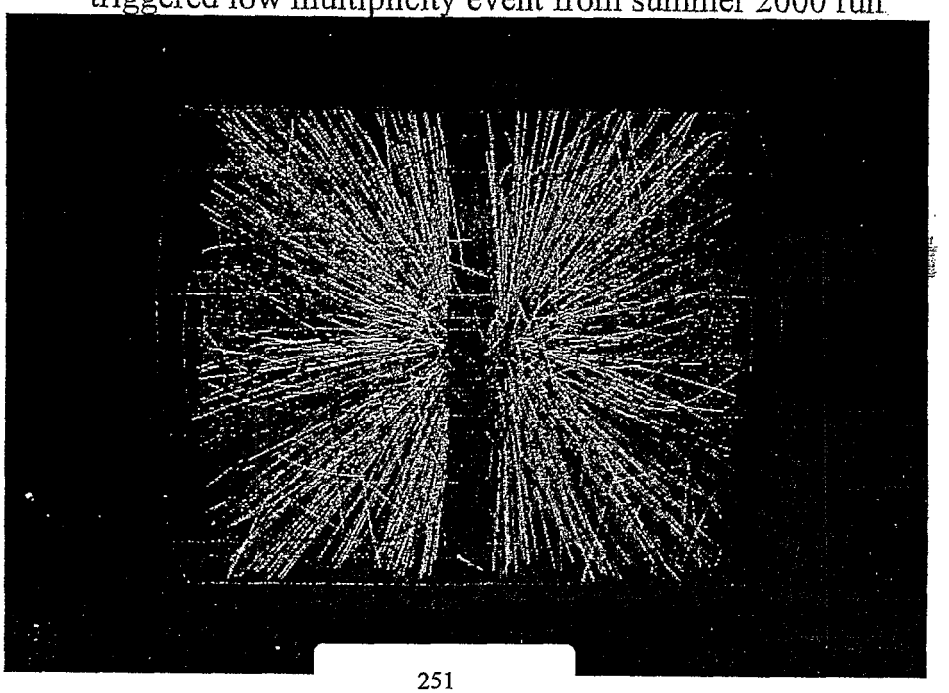

$Au + Au \rightarrow Au + Au + \rho^0$
event candidate
taken 2000 summer
(rate stress test)

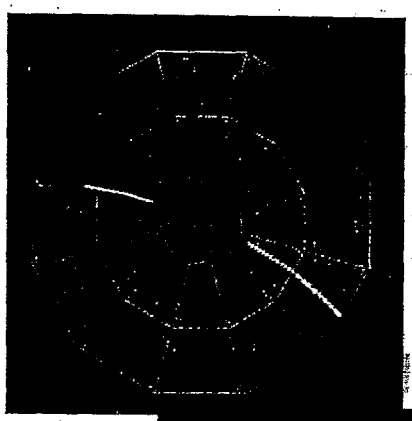

Pt=25MeV
m=716MeV

L0-DAQ worked >50Hz
Topological L0 trigger
(CTB North South coincidence
+ multiplicity cut)
20~30Hz

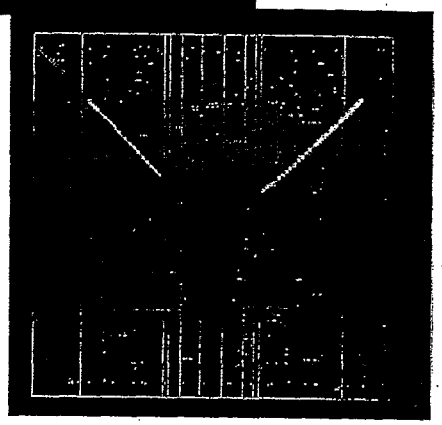

Trigger -DAQ - tape(HPSS) worked at
~ 30Hz

L3 reconstructed tracks
(for low multiplicity events) at >50Hz
L3 reduction to
~ 2Hz

Short comment

H.spinka

1) Calibrate the AGS polarimeter at several energies
$G\gamma$ = 7.5, 13.5, 24.5, (30.5?), 41.5, 46.5
Need to record ADC, TDC values for many events to estimate backgrounds

2) Determine ε(fishline)/ε(carbon) at a couple energies
$G\gamma$ = 7.5, 24.5, (41.5?), 46.5
Alternate fishline, carbon runs - many runs
Look for systematic effects

3) Map out asymmetry vs. beam position in the AGS
$G\gamma$ = 7.5, 46.5 especially
Polarimeter response vs position, P_{beam} vs position

4) Install and run CNI polarimeter in the AGS
Cross check previous measurements (Mar 1999)

5) Get a good measurement (>5σ) in the RHIC "elastic" polarimeter Cross check RHIC polarization from CI

6) Calibrate the RHIC CNI polarimeter (100, ... 250 GeV/c)
Must make ramp up/ramp down procedure work
measure after injection
accelerate
measure at 100 GeV/c etc
decelerate to injection energy
measure again
This 5 step procedure will need to be done MANY times to get good statistical errors

H. SPINKA 14 OCT 2000

Polarized Jet Target for Absolute Measurement of RHIC Proton Beam Polarization

T. Wise for the RHIC Jet Polarimeter Group (University of Wisconsin, USA)

Abstract

We will discuss the design of a polarized atomic hydrogen jet target, combined with a polarimeter ("Breit-Rabi" polarimeter, BRP) that will measure the nuclear polarization of the atomic jet to 2% or better. This target is to be used for an absolute polarization measurement of the RHIC proton beams. This absolute measurement can be used in turn to calibrate a secondary polarimeter reaction. The status of the design work of the atomic-beam source (ABS) and the BRP will be presented

ABSOLUTE POLARIMETER FOR RHIC

T. Wise U. of Wisconsin

* PROJECT IN EARLY STAGES OF DEVELOPMENT

* POSSIBLE MAJOR CONTRIBUTING INSTITUTIONS

	# OF PHYSICISTS(?)
UNIVERSITY of WISCONSIN	2
INDIANA UNIVERSITY -- IUCF	1-2
MIT -- BATES	1
V. U. AMSTERDAM	1
BNL --ACCELERATOR DIVISION	>2

* NO FORMAL COMMITMENTS HAVE BEEN MADE AT THIS TIME

PROPOSED METHOD

- USE RHIC PROTONS ON $\vec{H}$ JET TARGET

- OBSERVE LOW ENERGY ELASTIC RECOILS NEAR 90º IN LAB WITH **VERTICAL** TARGET AND **VERTICAL** BEAM POLARIZATION

- REACTION CROSS-SECTION,

Same A_y

$$\sigma_0(\theta)\{1 + P_y A_y(\theta)\cos\phi + Q_y A_y(\theta)\cos\phi + (A_{xx}(\theta)\sin^2\phi + A_{yy}(\theta)\cos^2\phi)P_y Q_y\}$$

σ_0	unpolarized cross-section
$A_y(\theta)$	analyzing power
P_y	beam polarization
Q_y	target polarization
$A_{xx}(\theta)$ $A_{yy}(\theta)$	spin correlation coefficients

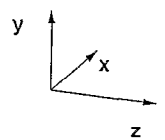

- USE SILICON DETECTORS TO COUNT RECOILS
  - RECOIL ENERGY FROM ~0.5MeV TO SEVERAL MeV.
  - INTEGRATE OVER θ, ϕ ACCEPTANCE OF DETECTORS

$$\sigma_0\{1 + P_y\bar{A}_y + Q_y\bar{A}_y + (\bar{A}_{xx} + \bar{A}_{yy})P_y Q_y\}$$

- WE EXPECT $\bar{A}_y \approx 0.03$ OVER $90º < \theta < 87º$.

BASIC CALIBRATION CONCEPT

$$\sigma_0\{1 + \cancel{P_y\bar{A}_y} + Q_y\bar{A}_y + \cancel{(\bar{A}_{xx} + \bar{A}_{yy})P_yQ_y}\}$$

1) MEASURE TARGET Q_y TO ≈ 2% ABSOLUTE

2) COLLECT DATA WITH UNPOLARIZED BEAM, POLARIZED TARGET (P_y =0, Q_y =±1) TO MEASURE A_y.

$Y_L = It\varepsilon_L\sigma_0\{1 + Q_y\bar{A}_y\}$ yield equation for left detector

$Y_R = \ldots$

3) COLLECT DATA WITH POLARIZED BEAM, UNPOLARIZED TARGET (P_y =±1, Q_y =0)

$Y_L = It\varepsilon_L\sigma_0\{1 + P_y\bar{A}_y\}$ yield equation for left detector

$Y_R = \ldots$

4) USE A_y TO DETERMINE P_y FROM #3.

I = beam current

t = target thickness

ε_L = efficiency of L detector

ACTUAL PROCEDURE

USE ± Q_y AND ± P_y ⇨ 4 POLARIZATION COMBINATIONS AND 8 SILICON YIELDS. IN RAPIDLY ALTERNATING CYCLE

$$Y_{L\uparrow\uparrow} = I_\uparrow t\varepsilon_L\sigma_0\{1 + P_\uparrow\bar{A}_y + Q_\uparrow\bar{A}_y + (\bar{A}_{xx} + \bar{A}_{yy})P_\uparrow Q_\uparrow\}$$

$$Y_{L\uparrow\downarrow} = I_\uparrow t\varepsilon_L\sigma_0\{1 + + P_\uparrow\bar{A}_y + Q_\downarrow\bar{A}_y + (\bar{A}_{xx} + \bar{A}_{yy})P_\uparrow Q_\downarrow\}$$

.

.

.

$$Y_{R\downarrow\downarrow} = I_\downarrow t\varepsilon_R\sigma_0\{1 + P_\downarrow\bar{A}_y + Q_\downarrow\bar{A}_y + (\bar{A}_{xx} + \bar{A}_{yy})P_\downarrow Q_\downarrow\}$$

SIX UNKNOWN TERMS:

A_y	$\varepsilon_L/\varepsilon_R$
$P\uparrow$	$I\uparrow/I\downarrow$
$P\downarrow$	
A_{yy}	

EIGHT EQUATION AND SIX UNKNOWNS.
SOLVE FOR ALL SIX USING METHOD OF DIAGIONAL SCALING

METHOD DESCRIBED IN
H.O. Meyer, Phys. Rev. C 56, 2074 (1997)

DURING DATA TAKING CAN SIMULTANEOUSLY RUN THE CNI CARBON POLARIMETER TO CALIBRATE IT

RATE ESTIMATES

EXPECTED JET THICKNESS 3×10^{11} H/cm^2.

MODERN ABS MAKES > 6×10^{16} ATOMS/S AT THERMAL VELOCITY OF $\sim 2 \times 10^5$ cm/s INTO 1 cm DIAMETER APERTURE

$\sigma_o \approx$ 80 mb
$I \approx$ 50 mA
$\Delta\phi \approx \pm 18°$ (10% of ϕ) } ~35 Hz

2×10^6 counts in 16 hours

$\Delta A_y / A_y \approx 0.02$ if $A_y \approx 0.035$.

OVERALL LAYOUT OF JET TARGET

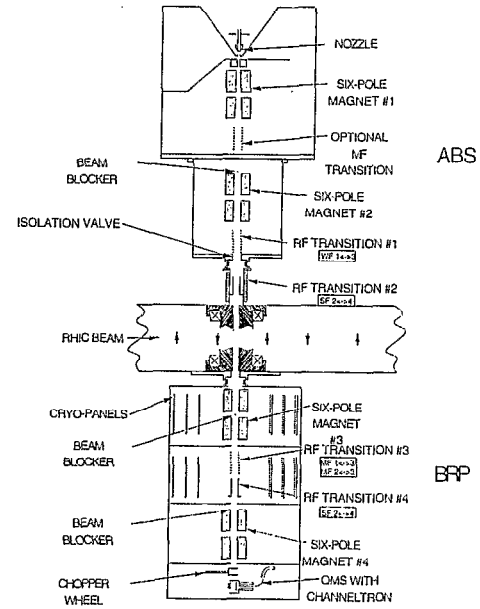

A more detaied proposal for target region follows

In this (HORIZONTAL) view silicon detectors are into and out of page.

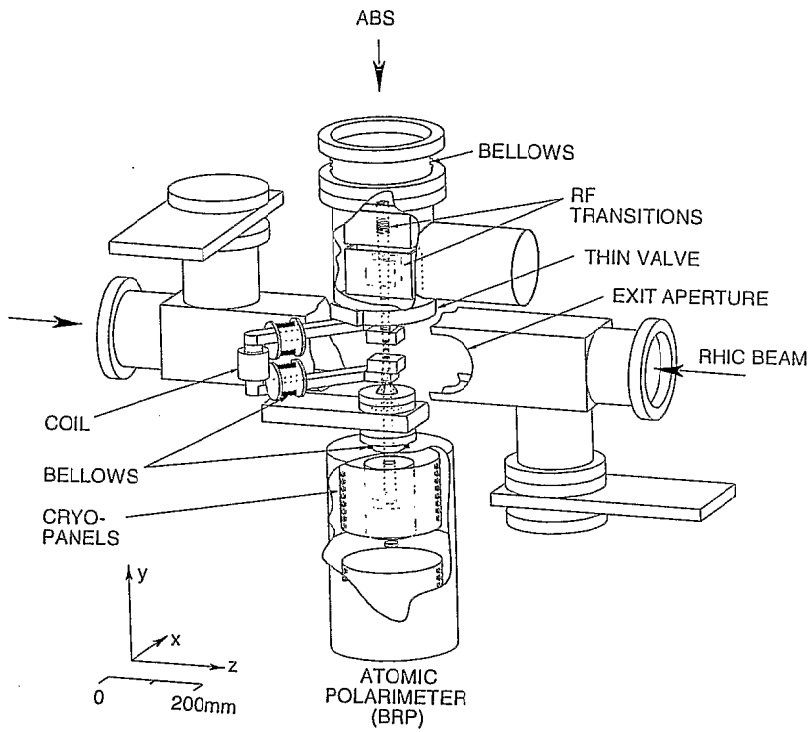

CHAMBER ALLOWS LARGE θ AND ϕ VIEW OF INTERACTION REGION:
±35° IN BOTH θ AND ϕ.

9000 LITER/S (geometric pumping speed)

POLE TIPS CAN RETRACT for unequal species operation of ring.

BEAM - TARGET - DETECTOR INTERACTIONS

1) BUNCH FIELD DEPOLARIZATION OF JET

2) GUIDE FIELD UNIFORMITY REQUIREMENTS

3) DEFLECTION OF LOW ENERGY RECOILS IN GUIDE FIELD

4) BACKGROUND GAS DILUTION OF JET--- FAST PUMPING REQUIRED

5) APERTURE REQUIREMENTS vs MAGNET GAP

6) SMOOTH BEAM PIPE REQUIREMENT

7) WEAK COMPENSATING MAGNET(S) MAY BE NEEDED

8) Beamline baking ⇔ Si detectors

GROUND STATE ATOM ENERGY LEVELS

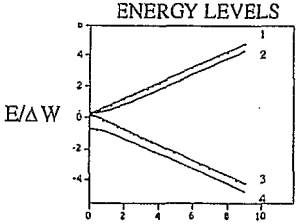

B in units of 50.7 mT

PROTON POLARIZATION

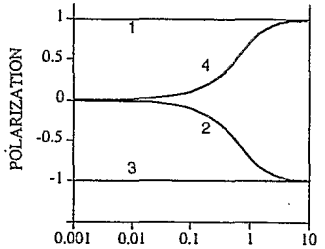

B in units of 50.7 mT

- ATOMIC BEAM SOURCE DELIVERS AN ATOMIC JET IN STATES 1+4 OR STATES 2+3. ALTERNATE RAPIDLY (<100 msec.) BETWEEN THESE CHOICES.

- RHIC BEAM IS BUNCHED AND IS A SOURCE FOR RF IN MULTIPLES OF 10 MHz. (UP TO 1 GHz)

- THIS RF WILL INDUCE TRANSITIONS BETWEEN H ENERGY LEVELS AND DEPOLARIZE THE JET WHEN

$$\Delta E = n * 10 mHz * h$$

BUNCHFIELD RESONANCES

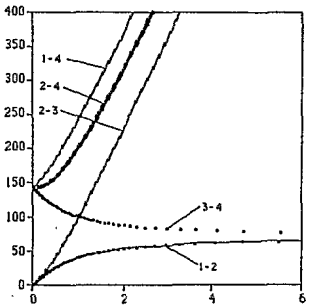

B in units of 50.7 mT

RELATIVE STRENGTH OF HARMONICS

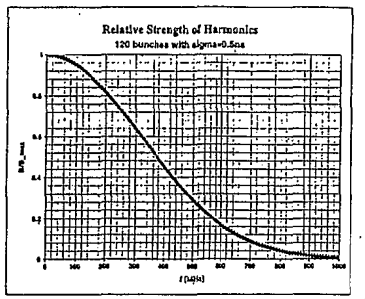

Above by Roser and Mackay, BNL

RESONANCE DETAIL NEAR 100 mT

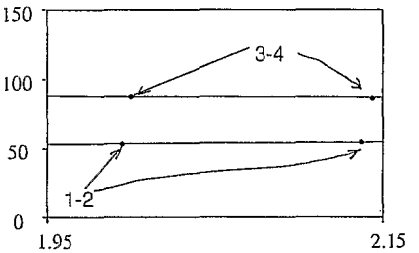

B in units of 50.7 mT

* 1-2 AND 3-4 LOCATIONS "SLIDE" IN OPPOSITE DIRECTIONS DEPENDING ON PRECISE BUNCH FREQUENCY.

* GAP BETWEEN RESONANCES COULD BE 1/2 THAT SHOWN.

* GUIDE FIELD MUST BE UNIFORM TO < 1/4 OF ΔB.

* $\Delta B/B = 6.3 \times 10^{-3}$ at B =0.1T.

VERTICAL JET AND VERTICAL POLARIZATION REQUIRE A 12mm HOLE IN POLE TIPS FOR JET.

CAN BOTH REQUIREMENTS BE MET?

CONSTRUCTED A PHYSICAL MODEL FROM SURPLUS MAGNET

B= 0.1T
GAP = 25MM
HOLE = 11MM
COIL POWER 112 WATTS

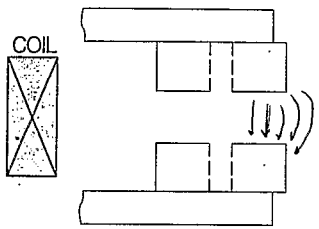

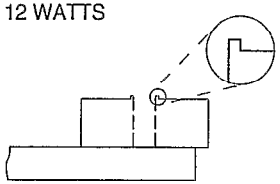

NO CORRECTION

WITH CORRECTION

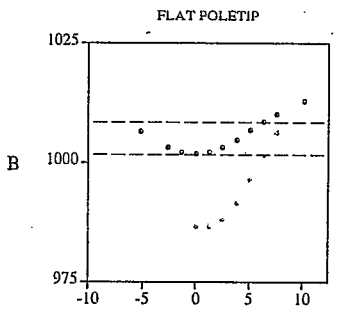

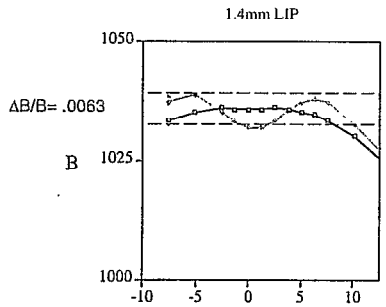

∘ B@x=y=0
• B@x=0,y=±5mm

MAGNET EASILY SCALED TO FULL SIZE

LOW ENERGY RECOIL DEFLECTION

IMPULSE APPROXIMATION

$$\Delta p_z = \int f dt = e \int B dx$$

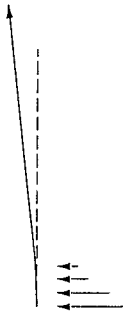

FOR THE PROPOSED MAGNET $\int B dx = 4.2X10^{-3}$ Tmeter

$$\tan\theta = \frac{\Delta p}{p} = \sqrt{e/2mV} \int B dx$$ V in Volts, B in Tesla

ENERGY	TAN θ	ΔZ AT 1 METER
0.3 MeV	0.053	53mm
0.5 MeV	0.041	41mm
5 Mev	0.013	13mm

MEASUREMENT OF JET TARGET POLARIZATION

WITH ATOMIC (BREIT-RABI) POLARIMETER (BRP)

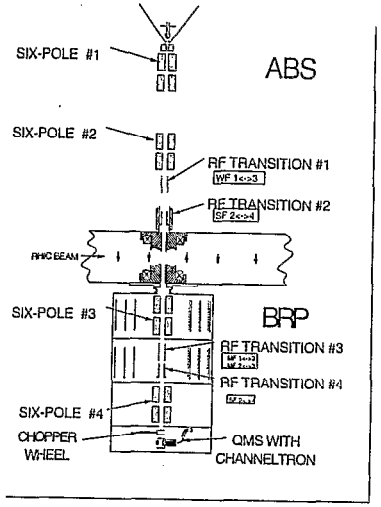

ABS WITH NO RF TRANSITIONS ON MAKES A BEAM WITH STATES 1+2.

NOTATION
ABS STATE "A"

$$\begin{pmatrix} N_1 \\ N_2 \\ 0 \\ 0 \end{pmatrix}$$

FOR Q=+1 THE 2-4 RF TRANSITION IS ON BUT EFFICIENCY IS ~95%.

ABS STATE "B"

$$\begin{pmatrix} N_1 \\ \varepsilon N_2 \\ 0 \\ (1-\varepsilon)N_2 \end{pmatrix}$$

$\varepsilon \approx .05$

NEED TO MEASURE ε.

BRP REJECTS STATES 3 AND 4 THEN MEASURES TWO BEAM INTENSITIES

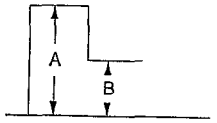

$$A = N_1 + N_2 \qquad B = N_1 + \varepsilon N_2$$

$$\frac{A-B}{A} = \frac{(1-\varepsilon)}{2} \qquad \frac{B}{A} = \frac{\varepsilon}{2}$$

IN PRACTICE THE MEASUREMENT IS MUCH MORE COMPLICATED.

20 INTENSITIES GENERATED BY 11 UNKNOWNS ARE MEASURED.

A CALIBRATION PROCEDURE CAN BE DONE WITHOUT RHIC BEAM.

CONCLUSION

- JET POLARIMETER ALLOWS ABSOLUTE CALLIBRATION OF RHIC PROTON POLARIZATION TO 5% OR BETTER IN 24 HOURS.
- NO DEDICATED UNPOLARIZED RUNNING IS REQUIRED AND CALIBRATION WILL INTERFERE MINIMALLY WITH RING OPERATION.
- VERTICAL JET DESIGN ALLOWS LARGE θ AND ϕ DETECTOR ACCEPTANCE.
- BEAM TARGET INTERACTIONS ARE MANAGEABLE.
- Major design study for Si detection system needed.

Room 302

Beyond Standard Model Physics at RHIC

Jiro Murata (RIKEN)

Abstract

One of the most vital tasks of an experiment using a polarized hadron collider in a new energy region must be a study of physics beyond the standard model. In the last few years, several theoretical articles have been devoted to the study of (1) quark compositeness and a contact interaction, (2) new gauge bosons $W^{\pm}$ and Z', and (3) CP-violation. In the theoretical work [1,2,3], it is shown that RHIC can reach a similar sensitivity for the TEVATRON, due to its polarized beam. The purpose of the present study is to explore the discovery potential for physics beyond standard model, from the experimental perspective. In order to study a physics sensitivity and to determine a search window, event generator based simulation studies are indispensable. A lot of non-standard model scenarios can be examined using PYTHIA.

A contact interaction, phenomenologically introduced as a "residual interaction" which originates in interactions between quark-and lepton-subconstituents, is included in it. However, as same as for all other sub-processes, PYTHIA includes only helicity averaged cross sections for the contact interaction.

The author developed a plug-in program "POLEYOND" for PYTHIA by which helicity- dependent matrix elements and spin asymmetries for Drell-Yan and quark scattering process can be examined. Fig.1 shows the expected single spin asymmetries

$$A_L = \{\sigma(-) - \sigma(+)\} / \{\sigma(-) + \sigma(+)\} \quad (1)$$

at RHIC ($\sqrt{S}$=500 GeV) in $\mu^+\mu^-$ pair production assuming full acceptance and detection efficiency. The results were obtained for various Λ, which is a model-independent scale parameter of the contact interaction, defined as $F(Q^2)=(1+Q^2/\Lambda^2)^{-1}$, where $F(Q^2)$ is a "form factor" of the quark or lepton. Helicity-dependent matrix elements including contact interaction terms were obtained by crossing the electron quark scattering formula shown in [4], from s-channel to t-channel. Final hadronic spin asymmetries were estimated using a weighting method. The weight factor consists of partonic-level helicity-dependent cross sections, polarized and unpolarized parton distribution- functions. The event generation was controlled by the unpolarized sub-processes, which are already included in PYTHIA for fermion pair creation via γ^*/Z production including contact interaction effects. The present result shows that we can expect to observe an anomalous parity violation if $\Lambda \sim 1$ TeV, however, at least the realistic acceptance for a detector should be considered in order to predict more accurate search limit. Furthermore, a full detector simulation is also possible using PYTHIA POL BEYOND.

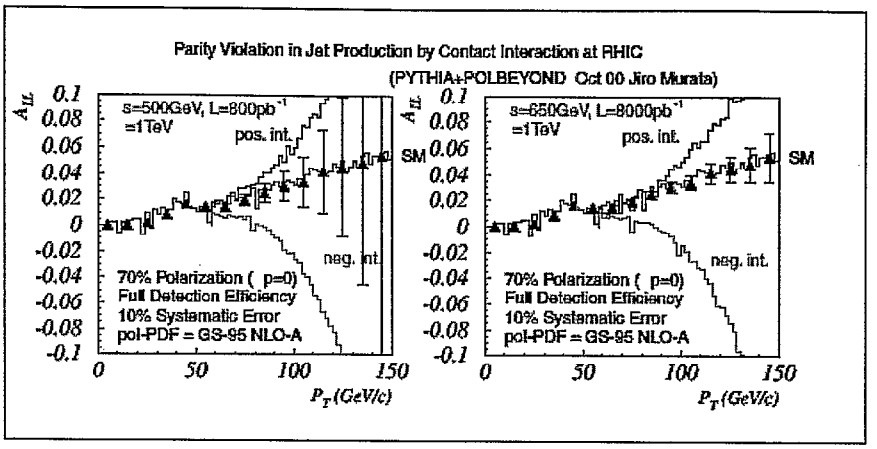

Figure 1:Single spin asymmetries A_L are plotted as functions of Drell-Yan Mass with selections of Λ =1,2 ,3 ,4 ,5 TeV and for the case of the Standard Model ($\Lambda \rightarrow \infty$) obtained by PYTHIA POLEYOND. Present results are for the reaction of $pp \rightarrow \mu^+\mu^-$ at $\sqrt{S}$ =500 GeV, with a constructive interference between the Standard Model and left-handed contact interaction.GS-95 NLO-A is used as a polarized parton distribution function.

Although Drell-Yan is a clean process, other processes, which have larger cross section, must be studied. It is because the present limit is considered as Λ 3 TeV from TEVATRON, atomic parity violation experiments, etc. For this reason, parity violation in jet production is also studied, as shown in Fig.2.From this jet study, it is shown that we can reach above 3 TeV sensitivity, which is higher than the current limit of 2.7 TeV, within original $\sqrt{S}$ =500GeV with 800 pb^{-1} plan. Here we can also see that by the energy and luminosity upgrade plan which is now under discussion, the sensitivity must be improved in order of magnitude. Indeed, it is also shown that the sensitivity limit can be above 6 TeV by the RHIC upgrade. We note that the observation of an anomalous parity violation would directly indicate the presence of new physics.

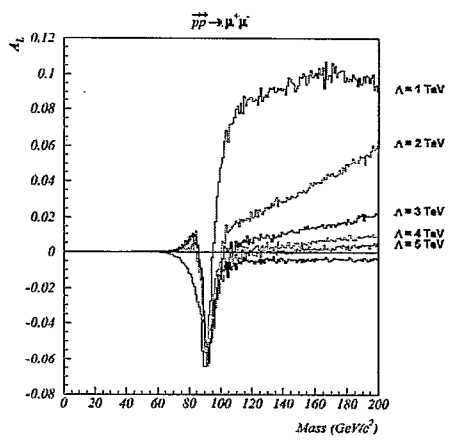

Figure 2: Parity violating double spin asymmetries A_{LL}^{PV} are plotted as functions of Jet P t for $\sqrt{S}$ =500 GeV with 800 pb^{-1} and $\sqrt{S}$ =650 GeV with 8000 pb^{-1}.

[1] P.Taxil,Nuo.Cim.Vol.16,N 11 (1993); P.Taxil and J.-M.Virey,Phys.Rev.D 55 4408 (1997)
[2] P.Taxil and J.-M.Virey,Phys.Lett.B 404 302 (1997);441 376 (1998)
[3] V.L.Rykov,hep-ex/9908050;S.Kovalenko et al.,hep-ph/9912529
[4] J.-M.Virey,Eur.Phys.J.C 8 283 (1999)

Beyond Standard Model Physics at RHIC

RIKEN Jiro Murata

Contents

- Introduction of BYSM at RHIC
- Simulation Study
- Contact Interaction
- Results on Drell-Yan
- Results on Jet Production
- New Gauge Boson ...

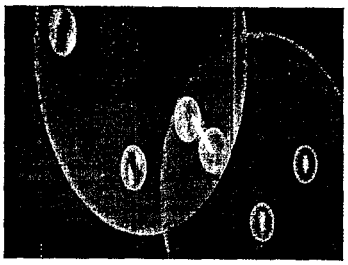

Motivation

Symmetry Test @ RHIC
⇒ Physics Beyond Standard Model !?
NEED Simulation as SM Reference

un-polarized	polarized
New Physics in PYTHIA 4th generation fermions New gauge boson Leptoquarks Compositeness Excited fermions Technicolor	Theoretical Calculation HERA (eq), RHIC (Jet) ⇨ RHIC (DY) HERA (eq), RHIC (Jet) ⇨ RHIC (DY)
CP-Violation Extra Dimension	RHIC (W,DY)

J.-M. Virey
(hep-ph/9707470)

Simulation using Event Generator for qqCI, lqCI(DY), Z', W', etc...

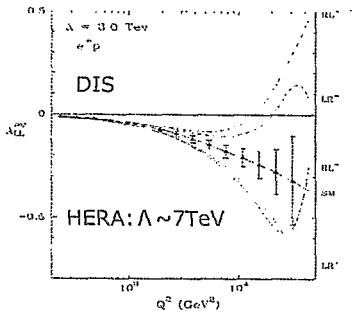

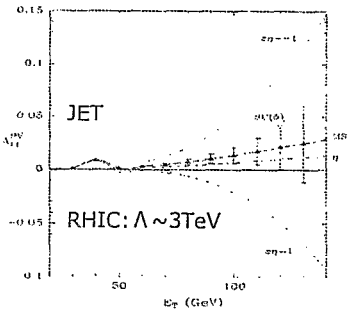

How to Simulate

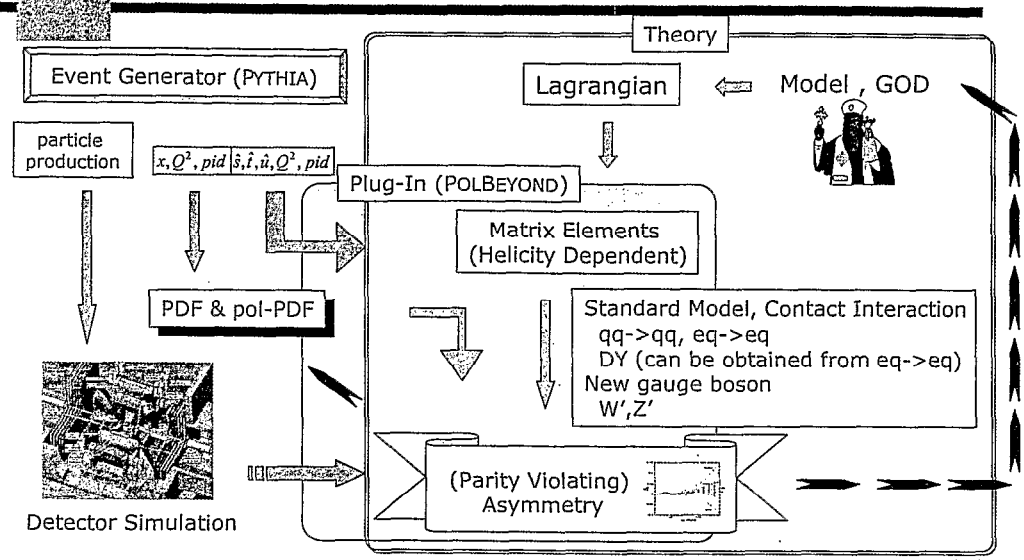

Contact Interaction

Residual Interactions between quark (lepton) sub-constituents

→ (MODEL)? → Parity Violation

Model Independent Scale Parameter Λ

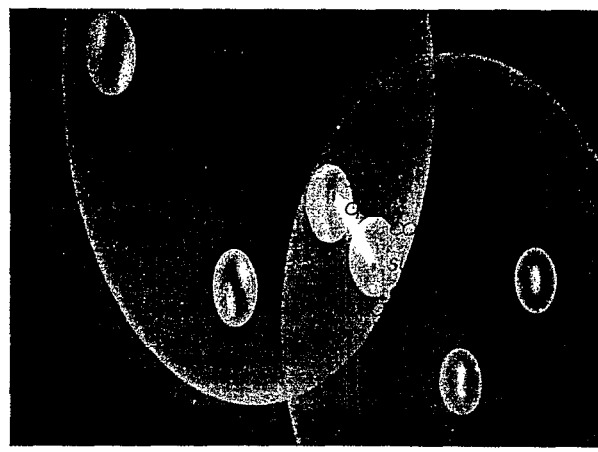

quark (lepton) Form Factor

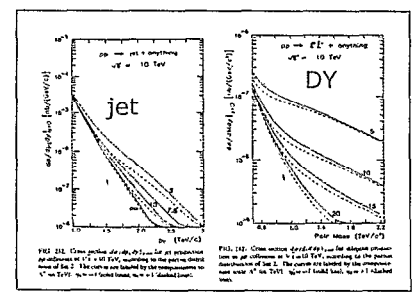

E. Eichten et all;
Rev.Mod.Phys.v56,n4 (84) 579

Matrix Elements to Asymmetries

Total Partonic Cross Section	$\hat{\sigma}^{\lambda_1\lambda_2} = (\lambda_1\lambda_2) = \sum_{\alpha\beta} \lvert M_{\alpha\beta}^{\lambda_1\lambda_2} \rvert^2$
Total Hadronic Cross Section	$\sigma^{\lambda_1\lambda_2} = \sum_{\lambda_1\lambda_2} \hat{\sigma}^{\lambda_1\lambda_2} \otimes q_1^{\lambda_1} q_2^{\lambda_2}$

Analytic Asymmetry (sum over q) and Weight Factor in Event Generator

$$\bar{A}_{LL}^{PV} = \frac{\sigma^{-+} - \sigma^{+-}}{\sigma^{-+} + \sigma^{+-}}$$

$$W(\bar{A}_{LL}^{PV}) = \frac{(q_1^- q_2^+ - q_1^+ q_2^-)(\hat{\sigma}^{--} - \hat{\sigma}^{++}) + (q_1^- q_2^- - q_1^+ q_2^+)(\hat{\sigma}^{-+} - \hat{\sigma}^{+-})}{(q_1^- q_2^+ + q_1^+ q_2^-)(\hat{\sigma}^{--} + \hat{\sigma}^{++}) + (q_1^- q_2^- + q_1^+ q_2^+)(\hat{\sigma}^{-+} + \hat{\sigma}^{+-})}$$

$$A_{LL}^{PV} = \frac{\sigma^{--} - \sigma^{++}}{\sigma^{--} + \sigma^{++}}$$

$$W(A_{LL}^{PV}) = \frac{(q_1^+ q_2^+ - q_1^- q_2^-)(\hat{\sigma}^{--} - \hat{\sigma}^{++}) + (q_1^- q_2^+ - q_1^+ q_2^-)(\hat{\sigma}^{-+} - \hat{\sigma}^{+-})}{(q_1^+ q_2^+ + q_1^- q_2^-)(\hat{\sigma}^{--} + \hat{\sigma}^{++}) + (q_1^- q_2^+ + q_1^+ q_2^-)(\hat{\sigma}^{-+} + \hat{\sigma}^{+-})}$$

$$A_L = \frac{\sigma^- - \sigma^+}{\sigma^- + \sigma^+}$$

$$W(A_L) = \frac{\Delta q}{q} \cdot \frac{\hat{\sigma}^- - \hat{\sigma}^+}{\hat{\sigma}^- + \hat{\sigma}^+}$$

DY Case

$$\lvert M_{\alpha\beta}^{\lambda\lambda} \rvert^2 = 0$$

$$\alpha, \beta = \gamma\gamma, ZZ, \gamma Z, CICI, \gamma CI, ZCI$$

$$A = \sum_{event} W^{event} \Big/ \sum_{event} 1$$

Drell-Yan Type Formalism

$e^- q \to e^- q$
Calculation for HERA by J.-M.Virey

Crossing

$q\bar{q} \to e^+ e^-$
Calculation for RHIC

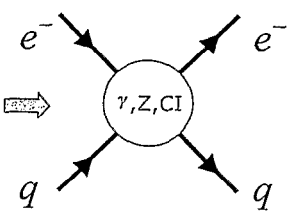

$$(s,t,u) \to (u,s,t)$$

$$\frac{1}{t - M_Z^2} \to \frac{s - M_Z^2}{(s - M_Z^2) + M_Z^2/\Gamma_Z^2}$$

$$\frac{1}{(t - M_Z^2)^2} \to \frac{1}{(s - M_Z^2) + M_Z^2/\Gamma_Z^2}$$

$\lambda_e \to -\lambda_1$ except for $\hat{u}$ term

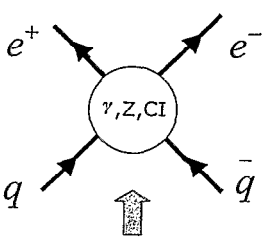

Helicity Depending Matrix Elements for
γ , Z, γ -Z interference
CI, γ -CI interference and Z-CI interference

Event Generation Results

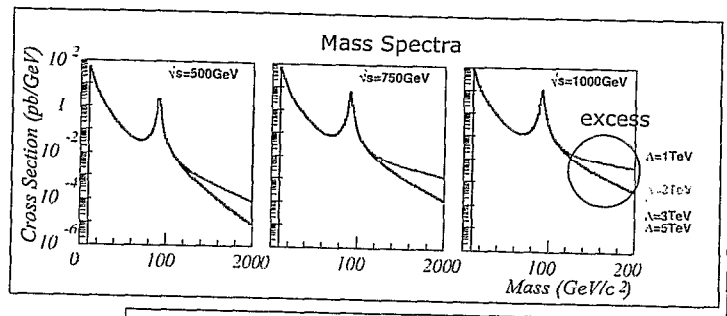

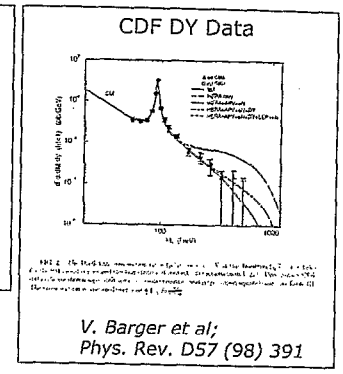

PYTHIA ONLY
Constructive Interference ($\varepsilon = 1$)
MSTP(5)=4 all quarks are composite
KFPR(165)=13 CI goes muon channel
Pure Left-handed (Small Effect)

Dominant Term $\propto 1/\Lambda^2$

Expected Parity Violation for Drell-Yan

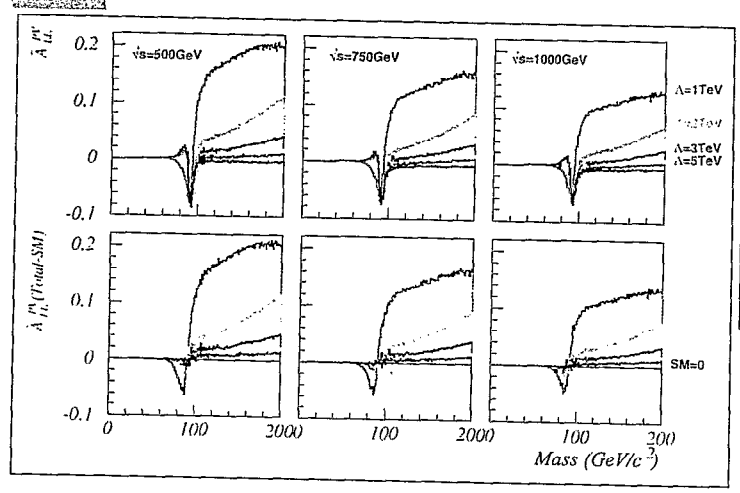

Constructive Interference
Pure Left-handed
PDF: GS95NLO-A
pp->dimuon

Sensitive Region
1. ~80GeV < Mass < Z
2. Mass > Z

Required Luminosity for Discovery on Drell-Yan

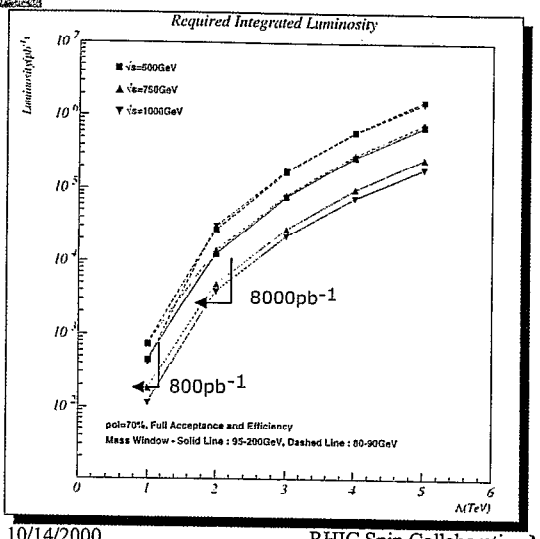

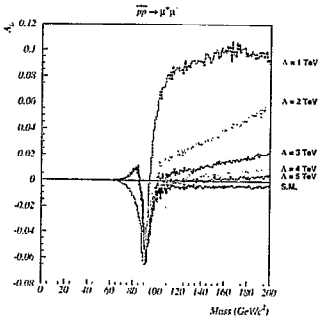

Improve factor 2-3 using A_L
Anyway Need Huge Luminosity ... !

$\Lambda < 1.2$ TeV : 800 pb^{-1}
$\Lambda < 2.2$ TeV : 8000 pb^{-1}

LHC !?

Simulate quark-quark Contact Interaction

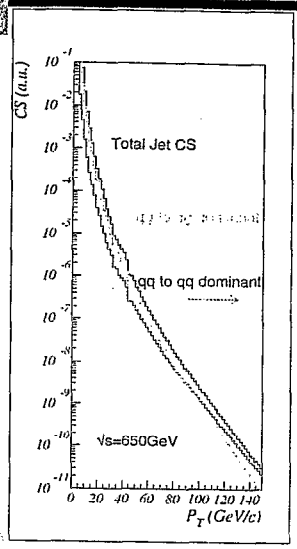

$gg \to gg$ $gg \to q\bar{q}$ $q\bar{q} \to gg$ $qg \to qg$	g

82 Terms [DY:6 Terms]

$qq \to qq$ $\bar{q}\bar{q} \to \bar{q}\bar{q}$ $q\bar{q} \to q\bar{q}$	g, γ, Z, g-γ, g-Z, γ-Z CI, g-CI, γ-CI, Z-CI
$qq' \to qq'$ $\bar{q}\bar{q}' \to \bar{q}\bar{q}'$ $q\bar{q}' \to q\bar{q}'$ $q\bar{q} \to q'\bar{q}'$	g, γ, Z, W, γ-Z, g-W, γ-W, Z-W CI, γ-CI, Z-CI, W-CI

Should Have C.I. Sensitivity on high Pt !

Expected Parity Violation

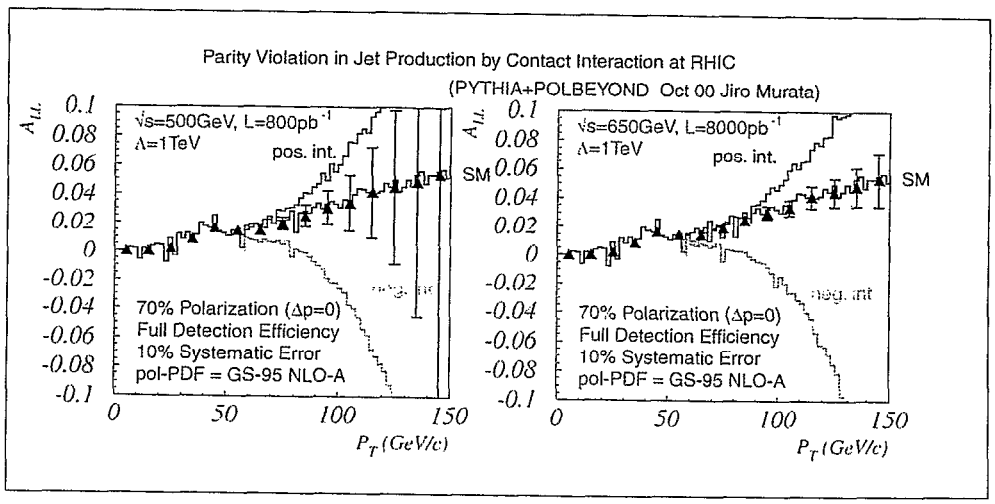

Discovery Limit on Jet Production

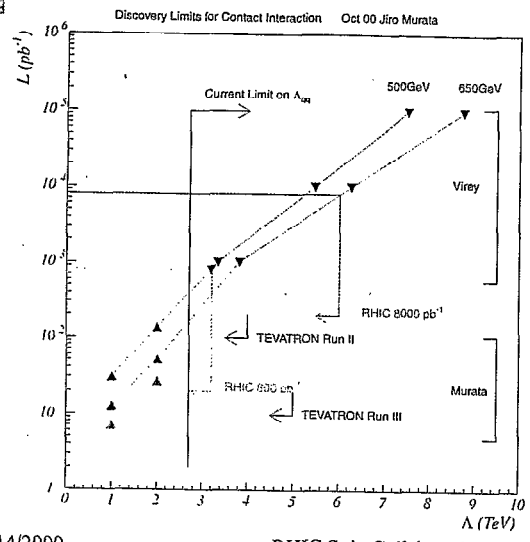

Luminosity Upgrade is Essential
500 -> 650GeV ~ x 2 Luminosity

New gauge boson

SUSY, String (E_6) -> additional U(1)'
CI and Z' is similar
(Model Dependent)
Mz'>690 GeV, Mw'>720 GeV

$$\frac{\alpha_{Z'} C'_{ei} C'_{qj}}{-M_{Z'}^2} \approx \frac{\varepsilon}{(\Lambda_{ij}^q)^2}$$

Matrix Elements

$qq \to qq$ $\bar{q}\bar{q} \to \bar{q}\bar{q}$ $q\bar{q} \to q\bar{q}$	SM Z', g-Z', γ-Z', Z-Z'
$qq' \to qq'$ $\bar{q}\bar{q}' \to \bar{q}\bar{q}'$ $q\bar{q}' \to q\bar{q}'$ $q\bar{q} \to q'\bar{q}'$	SM Z', γ-Z', Z-Z', Z'-W W', g-W', γ-W', Z-W', W-W'
$eq \to eq$ $q\bar{q} \to ee$	SM Z', γ-Z', Z-Z'

Jean-Marc Virey, Doctor Thesis, 1997

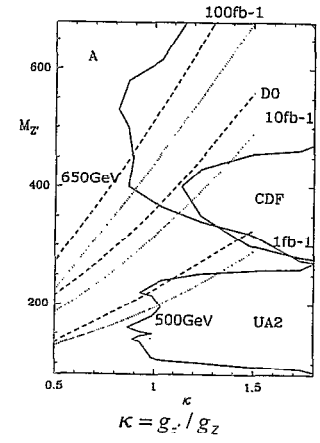

Next Step ...
Z' in DY is Interesting

Summary

- Procedure of including polarized BYSM effects into Pythia has been established.
- Obtained DY Mass dep. of Asymmetries, Pt dep. Jet Asymmetries were obtained.
- CI in DY need huge luminosity (Sufficient for pol-PDF study in SM)
- CI in quark sector can reach $\Lambda \sim 6$TeV with 8000pb-1, 650GeV upgrade.
- Including new gauge bosons Z′,W′ is also possible for DY and Jet.
- By the UPGRADE, WE CAN BE A VERY HIGH ENERGY FRONTIER !!!

Quark and Lepton Compositeness, Searches for

Scale Limits Λ for Contact Interactions (the lowest dimensional interactions with four fermions)

If the Lagrangian has the form

$$\pm \frac{g^2}{2\Lambda^2} \bar{\psi}_L \gamma_\mu \psi_L \bar{\psi}_L \gamma^\mu \psi_L$$

(with $g^2/4\pi$ set equal to 1), then we define $\Lambda \equiv \Lambda^{\pm}_{LL}$. For the full definitions and for other forms, see the Note in the Listings on Searches for Quark and Lepton Compositeness in the full *Review* and the original literature.

$\Lambda^+_{LL}(eeee)$	> 3.5 TeV, CL = 95%
$\Lambda^-_{LL}(eeee)$	> 3.8 TeV, CL = 95%
$\Lambda^+_{LL}(ee\mu\mu)$	> 4.5 TeV, CL = 95%
$\Lambda^-_{LL}(ee\mu\mu)$	> 4.7 TeV, CL = 95%
$\Lambda^+_{LL}(ee\tau\tau)$	> 3.9 TeV, CL = 95%
$\Lambda^-_{LL}(ee\tau\tau)$	> 4.0 TeV, CL = 95%
$\Lambda^+_{LL}(\ell\ell\ell\ell)$	> 5.3 TeV, CL = 95%
$\Lambda^-_{LL}(\ell\ell\ell\ell)$	> 5.5 TeV, CL = 95%
$\Lambda^+_{LL}(eeqq)$	> 5.4 TeV, CL = 95%
$\Lambda^-_{LL}(eeqq)$	> 6.2 TeV, CL = 95%
$\Lambda^+_{LL}(eebb)$	> 5.6 TeV, CL = 95%
$\Lambda^-_{LL}(eebb)$	> 4.9 TeV, CL = 95%
$\Lambda^+_{LL}(\mu\mu qq)$	> 2.9 TeV, CL = 95%
$\Lambda^-_{LL}(\mu\mu qq)$	> 4.2 TeV, CL = 95%
$\Lambda^{\pm}_{LR}(\nu_\mu \nu_e \mu e)$	> 3.1 TeV, CL = 90%
$\Lambda^+_{LL}(qqqq)$	> 2.7 TeV, CL = 95%
$\Lambda^-_{LL}(qqqq)$	> 2.4 TeV, CL = 95%
$\Lambda^+_{LL}(\nu\nu qq)$	> 5.0 TeV, CL = 95%
$\Lambda^-_{LL}(\nu\nu qq)$	> 5.4 TeV, CL = 95%

Summary of Previous meeting (Aug 3rd)

S.Vigdor

Summary of August 3, 2000 Meeting on Year 2 RHIC Spin Program

Questions Addressed:

1) What hardware will be available for spin manipulation in Year 2? How will it be implemented?

2) Can STAR & PHENIX agree on joint goals for beam use request?

3) What year 2 program of measurements will optimize the impact of RHIC Spin?

S. Vigdor
RSC 2000
Kyoto

Answers:

1) 2 Snakes + 1 CNI polarimeter per ring. spin flip for both beams; no spin rotators
$\Rightarrow$ 2 modes of running possible @ $\sqrt{s} = 200$ GeV
a) ramp to 100 GeV, adiabatically turn off 1 snake/ring, run horizontal spin orient'n set by precise E_{beam} tuning $\Rightarrow$ different orientations possible at different IR's
b) keep both snakes on in both rings
$\Rightarrow$ vertical spin at each IR, independent of E_{beam}

2) Yes, we must agree for strength of overall program, priority vis-a-vis A+A

3) Reasonable people with common goals, but different experiences and detectors, can come to very different conclusions about optimal Year 2 program

Basic Conflict:

PHENIX -- "Let's get on with placing meaningful constraint on ΔG, via 32 pb^{-1} A_{LL} measurement for inclusive π^0 production"

STAR -- "Let's understand how to make credible measurements in this completely new regime ⇒ begin understanding systematic errors, publish first A_T measurements (preferably with vertical spin)"

Year 2 is the Engineering Run for RHIC Spin:

Goals:

1) Demonstrate pp collisions with good, and reliably measurable, P_{beam}
2) Demonstrate that detectors can measure small asymmetries reliably.
3) Produce first publishable (i.e., credible, enduring, essential) spin physics results

STAR View: goals are most likely to be met by concentration on vertically pol'd beam + meas'ment of single-spin transverse asymmetry at high p_T

Part of 5-year STAR spin plan ⇒ staged, matched progression of:
spin manipulation hardware;
STAR det. hardware; learning curve;
physics goals

Systematic Error Concerns:

1) $|P_{beam}|$ scale uncertainty -- will have to work very hard (+ plan ahead) to do better than $\pm 25\%$ in YEAR 2 or 3!

multi-stage calibration requires extensive time for measurements:

$\vec{p}p$ database $\rightarrow$ AGS fishline
AGS fishline $\rightarrow$ AGS CNI
AGS CNI $\rightarrow$ RHIC CNI ($E_{injection}$)
RHIC CNI (E_{inj}) $\rightarrow$ RHIC CNI ($E_{ramp-top}$)

2) To reach horizontal spin orientation precision of $\lesssim \pm 10°$ requires:

absolute E_{beam} accuracy $\sim 10^{-4}$
beam momentum dir'n errors < 1 mrad

$\Rightarrow$ detectors well advised to include local orientation monitoring via A_T

3) $\mathcal{L}$ monitoring: to measure A_{LL} to $\sim \pm .001$ precision with $P_{beam} = 0.5$ ($\Rightarrow P^2 A_{LL}$ uncertainty $\sim \pm 3 \times 10^{-4}$), need

$$\left(\frac{\delta \mathcal{L}}{\mathcal{L}}\right)_{relative} \sim 10^{-4}$$

This includes any real A_{LL} spin-dependence in $\mathcal{L}$-monitor processes.

All of these require measurement programs + planning of their own.

meeting concluded by enumerating many areas of agreement between the two groups, which should lead to a joint polarized beam use request for year 2:

- The chances of a healthy and productive RHIC spin program are greatly enhanced by cooperation among all the interested groups.
- Sufficient polarized beam operation will be needed in RHIC year 2 to permit commissioning of polarized proton collisions, systematic studies of CNI polarimeter operation and reproducibility, studies relevant to calibrating other systematic errors discussed above, and production running with both longitudinally and transversely polarized beams. It was estimated that 10 weeks of running would probably be needed to accomplish all these goals, but a detailed time request must await further work outlined below.
- The deployment of all four Siberian snakes for the year 2 run was strongly endorsed, as it provides the flexibility to meet needs of all the interested experiments.
- Some of the engineering run goals outlined by Vigdor should be accomplished during the anticipated September 2000 polarized beam commissioning study within the blue ring. Therefore, a more informed decision regarding the optimal breakdown of requested time among the goals listed above can be made after the Sept. 19 end of the current running period. The spin groups will reconvene shortly thereafter to try to converge on a beam use request.
- In the time before the next meeting, more detailed thought needs to be given to quantitative year 2 systematic error concerns and goals for both STAR and PHENIX, and to realistic measurement plans aimed at assessing whether these goals have been achieved. Progress on relevant calculations will be a prominent topic of discussion at the next meeting.
- The STAR spin group should consider in more detail the possibility of measuring transverse asymmetries with radially polarized beam. BRAHMS collaborators should be approached to gauge their interest and capabilities for transverse asymmetry measurements in inclusive hadron production at high x_F and p_T values.
- The PHENIX spin group should reassess the beam time needed for year 2 A_{LL} measurements, in light of more realistic estimates of integrated luminosity likely to be available, and in light of more realistic assessments of systematic errors. It makes no sense to push statistical uncertainties to levels far smaller than the systematic ones.
- Installation of a full complement of spin rotators at both STAR and PHENIX at the earliest possible date is crucial to the future of the RHIC spin program. Different installation schedules for relevant equipment within the two detectors will inevitably lead to continuing differences in beam time demands for the various beam spin orientations. The rotators provide the flexibility to accommodate the needs of both collaborations. Continued cooperation will still be needed in dividing time between different beam energies.

Discussion for FY2001 running and beyond

G. Bunce discussion leader

Proposed

0) AGS commissioning time : ? weeks

1) 2 weeks pp collision commissioning

2) 1 week spin commissioning

3) 5 weeks $\vec{p}\vec{p}$ 5-6 pb^{-1}

---

8 weeks

But : does not fit into 25 weeks.

$\Rightarrow$ 1 extra month.

RSC 2000
Oct. 2000
Kyoto
G. Bunce

Remarks / Discussion: Next Year — FY2001 Spin Program

From Sept. 2000 commissioning:

1) pC CNI clean, $\Delta P \leq \pm 2\%$, systematics $\leq \pm 2\%$

2) absolute polarization still work in progress. Based on pp, $-t \simeq .15$ — comments from Naduto, Haixin, Hal, ... Expect $\frac{\Delta P}{P} \approx \pm 7\% \,|\, \pm 10\% \,|\, \approx \pm 15\%$

E925 stats | pp A_N

at AGS injection. But, hadronic spin flip $\neq 0$. $\Rightarrow A_{N_{CNI}}(E)$? $\Rightarrow$ can we decellerate to measure $A_{N_{CNI}}(E)$? Why didn't pp quasi-el. work in RHIC? (Do we need it?)

3) polarimeter commissioning with RHIC ≤ 12 hours! For FY2001 will have 10x rate/crossing, new readout to commission.

4) 2 snakes / ring much preferred
   – P × 1/.6, RHIC tune dep. at injection, ...

5) 1 snake running stable, as predicted

6) large bunch intensity variation (factor 2)
   – from AGS extraction jitter? Variation of other beam characteristics?

7) polarization only ≈ 20%. 2 snakes: × 1/.6 ?
   AGS problem at injection? P = .5 next year?

8) assume 1.5 pb^{-1} / week

From Aug. 3 mtg.

1) 5 pb^{-1} and P = .5 more realistic. ✓

2) systematics of polarimetry ($\lesssim \pm 2\% = \Delta P$) ✓

3) absolute $\Delta P/P = \pm$ 20% or 30%? ✓

4) luminosity monitoring by crossing — necessary if $N_i = 2N_j$ ✓
   – but, spin flipper?

5) measure A_N, show $A_N \to 0$ for $\sqrt{s} \to$ large
   – can only do this at Brahms now
   – see Bravar talk at Transv. Workshop
   → possible

6) measure non-zero asymmetry at detectors
   ⇒ handling data properly

7) measure transverse asym. → absence for long. polarization

→ add γ/π^0 forward detectors at expts.!
   – see Yuji Goto / Ken Imai

Straw-man FY2001 Spin Plan

1) 1 week for AGS pol. proton commissioning

2) set up pp collisions, tune closed orbit
   → 2 weeks – changed to heavy ions
   – set up both polarimeter, expt. lum. monitors, 4 snakes (also during heavy ions)

3) commission pol. proton collisions → 1 week
   – each ring, polarization vs. E
   – spin flipping
   – 2 snakes → 1 snake
   – deceleration for $A_N(E)_{CNI}$

4) transverse pol. running → 1 week – 1.5 pb^{-1}
   – forward γ meas. at detectors
   – detector meas. with transv. pol., vs. ϕ

5) longitudinal pol. running → 5 weeks – 5 pb^{-1}
   – $\pi^{\pm}, \phi$ asym. → $\Delta G/G$
   – μ, e →

Total: spin: 1 week comm., 6 weeks running + 1
⇒ 8 weeks (heavy ion pp included)

Improvements for near and longer term spin program:

- 200 MeV polarimeter at high intensity
- AGS CNI polarimeter
- spin flipping in RHIC
- AGS polarization – several possibilities
  - helical snake?
  - hor. rf dipole
  - quads, ramp rate
- scheme for experiments using spin flipping, recogging → eliminate need for luminosity normalization?
- stabilize AGS extraction
  - new hardware?
- polarized hydrogen jet target: $\frac{\Delta P}{P} \leq \pm 5\%$

RSC 2000
G. Bunce

RHIC Spin and the U.S. Nuclear Physics Long Range Plan

"what you want to do for the next 5 years, and what you want to build beyond that; argue for anything beyond the FY2002 budget" – Peter Bond

---

Nuclear Science Advisory Committee (Symons, chair)
→ 4 planning committees + 4 Town Meetings

---

2 Town Meetings overlap RHIC Spin:

Dec. 1-4, JLab: Electromagnetic and Hadronic Physics

Jan. 21-23, BNL: Nuclear Matter and Hadrons at High Energies

BNL asked Thomas Roser + GB to help organise RHIC spin response.

Goals toward RHIC Spin response:

1) contact chairs of Town Meetings, get slots for presentations for RHIC spin (Murtagh → JLab)
2) discuss, think, decide on focus for longer range spin physics at RHIC
3) decide on what presentations and who
4) write something short and sweet in time for Dec. 1-4 meeting at JLab

---

Formed a committee: inclusive

Naohito Saito, Mike Tannenbaum, Yousef Makdisi, Matthias Grosse Perdekamp, Les Bland, Steve Vigdor, Hal Spinka, Bob Jaffe, Jacques Soffer, Werner Vogelsang, Wlodek Guryn, Thomas Roser, Gerry Bunce, ...

Meetings: Sept. 15, BNL
Sept. 19, BNL
→ Oct. 14, Kyoto

Some notes on Sept. 15, 19 meetings:

1. main emphasis: our present RHIC spin plan
   → 5 to 7 year plan as it is

2. any "beyond RSC" must be physics-driven, qualitatively new reach beyond (1).

3. discussion around
   - 10× luminosity
   - $\sqrt{s} \to 650$ GeV at one IP
   - $\sqrt{s} = 50$ GeV with high luminosity
   - $\vec{p}A$ collisions with parity violation probe
   - $^3\vec{He}\,\vec{p}$ collisions
   - new detector for spin at RHIC
     - need new reach
     - is it a bad idea to emphasize this now?
     - phasing with eRHIC?
   - connect with physics of $\vec{e}\,\vec{p}$ collider
   - transversity physics?

4. For any "beyond RSC" areas, need to have advocate, set up group to develop arguments.

Note: RHIC spin has considerable support:
- emphasized in email setting up meetings
- Les Bland, Tim Hallman on NSAC (also Jim Symons)
- Joel Moss, Al Mueller, Dave Hertzog, Peter Paul on JLab planning committee
- Steve Vigdor on BNL planning committee

286

Present tentative conclusions:
- presentations at JLab:
  - $\Delta G/G$, $\Delta q/q$ program — Vigdor, Bland, ...
  - transversity (motivate!) — Jaffe, Grosse, Pantelkamp
  - RHIC spin accelerator + commissioning — Russo
  - future with eRHIC?
- presentations at BNL:
  - summary of proton spin
  - beyond SM
  - $pp \to pp$ — $\vec{p}A$

For information please contact:

Ms. Tammy Heinz
RIKEN BNL Research Center
Building 510A, Brookhaven National Laboratory
Upton, N.Y. 11973-5000, USA

Phone: (631) 344-5864
Fax: (631) 344-2562
E-Mail: theinz@bnl.gov

Homepage: http://quark.phy.bnl.gov/www/riken.html
http://penguin.phy.bnl.gov/www/riken.html

inside back cover

RHIC SPIN PHYSICS III & IV
POLARIZED PARTONS AT HIGH Q^2 REGION

AUG. 3, 2000 AT BNL **OCT. 14, 2000 AT KYOTO UNIVERSITY**

Li Keran

Copyright©CCASTA

Nuclei as heavy as bulls
Through collision
Generate new states of matter.
T. D. Lee

Speakers:

M. Bai, K. Barish, D. Boer, G. Bunce, M. Grosse Perdekamp, Haixin Huang, Hanwen Huang, H. Kobayashi, E. Leader, A. Lehrach, J. Murata, A. Ogawa, K. Ohkuma, M. Okamura, T. Roser, J. Soffer, J. Soeren Lange, H. Spinka, D. Svirida, S. Vigdor, W. Vogelsang, T. Wise, M. Xiao, A. Zelenski

Organizers: Aug. 3: G. Bunce & S. Vigdor
Oct. 14: K. Imai, H. En'yo, N. Saito, T. Kunihiro, T. Uematsu, S. Kumano, Y. Koike, M. Okamura

Scientific Advisor Committee: T. Roser, D. Underwood, X. Ji, J. Soffer, L.C. Bland, K. Yazaki, A. Masaike